ATTACHMENT 1

Program Areas & Departments > Standards > Project 2013-03 Geomagnetic Disturbance Mitigation

Project 2013-03 Geomagnetic Disturbance Mitigation

Related Files

Status

A 30-day comment period on revised project white papers is available until **8 p.m. Eastern, Monday, June 13, 2016**.

Board Adopted: December 17, 2014 - TPL-007-1

Filed with FERC: January 21, 2015

Order Effective:

Enforcement Date:

Background:

FERC issued order 779 in May 2013 directing NERC to develop reliability standards to address the potential impact of geomagnetic disturbances (GMDs) on the reliability operation of the Bulk-Power System. Since 2010, industry has taken steps to address the GMD risk scenario identified in the 2010 High Impact Low Frequency (HILF) Event joint report through the Geomagnetic Disturbance (GMD) Task Force, which is comprised of industry representatives, government partners, and GMD experts. The GMD Task Force published an interim report on the effects of GMD on the Bulk-Power System in April 2012 and provided recommendations to manage risk. The task force's current project is focused on providing tools for system operators and planners to assess GMD effects on the system and implement mitigating strategies when needed.

Purpose / Industry Need:

Project 2013-03 will develop reliability standards to mitigate the risk of instability, uncontrolled separation, and Cascading as a result of geomagnetic disturbances (GMDs) through application of Operating Procedures and strategies that address potential impacts identified in a registered entity's assessment as directed in FERC Order 779.

While the impacts of space weather are complex and depend on numerous factors, space weather has demonstrated the potential to effect the reliable operation of the Bulk-Power System. During a GMD event, geomagnetically-induced current (GIC) flow in transformers may cause half-cycle saturation, which can increase absorption of Reactive Power, generate harmonic currents, and cause transformer hot spot heating. Increased transformer Reactive Power absorption and harmonic currents associated with GMD events can also cause protection system Misoperation and loss of Reactive Power sources, the combination of which can lead to voltage collapse.

The project will develop requirements for registered entities to employ strategies that mitigate risks of instability, uncontrolled separation and Cascading caused by GMD in two stages as directed in order 779:

1. Stage 1 standard(s) will require applicable registered entities to develop and implement Operating Procedures that can mitigate the effects of GMD events.
2. Stage 2 standard(s) will require applicable registered entities to conduct initial and on-going assessments of the potential impact of benchmark GMD events on their respective system as directed in order 779. The Second Stage GMD Reliability Standards must identify benchmark GMD events that specify what severity GMD events applicable registered entities must assess for potential impacts on the Bulk-Power System. If the assessments identify potential impacts from benchmark GMD events, the Reliability Standards will require the registered entity to develop and implement a plan to mitigate the risk of instability, uncontrolled separation, or Cascading as a result of a benchmark GMD event. The development of this plan cannot be limited to considering operational procedures or

enhanced training alone, but will, subject to the potential impacts of the benchmark GMD events identified in the assessments, contain strategies for mitigating the potential impact of GMDs based on factors such as the age, condition, technical specifications, system configuration, or location of specific equipment.

As directed in order 779, stage 1 standards must be filed by January 2014, and stage 2 standards must be filed by January 2015.

Draft	Action	Dates	Results	Consideration of Comments
Project White Papers Benchmark GMD Event White Paper **(11)**[unchanged from clean version below] Thermal Screening Criterion White Paper **(12)** [unchanged from clean version below] Transformer Thermal Impact Assessment White Paper Clean **(13)** | Redline to Last Posted **(14)**				
Revisions to Project White Papers Benchmark GMD Event White Paper Clean **(1)** | Redline to Last Posted **(2)** Transformer Thermal Impact Assessment White Paper	Comment Period Info **(8)** Submit Comments	05/12/16 - 06/13/16	Comments Received **(9)**	Consideration of Comments **(10)**

Clean **(3)** | Redline to Last Posted **(4)** Thermal Screening Criterion White Paper Clean **(5)**| Redline to Last Posted **(6)** **Supporting Materials** Unofficial Comment Form (Word) **(7)**				

NERC
NORTH AMERICAN ELECTRIC RELIABILITY CORPORATION

Benchmark Geomagnetic Disturbance Event Description

Project 2013-03 GMD Mitigation
Standard Drafting Team
May 12, 2016

RELIABILITY | ACCOUNTABILITY




Table of Contents

Preface

The North American Electric Reliability Corporation (NERC) is a not-for-profit international regulatory authority whose mission is to ensure the reliability of the Bulk-Power System (BPS) in North America. NERC develops and enforces Reliability Standards; annually assesses seasonal and long-term reliability; monitors the BPS through system awareness; and educates, trains, and certifies industry personnel. NERC's area of responsibility spans the continental United States, Canada, and the northern portion of Baja California, Mexico. NERC is the electric reliability organization (ERO) for North America, subject to oversight by the Federal Energy Regulatory Commission (FERC) and governmental authorities in Canada. NERC's jurisdiction includes users, owners, and operators of the BPS, which serves more than 334 million people.

The North American BPS is divided into several assessment areas within the eight Regional Entity (RE) boundaries, as shown in the map and corresponding table below.

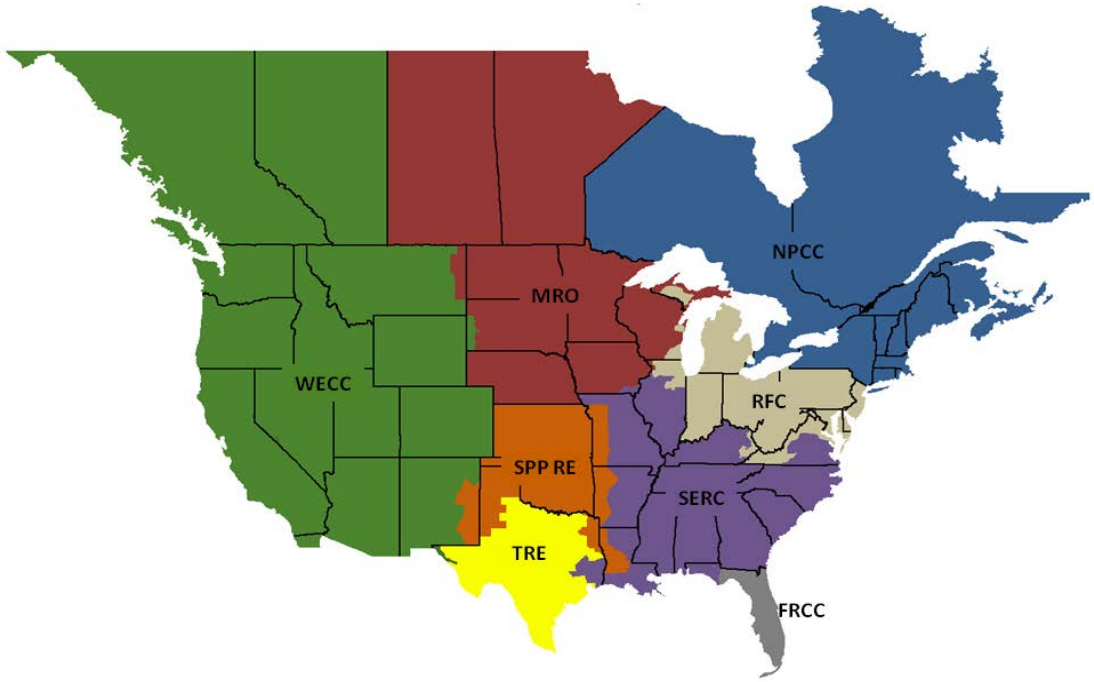

FRCC	Florida Reliability Coordinating Council
MRO	Midwest Reliability Organization
NPCC	Northeast Power Coordinating Council
RFC	Reliability*First* Corporation
SERC	SERC Reliability Corporation
SPP-RE	Southwest Power Pool Regional Entity
TRE	Texas Reliability Entity
WECC	Western Electric Coordinating Council

Introduction

Background

The purpose of the benchmark geomagnetic disturbance (GMD) event description is to provide a defined event for assessing system performance during a low probability, high magnitude GMD event as required by proposed standard TPL-007-1 – Transmission System Planned Performance for Geomagnetic Disturbance Events. The benchmark GMD event defines the geoelectric field values used to compute geomagnetically-induced current (GIC) flows for a GMD Vulnerability Assessment.

On May 16, 2013, FERC issued Order No. 779, directing NERC to develop Standards that address risks to reliability caused by geomagnetic disturbances in two stages:

- Stage 1 Standard(s) that require applicable entities to develop and implement Operating Procedures. EOP-010-1 – Geomagnetic Disturbance Operations was approved by FERC in June 2014.
- Stage 2 Standard(s) that require applicable entities to conduct assessments of the potential impact of benchmark GMD events on their systems. If the assessments identify potential impacts, the Standard(s) will require the applicable entity to develop and implement a plan to mitigate the risk.

TPL-007-1 is a new Reliability Standard developed to specifically address the Stage 2 directives in Order No. 779. The benchmark GMD event will define the scope of the Stage 2 Reliability Standard.

General Characteristics

The benchmark GMD event described herein takes into consideration the known characteristics of a severe GMD event and its impact on an interconnected transmission system. These characteristics include:

- Geomagnetic Latitude – The amplitude of the induced geoelectric field for a given GMD event is reduced as the observation point moves away from the earth's magnetic poles.
- Earth Conductivity – The amplitude and phase of the geoelectric field depends on the local or regional earth ground resistivity structure. Higher geoelectric field amplitudes are induced in areas of high resistivity.
- Transformer Electrical Response – Transformers can experience half-cycle saturation when subjected to GIC. Transformers under half-cycle saturation absorb increased amounts of reactive power (var) and inject harmonics into the system. However, half-cycle saturation does not occur instantaneously and depends on the electrical characteristics of the transformer and GIC amplitude [1]. Thus, the effects of transformer reactive power absorption and harmonic generation do not occur instantaneously, but instead may take up to several seconds. It is conservative, therefore, to assume that the effects of GIC on transformer var absorption and harmonic generation are instantaneous.
- Transformer Thermal Effects (e.g. hot spot transformer heating) – Heating of the winding and other structural parts can occur in power transformers during a GMD event. However, the thermal impacts are not instantaneous and are dependent on the thermal time constants of the transformer. Thermal time constants for hot spot heating in power transformers are in the 5-20 minute range.
- Geoelectric Field Waveshape – The geoelectric field waveshape has a strong influence on the hot spot heating of transformer windings and structural parts since thermal time constants of the transformer and time to peak of storm maxima are both on the order of minutes. The frequency content of the magnetic field (dB/dt) is a function of the waveshape, which in turn has a direct effect on the geoelectric field since the earth response to external dB/dt is frequency-dependent.
- Wide Area Geomagnetic Phenomena – The influence of GMD events is typically over a very broad area (e.g. continental scale); however, there can be pockets or very localized regions of enhanced geomagnetic activity. Since geomagnetic disturbance impacts within areas of influence of approximately 100-200 km do not have a widespread impact on the interconnected transmission system (see Appendix I), statistical methods used to assess the frequency of occurrence of a severe GMD event need to consider broad geographical regions to avoid bias caused by spatially localized geomagnetic phenomena.

Benchmark GMD Event Description

Severe geomagnetic disturbance events are high-impact, low-frequency (HILF) events [2]; thus, any benchmark event should consider the probability that the event will occur, as well as the impact or consequences of such an event. The benchmark event is composed of the following elements: 1) a reference peak geoelectric field amplitude (V/km) derived from statistical analysis of historical magnetometer data; 2) scaling factors to account for local geomagnetic latitude; 3) scaling factors to account for local earth conductivity; and 4) a reference geomagnetic field time series or waveshape to facilitate time-domain analysis of GMD impact on equipment.

Reference Geoelectric Field Amplitude

The reference geoelectric field amplitude was determined through statistical analysis using the plane wave method [3]-[10] geomagnetic field measurements from geomagnetic observatories in northern Europe [11] and the reference (Quebec) earth model shown in **Table 1** [12]. For details of the statistical considerations, see Appendix I. The Quebec earth model is generally resistive and the geological structure is relatively well understood.

Table 1: Reference earth model (Quebec)

Thickness (km)	Resistivity (Ω-m)
15	20,000
10	200
125	1,000
200	100
∞	3

The statistical analysis (see Appendix II) resulted in a conservative peak geoelectric field amplitude of approximately 8 V/km. For steady-state GIC and load flow analysis, the direction of the geoelectric field is assumed to be variable meaning that it can be in any direction (Eastward, Northward, or a vectorial combination thereof).

The frequency of occurrence of this benchmark GMD event is estimated to be approximately 1 in 100 years (see Appendix I). The selected frequency of occurrence is consistent with utility practices where a design basis frequency of 1 in 50 years is currently used as the storm return period for determining wind and ice loading of transmission infrastructure [13], for example.

The regional geoelectric field peak amplitude, E_{peak}, to be used in calculating GIC in the GIC system model can be obtained from the reference value of 8 V/km using the following relationship

$$E_{peak} = 8 \times \alpha \times \beta \text{ (V/km)} \quad (1)$$

where α is the scaling factor to account for local geomagnetic latitude, and β is a scaling factor to account for the local earth conductivity structure (see Appendix II).

Reference Geomagnetic Field Waveshape

The reference geomagnetic field waveshape was selected after analyzing a number of recorded GMD events, including the reference storm of the NERC interim report of 2012 [14], measurements at the Nurmijarvi (NUR) and Memanbetsu (MMB) geomagnetic observatories for the "Halloween event" of October 29-31, 2003, and the March 1989 GMD event that caused the Hydro Quebec blackout. The geomagnetic field measurement record of the March 13-14 1989 GMD event, measured at NRCan's Ottawa geomagnetic observatory, was selected as the

reference geomagnetic field waveform because it provides generally conservative results when performing thermal analysis of power transformers (see Appendix I). The reference geomagnetic field waveshape is used to calculate the GIC time series, GIC(t), required for transformer thermal impact assessment.

The geomagnetic latitude of the Ottawa geomagnetic observatory is 55°; therefore, the amplitude of the geomagnetic field measurement data were scaled up to the 60° reference geomagnetic latitude (see **Figure 1**) such that the resulting peak geoelectric field amplitude computed using the reference earth model was 8 V/km (see **Figures 2** and **3**). Sampling rate for the geomagnetic field waveshape is 10 seconds.

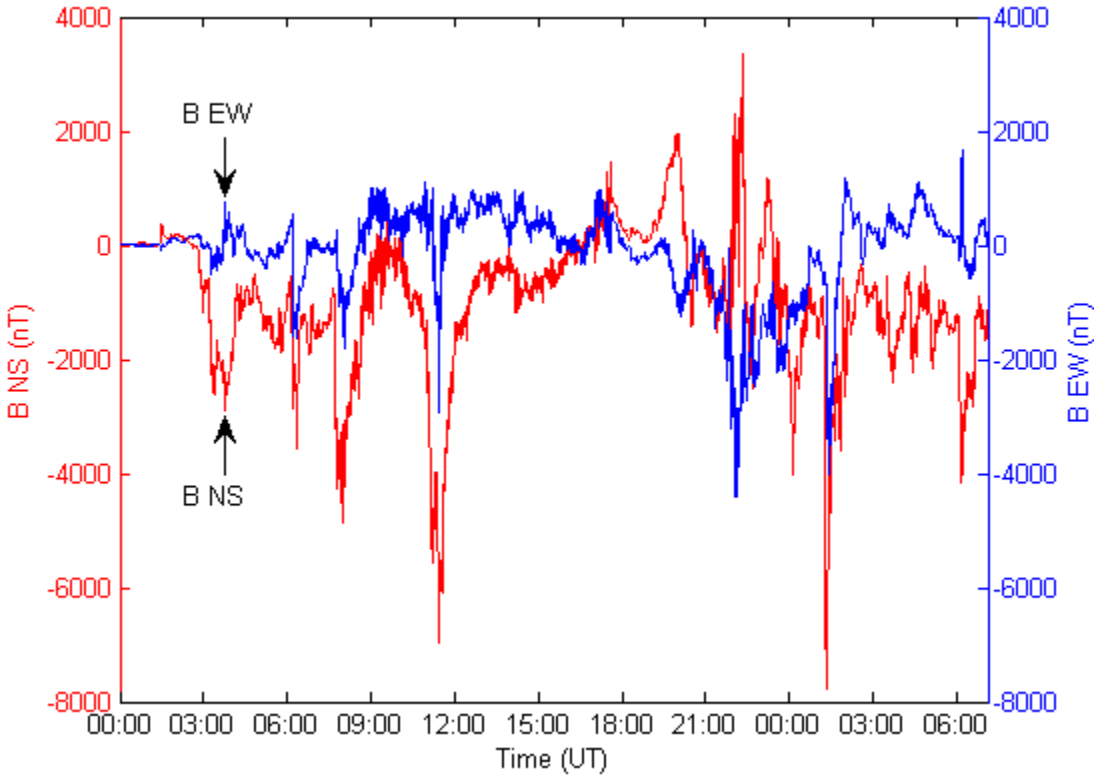

Figure 1: Benchmark Geomagnetic Field Waveshape
Red Bn (Northward), Blue Be (Eastward)
Referenced to pre-event quiet conditions

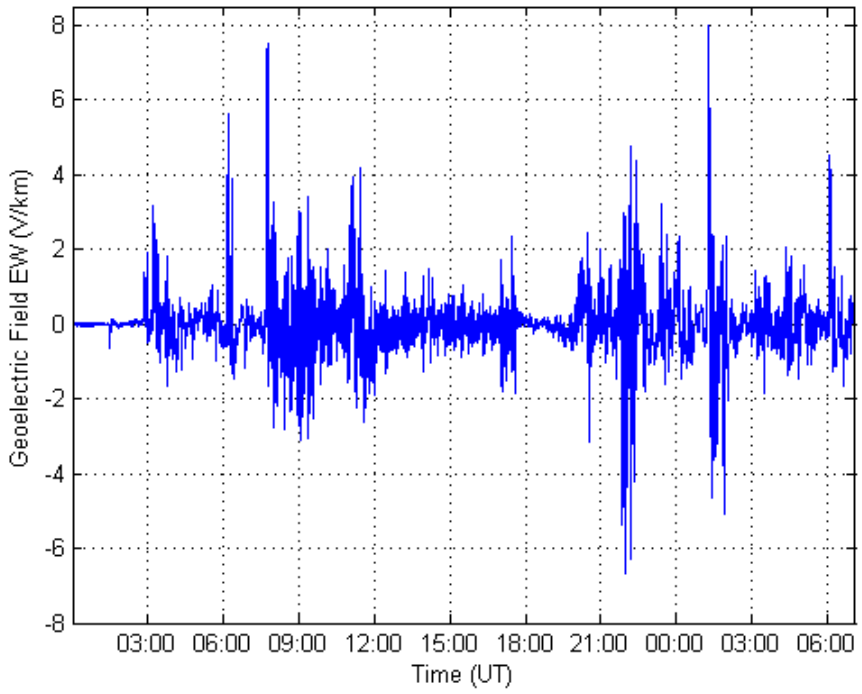

Figure 2: Benchmark Geoelectric Field Waveshape (E_E Eastward)

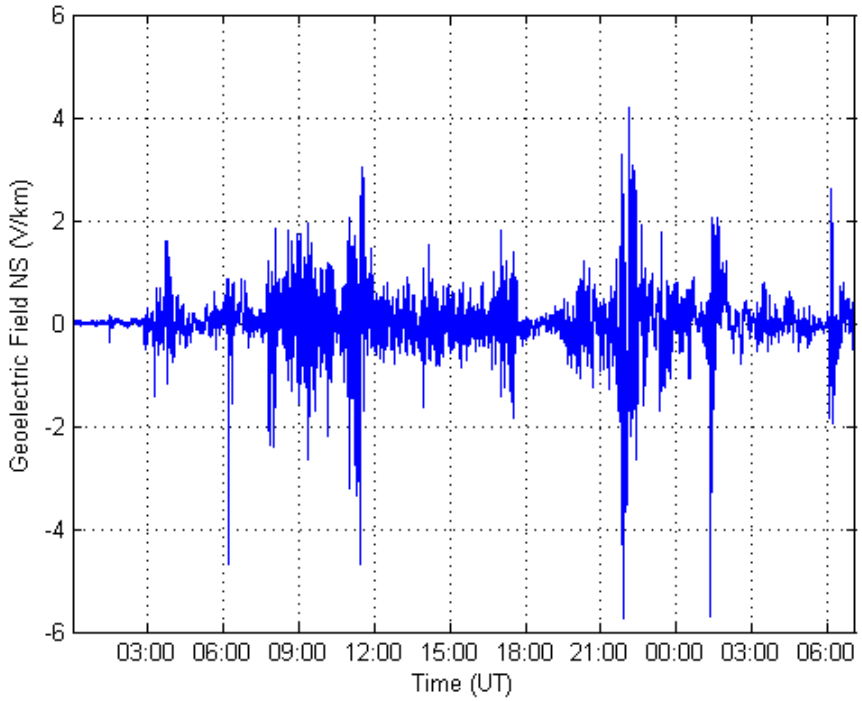

Figure 3: Benchmark Geoelectric Field Waveshape (E_N Northward)

Appendix I – Technical Considerations

The following sections describe the technical justification of the assumptions that were made in the development of the benchmark GMD event.

Statistical Considerations

Due to the lack of long-term accurate geomagnetic field observations, assigning probabilities to the occurrence of historical extreme geomagnetic storms is difficult because of the lack of high fidelity geomagnetic recordings of events prior to the 1980s. This is particularly true for the Carrington event for which data that allow the direct determination of the geoelectric fields experienced during the storm are not available [15].

The storm-time disturbance index Dst has often been used as a measure of storm strength even though it does not provide a direct correspondence with GIC[1]. One of the reasons for using Dst in statistical analysis is that Dst data are available for events occurring prior to 1980. Extreme value analysis of GMD events, including the Carrington, September 1859 and March 1989 events, has been carried out using Dst as an indicator of storm strength. In one such study [16], the (one sigma) range of 10-year occurrence probability for another March 1989 event was estimated to be between 9.4-27.8 percent. The range of 10-year occurrence probability for Carrington event in Love's analysis is 1.6-13.7 percent. These translate to occurrence rates of approximately 1 in 30-100 years for the March 1989 event and 1 in 70-600 years for the Carrington event. The error bars in such analysis are significant, however, it is reasonable to conclude that statistically the March 1989 event is likely more frequent than 1-in-100 years and the Carrington event is likely less frequent than 1-in-100 years.

The benchmark GMD event is based on a 1 in 100 year frequency of occurrence which is a conservative design basis for power systems. Also, the benchmark GMD event is not biased towards local geomagnetic field enhancements, since it must address wide-area effects in the interconnected power system. Therefore, the use of Dst-based statistical considerations is not adequate in this context and only relatively modern data have been used.

The benchmark GMD event is derived from modern geomagnetic field data records and corresponding calculated geoelectric field amplitudes. Using such data allows rigorous statistical analysis of the occurrence rates of the physical parameter (i.e. rate of change in geomagnetic field, dB/dt) directly related to the geoelectric field. Geomagnetic field measurements from the IMAGE magnetometer chain for 1993-2013 have been used to study the occurrence rates of the geoelectric field amplitudes.

With the use of modern data it is possible to avoid bias caused by localized geomagnetic field enhancements. The spatial structure of high-latitude geoelectric fields can be very complex during strong geomagnetic storm events [17]-[18]. One reflection of this spatial complexity is localized geomagnetic field enhancements that result in high amplitude geoelectric fields in regions of a few hundred kilometers or less. **Figure I-1**[2] illustrates this spatial complexity of the storm-time geoelectric fields. In areas indicated by the bright red location, the geoelectric field can be a factor of 2-3 larger than at neighboring locations. Localized geomagnetic phenomena should not be confused with local earth structure/conductivity features that result in consistently high geoelectric fields (e.g., coastal effects). Localized field enhancements can occur at any region exposed to auroral ionospheric electric current fluctuations.

[1] Dst index quantifies the amplitude of the main phase disturbance of a magnetic storm. The index is derived from magnetic field variations recorded at four low-latitude observatories. The data is combined to provide a measure of the average main-phase magnetic storm amplitude around the world.

[2] **Figure I-1** is for illustration purposes only, and is not meant to suggest that a particular area is more likely to experience a localized enhanced geoelectric field.

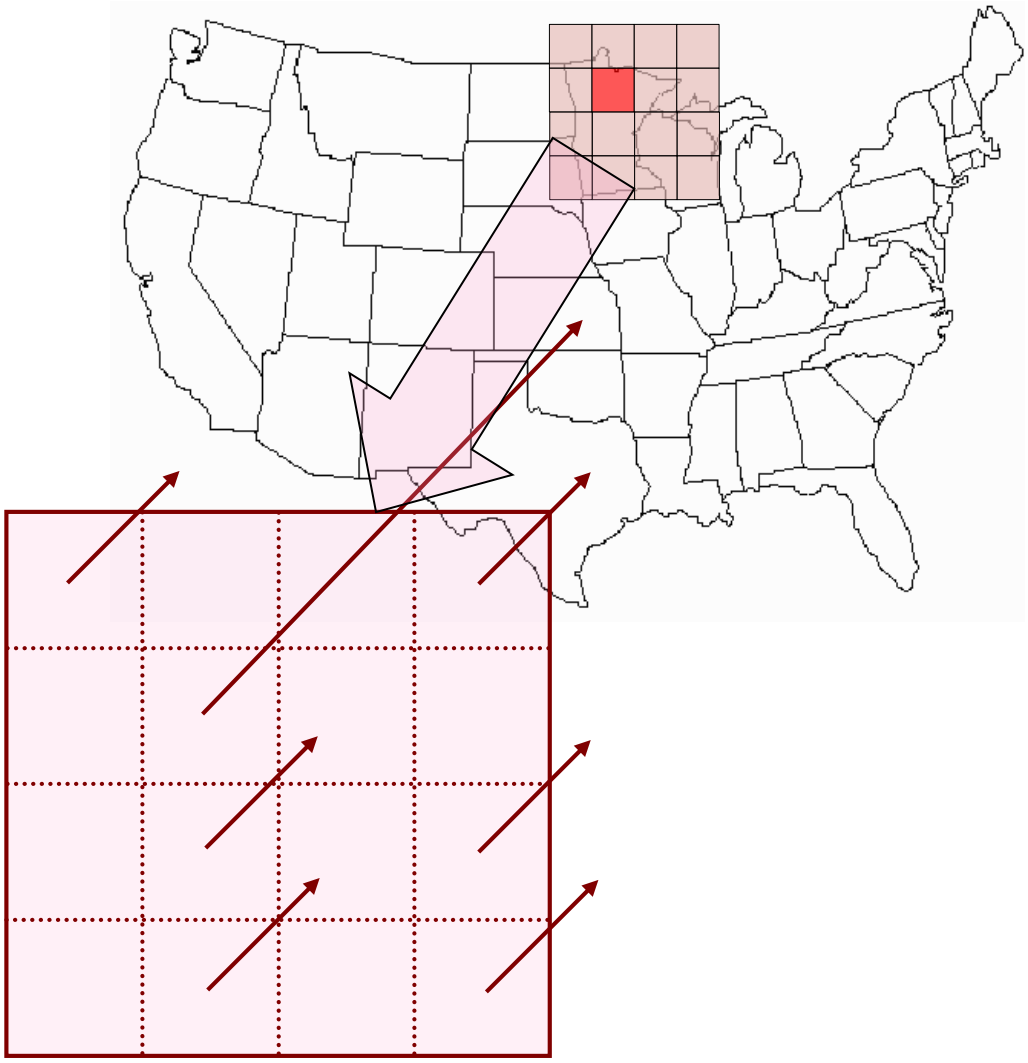

Figure I-1: Illustration of the Spatial Scale between Localized Enhancements and Larger Spatial Scale Amplitudes of Geoelectric Field Observed during a Strong Geomagnetic Storm.
In this illustration, the red square illustrates a spatially localized field enhancement.

The benchmark event is designed to address wide-area effects caused by a severe GMD event, such as increased var absorption and voltage depressions. Without characterizing GMD on regional scales, statistical estimates could be weighted by local effects and suggest unduly pessimistic conditions when considering cascading failure and voltage collapse. It is important to note that most earlier geoelectric field amplitude statistics and extreme amplitude analyses have been built for individual stations thus reflecting only localized spatial scales [10], [19]-[22]. A modified analysis is required to account for geoelectric field amplitudes at larger spatial scales. Consequently, analysis of spatially averaged geoelectric field amplitudes is presented below.

Figure I-2 shows statistical occurrence of spatially averaged high latitude geoelectric field amplitudes for the period of January 1, 1993 – December 31, 2013. The geoelectric field amplitudes were calculated using 10-s IMAGE magnetometer array observations and the Quebec ground conductivity model, which is used as a reference in the benchmark GMD event. Spatial averaging was carried out over four different station groups spanning a square area of approximately 500 km in width. For the schematic situation in **Figure I-1** the averaging process involves taking the average of the geoelectric field amplitudes over all 16 points or squares.

As can be seen from **Figure I-2**, the computed spatially averaged geoelectric field amplitude statistics indicate the 1-in-100 year amplitude is approximately between 3-8 V/km. Using extreme value analysis as described in the next section, it can be shown that the upper limit of the 95% confidence interval for a 100-year return level is more precisely 5.77 V/km.

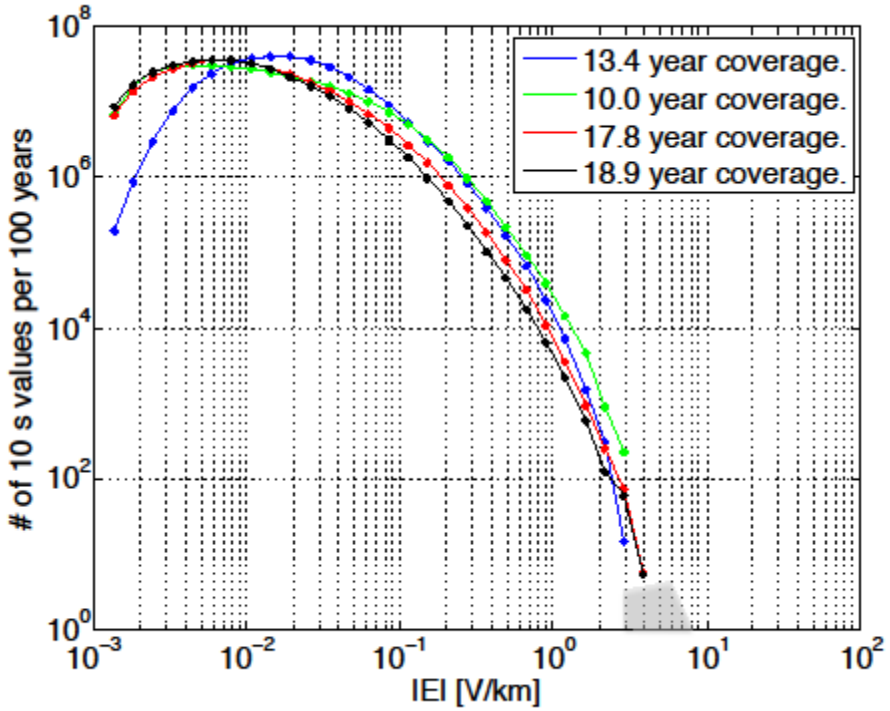

Figure I-2: Statistical Occurrence of Spatially Averaged Geoelectric Field Amplitudes.
Four curves with dots correspond to different station groups and the gray area shows a visual extrapolation to 1-in-100 year amplitudes. The legend shows the data coverage for each station group used in computing the averaged geoelectric field amplitudes.

Extreme Value Analysis

The objective of extreme value analysis is to describe the behavior of a stochastic process at extreme deviations from the median. In general, the intent is to quantify the probability of an event more extreme than any previously observed. In particular, we are concerned with estimating the 95 percent confidence interval of the maximum geoelectric field amplitude to be expected within a 100-year return period.[3] In the context of this document, extreme value analysis has been used to rigorously support the extrapolation estimates used in the statistical considerations of the previous section.

The data set consists of 21 years of daily maximum geoelectric field amplitudes derived from the IMAGE magnetometer chain, using the Quebec earth model as reference. **Figure I-3** shows a scatter plot of the 10-largest geoelectric field amplitudes per year across the IMAGE stations. The plot indicates that both the amplitude and standard deviation of extreme geoelectric fields are not independent of the solar cycle. The data clearly exhibits heteroskedasticity[4] and an 11-year seasonality in the mean.

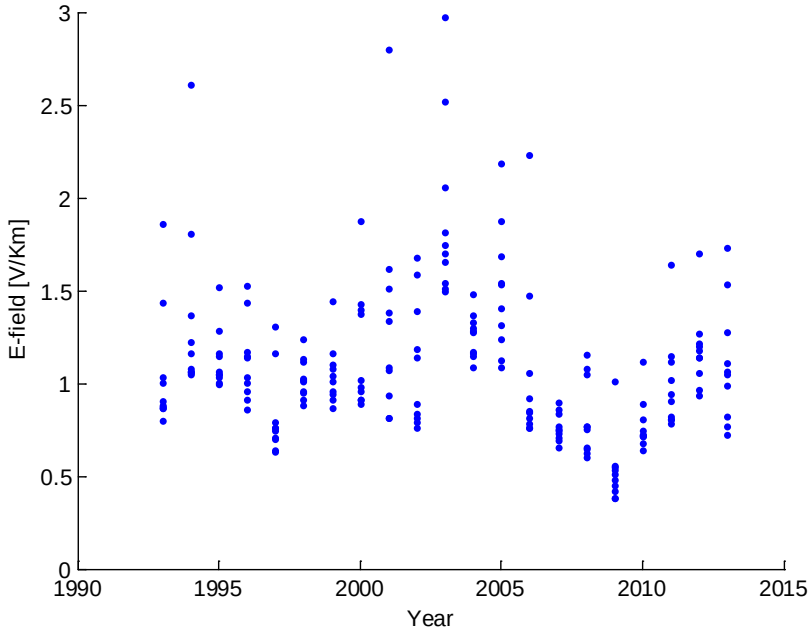

Figure I-3: Scatter Plot of Ten Largest Geoelectric Fields per Year

Data source: IMAGE magnetometer chain from 1993-2013

Several statistical methods can be used to conduct extreme value analysis. The most commonly applied include: Generalized Extreme Value (GEV), Point Over Threshold (POT), R-Largest, and Point Process (PP). In general, all methods assume independent and identically distributed (iid) data [23].

Two of these methods, GEV and POT, have been applied to the geoelectric field data, and their suitability for this application has been examined. **Table I-1** shows a summary of the estimated parameters and return levels obtained from GEV and POT methods. The parameters were estimated using the Maximum Likelihood Estimator (MLE). Since the distribution parameters do not have an intuitive interpretation, the expected geoelectric field amplitude for a 100-year return period is also included in **Table I-1.** The 95 percent confidence interval of the 100-year return level was calculated using the delta method and the profile likelihood. The delta method relies on the

[3] A 95 percent confidence interval means that, if repeated samples were obtained, the return level would lie within the confidence interval for 95 percent of the samples.

[4] Heteroskedasticity means that the skedastic function depends on the values of the conditioning variable; i.e., *var(Y|X=x) = f(x)*.

Gaussian approximation to the distribution of the MLE; this approximation can be poor for long return periods. In general, the profile likelihood provides a better description of the return level.

Table I-1: Extreme Value Analysis

Statistical Method	Estimated Parameters	Hypothesis Testing	100 Year Return Level Mean [V/km]	95% CI [V/km]	95% CI P-Likelihood [V/km]
(1) GEV	μ=1.4499 (0.1090) σ=0.4297 (0.0817) ξ=0.0305 (0.2011)	H0: ξ=0 p = 0.877	3.57	[1.77 , 5.36]	[2.71, 10.26]
(2) GEV $\mu = \beta_0 + \beta_1 \cdot \sin\left(\frac{t}{T} + \phi\right)$	β_0=1.5047 (0.0753) β_1=0.3722 (0.0740) σ=0.2894 (0.0600) ξ=0.1891 (0.2262)	H0: β_1=0 p= 0.0003 H0: ξ=0 p = 0.38	4	[2.64, 4.81]	[2.92, 12.33]
(3) POT, threshold=1V/km	σ=0.3163 (0.0382) ξ=0.0430 (0.0893)		3.4	[2.28, 4.52]	[2.72,5.64]
(4) POT, threshold=1V/km $\sigma = \alpha_0 + \alpha_1 \cdot \sin\left(\frac{t}{T} + \phi\right)$	α_0=0.2920 (0.0339) α_1=0.1660 (0.0368) ξ=-0.0308 (0.0826)	H0: α_1=0 p= 3.7e-5	3.724	[2.64, 4.81]	[3.02, 5.77]

Statistical model (1) in **Table I-1** is the traditional GEV estimation using blocks of 1 year maxima; i.e., only 21 data points are used in the estimation. The mean expected amplitude of the geolectric field for a 100-year return level is 3.57 V/km. Since GEV works with blocks of maxima, it is typically regarded as a wasteful approach. This is reflected in the comparatively large confidence intervals: [1.77, 5.36] V/km for the delta method and [2.71, 10.26] V/km for the profile likelihood.

As discussed previously, GEV assumes that the data is iid. Based on the scatter plot shown in **Figure 1-3**, the iid statistical assumption is not warranted by the data. Statistical model (2) in **Table I-1** is a re-parameterization of the GEV distribution contemplating the 11-year seasonality in the mean,

$$\mu = \beta_0 + \beta_1 \cdot \sin\left(\frac{t}{T} + \phi\right)$$

where β_0 represents the offset in the mean, β_1 describes the 11-year seasonality, T is the period (11 years), and ϕ is a constant phase shift.

A likelihood ratio test is used to test the hypothesis that β_1 is zero. The null hypothesis, H0: β_1=0, is rejected with a p-value of 0.0003; as expected, the 11-year seasonality has explanatory power. The blocks of maxima during the solar minimum are better represented in the re-parameterized GEV. The benefit is an increase in the mean return

level to 4 V/km and a wider confidence interval: [2.63, 4.81] V/km for the delta method and [2.92, 12.33] V/km for the profile likelihood (calculated at solar maximum).

Statistical model (3) in **Table I-1** is the traditional POT estimation using a threshold *u* of 1 V/km; the data was de-clustered using a 1-day run. The data set consists of normalized excesses over a threshold, and therefore, the sample size for POT is increased if more than one extreme observation per year is available (in the GEV approach, only the maximum observation over the year was taken; in the POT method, a single year can have multiple observations over the threshold). The selection of the threshold *u* is a compromise between bias and variance. The asymptotic basis of the model relies on a high threshold; a threshold that is too low will likely lead to bias. On the other hand, a threshold that is too high will reduce the sample size and result in high variance. The stability of parameter estimates can guide the selection of an appropriate threshold. **Figure I-4** shows the estimated parameters (modified scale $\sigma^*=\sigma_u-\xi\cdot u$, and shape ξ) for a range of thresholds. The objective is to select the lowest threshold for which the estimates remain near constant; 1V/km appears to be a good choice.

The mean return level for statistical model (3), 3.4 V/km, is similar to the GEV estimates. However, due to the larger sample size, the POT method is more efficient, and consequently, the confidence intervals are significantly reduced: [2.28, 4.52] V/km for the delta method, and [2.72, 5.64] V/km for the profile likelihood method.

In order to cope with the heteroskedasticity exhibited by the data, a re-parameterization of POT is used in statistical model (4) in **Table I-1**,

$$\sigma = \alpha_0 + \alpha_1 \cdot \sin\left(\frac{t}{T} + \phi\right)$$

where α_0 represents the offset in the standard deviation, α_1 describes the 11-year seasonality, *T* is the period ($365.25 \cdot 11$), and ϕ is a constant phase shift.

The parameter α_1 is statistically significant; the null hypothesis, H0: $\alpha_1=0$, is rejected with a p-value of 3.7e-5. The mean return level has slightly increased to 3.72 V/km. The upper limit of the confidence interval, calculated at solar maximum, also increases: [2.63, 4.81] V/km for the delta method and [3.02, 5.77] V/km for the profile likelihood method. As a final remark, it is emphasized that the confidence interval obtained using the profile likelihood is preferred over the delta method. **Figure I-5** shows the profile likelihood of the 100-year return level of statistical model (4). Note that the profile likelihood is highly asymmetric with a positive skew, rendering a larger upper limit for the confidence interval. Recall that the delta method assumes a normal distribution for the MLEs, and therefore, the confidence interval is symmetric around the mean.

To conclude, traditional GEV (1) and POT (3) models are misspecified; the statistical assumptions (iid) are not warranted by the data. The models were re-parameterized to cope with heteroskedasticity and the 11-year seasonality in the mean. Statistical model (4) better utilizes the available extreme measurements and it is therefore preferred over statistical model (2). The upper limit of the 95 percent confidence interval for a 100-year return level is 5.77 V/km. This analysis is consistent with the selection of a geoelectric field amplitude of 8 V/km for the 100-year GMD benchmark. .

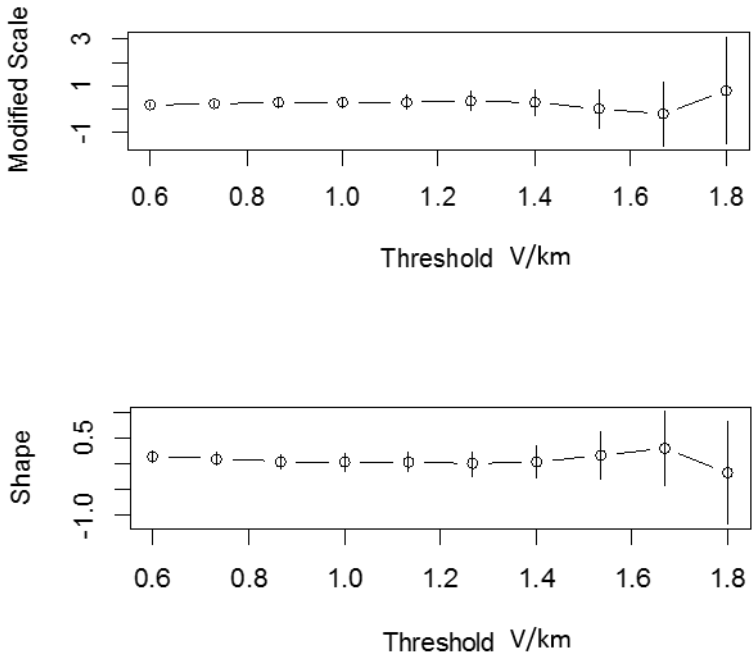

Figure I-4: Parameter Estimates Against Threshold for Statistical Model (3)

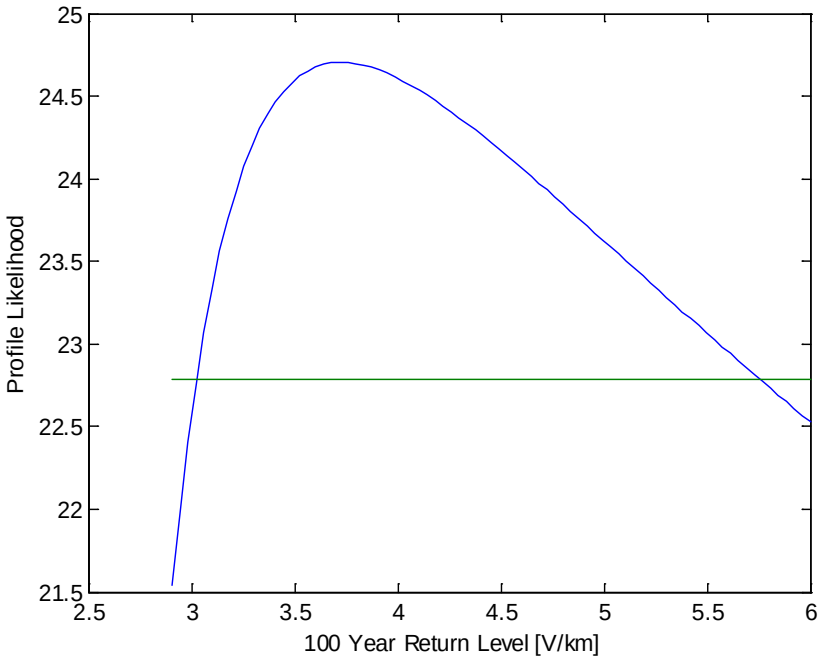

Figure I-5: Profile Likelihood for 100-year Return Level for Statistical Model (4)

Impact of Local Geomagnetic Disturbances on GIC

The impact of local disturbances on a power network is illustrated with the following example. A 500 km by 500 km section of a North American transmission network is subdivided into 100 km by 100 km sections. The geoelectric field is assumed to be uniform within each section. The analysis is performed by scaling the geoelectric field in each section individually by an intensification factor of 2.5 and computing the corresponding GIC flows in the network, resulting in a total of 25 GIC distribution simulations.[5] In these simulations the peak geomagnetic field amplitude has been scaled according to geomagnetic latitude of the network under study.

Figure I-6 shows the number of transformers that experience a GIC increase greater than 10 Amps (in red), those that experienced a reduction in GIC of more than 10 Amps (in blue), and those that remain essentially the same (in green). It can be observed that there is a small set of transformers that are affected by the local amplification of the geo-electric field but that the impact on the GIC distribution of the entire network due to a local intensification of the geoelectric field in a "local peak" is minor. Therefore, it can be concluded that the effect of local disturbances on the larger transmission system is relatively minor and does not warrant further consideration in network analysis.

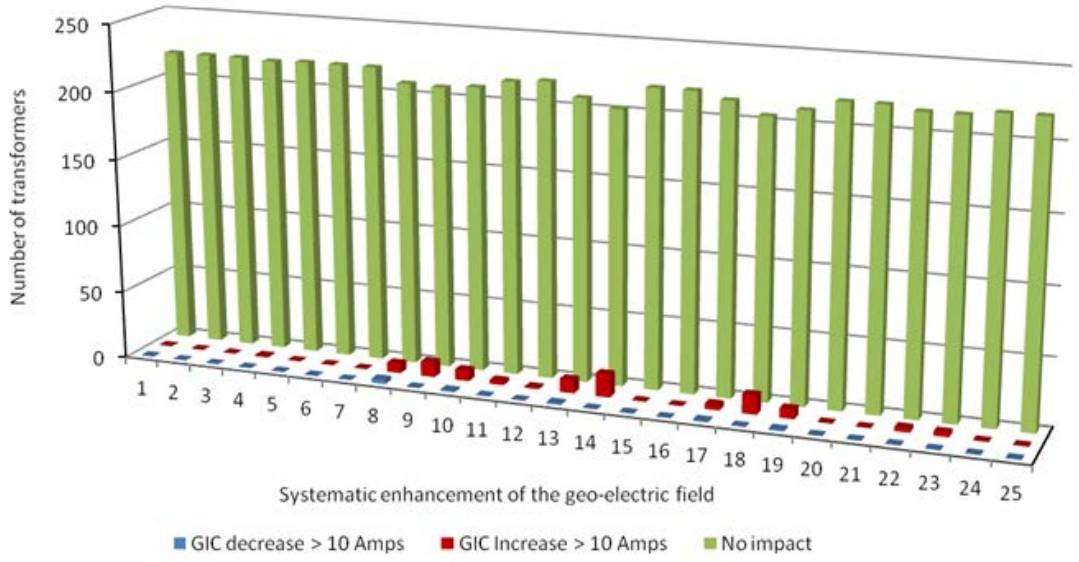

Figure I-6: Number of Transformers that see a 10 A/phase Change in GIC due to Local Geoelectric Field Intensification

Impact of Waveshape on Transformer Hot-spot Heating

Thermal effects (e.g. hot spot transformer heating) in power transformers are not instantaneous. Thermal time constants associated with hot spot heating in power transformers are in the 5-20 minute range; therefore, the waveshape of the geomagnetic and geoelectric field has a strong impact on transformer hot spot heating of windings and metallic parts since thermal time constants are of the same order of magnitude as the time-to-peak of storm maxima. The waveshape of the March 13-14 1989 GMD event measured at the Ottawa geomagnetic observatory was found to be a conservative choice when compared with other events of the last 20 years, such

[5] An intensification factor of 2.5 would make a general 8 V/km peak geoelectric field in the entire network show a 20 V/km intensified geoelectric field in one of the twenty five 100 km by 100 km sections.

as the measurements at the Nurmijarvi (NUR) and Memanbetsu (MMB) geomagnetic observatories for the "Halloween event" of October 29-31, 2003 described in the NERC GMD interim report of 2012 [14].

To illustrate, the results of a thermal analysis performed on a relatively large test network with a diverse mix of circuit lengths and orientations is provided in **Figures I-7** and **I-8**. **Figure I-9** shows a more systematic way to compare the relative effects of storm waveshape on the thermal response of a transformer. It shows the results of 33,000 thermal assessments for all combinations of effective GIC due to circuit orientation (similar **to Figures I-7** and **I-8** but systematically taking into account all possible circuit orientations). These results illustrate the relative effect of different waveshapes in a broad system setting and should not be interpreted as a vulnerability assessment of any particular network.

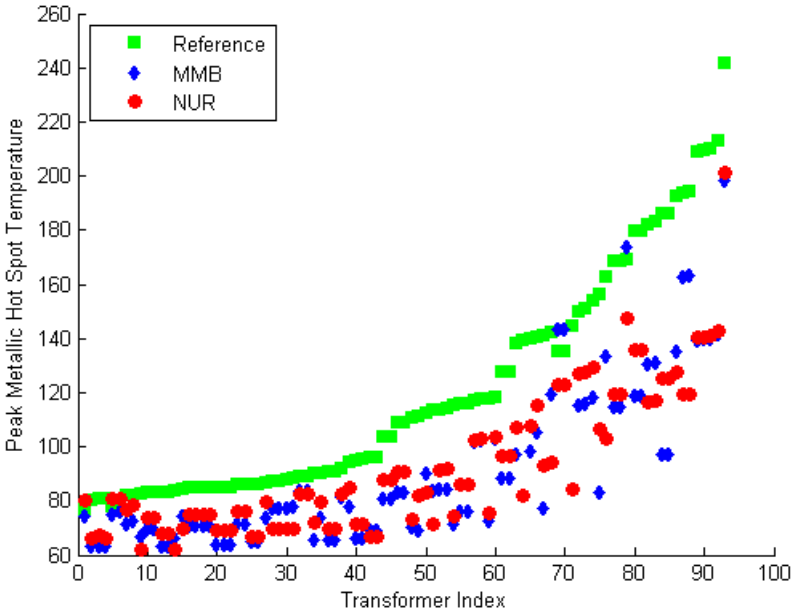

Figure I-7: Calculated Peak Metallic Hot Spot Temperature for All Transformers in a Test System with a Temperature Increase of More Than 20°C for Different GMD Events Scaled to the Same Peak Geoelectric Field

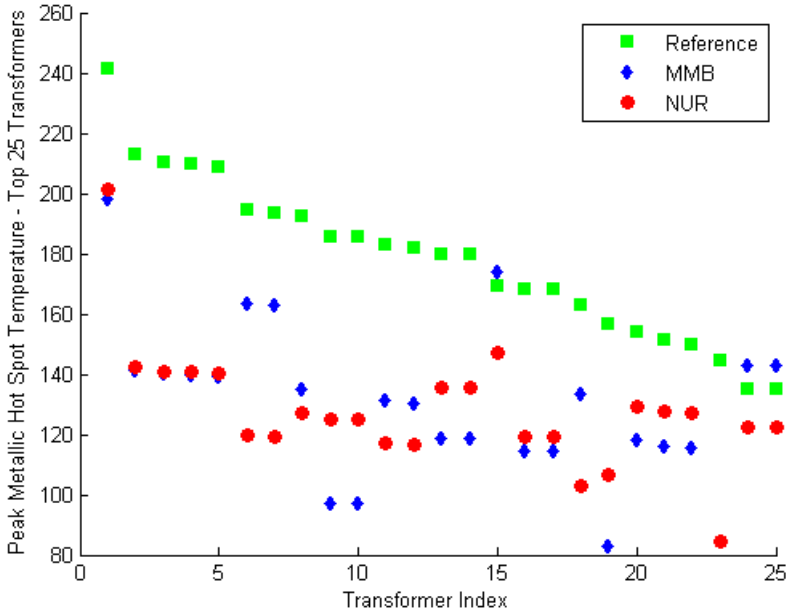

Figure I-8: Calculated Peak Metallic Hot Spot Temperature for the Top 25 Transformers in a Test System for Different GMD Events Scaled to the Same Peak Geoelectric Field

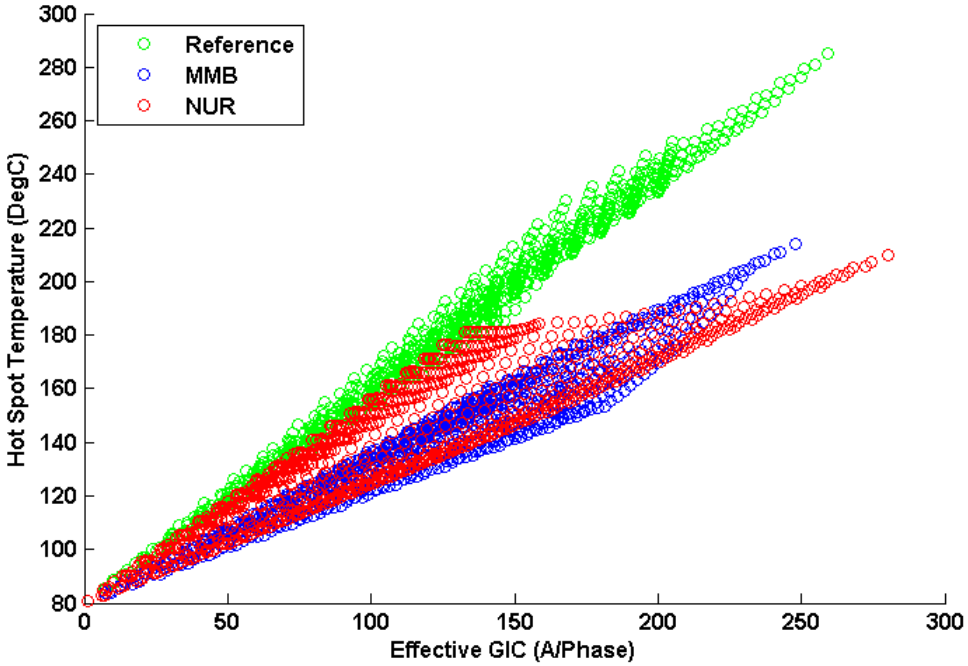

Figure I-9: Calculated Peak Metallic Hot Spot Temperature for all possible circuit orientations and effective GIC.

Appendix II – Scaling the Benchmark GMD Event

The intensity of a GMD event depends on geographical considerations such as geomagnetic latitude[6] and local earth conductivity[7] [3]**.** Scaling factors for geomagnetic latitude take into consideration that the intensity of a GMD event varies according to latitude-based geographical location. Scaling factors for earth conductivity take into account that the induced geoelectric field depends on earth conductivity, and that different parts of the continent have different earth conductivity and deep earth structure.

Scaling the Geomagnetic Field

The benchmark GMD event is defined for geomagnetic latitude of 60° and it must be scaled to account for regional differences based on geomagnetic latitude. To allow usage of the reference geomagnetic field waveshape in other locations, **Table II-1** summarizes the scaling factor α correlating peak geoelectric field to geomagnetic latitude as described in **Figure II-1** [3]. This scaling factor α has been obtained from a large number of global geomagnetic field observations of all major geomagnetic storms since the late 1980s [15], [24]-[25], and can be approximated with the empirical expression in (II.1)

$$\alpha = 0.001 \cdot e^{(0.115 \cdot L)} \qquad \text{(II.1)}$$

where L is the geomagnetic latitude in degrees and $0.1 \leq \alpha \leq 1.0$.

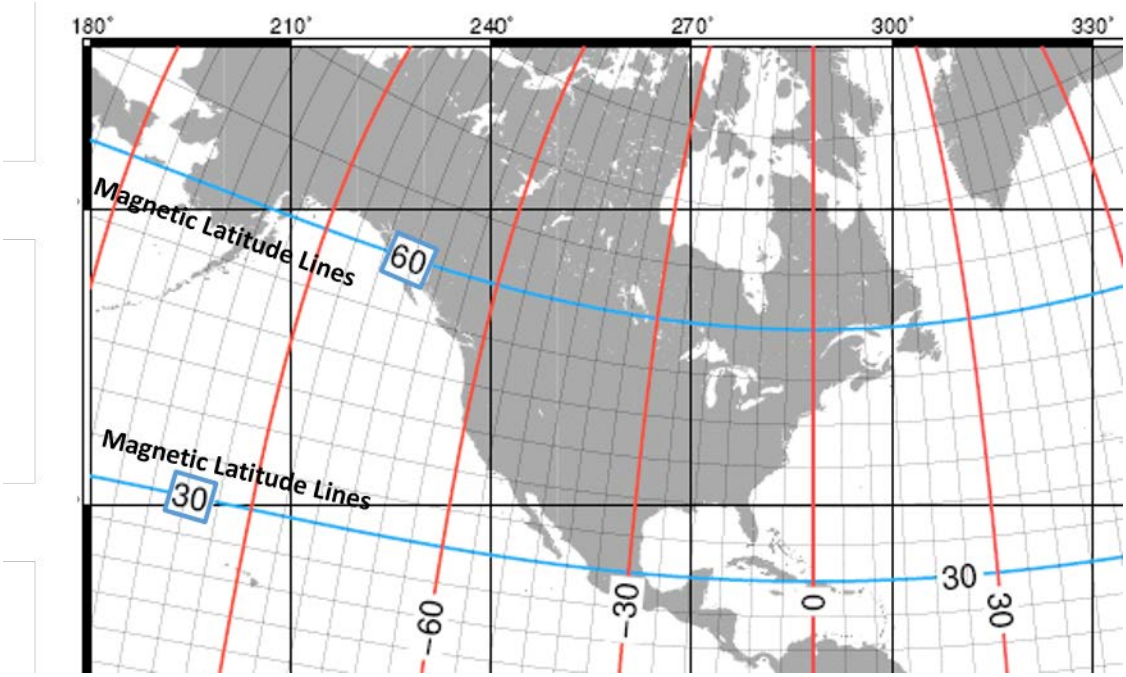

Figure II-1: Geomagnetic Latitude Lines in North America

[6] Geomagnetic latitude is analogous to geographic latitude, except that bearing is in relation to the magnetic poles, as opposed to the geographic poles. Geomagnetic phenomena are often best organized as a function of geomagnetic coordinates.

[7] Local earth conductivity refers to the electrical characteristics to depths of hundreds of km down to the earth's mantle. In general terms, lower ground conductivity results in higher geoelectric field amplitudes.

Table II-1: Geomagnetic Field Scaling Factors	
Geomagnetic Latitude (Degrees)	Scaling Factor1 (α)
≤ 40	0.10
45	0.2
50	0.3
54	0.5
56	0.6
57	0.7
58	0.8
59	0.9
≥ 60	1.0

Scaling the Geoelectric Field

The benchmark GMD event is defined for the reference Quebec earth model provided in **Table 1**. This earth model has been used in many peer-reviewed technical articles [12, 15]. The peak geoelectric field depends on the geomagnetic field waveshape and the local earth conductivity. Ideally, the peak geoelectric field, E_{peak}, is obtained by calculating the geoelectric field from the scaled geomagnetic waveshape using the plane wave method and taking the maximum value of the resulting waveforms

$$E_N = (z(t)/\mu_o) * B_E(t)$$
$$E_E = -(z(t)/\mu_o) * B_N(t) \qquad \text{(II.2)}$$
$$E_{peak} = \max\left\{\left|E_E(t), E_N(t)\right|\right\}$$

where,

* denotes convolution in the time domain,

z(t) is the impulse response for the earth surface impedance calculated from the laterally uniform or 1D earth model,

$B_E(t)$, $B_N(t)$ are the scaled Eastward and Northward geomagnetic field waveshapes,

$E_E(t)$, $E_N(t)|$ are the magnitudes of the calculated Eastward and Northward geoelectric field $E_E(t)$ and $E_N(t)$.

As noted previously, the response of the earth to B(t) (and dB/dt) is frequency dependent. **Figure II-2** shows the magnitude of Z(ω) for the reference earth model.

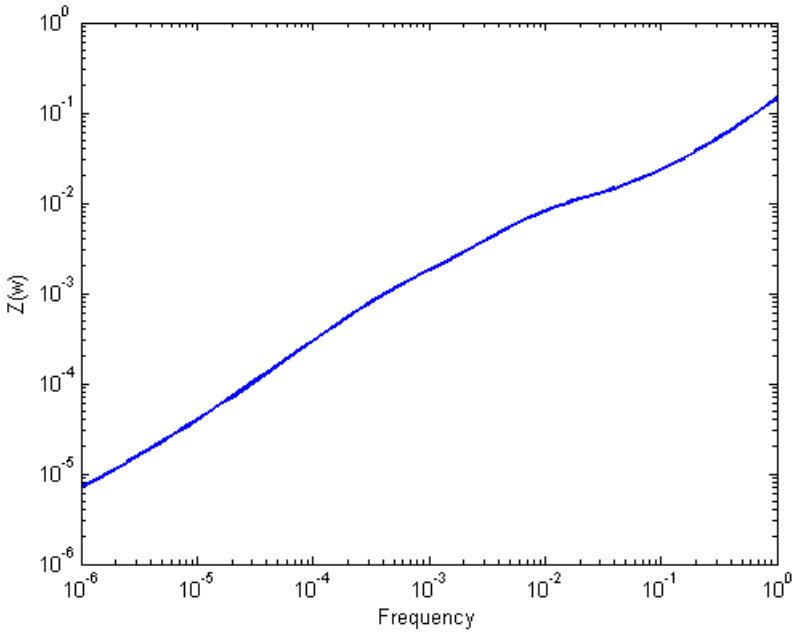

Figure II-2: Magnitude of the Earth Surface Impedance for the Reference Earth Model

If a utility does not have the capability of calculating the waveshape or time series for the geoelectric field, an earth conductivity scaling factor β can be obtained from **Table II-2**. Using α and β, the peak geoelectric field E_{peak} for a specific service territory shown in **Figure II-3** can be obtained using (II.3)

$$E_{peak} = 8 \times \alpha \times \beta \text{ (V/km)} \quad \text{(II.3)}$$

It should be noted that (II.3) is an approximation based on the following assumptions:

- The earth models used to calculate Table II-2 for the United States are from published information available on the USGS website.
- The models used to calculate Table II-2 for Canada were obtained from NRCan and reflect the average structure for large regions. When models are developed for sub-regions, there will be variance (to a greater or lesser degree) from the average model. For instance, detailed models for Ontario have been developed by NRCan and consist of seven major sub-regions.
- The conductivity scaling factor β is calculated as the quotient of the local geoelectric field peak amplitude in a physiographic region with respect to the reference peak amplitude value of 8 V/km. Both geoelectric field peaks amplitudes are calculated using the reference geomagnetic field time series. If a different geomagnetic field time series were used, the calculated scaling factors β would be different than the values in Table II-2 because the frequency content of storm maxima is, in principle, different for every storm. However, the reference time series produces generally more conservative values of β when compared to the time series of reference storm of the NERC interim report of 2012 [14], measurements at the Nurmijarvi (NUR) and Memanbetsu (MMB) geomagnetic observatories for the "Halloween event" of October 29-31, 2003, and other recordings of the March 1989 event at high latitudes (Meanook observatory, Canada). The average variation between minimum and maximum β is approximately 12 percent. **Figure II-4** illustrates the values of β calculated using the 10-second recordings for these geomagnetic field time series.
- If a utility has technically-sound earth models for its service territory and sub-regions thereof, then the use of such earth models is preferable to estimate E_{peak}.

- When a ground conductivity model is not available the planning entity should use the largest β factor of adjacent physiographic regions or a technically-justified value.

Physiographic Regions of the Continental United States

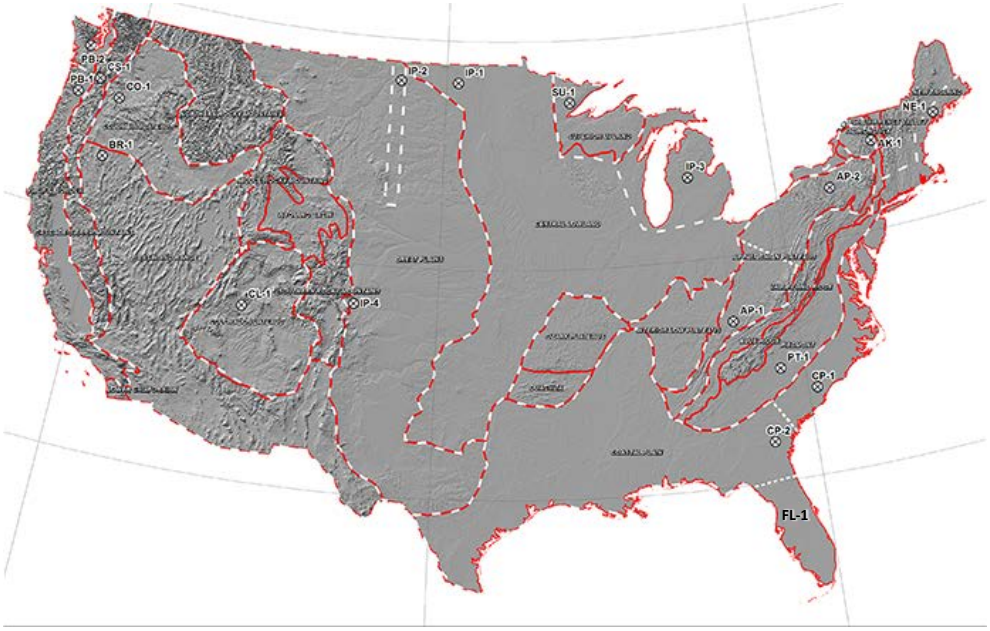

Physiographic Regions of Canada

Figure II-3: Physiographic Regions of North America

Table II-2 Geoelectric Field Scaling Factors	
USGS Earth model	Scaling Factor (β)
AK1A	0.56
AK1B	0.56
AP1	0.33
AP2	0.82
BR1	0.22
CL1	0.76
CO1	0.27
CP1	0.81
CP2	0.95
FL1	0.74
CS1	0.41
IP1	0.94
IP2	0.28
IP3	0.93
IP4	0.41
NE1	0.81
PB1	0.62
PB2	0.46
PT1	1.17
SL1	0.53
SU1	0.93
BOU	0.28
FBK	0.56
PRU	0.21
BC	0.67
PRAIRIES	0.96
SHIELD	1.0
ATLANTIC	0.79

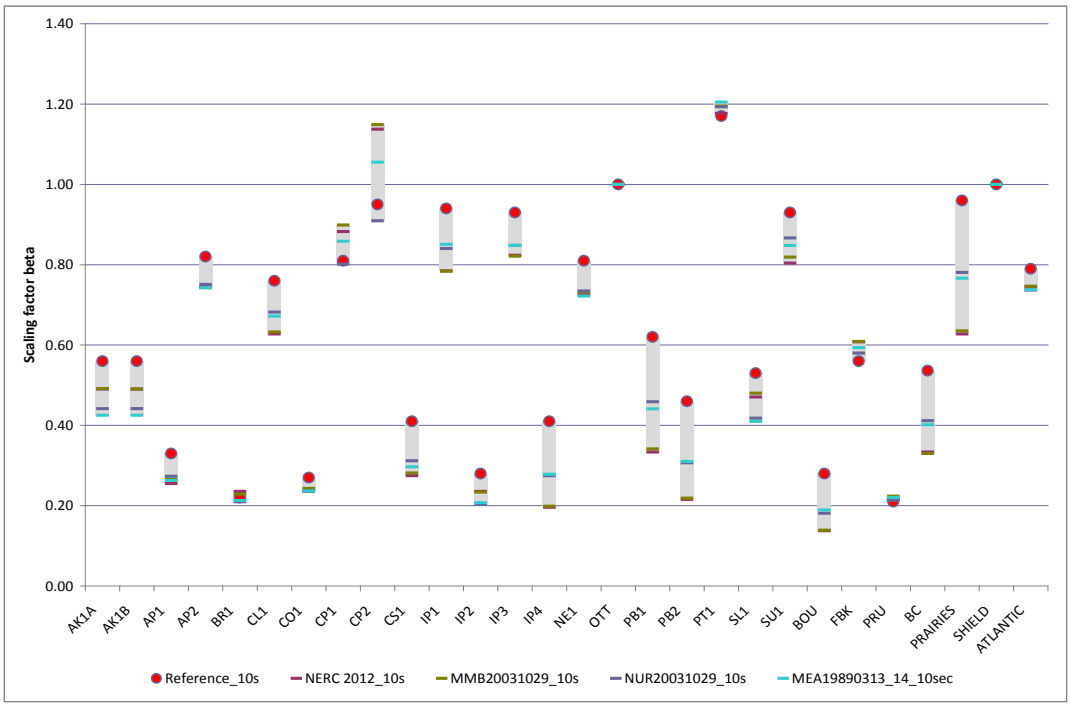

Figure II-4: Beta factors Calculated for Different GMD Events
Red circles correspond to the values in Table II-2

Example Calculations

Example 1

Consider a transmission service territory that lies in a geographical latitude of 45.5°, which translates to a geomagnetic latitude of 55°. The scaling factor α calculated using II.1 is 0.56; therefore, the benchmark waveshape and the peak geoelectric field will be scaled accordingly. If the service territory has the same earth conductivity as the benchmark then β=1, and the peak geoelectric field will be

$$\alpha = 0.56$$
$$\beta = 1.0$$
$$E_{peak} = 8 \times 0.56 \times 1 = 4.5 V/km$$

If the service territory spans more than one physiographic region (i.e. several locations within the service territory have a different earth model) then the largest α can be used across the entire service territory for conservative results. Alternatively, the network can be split into multiple subnetworks, and the corresponding geoelectric field amplitude can be applied to each subnetwork.

Example 2

Consider a service territory that lies in a geographical latitude of 45.5° which translates to a geomagnetic latitude of 55°. The scaling factor α calculated using II.1 is 0.56; therefore, the benchmark waveshape and the peak geoelectric field will be scaled accordingly.

The service territory has lower conductivity than the reference benchmark conductivity, therefore, according to the conductivity factor β from Table II-2., the calculation follows:

Conductivity factor β=1.17

$$\alpha = 0.56$$

$$E_{peak} = 8 \times 0.56 \times 1.17 = 5.2V / km$$

References

[1] L. Bolduc, A. Gaudreau, A. Dutil, "Saturation Time of Transformers Under dc Excitation", Electric Power Systems Research, 56 (2000), pp. 95-102

[2] *High-Impact, Low-Frequency Event Risk to the North American Bulk Power System*, A Jointly-Commissioned Summary Report of the North American Reliability Corporation and the U.S. Department of Energy's November 2009 Workshop.

[3] Application Guide: Computing Geomagnetically-Induced Current in the Bulk-Power System, NERC. NERC. http://www.nerc.com/comm/PC/Geomagnetic%20Disturbance%20Task%20Force%20GMDTF%202013/GIC%20Application%20Guide%202013_approved.pdf

[4] Kuan Zheng, Risto Pirjola, David Boteler, Lian-guang Liu, "Geoelectric Fields Due to Small-Scale and Large-Scale Source Currents", *IEEE Transactions on Power Delivery*, Vol. 28, No. 1, January 2013, pp. 442-449.

[5] Boteler, D. H. "Geomagnetically Induced Currents: Present Knowledge and Future Research", *IEEE Transactions on Power Delivery*, Vol. 9, No. 1, January 1994, pp. 50-58.

[6] Boteler, D. H. "Modeling Geomagnetically Induced Currents Produced by Realistic and Uniform Electric Fields", *IEEE Transactions on Power Delivery*, Vol. 13, No. 4, January 1998, pp. 1303-1308.

[7] J. L. Gilbert, W. A. Radasky, E. B. Savage, "A Technique for Calculating the Currents Induced by Geomagnetic Storms on Large High Voltage Power Grids", Electromagnetic Compatibility (EMC), 2012 IEEE International Symposium on.

[8] *How to Calculate Electric Fields to Determine Geomagnetically-Induced Currents.* EPRI, Palo Alto, CA: 2013. 3002002149.

[9] Pulkkinen, A., R. Pirjola, and A. Viljanen, Statistics of extreme geomagnetically induced current events, Space Weather, 6, S07001, doi:10.1029/2008SW000388, 2008.

[10] Boteler, D. H., Assessment of geomagnetic hazard to power systems in Canada, Nat. Hazards, 23, 101–120, 2001.

[11] Finnish Meteorological Institute's IMAGE magnetometer chain data available at: http://image.gsfc.nasa.gov/

[12] Boteler, D. H., and R. J. Pirjola, The complex-image method for calculating the magnetic and electric fields produced at the surface of the Earth by the auroral electrojet, Geophys. J. Int., 132(1), 31—40, 1998

[13] ANSI Standard C2, *National Electric Safety Code*, 2012, ISBN 978-0-7381-6588-2

[14] 2012 Special Reliability Assessment Interim Report: Effects of Geomagnetic Disturbances on the Bulk Power System. NERC. February 2012. http://www.nerc.com/pa/RAPA/ra/Reliability%20Assessments%20DL/2012GMD.pdf

[15] Pulkkinen, A., E. Bernabeu, J. Eichner, C. Beggan and A. Thomson, Generation of 100-year geomagnetically induced current scenarios, *Space Weather*, Vol. 10, S04003, doi:10.1029/2011SW000750, 2012.

[16] Love, J., Credible occurrence probabilities for extreme geophysical events: Earthquakes, volcanic eruptions, magnetic storms, Geophysical Research Letters, Vol. 39, L10301, doi:10.1029/2012GL051431, 2012.

[17] Pulkkinen, A., A. Thomson, E. Clarke, and A. Mckay, April 2000 geomagnetic storm: ionospheric drivers of large geomagnetically induced currents, Annales Geophysicae, 21, 709-717, 2003.

[18] Pulkkinen, A., S. Lindahl, A. Viljanen, and R. Pirjola, Geomagnetic storm of 29–31 October 2003: Geomagnetically induced currents and their relation to problems in the Swedish high-voltage power transmission system, Space Weather, 3, S08C03, doi:10.1029/2004SW000123, 2005.

[19] Pulkkinen, A., R. Pirjola, and A. Viljanen, Statistics of extreme geomagnetically induced current events, Space Weather, 6, S07001, doi:10.1029/2008SW000388, 2008.

[20] Langlois, P., L. Bolduc, and M. C. Chouteau, Probability of occurrence of geomagnetic storms based on a study of the distribution of the electric field amplitudes measured in Abitibi, Québec, in 1993–1994, J. Geomagn. Geoelectr., 48, 1033–1041, 1996.

[21] Pulkkinen, A., R. Pirjola, and A. Viljanen, Statistics of extreme geomagnetically induced current events, Space Weather, 6, S07001, doi:10.1029/2008SW000388, 2008.

[22] Campbell, W. C., Observation of electric currents in the Alaska oil pipeline resulting from auroral electrojet current sources, Geophys. J. R. Astron. Soc., 61, 437–449, 1980.

[23] Coles, Stuart (2001). An Introduction to Statistical Modelling of Extreme Values. Springer.

[24] Ngwira, C., A. Pulkkinen, F. Wilder, and G. Crowley, Extended study of extreme geoelectric field event scenarios for geomagnetically induced current applications, Space Weather, Vol. 11, 121–131, doi:10.1002/swe.20021, 2013.

[25] Thomson, A., S. Reay, and E. Dawson. Quantifying extreme behavior in geomagnetic activity, Space Weather, 9, S10001, doi:10.1029/2011SW000696, 2011.

NERC
NORTH AMERICAN ELECTRIC RELIABILITY CORPORATION

Benchmark Geomagnetic Disturbance Event Description

Project 2013-03 GMD Mitigation
Standard Drafting Team

~~December 5, 2014~~May 12, 2016

RELIABILITY | ACCOUNTABILITY

Table of Contents

Preface

The North American Electric Reliability Corporation (NERC) is a not-for-profit international regulatory authority whose mission is to ensure the reliability of the Bulk-Power System (BPS) in North America. NERC develops and enforces Reliability Standards; annually assesses seasonal and long-term reliability; monitors the BPS through system awareness; and educates, trains, and certifies industry personnel. NERC's area of responsibility spans the continental United States, Canada, and the northern portion of Baja California, Mexico. NERC is the electric reliability organization (ERO) for North America, subject to oversight by the Federal Energy Regulatory Commission (FERC) and governmental authorities in Canada. NERC's jurisdiction includes users, owners, and operators of the BPS, which serves more than 334 million people.

The North American BPS is divided into several assessment areas within the eight Regional Entity (RE) boundaries, as shown in the map and corresponding table below.

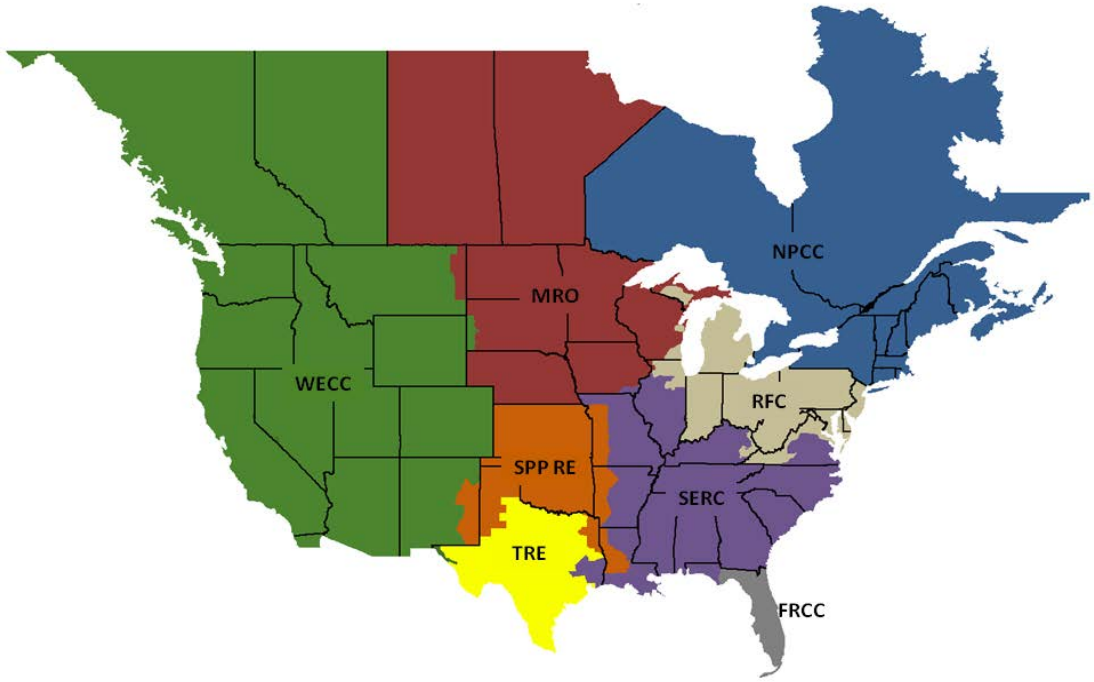

FRCC	Florida Reliability Coordinating Council
MRO	Midwest Reliability Organization
NPCC	Northeast Power Coordinating Council
RFC	Reliability*First* Corporation
SERC	SERC Reliability Corporation
SPP-RE	Southwest Power Pool Regional Entity
TRE	Texas Reliability Entity
WECC	Western Electric Coordinating Council

Introduction

Background

The purpose of the benchmark geomagnetic disturbance (GMD) event description is to provide a defined event for assessing system performance during a low probability, high magnitude GMD event as required by proposed standard TPL-007-1 – Transmission System Planned Performance for Geomagnetic Disturbance Events. The benchmark GMD event defines the geoelectric field values used to compute geomagnetically-induced current (GIC) flows for a GMD Vulnerability Assessment.

On May 16, 2013, FERC issued Order No. 779, directing NERC to develop Standards that address risks to reliability caused by geomagnetic disturbances in two stages:

- Stage 1 Standard(s) that require applicable entities to develop and implement Operating Procedures. EOP-010-1 – Geomagnetic Disturbance Operations was approved by FERC in June 2014.
- Stage 2 Standard(s) that require applicable entities to conduct assessments of the potential impact of benchmark GMD events on their systems. If the assessments identify potential impacts, the Standard(s) will require the applicable entity to develop and implement a plan to mitigate the risk.

TPL-007-1 is a new Reliability Standard developed to specifically address the Stage 2 directives in Order No. 779. The benchmark GMD event will define the scope of the Stage 2 Reliability Standard.

General Characteristics

The benchmark GMD event described herein takes into consideration the known characteristics of a severe GMD event and its impact on an interconnected transmission system. These characteristics include:

- Geomagnetic Latitude – The amplitude of the induced geoelectric field for a given GMD event is reduced as the observation point moves away from the earth's magnetic poles.
- Earth Conductivity – The amplitude and phase of the geoelectric field depends on the local or regional earth ground resistivity structure. Higher geoelectric field amplitudes are induced in areas of high resistivity.
- Transformer Electrical Response – Transformers can experience half-cycle saturation when subjected to GIC. Transformers under half-cycle saturation absorb increased amounts of reactive power (var) and inject harmonics into the system. However, half-cycle saturation does not occur instantaneously and depends on the electrical characteristics of the transformer and GIC amplitude [1]. Thus, the effects of transformer reactive power absorption and harmonic generation do not occur instantaneously, but instead may take up to several seconds. It is conservative, therefore, to assume that the effects of GIC on transformer var absorption and harmonic generation are instantaneous.
- Transformer Thermal Effects (e.g. hot spot transformer heating) – Heating of the winding and other structural parts can occur in power transformers during a GMD event. However, the thermal impacts are not instantaneous and are dependent on the thermal time constants of the transformer. Thermal time constants for hot spot heating in power transformers are in the 5-20 minute range.
- Geoelectric Field Waveshape – The geoelectric field waveshape has a strong influence on the hot spot heating of transformer windings and structural parts since thermal time constants of the transformer and time to peak of storm maxima are both on the order of minutes. The frequency content of the magnetic field (dB/dt) is a function of the waveshape, which in turn has a direct effect on the geoelectric field since the earth response to external dB/dt is frequency-dependent.
- Wide Area Geomagnetic Phenomena – The influence of GMD events is typically over a very broad area (e.g. continental scale); however, there can be pockets or very localized regions of enhanced geomagnetic activity. Since geomagnetic disturbance impacts within areas of influence of approximately 100-200 km do not have a widespread impact on the interconnected transmission system (see Appendix I), statistical methods used to assess the frequency of occurrence of a severe GMD event need to consider broad geographical regions to avoid bias caused by spatially localized geomagnetic phenomena.

Benchmark GMD Event Description

Severe geomagnetic disturbance events are high-impact, low-frequency (HILF) events [2]; thus, any benchmark event should consider the probability that the event will occur, as well as the impact or consequences of such an event. The benchmark event is composed of the following elements: 1) a reference peak geoelectric field amplitude (V/km) derived from statistical analysis of historical magnetometer data; 2) scaling factors to account for local geomagnetic latitude; 3) scaling factors to account for local earth conductivity; and 4) a reference geomagnetic field time series or waveshape to facilitate time-domain analysis of GMD impact on equipment.

Reference Geoelectric Field Amplitude

The reference geoelectric field amplitude was determined through statistical analysis using the plane wave method [3]-[10] geomagnetic field measurements from geomagnetic observatories in northern Europe [11] and the reference (Quebec) earth model shown in **Table 1** [12]. For details of the statistical considerations, see Appendix I. The Quebec earth model is generally resistive and the geological structure is relatively well understood.

Table 1: Reference earth model (Quebec)

Thickness (km)	Resistivity (Ω-m)
15	20,000
10	200
125	1,000
200	100
∞	3

The statistical analysis (see Appendix II) resulted in a conservative peak geoelectric field amplitude of approximately 8 V/km. For steady-state GIC and load flow analysis, the direction of the geoelectric field is assumed to be variable meaning that it can be in any direction (Eastward, Northward, or a vectorial combination thereof).

The frequency of occurrence of this benchmark GMD event is estimated to be approximately 1 in 100 years (see Appendix I). The selected frequency of occurrence is consistent with utility practices where a design basis frequency of 1 in 50 years is currently used as the storm return period for determining wind and ice loading of transmission infrastructure [13], for example.

The regional geoelectric field peak amplitude, E_{peak}, to be used in calculating GIC in the GIC system model can be obtained from the reference value of 8 V/km using the following relationship

$$E_{peak} = 8 \times \alpha \times \beta \text{ (V/km)} \quad (1)$$

where α is the scaling factor to account for local geomagnetic latitude, and β is a scaling factor to account for the local earth conductivity structure (see Appendix II).

Reference Geomagnetic Field Waveshape

The reference geomagnetic field waveshape was selected after analyzing a number of recorded GMD events, including the reference storm of the NERC interim report of 2012 [14], measurements at the Nurmijarvi (NUR) and Memanbetsu (MMB) geomagnetic observatories for the "Halloween event" of October 29-31, 2003, and the March 1989 GMD event that caused the Hydro Quebec blackout. The geomagnetic field measurement record of the March 13-14 1989 GMD event, measured at NRCan's Ottawa geomagnetic observatory, was selected as the

reference geomagnetic field waveform because it provides generally conservative results when performing thermal analysis of power transformers (see Appendix I). The reference geomagnetic field waveshape is used to calculate the GIC time series, GIC(t), required for transformer thermal impact assessment.

The geomagnetic latitude of the Ottawa geomagnetic observatory is 55°; therefore, the amplitude of the geomagnetic field measurement data were scaled up to the 60° reference geomagnetic latitude (see **Figure 1**) such that the resulting peak geoelectric field amplitude computed using the reference earth model was 8 V/km (see **Figures 2** and **3**). Sampling rate for the geomagnetic field waveshape is 10 seconds.

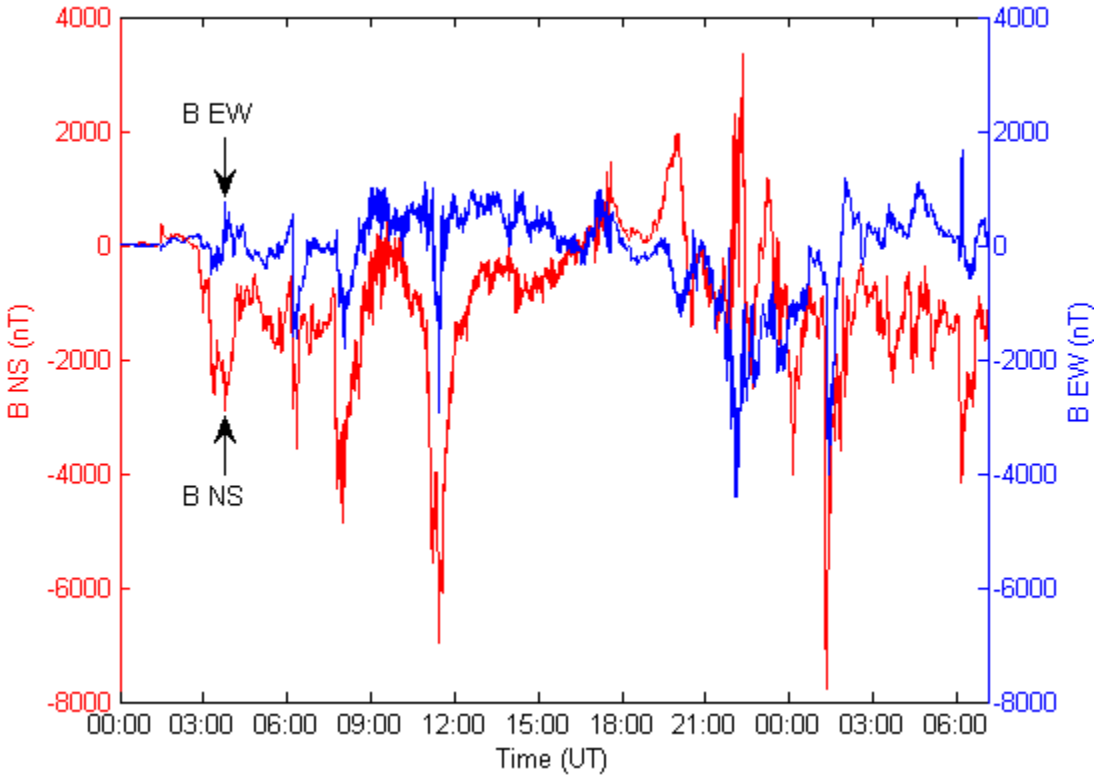

Figure 1: Benchmark Geomagnetic Field Waveshape
Red Bn (Northward), Blue Be (Eastward)
Referenced to pre-event quiet conditions

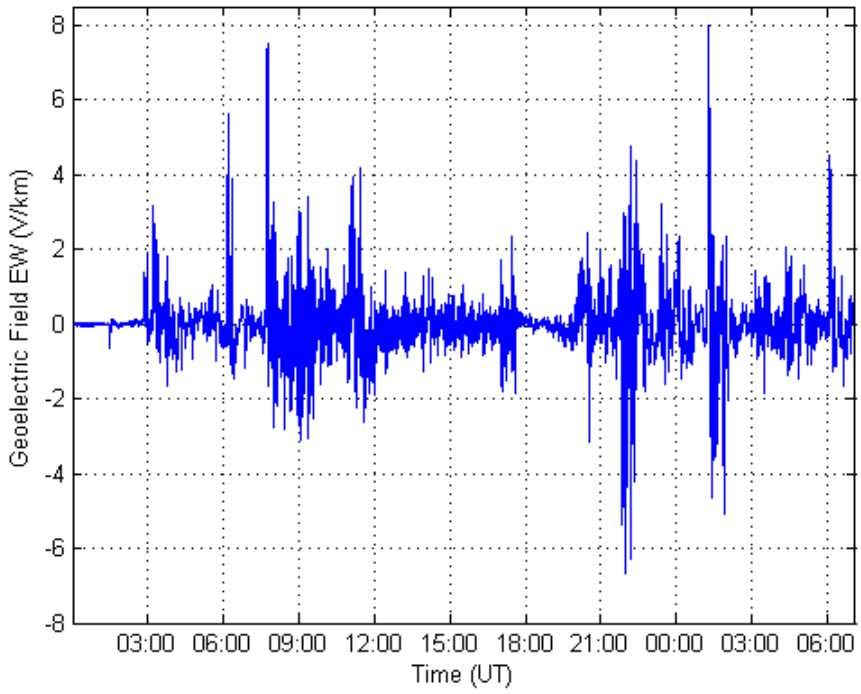

Figure 2: Benchmark Geoelectric Field Waveshape (E_E Eastward)

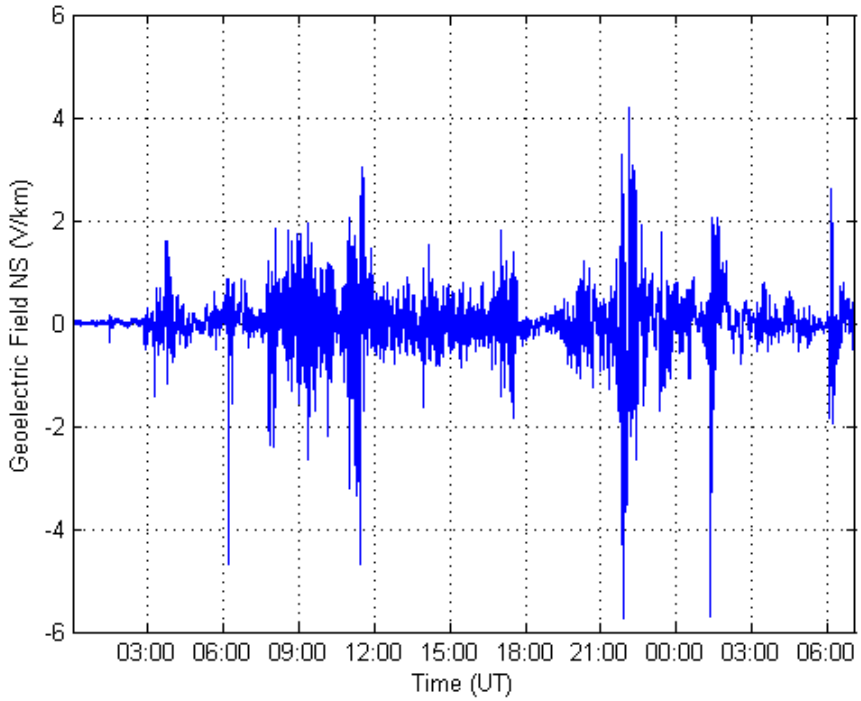

Figure 3: Benchmark Geoelectric Field Waveshape (E_N Northward)

Appendix I – Technical Considerations

The following sections describe the technical justification of the assumptions that were made in the development of the benchmark GMD event.

Statistical Considerations

Due to the lack of long-term accurate geomagnetic field observations, assigning probabilities to the occurrence of historical extreme geomagnetic storms is difficult because of the lack of high fidelity geomagnetic recordings of events prior to the 1980s. This is particularly true for the Carrington event for which data that allow the direct determination of the geoelectric fields experienced during the storm are not available [15].

The storm-time disturbance index Dst has often been used as a measure of storm strength even though it does not provide a direct correspondence with GIC[1]. One of the reasons for using Dst in statistical analysis is that Dst data are available for events occurring prior to 1980. Extreme value analysis of GMD events, including the Carrington, September 1859 and March 1989 events, has been carried out using Dst as an indicator of storm strength. In one such study [16], the (one sigma) range of 10-year occurrence probability for another March 1989 event was estimated to be between 9.4-27.8 percent. The range of 10-year occurrence probability for Carrington event in Love's analysis is 1.6-13.7 percent. These translate to occurrence rates of approximately 1 in 30-100 years for the March 1989 event and 1 in 70-600 years for the Carrington event. The error bars in such analysis are significant, however, it is reasonable to conclude that statistically the March 1989 event is likely more frequent than 1-in-100 years and the Carrington event is likely less frequent than 1-in-100 years.

The benchmark GMD event is based on a 1 in 100 year frequency of occurrence which is a conservative design basis for power systems. Also, the benchmark GMD event is not biased towards local geomagnetic field enhancements, since it must address wide-area effects in the interconnected power system. Therefore, the use of Dst-based statistical considerations is not adequate in this context and only relatively modern data have been used.

The benchmark GMD event is derived from modern geomagnetic field data records and corresponding calculated geoelectric field amplitudes. Using such data allows rigorous statistical analysis of the occurrence rates of the physical parameter (i.e. rate of change in geomagnetic field, dB/dt) directly related to the geoelectric field. Geomagnetic field measurements from the IMAGE magnetometer chain for 1993-2013 have been used to study the occurrence rates of the geoelectric field amplitudes.

With the use of modern data it is possible to avoid bias caused by localized geomagnetic field enhancements. The spatial structure of high-latitude geoelectric fields can be very complex during strong geomagnetic storm events [17]-[18]. One reflection of this spatial complexity is localized geomagnetic field enhancements that result in high amplitude geoelectric fields in regions of a few hundred kilometers or less. **Figure I-1**[2] illustrates this spatial complexity of the storm-time geoelectric fields. In areas indicated by the bright red location, the geoelectric field can be a factor of 2-3 larger than at neighboring locations. Localized geomagnetic phenomena should not be confused with local earth structure/conductivity features that result in consistently high geoelectric fields (e.g., coastal effects). Localized field enhancements can occur at any region exposed to auroral ionospheric electric current fluctuations.

[1] Dst index quantifies the amplitude of the main phase disturbance of a magnetic storm. The index is derived from magnetic field variations recorded at four low-latitude observatories. The data is combined to provide a measure of the average main-phase magnetic storm amplitude around the world.

[2] **Figure I-1** is for illustration purposes only, and is not meant to suggest that a particular area is more likely to experience a localized enhanced geoelectric field.

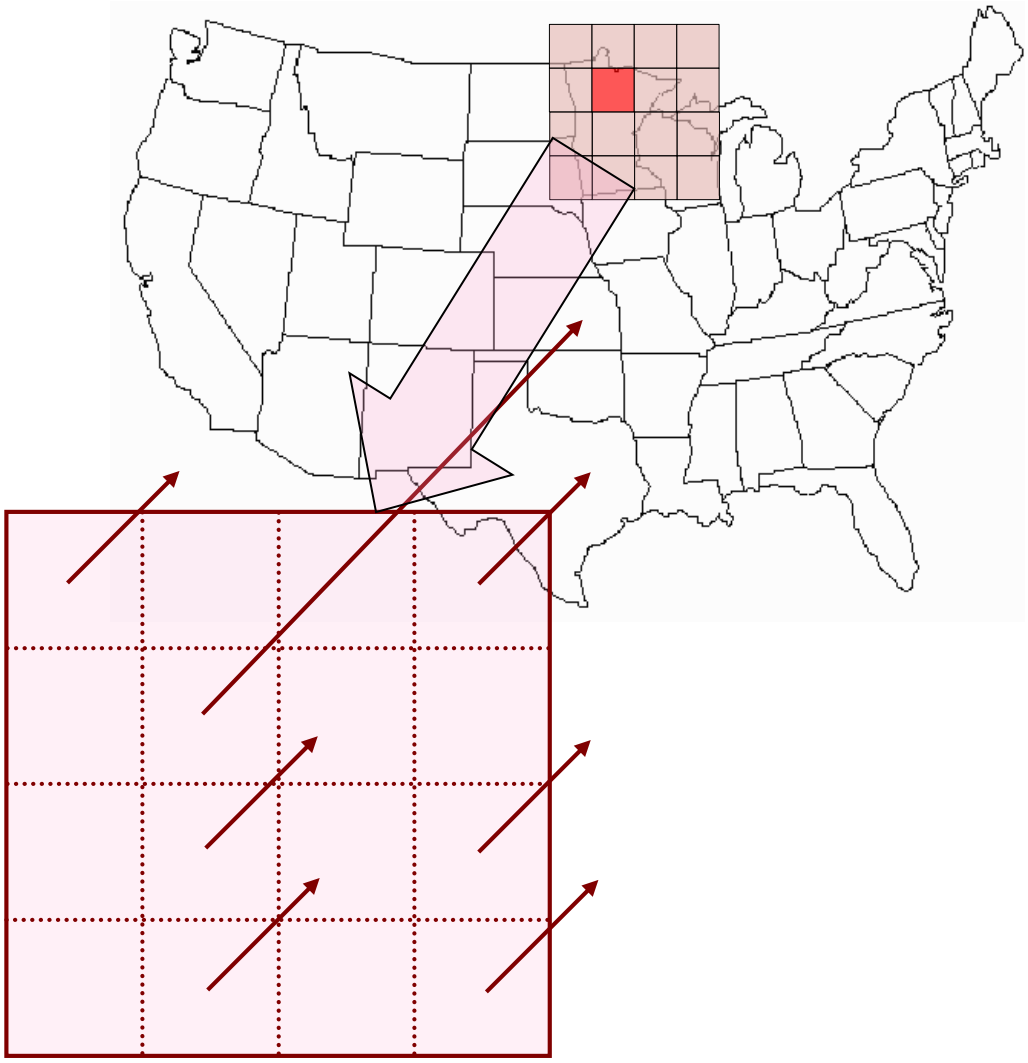

Figure I-1: Illustration of the Spatial Scale between Localized Enhancements and Larger Spatial Scale Amplitudes of Geoelectric Field Observed during a Strong Geomagnetic Storm.
In this illustration, the red square illustrates a spatially localized field enhancement.

The benchmark event is designed to address wide-area effects caused by a severe GMD event, such as increased var absorption and voltage depressions. Without characterizing GMD on regional scales, statistical estimates could be weighted by local effects and suggest unduly pessimistic conditions when considering cascading failure and voltage collapse. It is important to note that most earlier geoelectric field amplitude statistics and extreme amplitude analyses have been built for individual stations thus reflecting only localized spatial scales [10], [19]-[22]. A modified analysis is required to account for geoelectric field amplitudes at larger spatial scales. Consequently, analysis of spatially averaged geoelectric field amplitudes is presented below.

Figure I-2 shows statistical occurrence of spatially averaged high latitude geoelectric field amplitudes for the period of January 1, 1993 – December 31, 2013. The geoelectric field amplitudes were calculated using 10-s IMAGE magnetometer array observations and the Quebec ground conductivity model, which is used as a reference in the benchmark GMD event. Spatial averaging was carried out over four different station groups spanning a square area of approximately 500 km in width. For the schematic situation in **Figure I-1** the averaging process involves taking the average of the geoelectric field amplitudes over all 16 points or squares.

As can be seen from **Figure I-2**, the computed spatially averaged geoelectric field amplitude statistics indicate the 1-in-100 year amplitude is approximately between 3-8 V/km. Using extreme value analysis as described in the next section, it can be shown that the upper limit of the 95% confidence interval for a 100-year return level is more precisely 5.77 V/km.

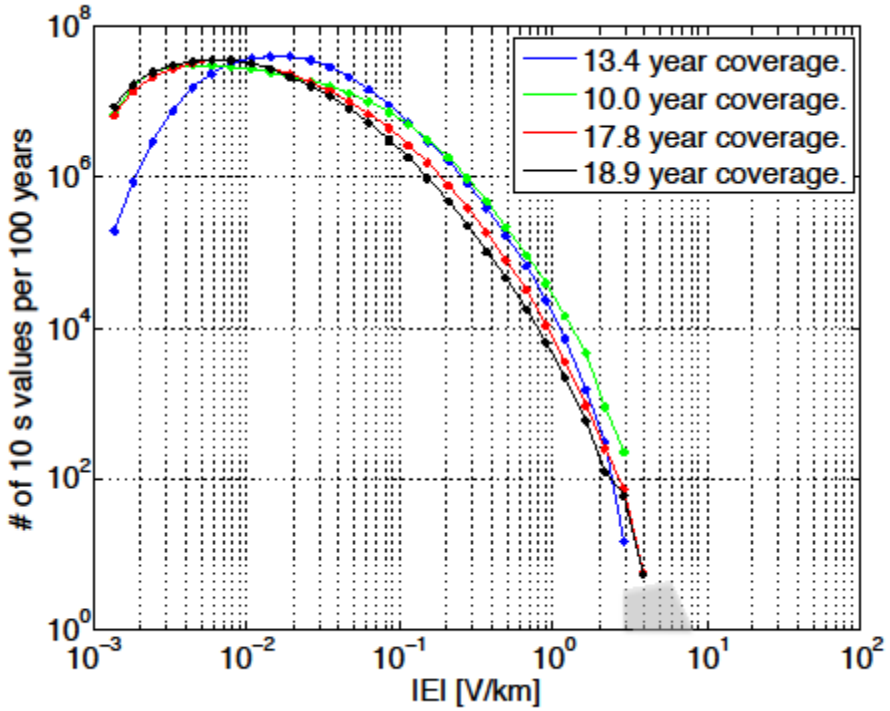

Figure I-2: Statistical Occurrence of Spatially Averaged Geoelectric Field Amplitudes.
Four curves with dots correspond to different station groups and the gray area shows a visual extrapolation to 1-in-100 year amplitudes. The legend shows the data coverage for each station group used in computing the averaged geoelectric field amplitudes.

Extreme Value Analysis

The objective of extreme value analysis is to describe the behavior of a stochastic process at extreme deviations from the median. In general, the intent is to quantify the probability of an event more extreme than any previously observed. In particular, we are concerned with estimating the 95 percent confidence interval of the maximum geoelectric field amplitude to be expected within a 100-year return period.[3] In the context of this document, extreme value analysis has been used to rigorously support the extrapolation estimates used in the statistical considerations of the previous section.

The data set consists of 21 years of daily maximum geoelectric field amplitudes derived from the IMAGE magnetometer chain, using the Quebec earth model as reference. **Figure I-3** shows a scatter plot of the 10-largest geoelectric field amplitudes per year across the IMAGE stations. The plot indicates that both the amplitude and standard deviation of extreme geoelectric fields are not independent of the solar cycle. The data clearly exhibits heteroskedasticity[4] and an 11-year seasonality in the mean.

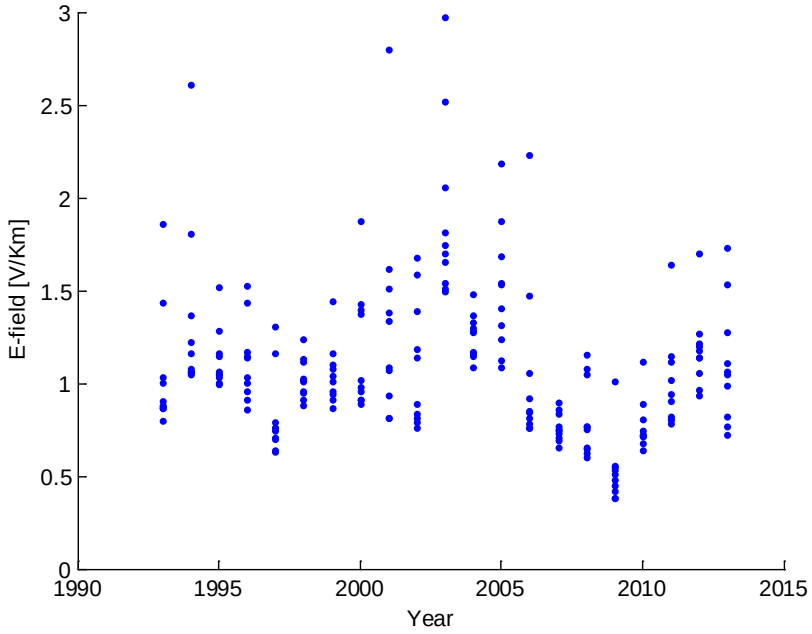

Figure I-3: Scatter Plot of Ten Largest Geoelectric Fields per Year

Data source: IMAGE magnetometer chain from 1993-2013

Several statistical methods can be used to conduct extreme value analysis. The most commonly applied include: Generalized Extreme Value (GEV), Point Over Threshold (POT), R-Largest, and Point Process (PP). In general, all methods assume independent and identically distributed (iid) data [23].

Two of these methods, GEV and POT, have been applied to the geoelectric field data, and their suitability for this application has been examined. **Table I-1** shows a summary of the estimated parameters and return levels obtained from GEV and POT methods. The parameters were estimated using the Maximum Likelihood Estimator (MLE). Since the distribution parameters do not have an intuitive interpretation, the expected geoelectric field amplitude for a 100-year return period is also included in **Table I-1.** The 95 percent confidence interval of the 100-year return level was calculated using the delta method and the profile likelihood. The delta method relies on the

[3] A 95 percent confidence interval means that, if repeated samples were obtained, the return level would lie within the confidence interval for 95 percent of the samples.

[4] Heteroskedasticity means that the skedastic function depends on the values of the conditioning variable; i.e., *var(Y|X=x) = f(x)*.

Gaussian approximation to the distribution of the MLE; this approximation can be poor for long return periods. In general, the profile likelihood provides a better description of the return level.

Table I-1: Extreme Value Analysis

Statistical Method	Estimated Parameters	Hypothesis Testing	100 Year Return Level Mean [V/km]	95% CI [V/km]	95% CI P-Likelihood [V/km]
(1) GEV	μ=1.4499 (0.1090) σ=0.4297 (0.0817) ξ=0.0305 (0.2011)	H0: ξ=0 p = 0.877	3.57	[1.77 , 5.36]	[2.71, 10.26]
(2) GEV $\mu = \beta_0 + \beta_1 \cdot \sin\left(\frac{t}{T} + \phi\right)$	β_0=1.5047 (0.0753) β_1=0.3722 (0.0740) σ=0.2894 (0.0600) ξ=0.1891 (0.2262)	H0: β_1=0 p= 0.0003 H0: ξ=0 p = 0.38	4	[2.64, 4.81]	[2.92, 12.33]
(3) POT, threshold=1V/km	σ=0.3163 (0.0382) ξ=0.0430 (0.0893)		3.4	[2.28, 4.52]	[2.72,5.64]
(4) POT, threshold=1V/km $\sigma = \alpha_0 + \alpha_1 \cdot \sin\left(\frac{t}{T} + \phi\right)$	α_0=0.2920 (0.0339) α_1=0.1660 (0.0368) ξ=-0.0308 (0.0826)	H0: α_1=0 p= 3.7e-5	3.724	[2.64, 4.81]	[3.02, 5.77]

Statistical model (1) in **Table I-1** is the traditional GEV estimation using blocks of 1 year maxima; i.e., only 21 data points are used in the estimation. The mean expected amplitude of the geolectric field for a 100-year return level is 3.57 V/km. Since GEV works with blocks of maxima, it is typically regarded as a wasteful approach. This is reflected in the comparatively large confidence intervals: [1.77, 5.36] V/km for the delta method and [2.71, 10.26] V/km for the profile likelihood.

As discussed previously, GEV assumes that the data is iid. Based on the scatter plot shown in **Figure 1-3**, the iid statistical assumption is not warranted by the data. Statistical model (2) in **Table I-1** is a re-parameterization of the GEV distribution contemplating the 11-year seasonality in the mean,

$$\mu = \beta_0 + \beta_1 \cdot \sin\left(\frac{t}{T} + \phi\right)$$

where β_0 represents the offset in the mean, β_1 describes the 11-year seasonality, *T* is the period (11 years), and ϕ is a constant phase shift.

A likelihood ratio test is used to test the hypothesis that β_1 is zero. The null hypothesis, H0: β_1=0, is rejected with a p-value of 0.0003; as expected, the 11-year seasonality has explanatory power. The blocks of maxima during the solar minimum are better represented in the re-parameterized GEV. The benefit is an increase in the mean return

level to 4 V/km and a wider confidence interval: [2.63, 4.81] V/km for the delta method and [2.92, 12.33] V/km for the profile likelihood (calculated at solar maximum).

Statistical model (3) in **Table I-1** is the traditional POT estimation using a threshold *u* of 1 V/km; the data was de-clustered using a 1-day run. The data set consists of normalized excesses over a threshold, and therefore, the sample size for POT is increased if more than one extreme observation per year is available (in the GEV approach, only the maximum observation over the year was taken; in the POT method, a single year can have multiple observations over the threshold). The selection of the threshold *u* is a compromise between bias and variance. The asymptotic basis of the model relies on a high threshold; a threshold that is too low will likely lead to bias. On the other hand, a threshold that is too high will reduce the sample size and result in high variance. The stability of parameter estimates can guide the selection of an appropriate threshold. **Figure I-4** shows the estimated parameters (modified scale $\sigma^*=\sigma_u-\xi\cdot u$, and shape ξ) for a range of thresholds. The objective is to select the lowest threshold for which the estimates remain near constant; 1V/km appears to be a good choice.

The mean return level for statistical model (3), 3.4 V/km, is similar to the GEV estimates. However, due to the larger sample size, the POT method is more efficient, and consequently, the confidence intervals are significantly reduced: [2.28, 4.52] V/km for the delta method, and [2.72, 5.64] V/km for the profile likelihood method.

In order to cope with the heteroskedasticity exhibited by the data, a re-parameterization of POT is used in statistical model (4) in **Table I-1**,

$$\sigma = \alpha_0 + \alpha_1 \cdot \sin\left(\frac{t}{T} + \phi\right)$$

where α_0 represents the offset in the standard deviation, α_1 describes the 11-year seasonality, *T* is the period ($365.25 \cdot 11$), and ϕ is a constant phase shift.

The parameter α_1 is statistically significant; the null hypothesis, H0: $\alpha_1=0$, is rejected with a p-value of 3.7e-5. The mean return level has slightly increased to 3.72 V/km. The upper limit of the confidence interval, calculated at solar maximum, also increases: [2.63, 4.81] V/km for the delta method and [3.02, 5.77] V/km for the profile likelihood method. As a final remark, it is emphasized that the confidence interval obtained using the profile likelihood is preferred over the delta method. **Figure I-5** shows the profile likelihood of the 100-year return level of statistical model (4). Note that the profile likelihood is highly asymmetric with a positive skew, rendering a larger upper limit for the confidence interval. Recall that the delta method assumes a normal distribution for the MLEs, and therefore, the confidence interval is symmetric around the mean.

To conclude, traditional GEV (1) and POT (3) models are misspecified; the statistical assumptions (iid) are not warranted by the data. The models were re-parameterized to cope with heteroskedasticity and the 11-year seasonality in the mean. Statistical model (4) better utilizes the available extreme measurements and it is therefore preferred over statistical model (2). The upper limit of the 95 percent confidence interval for a 100-year return level is 5.77 V/km. This analysis is consistent with the selection of a geoelectric field amplitude of 8 V/km for the 100-year GMD benchmark. .

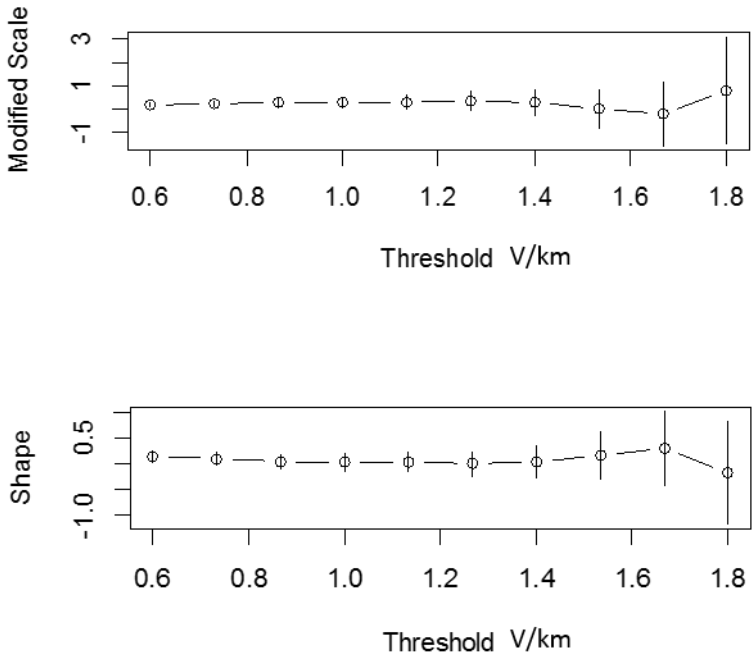

Figure I-4: Parameter Estimates Against Threshold for Statistical Model (3)

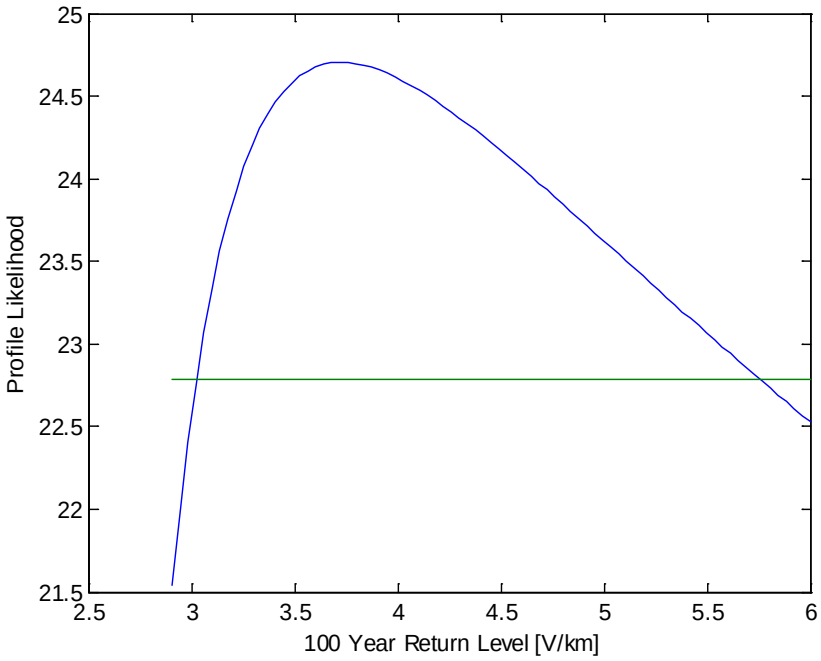

Figure I-5: Profile Likelihood for 100-year Return Level for Statistical Model (4)

Impact of Local Geomagnetic Disturbances on GIC

The impact of local disturbances on a power network is illustrated with the following example. A 500 km by 500 km section of a North American transmission network is subdivided into 100 km by 100 km sections. The geoelectric field is assumed to be uniform within each section. The analysis is performed by scaling the geoelectric field in each section individually by an intensification factor of 2.5 and computing the corresponding GIC flows in the network, resulting in a total of 25 GIC distribution simulations.[5] In these simulations the peak geomagnetic field amplitude has been scaled according to geomagnetic latitude of the network under study.

Figure I-6 shows the number of transformers that experience a GIC increase greater than 10 Amps (in red), those that experienced a reduction in GIC of more than 10 Amps (in blue), and those that remain essentially the same (in green). It can be observed that there is a small set of transformers that are affected by the local amplification of the geo-electric field but that the impact on the GIC distribution of the entire network due to a local intensification of the geoelectric field in a "local peak" is minor. Therefore, it can be concluded that the effect of local disturbances on the larger transmission system is relatively minor and does not warrant further consideration in network analysis.

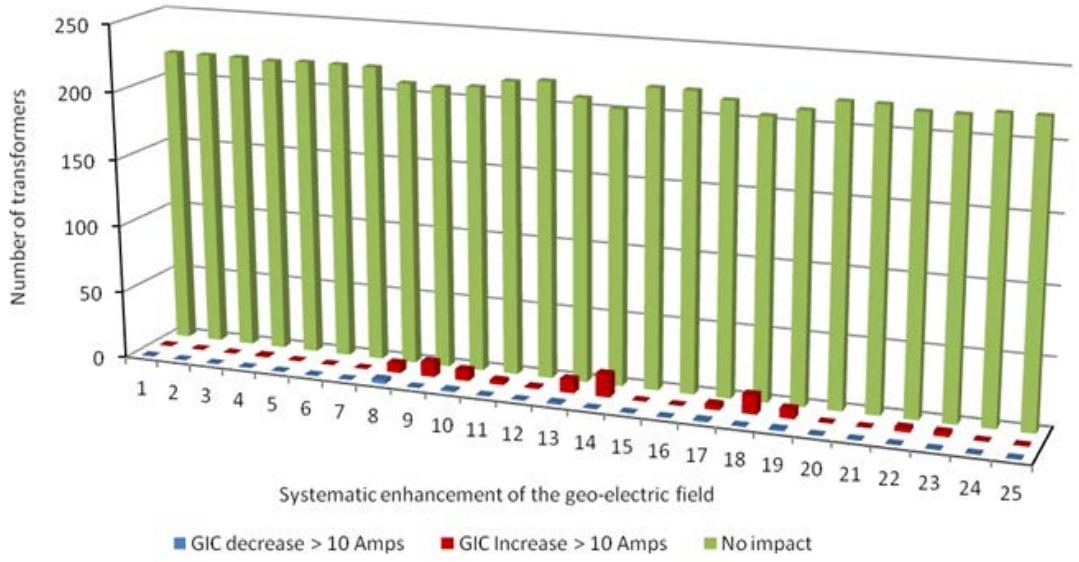

Figure I-6: Number of Transformers that see a 10 A/phase Change in GIC due to Local Geoelectric Field Intensification

Impact of Waveshape on Transformer Hot-spot Heating

Thermal effects (e.g. hot spot transformer heating) in power transformers are not instantaneous. Thermal time constants associated with hot spot heating in power transformers are in the 5-20 minute range; therefore, the waveshape of the geomagnetic and geoelectric field has a strong impact on transformer hot spot heating of windings and metallic parts since thermal time constants are of the same order of magnitude as the time-to-peak of storm maxima. The waveshape of the March 13-14 1989 GMD event measured at the Ottawa geomagnetic observatory was found to be a conservative choice when compared with other events of the last 20 years, such

[5] An intensification factor of 2.5 would make a general 8 V/km peak geoelectric field in the entire network show a 20 V/km intensified geoelectric field in one of the twenty five 100 km by 100 km sections.

as the ~~reference storm of the NERC interim report of 2012 [14], and~~ measurements at the Nurmijarvi (NUR) and Memanbetsu (MMB) geomagnetic observatories for the "Halloween event" of October 29-31, 2003~~.~~ described in the NERC GMD interim report of 2012 [14].

To illustrate, the results of a thermal analysis performed on a relatively large test network with a diverse mix of circuit lengths and orientations is provided in **Figures I-7** and **I-8**. **Figure I-9** shows a more systematic way to compare the relative effects of storm waveshape on the thermal response of a transformer. It shows the results of 33,000 thermal assessments for all combinations of effective GIC due to circuit orientation (similar **to Figures I-7** and **I-8** but systematically taking into account all possible circuit orientations). These results illustrate the relative effect of different waveshapes in a broad system setting and should not be interpreted as a vulnerability assessment of any particular network.

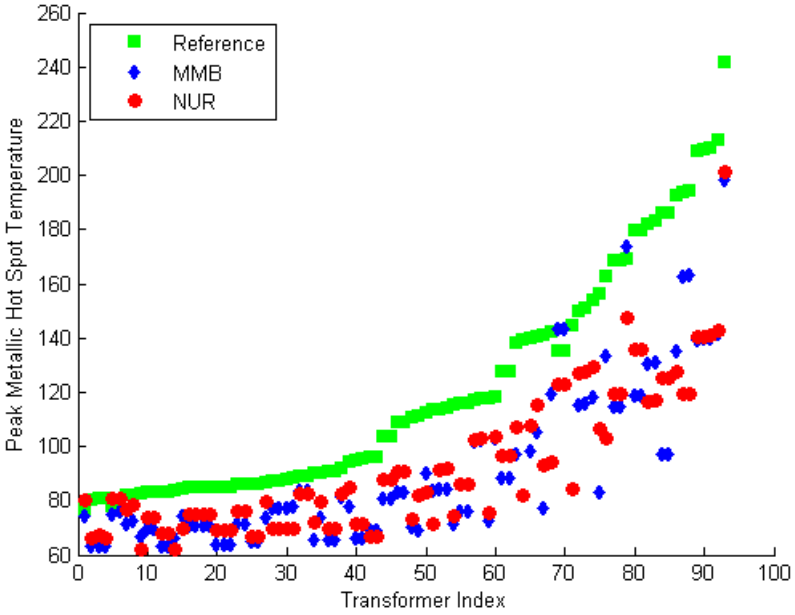

Figure I-7: Calculated Peak Metallic Hot Spot Temperature for All Transformers in a Test System with a Temperature Increase of More Than 20°C for Different GMD Events Scaled to the Same Peak Geoelectric Field

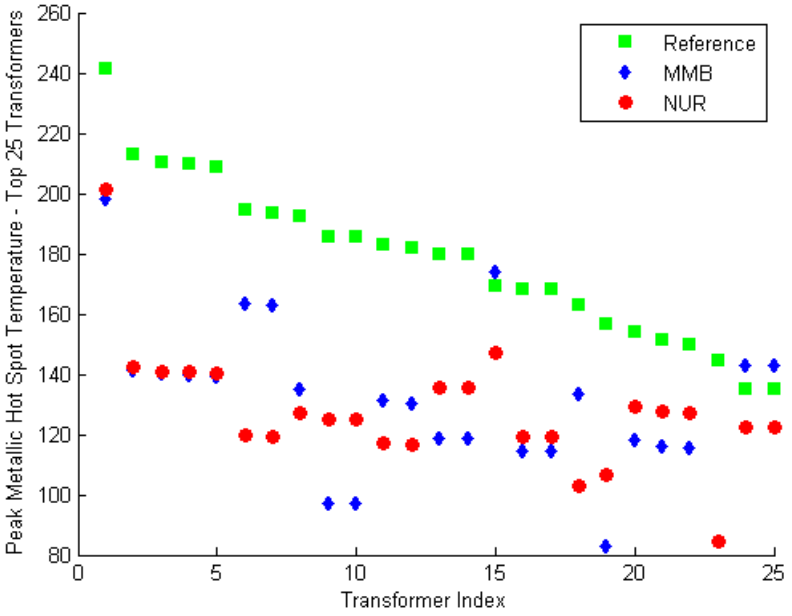

Figure I-8: Calculated Peak Metallic Hot Spot Temperature for the Top 25 Transformers in a Test System for Different GMD Events Scaled to the Same Peak Geoelectric Field

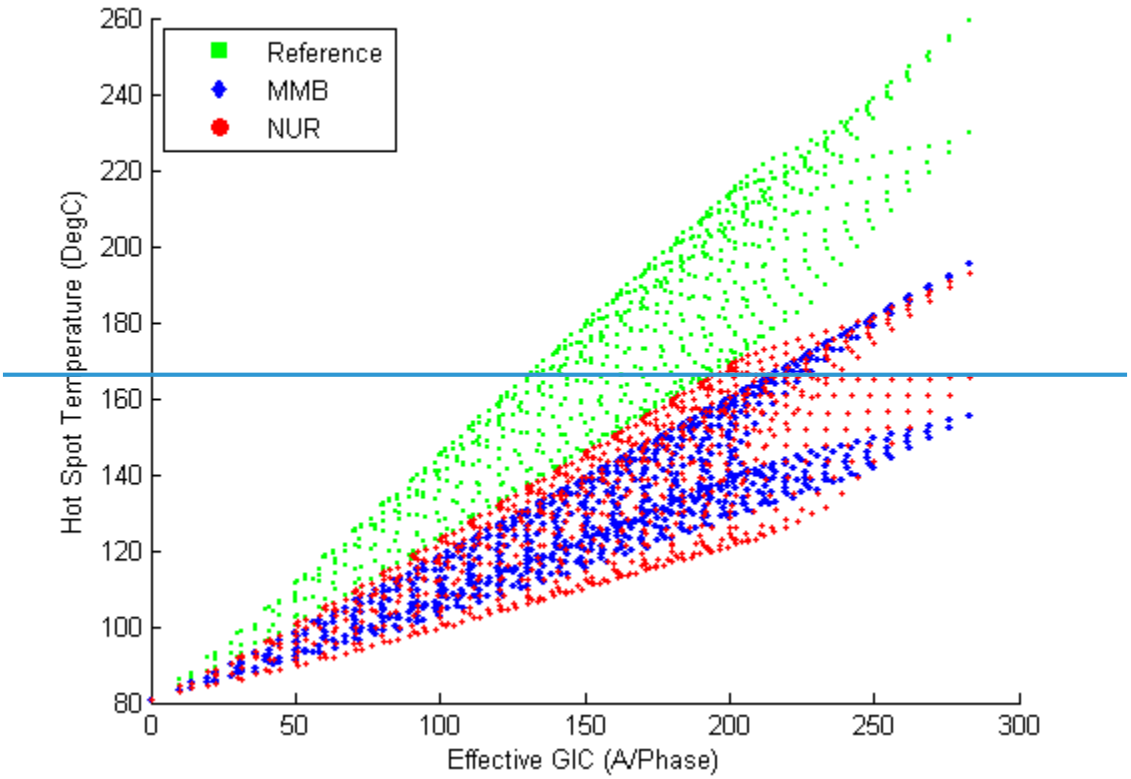

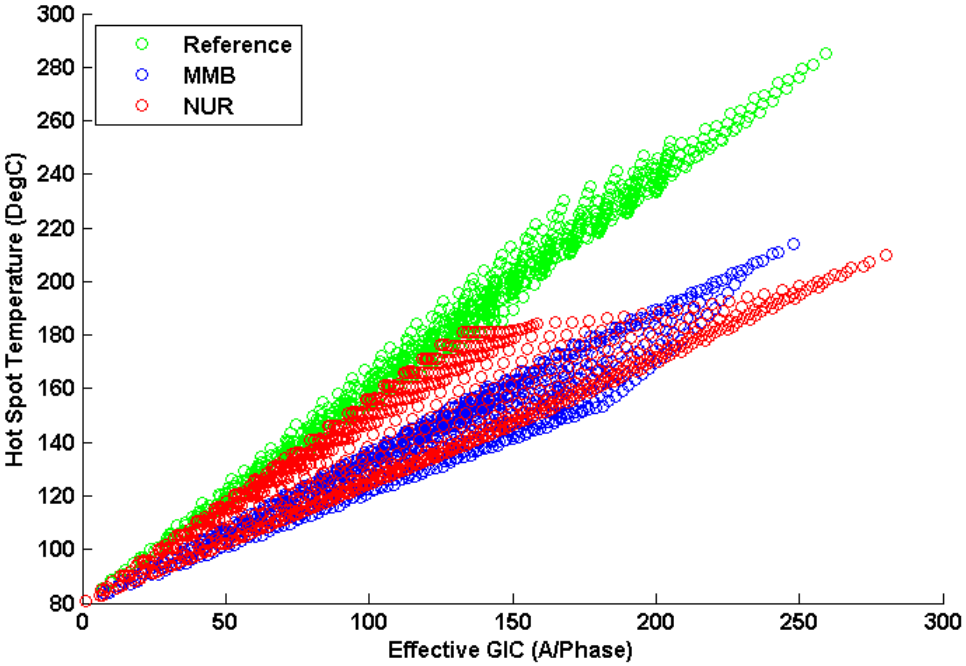

Figure I-9: Calculated Peak Metallic Hot Spot Temperature for all possible circuit orientations and effective GIC.

Appendix II – Scaling the Benchmark GMD Event

The intensity of a GMD event depends on geographical considerations such as geomagnetic latitude[6] and local earth conductivity[7] [3]**.** Scaling factors for geomagnetic latitude take into consideration that the intensity of a GMD event varies according to latitude-based geographical location. Scaling factors for earth conductivity take into account that the induced geoelectric field depends on earth conductivity, and that different parts of the continent have different earth conductivity and deep earth structure.

Scaling the Geomagnetic Field

The benchmark GMD event is defined for geomagnetic latitude of 60° and it must be scaled to account for regional differences based on geomagnetic latitude. To allow usage of the reference geomagnetic field waveshape in other locations, **Table II-1** summarizes the scaling factor α correlating peak geoelectric field to geomagnetic latitude as described in **Figure II-1** [3]. This scaling factor α has been obtained from a large number of global geomagnetic field observations of all major geomagnetic storms since the late 1980s [15], [24]-[25], and can be approximated with the empirical expression in (II.1)

$$\alpha = 0.001 \cdot e^{(0.115 \cdot L)} \qquad \text{(II.1)}$$

where L is the geomagnetic latitude in degrees and $0.1 \leq \alpha \leq 1.0$.

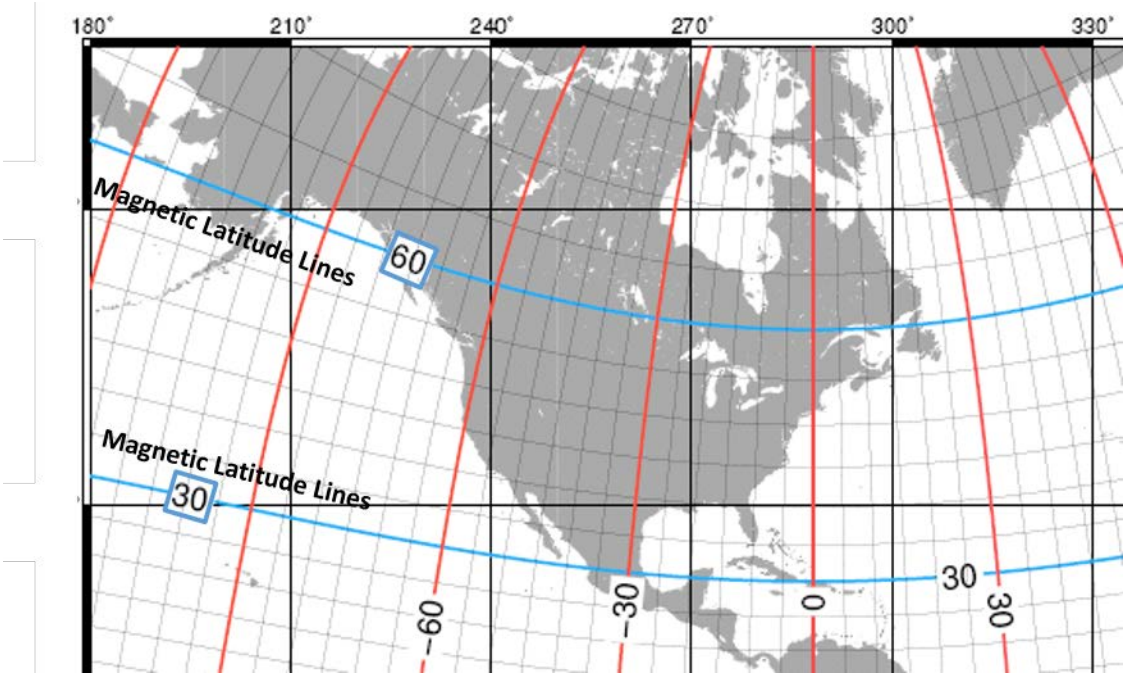

Figure II-1: Geomagnetic Latitude Lines in North America

[6] Geomagnetic latitude is analogous to geographic latitude, except that bearing is in relation to the magnetic poles, as opposed to the geographic poles. Geomagnetic phenomena are often best organized as a function of geomagnetic coordinates.

[7] Local earth conductivity refers to the electrical characteristics to depths of hundreds of km down to the earth's mantle. In general terms, lower ground conductivity results in higher geoelectric field amplitudes.

Table II-1: Geomagnetic Field Scaling Factors	
Geomagnetic Latitude (Degrees)	Scaling Factor1 (α)
≤ 40	0.10
45	0.2
50	0.3
54	0.5
56	0.6
57	0.7
58	0.8
59	0.9
≥ 60	1.0

Scaling the Geoelectric Field

The benchmark GMD event is defined for the reference Quebec earth model provided in **Table 1**. This earth model has been used in many peer-reviewed technical articles [12, 15]. The peak geoelectric field depends on the geomagnetic field waveshape and the local earth conductivity. Ideally, the peak geoelectric field, E_{peak}, is obtained by calculating the geoelectric field from the scaled geomagnetic waveshape using the plane wave method and taking the maximum value of the resulting waveforms

$$E_N = (z(t)/\mu_o) * B_E(t)$$
$$E_E = -(z(t)/\mu_o) * B_N(t) \qquad \text{(II.2)}$$
$$E_{peak} = \max\left\{\left|E_E(t), E_N(t)\right|\right\}$$

where,

* denotes convolution in the time domain,

z(t) is the impulse response for the earth surface impedance calculated from the laterally uniform or 1D earth model,

$B_E(t)$, $B_N(t)$ are the scaled Eastward and Northward geomagnetic field waveshapes,

$E_E(t)$, $E_N(t)|$ are the magnitudes of the calculated Eastward and Northward geoelectric field $E_E(t)$ and $E_N(t)$.

As noted previously, the response of the earth to B(t) (and dB/dt) is frequency dependent. **Figure II-2** shows the magnitude of Z(ω) for the reference earth model.

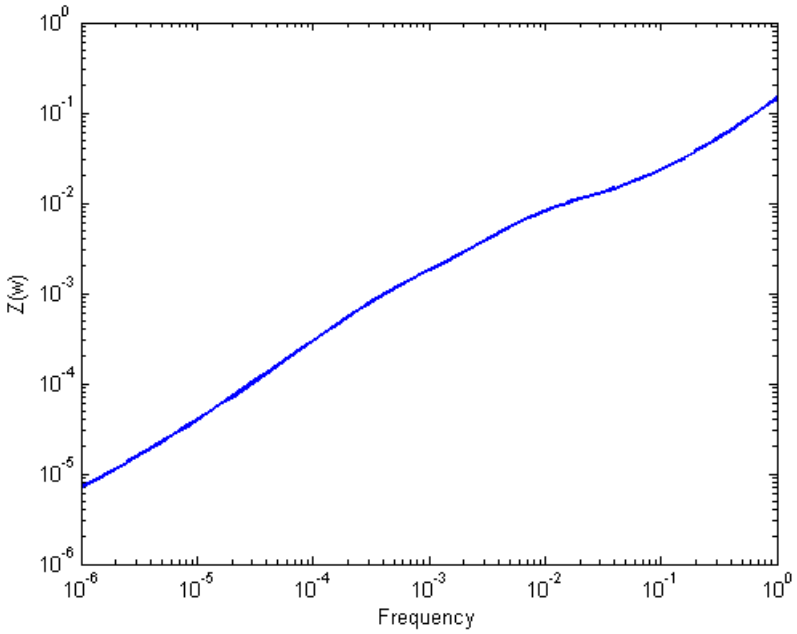

Figure II-2: Magnitude of the Earth Surface Impedance for the Reference Earth Model

If a utility does not have the capability of calculating the waveshape or time series for the geoelectric field, an earth conductivity scaling factor β can be obtained from **Table II-2**. Using α and β, the peak geoelectric field E_{peak} for a specific service territory shown in **Figure II-3** can be obtained using (II.3)

$$E_{peak} = 8 \times \alpha \times \beta \text{ (V/km)} \quad \text{(II.3)}$$

It should be noted that (II.3) is an approximation based on the following assumptions:

- The earth models used to calculate Table II-2 for the United States are from published information available on the USGS website.
- The models used to calculate Table II-2 for Canada were obtained from NRCan and reflect the average structure for large regions. When models are developed for sub-regions, there will be variance (to a greater or lesser degree) from the average model. For instance, detailed models for Ontario have been developed by NRCan and consist of seven major sub-regions.
- The conductivity scaling factor β is calculated as the quotient of the local geoelectric field peak amplitude in a physiographic region with respect to the reference peak amplitude value of 8 V/km. Both geoelectric field peaks amplitudes are calculated using the reference geomagnetic field time series. If a different geomagnetic field time series were used, the calculated scaling factors β would be different than the values in Table II-2 because the frequency content of storm maxima is, in principle, different for every storm. However, the reference time series produces generally more conservative values of β when compared to the time series of reference storm of the NERC interim report of 2012 [14], measurements at the Nurmijarvi (NUR) and Memanbetsu (MMB) geomagnetic observatories for the "Halloween event" of October 29-31, 2003, and other recordings of the March 1989 event at high latitudes (Meanook observatory, Canada). The average variation between minimum and maximum β is approximately 12 percent. **Figure II-4** illustrates the values of β calculated using the 10-second recordings for these geomagnetic field time series.
- If a utility has technically-sound earth models for its service territory and sub-regions thereof, then the use of such earth models is preferable to estimate E_{peak}.

- When a ground conductivity model is not available the planning entity should use the largest β factor of adjacent physiographic regions or a technically-justified value.

Physiographic Regions of the Continental United States

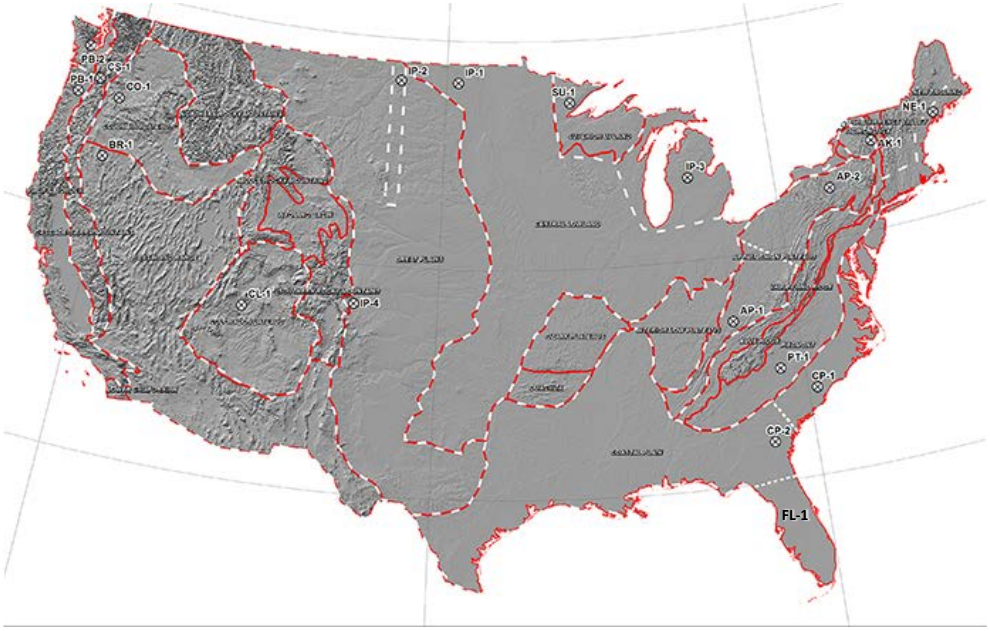

Physiographic Regions of Canada

Figure II-3: Physiographic Regions of North America

Table II-2 Geoelectric Field Scaling Factors	
USGS Earth model	Scaling Factor (β)
AK1A	0.56
AK1B	0.56
AP1	0.33
AP2	0.82
BR1	0.22
CL1	0.76
CO1	0.27
CP1	0.81
CP2	0.95
FL1	0.74
CS1	0.41
IP1	0.94
IP2	0.28
IP3	0.93
IP4	0.41
NE1	0.81
PB1	0.62
PB2	0.46
PT1	1.17
SL1	0.53
SU1	0.93
BOU	0.28
FBK	0.56
PRU	0.21
BC	0.67
PRAIRIES	0.96
SHIELD	1.0
ATLANTIC	0.79

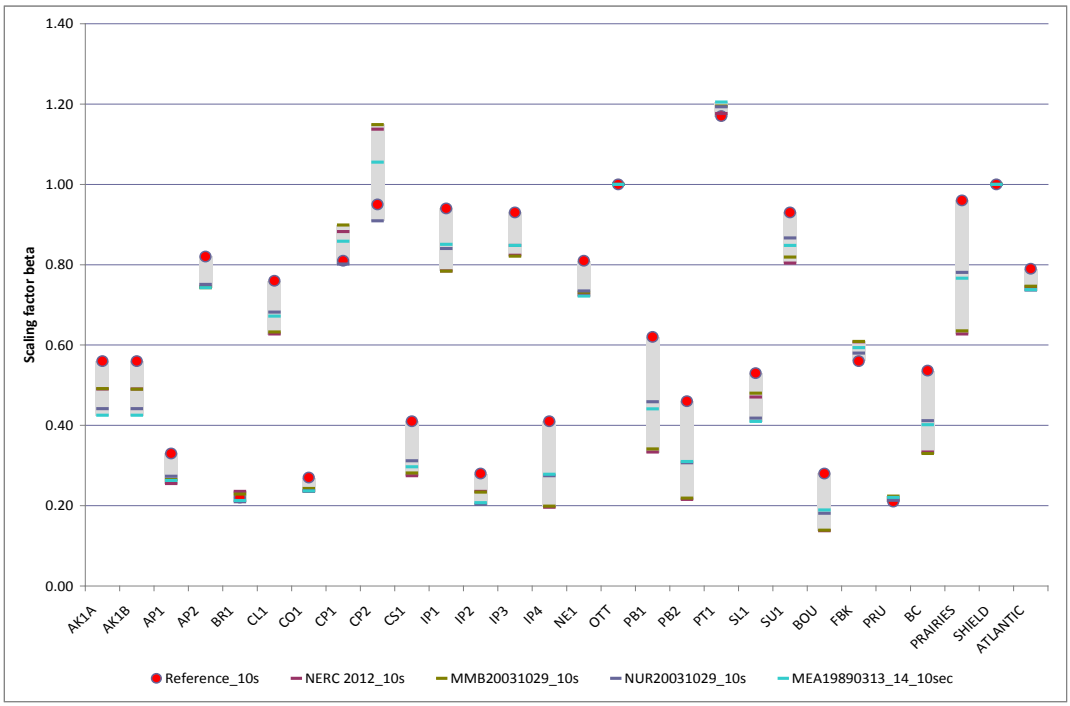

Figure II-4: Beta factors Calculated for Different GMD Events
Red circles correspond to the values in Table II-2

Example Calculations

Example 1

Consider a transmission service territory that lies in a geographical latitude of 45.5°, which translates to a geomagnetic latitude of 55°. The scaling factor α calculated using II.1 is 0.56; therefore, the benchmark waveshape and the peak geoelectric field will be scaled accordingly. If the service territory has the same earth conductivity as the benchmark then β=1, and the peak geoelectric field will be

$$\alpha = 0.56$$
$$\beta = 1.0$$
$$E_{peak} = 8 \times 0.56 \times 1 = 4.5 V/km$$

If the service territory spans more than one physiographic region (i.e. several locations within the service territory have a different earth model) then the largest α can be used across the entire service territory for conservative results. Alternatively, the network can be split into multiple subnetworks, and the corresponding geoelectric field amplitude can be applied to each subnetwork.

Example 2

Consider a service territory that lies in a geographical latitude of 45.5° which translates to a geomagnetic latitude of 55°. The scaling factor α calculated using II.1 is 0.56; therefore, the benchmark waveshape and the peak geoelectric field will be scaled accordingly.

The service territory has lower conductivity than the reference benchmark conductivity, therefore, according to the conductivity factor β from Table II-2., the calculation follows:

Conductivity factor β=1.17

$$\alpha = 0.56$$

$$E_{peak} = 8 \times 0.56 \times 1.17 = 5.2V / km$$

References

[1] L. Bolduc, A. Gaudreau, A. Dutil, "Saturation Time of Transformers Under dc Excitation", Electric Power Systems Research, 56 (2000), pp. 95-102

[2] *High-Impact, Low-Frequency Event Risk to the North American Bulk Power System*, A Jointly-Commissioned Summary Report of the North American Reliability Corporation and the U.S. Department of Energy's November 2009 Workshop.

[3] Application Guide: Computing Geomagnetically-Induced Current in the Bulk-Power System, NERC. NERC. http://www.nerc.com/comm/PC/Geomagnetic%20Disturbance%20Task%20Force%20GMDTF%202013/GIC%20Application%20Guide%202013_approved.pdf

[4] Kuan Zheng, Risto Pirjola, David Boteler, Lian-guang Liu, "Geoelectric Fields Due to Small-Scale and Large-Scale Source Currents", *IEEE Transactions on Power Delivery*, Vol. 28, No. 1, January 2013, pp. 442-449.

[5] Boteler, D. H. "Geomagnetically Induced Currents: Present Knowledge and Future Research", *IEEE Transactions on Power Delivery*, Vol. 9, No. 1, January 1994, pp. 50-58.

[6] Boteler, D. H. "Modeling Geomagnetically Induced Currents Produced by Realistic and Uniform Electric Fields", *IEEE Transactions on Power Delivery*, Vol. 13, No. 4, January 1998, pp. 1303-1308.

[7] J. L. Gilbert, W. A. Radasky, E. B. Savage, "A Technique for Calculating the Currents Induced by Geomagnetic Storms on Large High Voltage Power Grids", Electromagnetic Compatibility (EMC), 2012 IEEE International Symposium on.

[8] *How to Calculate Electric Fields to Determine Geomagnetically-Induced Currents.* EPRI, Palo Alto, CA: 2013. 3002002149.

[9] Pulkkinen, A., R. Pirjola, and A. Viljanen, Statistics of extreme geomagnetically induced current events, Space Weather, 6, S07001, doi:10.1029/2008SW000388, 2008.

[10] Boteler, D. H., Assessment of geomagnetic hazard to power systems in Canada, Nat. Hazards, 23, 101–120, 2001.

[11] Finnish Meteorological Institute's IMAGE magnetometer chain data available at: http://image.gsfc.nasa.gov/

[12] Boteler, D. H., and R. J. Pirjola, The complex-image method for calculating the magnetic and electric fields produced at the surface of the Earth by the auroral electrojet, Geophys. J. Int., 132(1), 31—40, 1998

[13] ANSI Standard C2, *National Electric Safety Code*, 2012, ISBN 978-0-7381-6588-2

[14] 2012 Special Reliability Assessment Interim Report: Effects of Geomagnetic Disturbances on the Bulk Power System. NERC. February 2012. http://www.nerc.com/pa/RAPA/ra/Reliability%20Assessments%20DL/2012GMD.pdf

[15] Pulkkinen, A., E. Bernabeu, J. Eichner, C. Beggan and A. Thomson, Generation of 100-year geomagnetically induced current scenarios, *Space Weather*, Vol. 10, S04003, doi:10.1029/2011SW000750, 2012.

[16] Love, J., Credible occurrence probabilities for extreme geophysical events: Earthquakes, volcanic eruptions, magnetic storms, Geophysical Research Letters, Vol. 39, L10301, doi:10.1029/2012GL051431, 2012.

[17] Pulkkinen, A., A. Thomson, E. Clarke, and A. Mckay, April 2000 geomagnetic storm: ionospheric drivers of large geomagnetically induced currents, Annales Geophysicae, 21, 709-717, 2003.

[18] Pulkkinen, A., S. Lindahl, A. Viljanen, and R. Pirjola, Geomagnetic storm of 29–31 October 2003: Geomagnetically induced currents and their relation to problems in the Swedish high-voltage power transmission system, Space Weather, 3, S08C03, doi:10.1029/2004SW000123, 2005.

[19] Pulkkinen, A., R. Pirjola, and A. Viljanen, Statistics of extreme geomagnetically induced current events, Space Weather, 6, S07001, doi:10.1029/2008SW000388, 2008.

[20] Langlois, P., L. Bolduc, and M. C. Chouteau, Probability of occurrence of geomagnetic storms based on a study of the distribution of the electric field amplitudes measured in Abitibi, Québec, in 1993–1994, J. Geomagn. Geoelectr., 48, 1033–1041, 1996.

[21] Pulkkinen, A., R. Pirjola, and A. Viljanen, Statistics of extreme geomagnetically induced current events, Space Weather, 6, S07001, doi:10.1029/2008SW000388, 2008.

[22] Campbell, W. C., Observation of electric currents in the Alaska oil pipeline resulting from auroral electrojet current sources, Geophys. J. R. Astron. Soc., 61, 437–449, 1980.

[23] Coles, Stuart (2001). An Introduction to Statistical Modelling of Extreme Values. Springer.

[24] Ngwira, C., A. Pulkkinen, F. Wilder, and G. Crowley, Extended study of extreme geoelectric field event scenarios for geomagnetically induced current applications, Space Weather, Vol. 11, 121–131, doi:10.1002/swe.20021, 2013.

[25] Thomson, A., S. Reay, and E. Dawson. Quantifying extreme behavior in geomagnetic activity, Space Weather, 9, S10001, doi:10.1029/2011SW000696, 2011.

NERC
NORTH AMERICAN ELECTRIC RELIABILITY CORPORATION

Transformer Thermal Impact Assessment White Paper

Project 2013-03 (Geomagnetic Disturbance Mitigation)

TPL-007-1 Transmission System Planned Performance for Geomagnetic Disturbance Events

Background

On May 16, 2013, FERC issued Order No. 779, directing NERC to develop Standards that address risks to reliability caused by geomagnetic disturbances (GMDs) in two stages:

- Stage 1 Standard(s) that require applicable entities to develop and implement Operating Procedures. EOP-010-1 – Geomagnetic Disturbance Operations was approved by FERC in June 2014.
- Stage 2 Standard(s) that require applicable entities to conduct assessments of the potential impact of benchmark GMD events on their systems. If the assessments identify potential impacts, the Standard(s) will require the applicable entity to develop and implement a plan to mitigate the risk.

TPL-007-1 is a new Reliability Standard to specifically address the Stage 2 directives in Order No. 779.

Large power transformers connected to the EHV transmission system can experience both winding and structural hot spot heating as a result of GMD events. TPL-007-1 will require owners of such transformers to conduct thermal analyses of their transformers to determine if the transformers will be able to withstand the thermal transient effects associated with the Benchmark GMD event. This paper discusses methods that can be employed to conduct such analyses, including example calculations.

The primary impact of GMDs on large power transformers is a result of the quasi-dc current that flows through wye-grounded transformer windings. This geomagnetically-induced current (GIC) results in an offset of the ac sinusoidal flux resulting in asymmetric or half-cycle saturation (see **Figure 1**).

Half-cycle saturation results in a number of known effects:

- Hot spot heating of transformer windings due to harmonics and stray flux;
- Hot spot heating of non-current carrying transformer metallic members due to stray flux;
- Harmonics;
- Increase in reactive power absorption; and
- Increase in vibration and noise level.

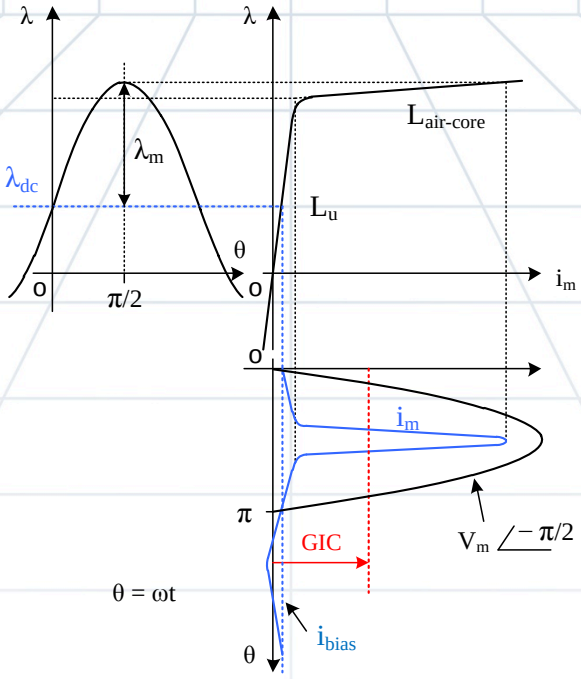

Figure 1: Mapping Magnetization Current to Flux through Core Excitation Characteristics

This paper focuses on hot spot heating of transformer windings and non current-carrying metallic parts. Effects such as the generation of harmonics, increase in reactive power absorption, vibration, and noise are not within the scope of this document.

Technical Considerations

The effects of half-cycle saturation on HV and EHV transformers, namely localized "hot spot" heating, are relatively well understood, but are difficult to quantify. A transformer GMD impact assessment must consider GIC amplitude, duration, and transformer physical characteristics such as design and condition (e.g., age, gas content, and moisture in the oil). A single threshold value of GIC cannot be justified as a "pass or fail" screening criterion where "fail" means that the transformer will suffer damage. A single threshold value of GIC only makes sense in the context where "fail" means that a more detailed study is required and that "pass" means that GIC in a particular transformer is so low that a detailed study is unnecessary. Such a threshold would have to be technically justifiable and sufficiently low to be considered a conservative value within the scope of the benchmark.

The following considerations should be taken into account when assessing the thermal susceptibility of a transformer to half-cycle saturation:

- In the absence of manufacturer specific information, use the temperature limits for safe transformer operation such as those suggested in the IEEE Std C57.91-2011 standard [1] for hot spot heating during short-term emergency operation. This standard does not suggest that exceeding these limits will result in transformer failure, but rather that it will result in additional aging of cellulose in the paper-oil insulation and the potential for the generation of gas bubbles in the bulk oil. Thus, from the point of view of evaluating

possible transformer damage due to increased hot spot heating, these thresholds can be considered conservative for a transformer in good operational condition.

- The worst case temperature rise for winding and metallic part (e.g., tie plate) heating should be estimated taking into consideration the construction characteristics of the transformer as they pertain to dc flux offset in the core (e.g., single-phase, shell, 5 and 3-leg three-phase construction).
- Bulk oil temperature due to ambient temperature and transformer loading must be added to the incremental temperature rise caused by hot spot heating. For planning purposes, maximum ambient and loading temperature should be used unless there is a technically justified reason to do otherwise.
- The time series or "waveshape" of the reference GMD event in terms of peak amplitude, duration, and frequency of the geoelectric field has an important effect on hot spot heating. Winding and metallic part hot spot heating have different thermal time constants, and their temperature rise will be different if the GIC currents are sustained for 2, 10, or 30 minutes for a given GIC peak amplitude.
- The "effective" GIC in autotransformers (reflecting the different GIC ampere-turns in the common and the series windings) must be used in the assessment. The effective current $I_{dc,eq}$ in an autotransformer is defined by [2].

$$I_{dc,eq} = I_H + (I_N/3 - I_H)V_X/V_H \quad (1)$$

where

I_H is the dc current in the high voltage winding;
I_N is the neutral dc current;
V_H is the rms rated voltage at HV terminals;
V_X is the rms rated voltage at the LV terminals.

Transformer Thermal Impact Assessment Process

A simplified thermal assessment may be based on Table 2 from the "Screening Criterion for Transformer Thermal Impact Assessment" white paper [7]. This table, shown as Table 1 below, provides the peak metallic hot spot temperatures that can be reached using conservative thermal models. To use Table 1, one must select the bulk oil temperature and the threshold for metallic hot spot heating, for instance, from reference [1] after allowing for possible de-rating due to transformer condition. If the effective GIC results in higher than threshold temperatures, then the use of a detailed thermal assessment as described below should be carried out.

Table 1: Upper Bound of Peak Metallic Hot Spot Temperatures Calculated Using the Benchmark GMD Event

Effective GIC (A/phase)	Metallic hot spot Temperature (°C)	Effective GIC(A/phase)	Metallic hot spot Temperature (°C)
0	80	100	182
10	107	110	186
20	128	120	190
30	139	130	193
40	148	140	204
50	157	150	213
60	169	160	221
70	170	170	230
75	172	180	234
80	175	190	241
90	179	200	247

Two different ways to carry out a detailed thermal impact assessment are discussed below. In addition, other approaches and models approved by international standard-setting organizations such as the Institute of Electrical and Electronic Engineers (IEEE) or International Council on Large Electric Systems (CIGRE) may also provide technically justified methods for performing thermal assessments. All thermal assessment methods should be demonstrably equivalent to assessments that use the benchmark GMD event.

1. Transformer manufacturer GIC capability curves. These curves relate permissible peak GIC (obtained by the user from a steady-state GIC calculation) and loading, for a specific transformer. An example of manufacturer capability curves is provided in **Figure 2**. Presentation details vary between manufacturers, and limited information is available regarding the assumptions used to generate these curves, in particular, the assumed waveshape or duration of the effective GIC. Some manufacturers assume that the waveshape of the GIC in the transformer windings is a square pulse of 2, 10, or 30 minutes in duration. In the case of the transformer capability curve shown in **Figure 2** [3], a square pulse of 900 A/phase with a duration of 2 minutes would cause the Flitch plate hot spot to reach a temperature of 180 °C at full load. While GIC capability curves are relatively simple to use, an amount of engineering judgment is necessary to ascertain which portion of a GIC waveshape is equivalent to, for example, a 2 minute pulse. Also, manufacturers generally maintain that in the absence of transformer standards defining thermal duty due to GIC, such capability curves must be developed for every transformer design and vintage.

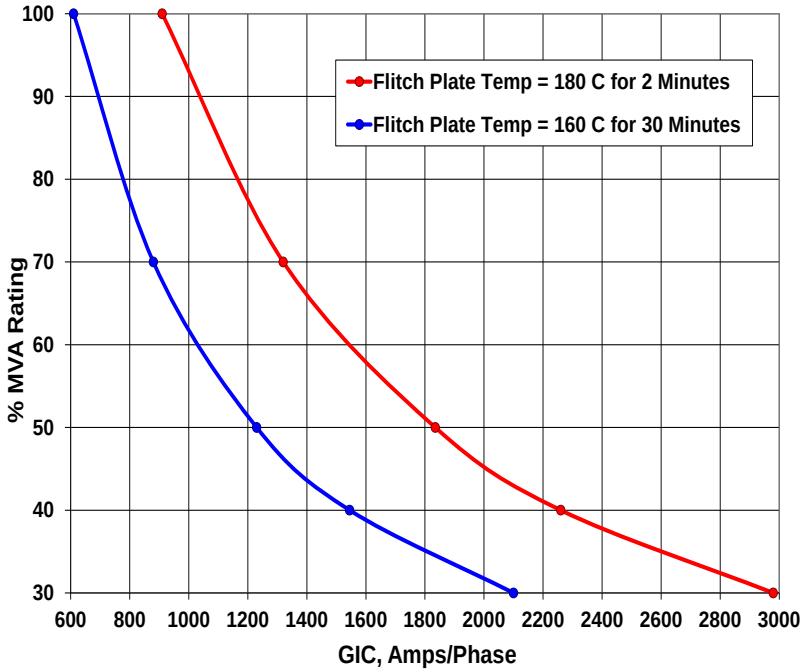

Figure 2: Sample GIC Manufacturer Capability Curve of a Large Single-Phase Transformer Design using the Flitch Plate Temperature Criteria [3]

2. Thermal response simulation[1]. The input to this type of simulation is the time series or waveshape of effective GIC flowing through a transformer (taking into account the actual configuration of the system), and the result of the simulation is the hot spot temperature (winding or metallic part) time sequence for a given transformer. An example of GIC input and hotspot temperature time series values from [4] are shown in **Figure 3**. The hot spot thermal transfer functions can be obtained from measurements or calculations provided by transformer manufacturers. Conservative default values can be used (e.g. those provided in [4]) when specific data are not available. Hot spot temperature thresholds shown in **Figure 3** are consistent with IEEE Std C57.91 emergency loading hot spot limits. Emergency loading time limit is usually 30 minutes.

[1] Technical details of this methodology can be found in [4].

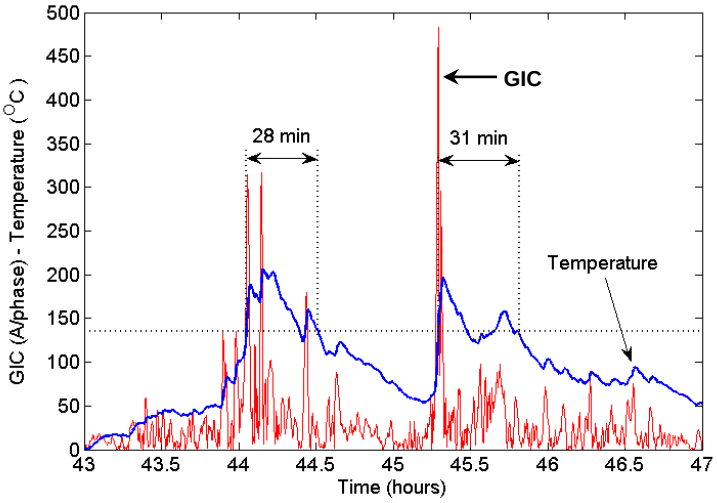

Figure 3: Sample Tie Plate Temperature Calculation
Blue trace is incremental temperature and red trace is the magnitude of the GIC/phase [4]

It is important to reiterate that the characteristics of the time sequence or "waveshape" are very important in the assessment of the thermal impact of GIC on transformers. Transformer hot spot heating is not instantaneous. The thermal time constants of transformer windings and metallic parts are typically on the order of minutes to tens of minutes; therefore, hot spot temperatures are heavily dependent on GIC history and rise time, amplitude and duration of GIC in the transformer windings, bulk oil temperature due to loading, ambient temperature and cooling mode.

Calculation of the GIC Waveshape for a Transformer

The following procedure can be used to generate time series GIC data, i.e. GIC(t), using a software program capable of computing GIC in the steady-state. The steps are as follows:

1. Calculate contribution of GIC due to eastward and northward geoelectric fields for the transformer under consideration;
2. Scale the GIC contribution according to the reference geoelectric field time series to produce the GIC time series for the transformer under consideration.

Most available GIC–capable software packages can calculate GIC in steady-state in a transformer assuming a uniform eastward geoelectric field of 1 V/km (GIC_E) while the northward geoelectric field is zero. Similarly, GIC_N can be obtained for a uniform northward geoelectric field of 1 V/km while the eastward geoelectric field is zero. GIC_E and GIC_N are the normalized GIC contributions for the transformer under consideration.

If the earth conductivity is assumed to be uniform (or laterally uniform) in the transmission system of interest, then the transformer GIC (in A/phase) for any value of $E_E(t)$ and $E_N(t)$ can be calculated using (2) [2].

$$GIC(t) = \left|E(t)\right| \cdot \left\{GIC_E \sin(\varphi(t)) + GIC_N \cos(\varphi(t))\right\} \quad (2)$$

where

$$|E(t)| = \sqrt{E_N^2(t) + E_E^2(t)} \quad (3)$$

$$\varphi(t) = \tan^{-1}\left(\frac{E_E(t)}{E_N(t)}\right) \quad (4)$$

$$GIC(t) = E_E(t) \cdot GIC_E + E_N(t) \cdot GIC_N \quad (5)$$

GIC_N is the effective GIC due to a northward geoelectric field of 1 V/km, and GIC_E is the effective GIC due to an eastward geoelectric field of 1 V/km. The units for GIC_N and GIC_E are A/phase/V/km)

The geoelectric field time series $E_N(t)$ and $E_E(t)$ is obtained, for instance, from the reference geomagnetic field time series [5] after the appropriate geomagnetic latitude scaling factor α is applied[2]. The reference geoelectric field time series is calculated using the reference earth model. When using this geoelectric field time series where a different earth model is applicable, it should be scaled with the conductivity scaling factor β[3]. Alternatively, the geoelectric field can be calculated from the reference geomagnetic field time series after the appropriate geomagnetic latitude scaling factor α is applied and the appropriate earth model is used. In such case, the conductivity scaling factor β is not applied because it is already accounted for by the use of the appropriate earth model.

Applying (5) to each point in $E_N(t)$ and $E_E(t)$ results in GIC(t).

GIC(t) Calculation Example

Let us assume that from the steady-state solution, the effective GIC in this transformer is GIC_E = -20 A/phase if E_N=0, E_E=1 V/km and GIC_N = 26 A/phase if E_N=1 V/km, E_E=0. Let us also assume the geomagnetic field time series corresponds to a geomagnetic latitude where α = 1 and that the earth conductivity corresponds to the reference earth model in [5]. The resulting geoelectric field time series is shown in **Figure 4**. Therefore:

$$GIC(t) = E_E(t) \cdot GIC_E + E_N(t) \cdot GIC_N \text{ (A/phase)} \quad (6)$$

$$GIC(t) = -E_E(t) \cdot 20 + \cdot E_N(t) \cdot 26 \text{ (A/phase)} \quad (7)$$

The resulting GIC waveshape GIC(t) is shown in **Figures 5 and 6** and can subsequently be used for thermal analysis.

[2] The geomagnetic factor α is described in [2] and is used to scale the geomagnetic field according to geomagnetic latitude. The lower the geomagnetic latitude (closer to the equator), the lower the amplitude of the geomagnetic field.

[3] The conductivity scaling factor β is described in [2], and is used to scale the geoelectric field according to the conductivity of different physiographic regions. Lower conductivity results in higher β scaling factors.

It should be emphasized that even for the same reference event, the GIC(t) waveshape in every transformer will be different, depending on the location within the system and the number and orientation of the circuits connecting to the transformer station. Assuming a single generic GIC(t) waveshape to test all transformers is incorrect.

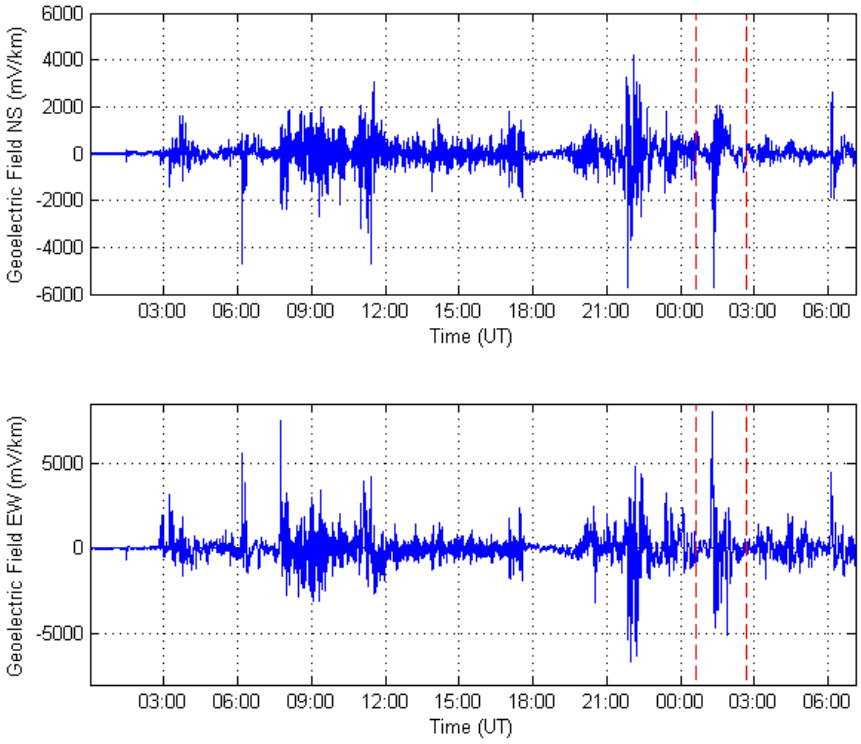

Figure 4: Calculated Geoelectric Field $E_N(t)$ and $E_E(t)$ Assuming $\alpha=1$ and $\beta=1$ (Reference Earth Model). Zoom area for subsequent graphs is highlighted. Dashed lines approximately show the close-up area for subsequent Figures.

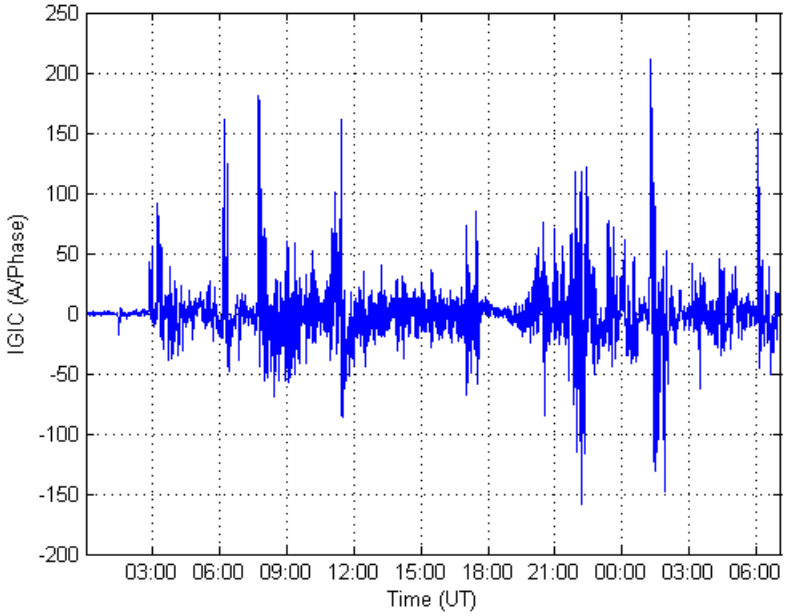

Figure 5: Calculated GIC(t) Assuming α=1 and β=1 (Reference Earth Model)

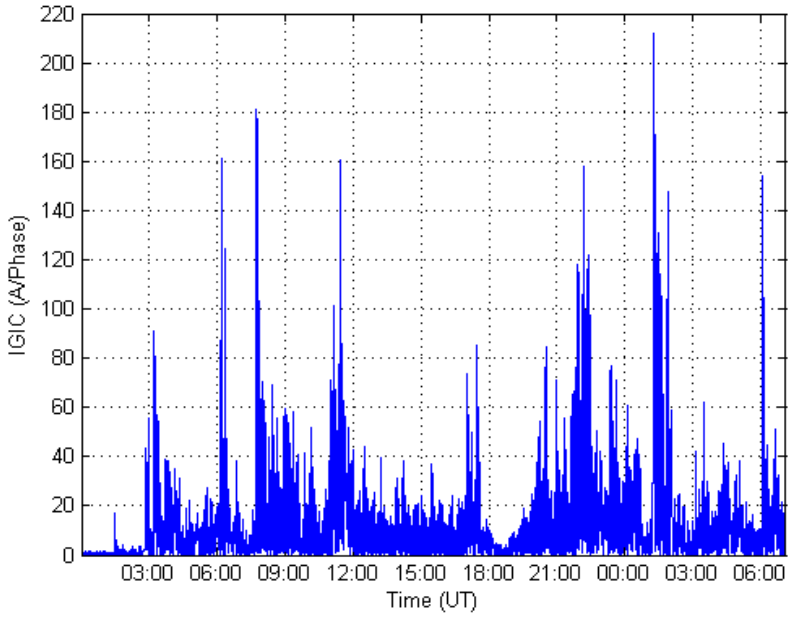

Figure 6: Calculated Magnitude of GIC(t) Assuming α=1 and β=1 (Reference Earth Model)

Transformer Thermal Assessment Examples

There are two basic ways to carry out a transformer thermal analysis once the GIC time series GIC(t) is known for a given transformer: 1) calculating the thermal response as a function of time; and 2) using manufacturer's capability curves.

Example 1: Calculating thermal response as a function of time using a thermal response tool

The thermal step response of the transformer can be obtained for both winding and metallic part hot spots from: 1) measurements; 2) manufacturer's calculations; or 3) generic published values. **Figure 7** shows the measured metallic hot spot thermal response to a dc step of 16.67 A/phase of the top yoke clamp from [6] that will be used in this example. **Figure 8** shows the measured incremental temperature rise (asymptotic response) of the same hot spot to long duration GIC steps.[4]

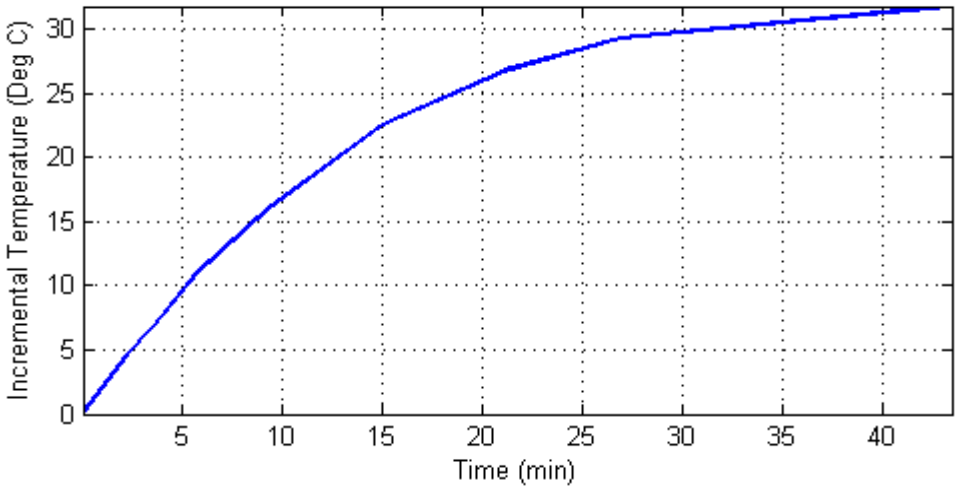

Figure 7: Thermal Step Response to a 16.67 Amperes per Phase dc Step
Metallic hot spot heating.

[4] Heating of bulk oil due to the hot spot temperature increase is not included in the asymptotic response because the time constant of bulk oil heating is at least an order of magnitude larger than the time constants of hot spot heating.

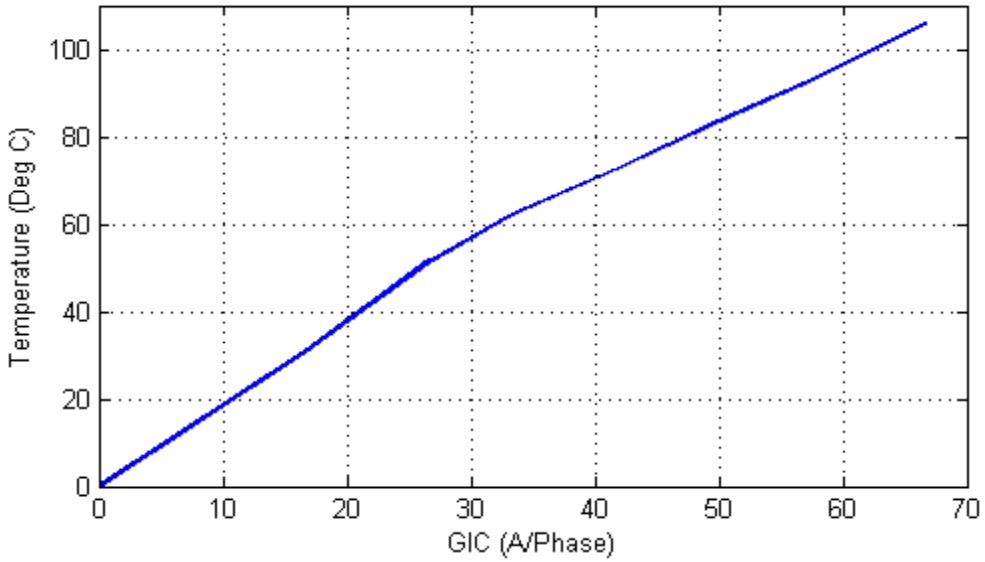

Figure 8: Asymptotic Thermal Step Response
Metallic hot spot heating.

The step response in **Figure 7** was obtained from the first GIC step of the tests carried out in [6]. The asymptotic thermal response in **Figure 8** was obtained from the final or near-final temperature values after each subsequent GIC step. **Figure 9** shows a comparison between measured temperatures and the calculated temperatures using the thermal response model used in the rest of this discussion.

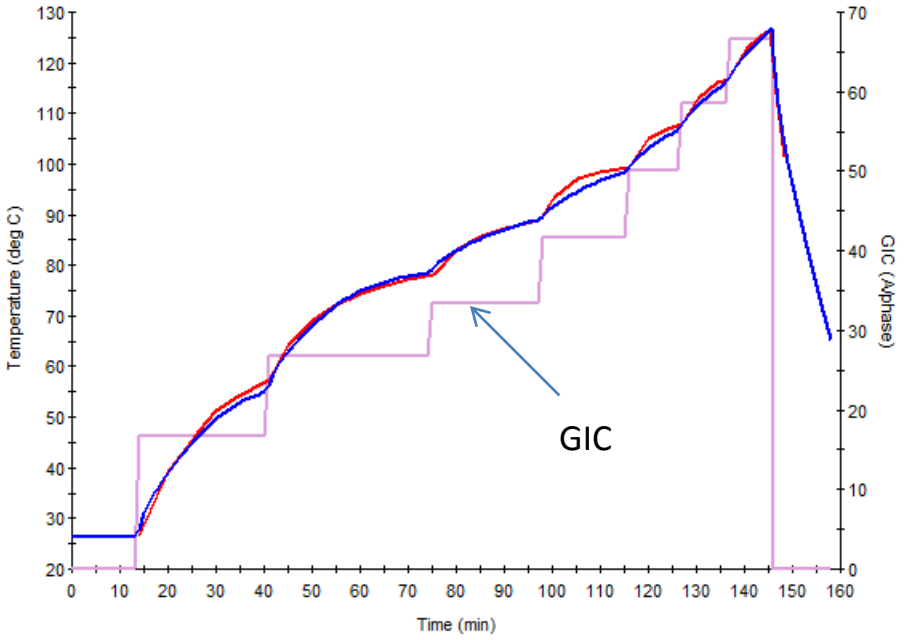

Figure 9: Comparison of measured temperatures (red trace) and simulation results (blue trace). Injected current is represented by the magenta trace.

To obtain the thermal response of the transformer to a GIC waveshape such as the one in **Figure 6**, a thermal response model is required. To create a thermal response model, the measured or manufacturer-calculated transformer thermal step responses (winding and metallic part) for various GIC levels are required. The GIC(t) time series or waveshape is then applied to the thermal model to obtain the incremental temperature rise as a function of time $\theta(t)$ for the GIC(t) waveshape. The total temperature is calculated by adding the oil temperature, for example, at full load.

Figure 10 illustrates the calculated GIC(t) and the corresponding hot spot temperature time series $\theta(t)$. **Figure 11** illustrates a close-up view of the peak transformer temperatures calculated in this example.

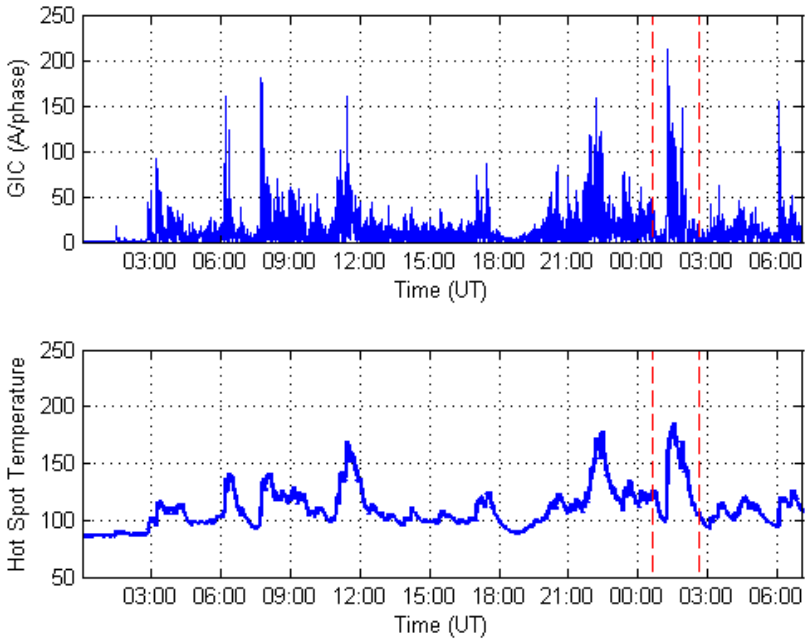

Figure 10: Magnitude of GIC(t) and Metallic Hot Spot Temperature $\theta(t)$ Assuming Full Load Oil Temperature of 85.3°C (40°C ambient). Dashed lines approximately show the close-up area for subsequent Figures.

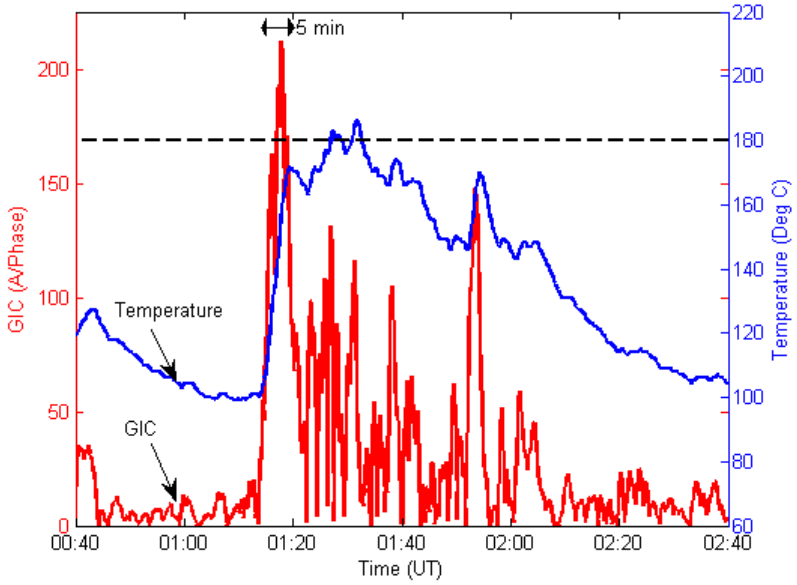

Figure 11: Close-up of Metallic Hot Spot Temperature Assuming a Full Load
(Blue trace is θ(t). Red trace is GIC(t))

In this example, the IEEE Std C57.91 emergency loading hot spot threshold of 200°C for metallic hot spot heating is not exceeded. Peak temperature is 186°C. The IEEE standard is silent as to whether the temperature can be higher than 200°C for less than 30 minutes. Manufacturers can provide guidance on individual transformer capability.

It is not unusual to use a lower temperature threshold of 180°C to account for calculation and data margins, as well as transformer age and condition. **Figure 11** shows that 180°C will be exceeded for 5 minutes.

At 75% loading, the initial temperature is 64.6 °C rather than 85.3 °C, and the hot spot temperature peak is 165°C, well below the 180°C threshold (see **Figure 12**).

If a conservative threshold of 160°C were used to account for the age and condition of the transformer, then the full load limits would be exceeded for approximately 22 minutes.

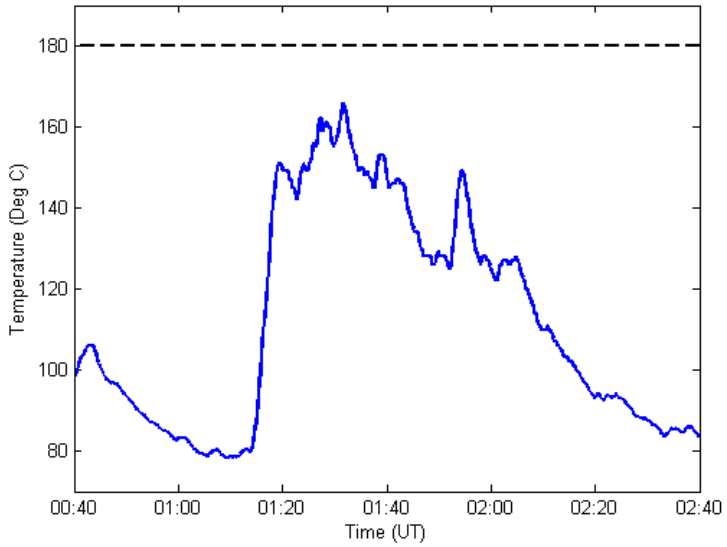

Figure 12: Close-up of Metallic Hot Spot Temperature Assuming a 75% Load
(Oil temperature of 64.5°C)

Example 2: Using a Manufacturer's Capability Curves

The capability curves used in this example are shown in **Figure 13**. To maintain consistency with the previous example, these particular capability curves have been reconstructed from the thermal step response shown in **Figures 7** and **8**, and the simplified loading curve shown in **Figure 14** (calculated using formulas from IEEE Std C57.91).

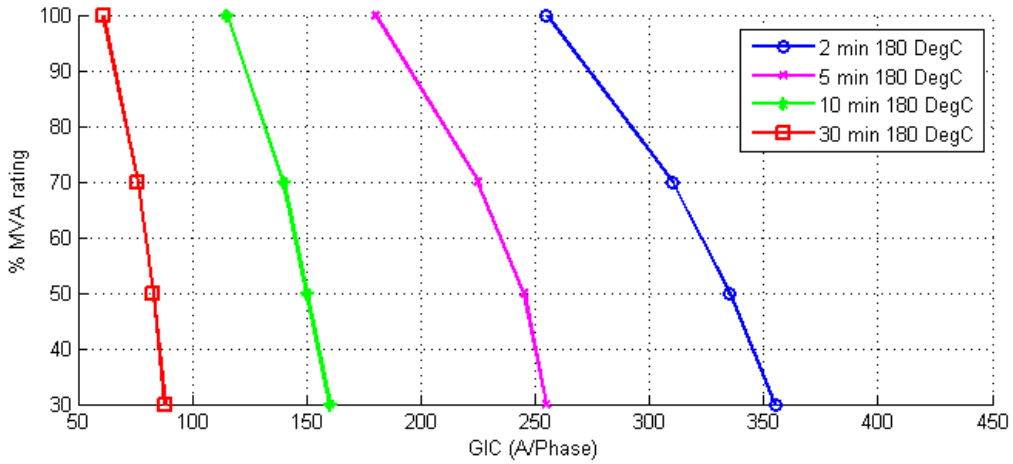

Figure 13: Capability Curve of a Transformer Based on the Thermal Response Shown in Figures 8 and 9.

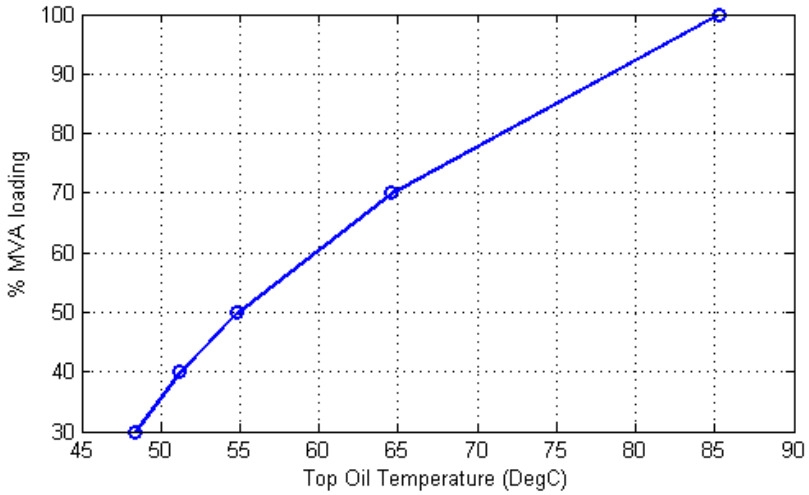

Figure 14: Simplified Loading Curve Assuming 40°C Ambient Temperature.

The basic notion behind the use of capability curves is to compare the calculated GIC in a transformer with the limits at different GIC pulse widths. A narrow GIC pulse has a higher limit than a longer duration or wider one. If the calculated GIC and assumed pulse width falls below the appropriate pulse width curve, then the transformer is within its capability.

To use these curves, it is necessary to estimate an equivalent square pulse that matches the waveshape of GIC(t), generally at a GIC(t) peak. **Figure 15** shows a close-up of the GIC near its highest peak superimposed to a 255 Amperes per phase, 2 minute pulse at 100% loading from **Figure 13**. Since a narrow 2-minute pulse is not representative of GIC(t) in this case, a 5 minute pulse with an amplitude of 180 A/phase at 100% loading has been superimposed on **Figure 16**. It should be noted that a 255 A/phase, 2 minute pulse is equivalent to a 180 A/phase 5 minute pulse from the point of view of transformer capability. Deciding what GIC pulse is equivalent to the portion of GIC(t) under consideration is a matter of engineering judgment.

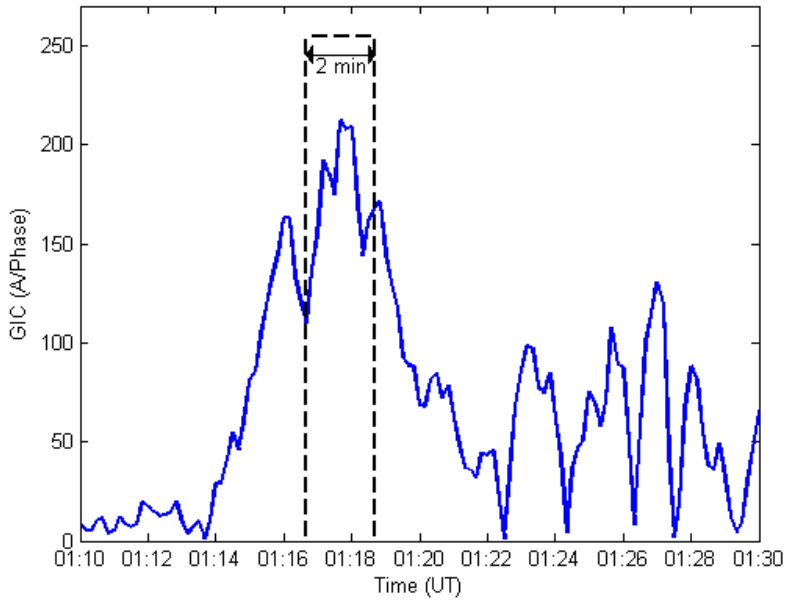

Figure 15: Close-up of GIC(t) and a 2 minute 255 A/phase GIC pulse at full load

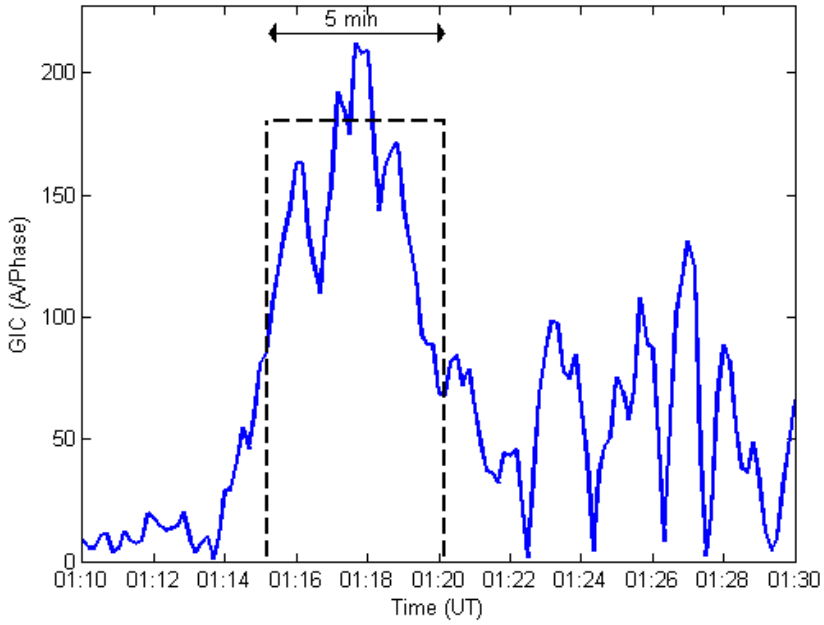

Figure 16: Close-up of GIC(t) and a Five Minute 180 A/phase GIC Pulse at Full Load

When using a capability curve, it should be understood that the curve is derived assuming that there is no hot spot heating due to prior GIC at the time the GIC pulse occurs (only an initial temperature due to loading). Therefore, in addition to estimating the equivalent pulse that matches GIC(t), prior hot spot heating must be accounted for. From

these considerations, it is unclear whether the capability curves would be exceeded at full load with a 180 °C threshold in this example.

At 70% loading, the two and five minute pulses from **Figure 13** would have amplitudes of 310 and 225 A/phase, respectively. The 5 minute pulse is illustrated in **Figure 17**. In this case, judgment is also required to assess if the GIC(t) is within the capability curve for 70% loading. In general, capability curves are easier to use when GIC(t) is substantially above, or clearly below the GIC thresholds for a given pulse duration.

If a conservative threshold of 160°C were used to account for the age and condition of the transformer, then a new set of capability curves would be required.

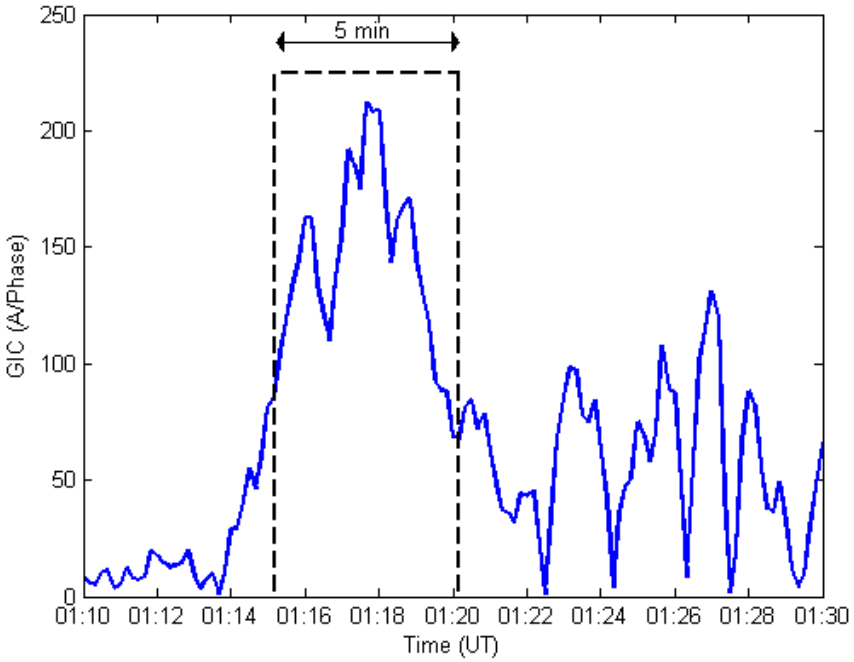

Figure 17: Close-up of GIC(t) and a 5 Minute 225 A/phase GIC Pulse Assuming 75% Load

References

[1] "IEEE Guide for loading mineral-oil-immersed transformers and step-voltage regulators." IEEE Std C57.91-2011 (Revision of IEEE Std C57.91-1995).

[2] Application Guide: Computing Geomagnetically-Induced Current in the Bulk-Power System, NERC. Available at: http://www.nerc.com/comm/PC/Geomagnetic%20Disturbance%20Task%20Force%20GMDTF%202013/GIC%20Application%20Guide%202013_approved.pdf

[3] Girgis, R.; Vedante, K. "Methodology for evaluating the impact of GIC and GIC capability of power transformer designs." IEEE PES 2013 General Meeting Proceedings. Vancouver, Canada.

[4] Marti, L., Rezaei-Zare, A., Narang, A. "Simulation of Transformer Hotspot Heating due to Geomagnetically Induced Currents." IEEE Transactions on Power Delivery, vol.28, no.1. pp 320-327. January 2013.

[5] Benchmark Geomagnetic Disturbance Event Description white paper. Developed by the Project 2013-03 (Geomagnetic Disturbance) standard drafting team. Available at:

http://www.nerc.com/pa/Stand/Pages/Project-2013-03-Geomagnetic-Disturbance-Mitigation.aspx

[6] Lahtinen, Matti. Jarmo Elovaara. "GIC occurrences and GIC test for 400 kV system transformer". IEEE Transactions on Power Delivery, Vol. 17, No. 2. April 2002.

[7] "Screening Criterion for Transformer Thermal Impact Assessment". Developed by the Project 2013-03 (Geomagnetic Disturbance) standard drafting team. Available at:

http://www.nerc.com/pa/Stand/Pages/Project-2013-03-Geomagnetic-Disturbance-Mitigation.aspx

NERC
NORTH AMERICAN ELECTRIC RELIABILITY CORPORATION

Transformer Thermal Impact Assessment White Paper

Project 2013-03 (Geomagnetic Disturbance Mitigation)

TPL-007-1 Transmission System Planned Performance for Geomagnetic Disturbance Events

Background

On May 16, 2013, FERC issued Order No. 779, directing NERC to develop Standards that address risks to reliability caused by geomagnetic disturbances (GMDs) in two stages:

- Stage 1 Standard(s) that require applicable entities to develop and implement Operating Procedures. EOP-010-1 – Geomagnetic Disturbance Operations was approved by FERC in June 2014.
- Stage 2 Standard(s) that require applicable entities to conduct assessments of the potential impact of benchmark GMD events on their systems. If the assessments identify potential impacts, the Standard(s) will require the applicable entity to develop and implement a plan to mitigate the risk.

TPL-007-1 is a new Reliability Standard to specifically address the Stage 2 directives in Order No. 779.

Large power transformers connected to the EHV transmission system can experience both winding and structural hot spot heating as a result of GMD events. TPL-007-1 will require owners of such transformers to conduct thermal analyses of their transformers to determine if the transformers will be able to withstand the thermal transient effects associated with the Benchmark GMD event. This paper discusses methods that can be employed to conduct such analyses, including example calculations.

The primary impact of GMDs on large power transformers is a result of the quasi-dc current that flows through wye-grounded transformer windings. This geomagnetically-induced current (GIC) results in an offset of the ac sinusoidal flux resulting in asymmetric or half-cycle saturation (see **Figure 1**).

Half-cycle saturation results in a number of known effects:

- Hot spot heating of transformer windings due to harmonics and stray flux;
- Hot spot heating of non-current carrying transformer metallic members due to stray flux;
- Harmonics;
- Increase in reactive power absorption; and
- Increase in vibration and noise level.

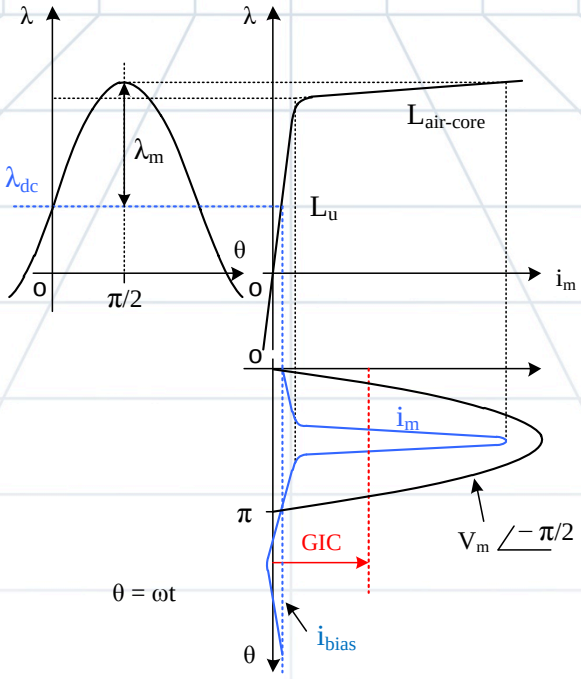

Figure 1: Mapping Magnetization Current to Flux through Core Excitation Characteristics

This paper focuses on hot spot heating of transformer windings and non current-carrying metallic parts. Effects such as the generation of harmonics, increase in reactive power absorption, vibration, and noise are not within the scope of this document.

Technical Considerations

The effects of half-cycle saturation on HV and EHV transformers, namely localized "hot spot" heating, are relatively well understood, but are difficult to quantify. A transformer GMD impact assessment must consider GIC amplitude, duration, and transformer physical characteristics such as design and condition (e.g., age, gas content, and moisture in the oil). A single threshold value of GIC cannot be justified as a "pass or fail" screening criterion where "fail" means that the transformer will suffer damage. A single threshold value of GIC only makes sense in the context where "fail" means that a more detailed study is required and that "pass" means that GIC in a particular transformer is so low that a detailed study is unnecessary. Such a threshold would have to be technically justifiable and sufficiently low to be considered a conservative value within the scope of the benchmark.

The following considerations should be taken into account when assessing the thermal susceptibility of a transformer to half-cycle saturation:

- In the absence of manufacturer specific information, use the temperature limits for safe transformer operation such as those suggested in the IEEE Std C57.91-2011 standard [1] for hot spot heating during short-term emergency operation. This standard does not suggest that exceeding these limits will result in transformer failure, but rather that it will result in additional aging of cellulose in the paper-oil insulation and the potential for the generation of gas bubbles in the bulk oil. Thus, from the point of view of evaluating

possible transformer damage due to increased hot spot heating, these thresholds can be considered conservative for a transformer in good operational condition.

- The worst case temperature rise for winding and metallic part (e.g., tie plate) heating should be estimated taking into consideration the construction characteristics of the transformer as they pertain to dc flux offset in the core (e.g., single-phase, shell, 5 and 3-leg three-phase construction).
- Bulk oil temperature due to ambient temperature and transformer loading must be added to the incremental temperature rise caused by hot spot heating. For planning purposes, maximum ambient and loading temperature should be used unless there is a technically justified reason to do otherwise.
- The time series or "waveshape" of the reference GMD event in terms of peak amplitude, duration, and frequency of the geoelectric field has an important effect on hot spot heating. Winding and metallic part hot spot heating have different thermal time constants, and their temperature rise will be different if the GIC currents are sustained for 2, 10, or 30 minutes for a given GIC peak amplitude.
- The "effective" GIC in autotransformers (reflecting the different GIC ampere-turns in the common and the series windings) must be used in the assessment. The effective current $I_{dc,eq}$ in an autotransformer is defined by [2].

$$I_{dc,eq} = I_H + (I_N/3 - I_H)V_X/V_H \quad (1)$$

where

I_H is the dc current in the high voltage winding;
I_N is the neutral dc current;
V_H is the rms rated voltage at HV terminals;
V_X is the rms rated voltage at the LV terminals.

Transformer Thermal Impact Assessment Process

A simplified thermal assessment may be based on Table 2 from the "Screening Criterion for Transformer Thermal Impact Assessment" white paper [7]. This table, shown as Table 1 below, provides the peak metallic hot spot temperatures that can be reached using conservative ~~screening~~ thermal models. To use Table 1, one must select the bulk oil temperature and the threshold for metallic hot spot heating, for instance, from reference [1] after allowing for possible de-rating due to transformer condition. If the effective GIC results in higher than threshold temperatures, then the use of a detailed thermal assessment as described below should be carried out.

Table 1: Upper Bound of Peak Metallic Hot Spot Temperatures Calculated Using the Benchmark GMD Event

Effective GIC (A/phase)	Metallic hot spot Temperature (°C)	Effective GIC(A/phase)	Metallic hot spot Temperature (°C)
0	80	~~140~~100	~~172~~182
10	~~106~~107	~~150~~110	~~180~~186
20	~~116~~128	~~160~~120	~~187~~190
30	~~125~~139	~~170~~130	~~194~~193
40	~~132~~148	~~180~~140	~~200~~204
50	~~138~~157	~~190~~150	~~208~~213
60	~~143~~169	~~200~~160	~~214~~221
70	~~147~~170	~~210~~170	~~221~~230
75	~~150~~172	~~220~~180	~~224~~234
80	~~152~~175	~~230~~190	~~228~~241
90	~~156~~179	~~240~~200	~~233~~247
~~100~~	~~159~~	~~250~~	~~239~~
~~110~~	~~163~~	~~260~~	~~245~~
~~120~~	~~165~~	~~270~~	~~251~~
~~130~~	~~168~~	~~280~~	~~257~~

Two different ways to carry out a detailed thermal impact assessment are discussed below. In addition, other approaches and models approved by international standard-setting organizations such as the Institute of Electrical and Electronic Engineers (IEEE) or International Council on Large Electric Systems (CIGRE) may also provide technically justified methods for performing thermal assessments. All thermal assessment methods should be demonstrably equivalent to assessments that use the benchmark GMD event.

1. Transformer manufacturer GIC capability curves. These curves relate permissible peak GIC (obtained by the user from a steady-state GIC calculation) and loading, for a specific transformer. An example of manufacturer capability curves is provided in **Figure 2**. Presentation details vary between manufacturers, and limited information is available regarding the assumptions used to generate these curves, in particular, the assumed waveshape or duration of the effective GIC. Some manufacturers assume that the waveshape of the GIC in the transformer windings is a square pulse of 2, 10, or 30 minutes in duration. In the case of the transformer capability curve shown in **Figure 2** [3], a square pulse of 900 A/phase with a duration of 2 minutes would

cause the Flitch plate hot spot to reach a temperature of 180 °C at full load. While GIC capability curves are relatively simple to use, an amount of engineering judgment is necessary to ascertain which portion of a GIC waveshape is equivalent to, for example, a 2 minute pulse. Also, manufacturers generally maintain that in the absence of transformer standards defining thermal duty due to GIC, such capability curves must be developed for every transformer design and vintage.

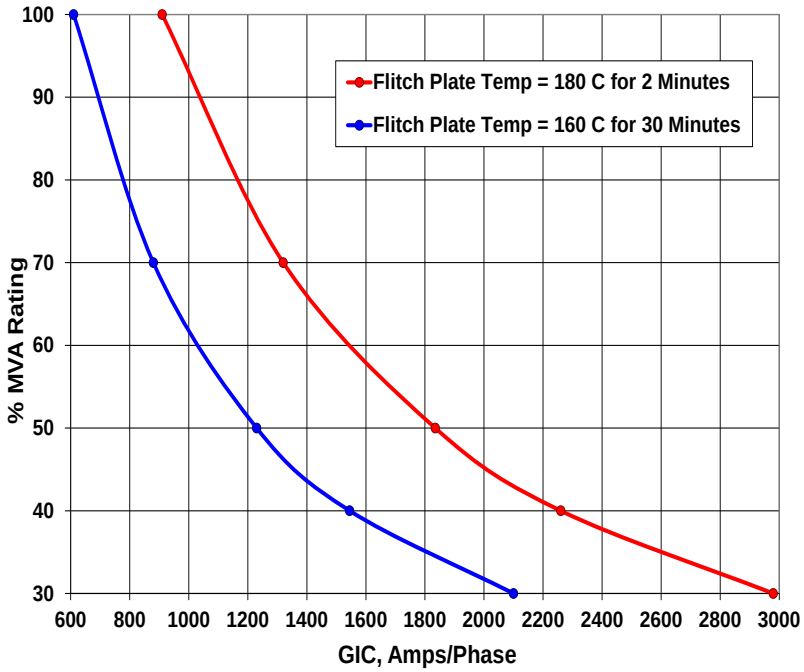

Figure 2: Sample GIC Manufacturer Capability Curve of a Large Single-Phase Transformer Design using the Flitch Plate Temperature Criteria [3]

2. Thermal response simulation[1]. The input to this type of simulation is the time series or waveshape of effective GIC flowing through a transformer (taking into account the actual configuration of the system), and the result of the simulation is the hot spot temperature (winding or metallic part) time sequence for a given transformer. An example of GIC input and hotspot temperature time series values from [4] are shown in **Figure 3**. The hot spot thermal transfer functions can be obtained from measurements or calculations provided by transformer manufacturers. Conservative default values can be used (e.g. those provided in [4]) when specific data are not available. Hot spot temperature thresholds shown in **Figure 3** are consistent with IEEE Std C57.91 emergency loading hot spot limits. Emergency loading time limit is usually 30 minutes.

[1] Technical details of this methodology can be found in [4].

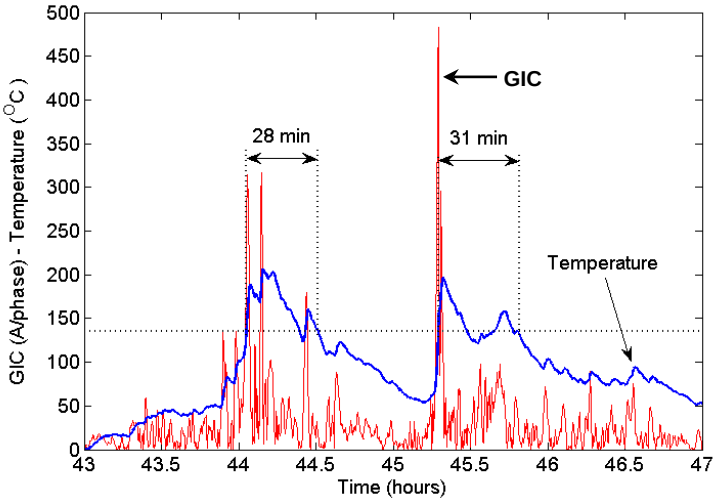

Figure 3: Sample Tie Plate Temperature Calculation
Blue trace is incremental temperature and red trace is the magnitude of the GIC/phase [4]

It is important to reiterate that the characteristics of the time sequence or "waveshape" are very important in the assessment of the thermal impact of GIC on transformers. Transformer hot spot heating is not instantaneous. The thermal time constants of transformer windings and metallic parts are typically on the order of minutes to tens of minutes; therefore, hot spot temperatures are heavily dependent on GIC history and rise time, amplitude and duration of GIC in the transformer windings, bulk oil temperature due to loading, ambient temperature and cooling mode.

Calculation of the GIC Waveshape for a Transformer

The following procedure can be used to generate time series GIC data, i.e. GIC(t), using a software program capable of computing GIC in the steady-state. The steps are as follows:

1. Calculate contribution of GIC due to eastward and northward geoelectric fields for the transformer under consideration;
2. Scale the GIC contribution according to the reference geoelectric field time series to produce the GIC time series for the transformer under consideration.

Most available GIC–capable software packages can calculate GIC in steady-state in a transformer assuming a uniform eastward geoelectric field of 1 V/km (GIC_E) while the northward geoelectric field is zero. Similarly, GIC_N can be obtained for a uniform northward geoelectric field of 1 V/km while the eastward geoelectric field is zero. GIC_E and GIC_N are the normalized GIC contributions for the transformer under consideration.

If the earth conductivity is assumed to be uniform (or laterally uniform) in the transmission system of interest, then the transformer GIC (in A/phase) for any value of $E_E(t)$ and $E_N(t)$ can be calculated using (2) [2].

$$GIC(t) = \left|E(t)\right| \cdot \left\{GIC_E \sin(\varphi(t)) + GIC_N \cos(\varphi(t))\right\} \quad (2)$$

where

$$|E(t)| = \sqrt{E_N^2(t) + E_E^2(t)} \quad (3)$$

$$\varphi(t) = \tan^{-1}\left(\frac{E_E(t)}{E_N(t)}\right) \quad (4)$$

$$GIC(t) = E_E(t) \cdot GIC_E + E_N(t) \cdot GIC_N \quad (5)$$

GIC_N is the effective GIC due to a northward geoelectric field of 1 V/km, and GIC_E is the effective GIC due to an eastward geoelectric field of 1 V/km. The units for GIC_N and GIC_E are A/phase/V/km)

The geoelectric field time series $E_N(t)$ and $E_E(t)$ is obtained, for instance, from the reference geomagnetic field time series [5] after the appropriate geomagnetic latitude scaling factor α is applied[2]. The reference geoelectric field time series is calculated using the reference earth model. When using this geoelectric field time series where a different earth model is applicable, it should be scaled with the conductivity scaling factor β[3]. Alternatively, the geoelectric field can be calculated from the reference geomagnetic field time series after the appropriate geomagnetic latitude scaling factor α is applied and the appropriate earth model is used. In such case, the conductivity scaling factor β is not applied because it is already accounted for by the use of the appropriate earth model.

Applying (5) to each point in $E_N(t)$ and $E_E(t)$ results in GIC(t).

GIC(t) Calculation Example

Let us assume that from the steady-state solution, the effective GIC in this transformer is GIC_E = -20 A/phase if E_N=0, E_E=1 V/km and GIC_N = 26 A/phase if E_N=1 V/km, E_E=0. Let us also assume the geomagnetic field time series corresponds to a geomagnetic latitude where α = 1 and that the earth conductivity corresponds to the reference earth model in [5]. The resulting geoelectric field time series is shown in **Figure 4**. Therefore:

$$GIC(t) = E_E(t) \cdot GIC_E + E_N(t) \cdot GIC_N \text{ (A/phase)} \quad (6)$$

$$GIC(t) = -E_E(t) \cdot 20 + \cdot E_N(t) \cdot 26 \text{ (A/phase)} \quad (7)$$

The resulting GIC waveshape GIC(t) is shown in **Figures 5 and 6** and can subsequently be used for thermal analysis.

[2] The geomagnetic factor α is described in [2] and is used to scale the geomagnetic field according to geomagnetic latitude. The lower the geomagnetic latitude (closer to the equator), the lower the amplitude of the geomagnetic field.

[3] The conductivity scaling factor β is described in [2], and is used to scale the geoelectric field according to the conductivity of different physiographic regions. Lower conductivity results in higher β scaling factors.

It should be emphasized that even for the same reference event, the GIC(t) waveshape in every transformer will be different, depending on the location within the system and the number and orientation of the circuits connecting to the transformer station. Assuming a single generic GIC(t) waveshape to test all transformers is incorrect.

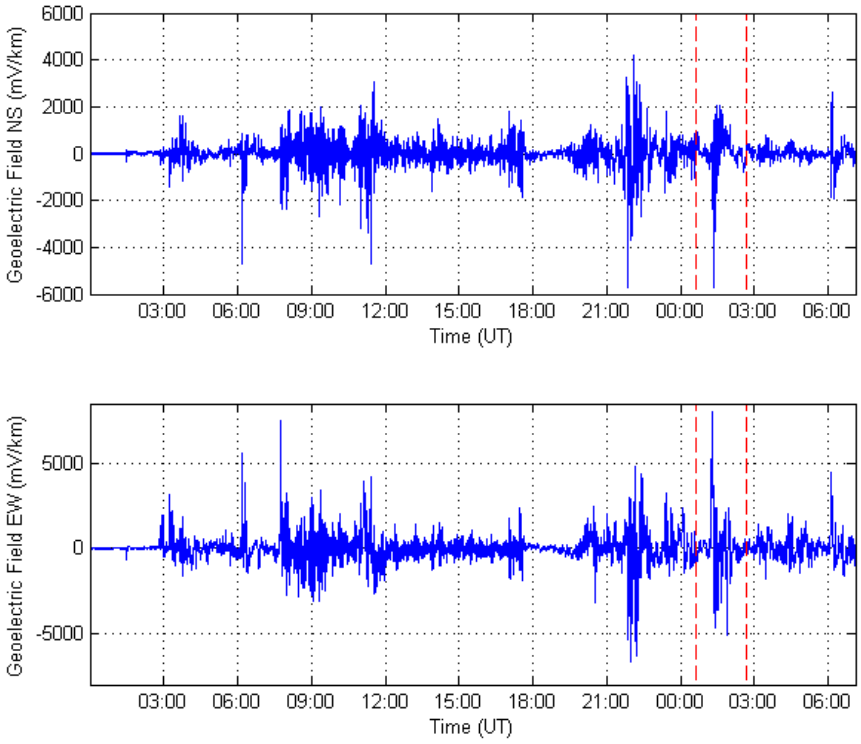

Figure 4: Calculated Geoelectric Field $E_N(t)$ and $E_E(t)$ Assuming $\alpha=1$ and $\beta=1$ (Reference Earth Model). Zoom area for subsequent graphs is highlighted. Dashed lines approximately show the close-up area for subsequent Figures.

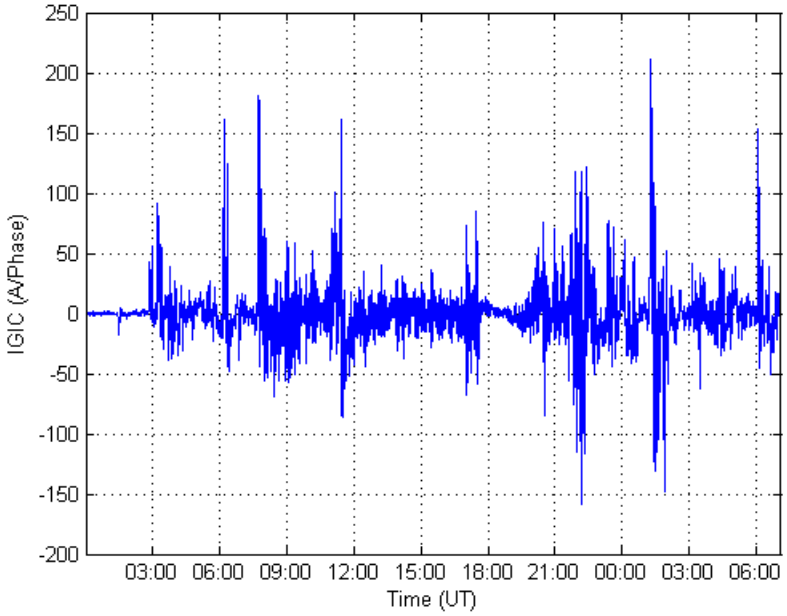

Figure 5: Calculated GIC(t) Assuming α=1 and β=1 (Reference Earth Model)

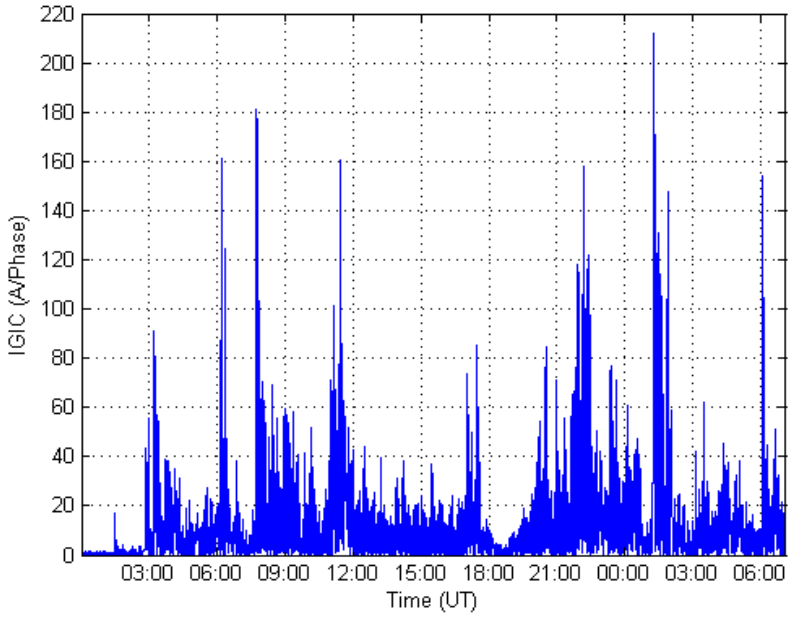

Figure 6: Calculated Magnitude of GIC(t) Assuming α=1 and β=1 (Reference Earth Model)

Transformer Thermal Assessment Examples

There are two basic ways to carry out a transformer thermal analysis once the GIC time series GIC(t) is known for a given transformer: 1) calculating the thermal response as a function of time; and 2) using manufacturer's capability curves.

Example 1: Calculating thermal response as a function of time using a thermal response tool

The thermal step response of the transformer can be obtained for both winding and metallic part hot spots from: 1) measurements; 2) manufacturer's calculations; or 3) generic published values. **Figure 7** shows the measured metallic hot spot thermal response to a dc step of 16.67 A/phase of the top yoke clamp from [6] that will be used in this example. **Figure 8** shows the measured incremental temperature rise (asymptotic response) of the same hot spot to long duration GIC steps.[4]

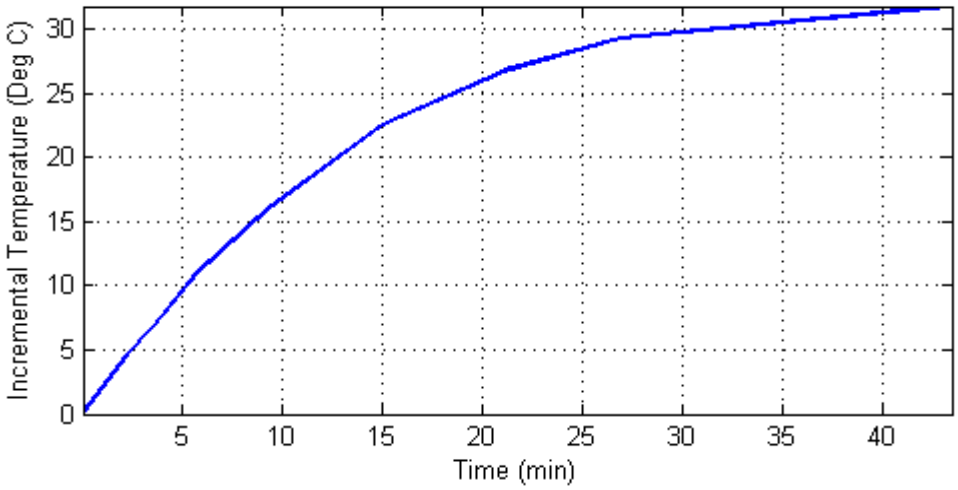

Figure 7: Thermal Step Response to a 16.67 Amperes per Phase dc Step
Metallic hot spot heating.

[4] Heating of bulk oil due to the hot spot temperature increase is not included in the asymptotic response because the time constant of bulk oil heating is at least an order of magnitude larger than the time constants of hot spot heating.

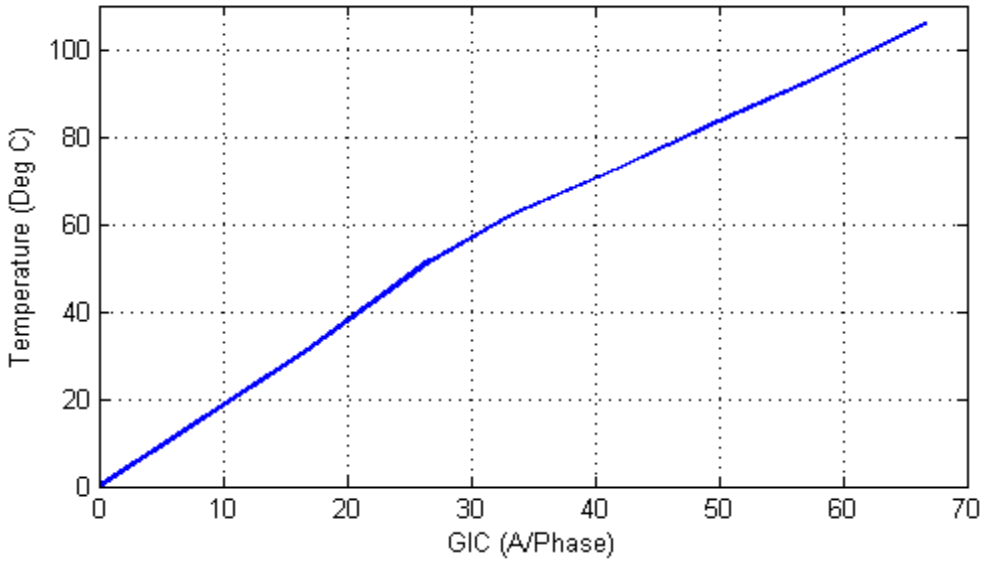

Figure 8: Asymptotic Thermal Step Response
Metallic hot spot heating.

The step response in **Figure 7** was obtained from the first GIC step of the tests carried out in [6]. The asymptotic thermal response in **Figure 8** was obtained from the final or near-final temperature values after each subsequent GIC step. **Figure 9** shows a comparison between measured temperatures and the calculated temperatures using the thermal response model used in the rest of this discussion.

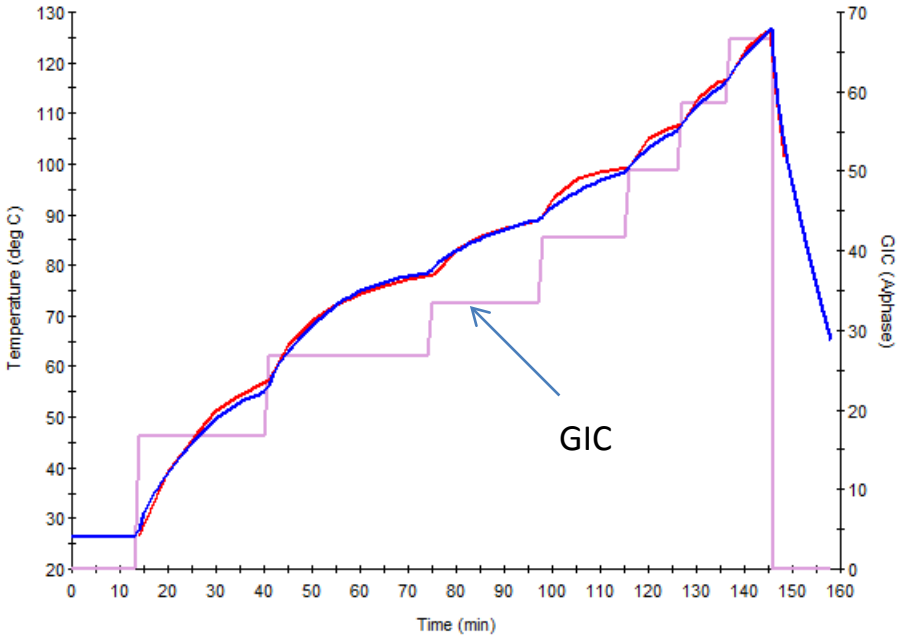

Figure 9: Comparison of measured temperatures (red trace) and simulation results (blue trace). Injected current is represented by the magenta trace.

To obtain the thermal response of the transformer to a GIC waveshape such as the one in **Figure 6**, a thermal response model is required. To create a thermal response model, the measured or manufacturer-calculated transformer thermal step responses (winding and metallic part) for various GIC levels are required. The GIC(t) time series or waveshape is then applied to the thermal model to obtain the incremental temperature rise as a function of time $\theta(t)$ for the GIC(t) waveshape. The total temperature is calculated by adding the oil temperature, for example, at full load.

Figure 10 illustrates the calculated GIC(t) and the corresponding hot spot temperature time series $\theta(t)$. **Figure 11** illustrates a close-up view of the peak transformer temperatures calculated in this example.

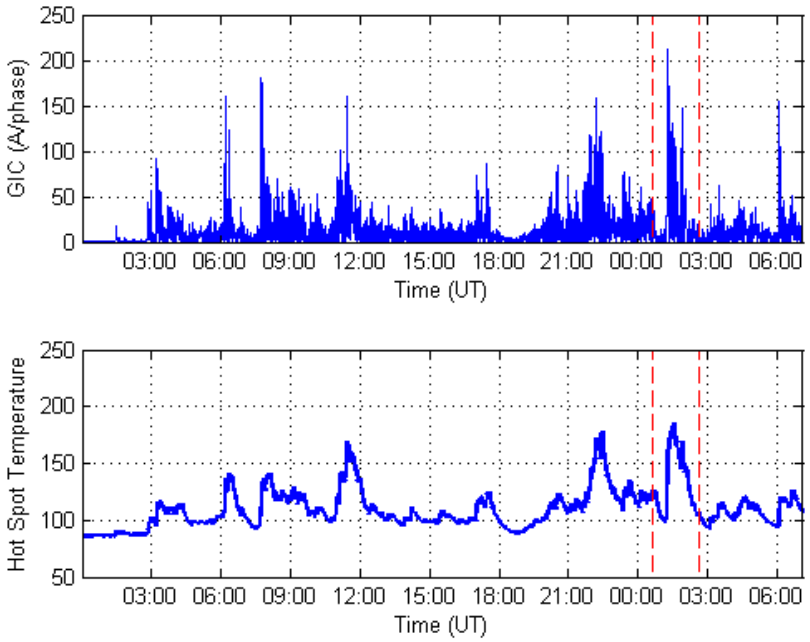

Figure 10: Magnitude of GIC(t) and Metallic Hot Spot Temperature $\theta(t)$ Assuming Full Load Oil Temperature of 85.3°C (40°C ambient). Dashed lines approximately show the close-up area for subsequent Figures.

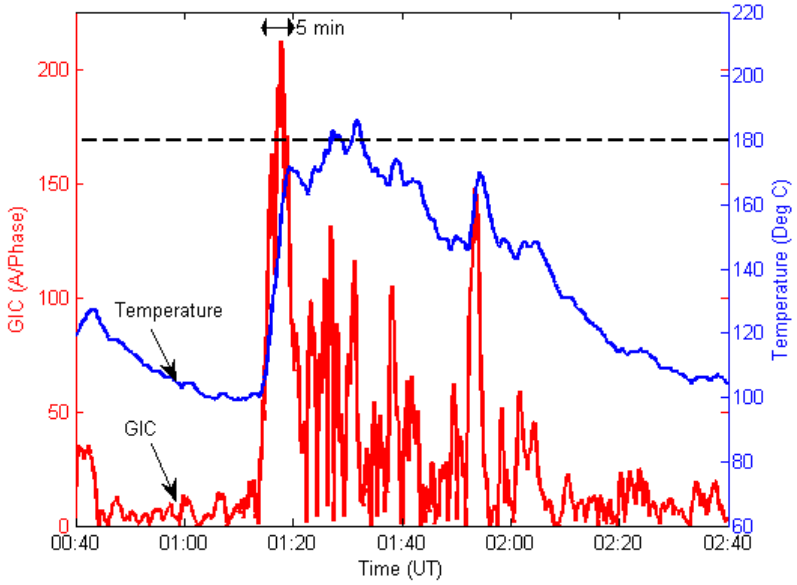

Figure 11: Close-up of Metallic Hot Spot Temperature Assuming a Full Load
(Blue trace is θ(t). Red trace is GIC(t))

In this example, the IEEE Std C57.91 emergency loading hot spot threshold of 200°C for metallic hot spot heating is not exceeded. Peak temperature is 186°C. The IEEE standard is silent as to whether the temperature can be higher than 200°C for less than 30 minutes. Manufacturers can provide guidance on individual transformer capability.

It is not unusual to use a lower temperature threshold of 180°C to account for calculation and data margins, as well as transformer age and condition. **Figure 11** shows that 180°C will be exceeded for 5 minutes.

At 75% loading, the initial temperature is 64.6 °C rather than 85.3 °C, and the hot spot temperature peak is 165°C, well below the 180°C threshold (see **Figure 12**).

If a conservative threshold of 160°C were used to account for the age and condition of the transformer, then the full load limits would be exceeded for approximately 22 minutes.

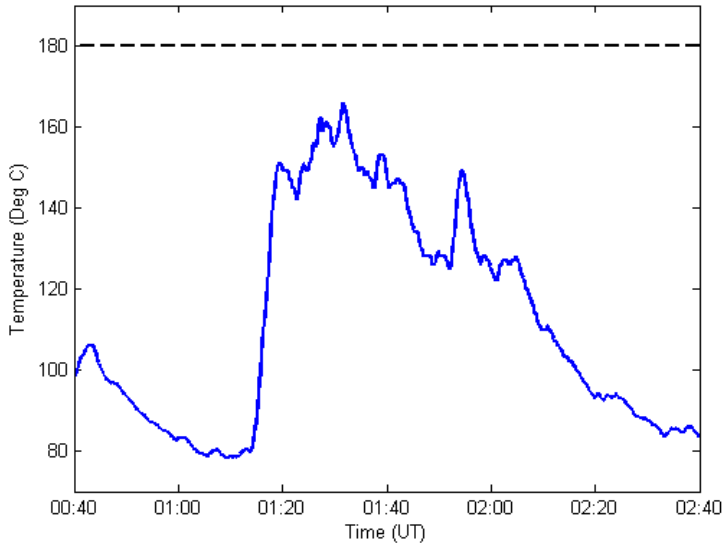

Figure 12: Close-up of Metallic Hot Spot Temperature Assuming a 75% Load
(Oil temperature of 64.5°C)

Example 2: Using a Manufacturer's Capability Curves

The capability curves used in this example are shown in **Figure 13**. To maintain consistency with the previous example, these particular capability curves have been reconstructed from the thermal step response shown in **Figures 7** and **8**, and the simplified loading curve shown in **Figure ~~13~~ 14** (calculated using formulas from IEEE Std C57.91).

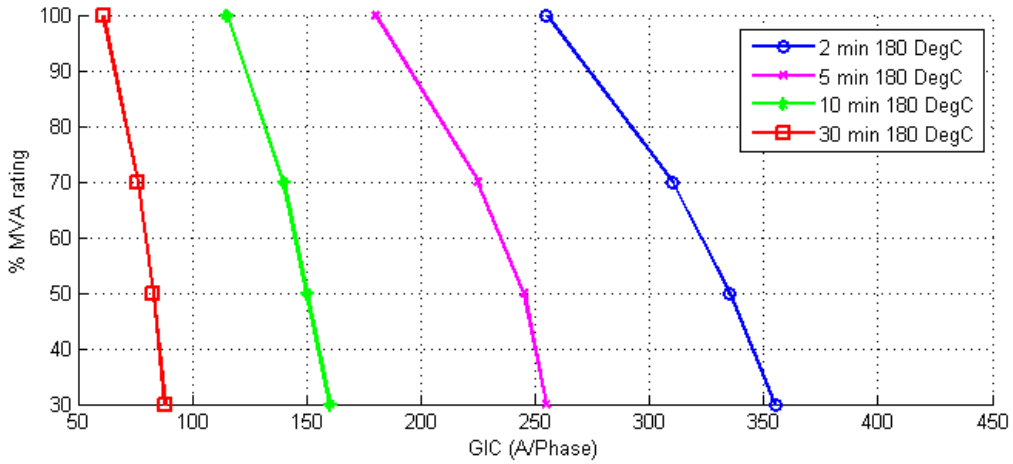

Figure 13: Capability Curve of a Transformer Based on the Thermal Response Shown in Figures 8 and 9.

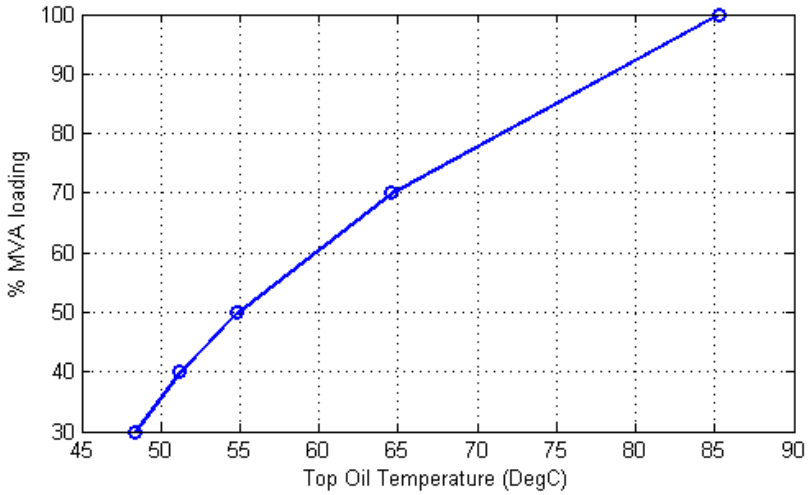

Figure 14: Simplified Loading Curve Assuming 40°C Ambient Temperature.

The basic notion behind the use of capability curves is to compare the calculated GIC in a transformer with the limits at different GIC pulse widths. A narrow GIC pulse has a higher limit than a longer duration or wider one. If the calculated GIC and assumed pulse width falls below the appropriate pulse width curve, then the transformer is within its capability.

To use these curves, it is necessary to estimate an equivalent square pulse that matches the waveshape of GIC(t), generally at a GIC(t) peak. **Figure 15** shows a close-up of the GIC near its highest peak superimposed to a 255 Amperes per phase, 2 minute pulse at 100% loading from **Figure 13**. Since a narrow 2-minute pulse is not representative of GIC(t) in this case, a 5 minute pulse with an amplitude of 180 A/phase at 100% loading has been superimposed on **Figure 16**. It should be noted that a 255 A/phase, 2 minute pulse is equivalent to a 180 A/phase 5 minute pulse from the point of view of transformer capability. Deciding what GIC pulse is equivalent to the portion of GIC(t) under consideration is a matter of engineering judgment.

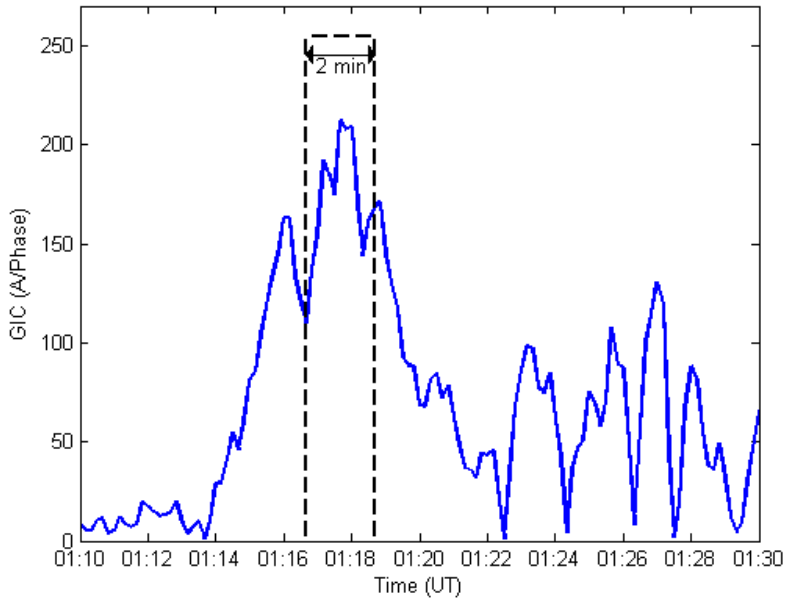

Figure 15: Close-up of GIC(t) and a 2 minute 255 A/phase GIC pulse at full load

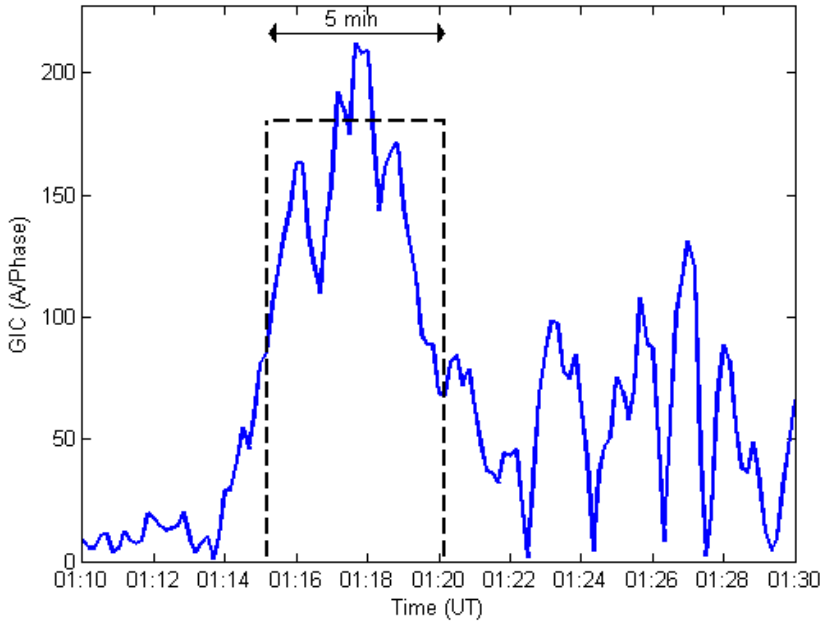

Figure 16: Close-up of GIC(t) and a Five Minute 180 A/phase GIC Pulse at Full Load

When using a capability curve, it should be understood that the curve is derived assuming that there is no hot spot heating due to prior GIC at the time the GIC pulse occurs (only an initial temperature due to loading). Therefore, in addition to estimating the equivalent pulse that matches GIC(t), prior hot spot heating must be accounted for. From

these considerations, it is unclear whether the capability curves would be exceeded at full load with a 180 °C threshold in this example.

At 70% loading, the two and five minute pulses from **Figure 13** would have amplitudes of 310 and 225 A/phase, respectively. The 5 minute pulse is illustrated in **Figure 17**. In this case, judgment is also required to assess if the GIC(t) is within the capability curve for 70% loading. In general, capability curves are easier to use when GIC(t) is substantially above, or clearly below the GIC thresholds for a given pulse duration.

If a conservative threshold of 160°C were used to account for the age and condition of the transformer, then a new set of capability curves would be required.

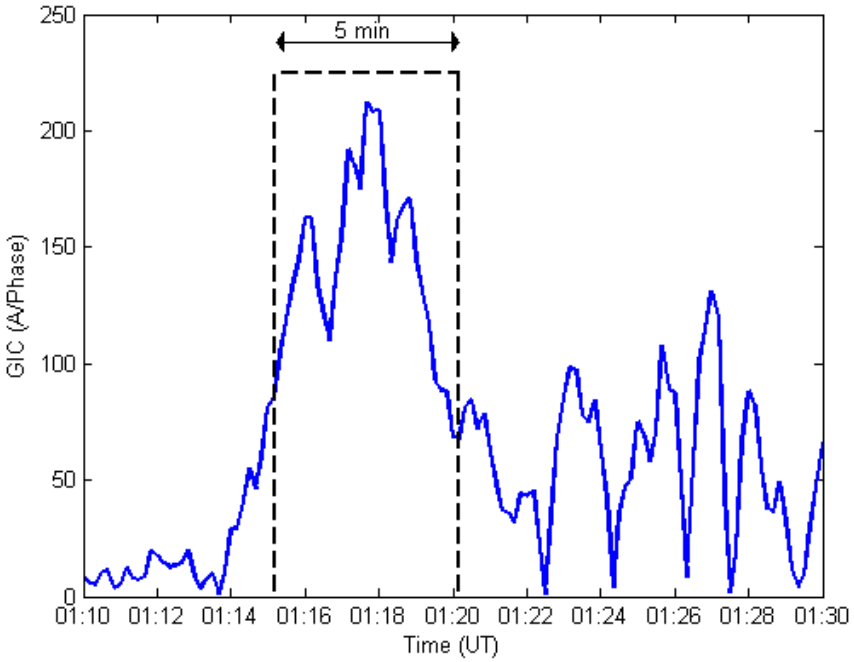

Figure 17: Close-up of GIC(t) and a 5 Minute 225 A/phase GIC Pulse Assuming 75% Load

References

[1] "IEEE Guide for loading mineral-oil-immersed transformers and step-voltage regulators." IEEE Std C57.91-2011 (Revision of IEEE Std C57.91-1995).

[2] Application Guide: Computing Geomagnetically-Induced Current in the Bulk-Power System, NERC. Available at: http://www.nerc.com/comm/PC/Geomagnetic%20Disturbance%20Task%20Force%20GMDTF%202013/GIC%20Application%20Guide%202013_approved.pdf

[3] Girgis, R.; Vedante, K. "Methodology for evaluating the impact of GIC and GIC capability of power transformer designs." IEEE PES 2013 General Meeting Proceedings. Vancouver, Canada.

[4] Marti, L., Rezaei-Zare, A., Narang, A. "Simulation of Transformer Hotspot Heating due to Geomagnetically Induced Currents." IEEE Transactions on Power Delivery, vol.28, no.1. pp 320-327. January 2013.

[5] Benchmark Geomagnetic Disturbance Event Description white paper. Developed by the Project 2013-03 (Geomagnetic Disturbance) standard drafting team. Available at:

http://www.nerc.com/pa/Stand/Pages/Project-2013-03-Geomagnetic-Disturbance-Mitigation.aspx

[6] Lahtinen, Matti. Jarmo Elovaara. "GIC occurrences and GIC test for 400 kV system transformer". IEEE Transactions on Power Delivery, Vol. 17, No. 2. April 2002.

[7] "Screening Criterion for Transformer Thermal Impact Assessment". ~~paper.~~ Developed by the Project 2013-03 (Geomagnetic Disturbance) standard drafting team. Available at:

http://www.nerc.com/pa/Stand/Pages/Project-2013-03-Geomagnetic-Disturbance-Mitigation.aspx

NERC
NORTH AMERICAN ELECTRIC RELIABILITY CORPORATION

Screening Criterion for Transformer Thermal Impact Assessment

Project 2013-03 (Geomagnetic Disturbance Mitigation)

TPL-007-1 Transmission System Planned Performance for Geomagnetic Disturbance Events

Summary

Proposed standard TPL-007-1 – Transmission System Planned Performance for Geomagnetic Disturbance Events requires applicable entities to conduct assessments of the potential impact of benchmark GMD events on their systems. The standard requires transformer thermal impact assessments to be performed on power transformers with high side, wye-grounded windings with terminal voltage greater than 200 kV. Transformers are exempt from the thermal impact assessment requirement if the maximum effective geomagnetically-induced current (GIC) in the transformer is less than 75 A per phase as determined by GIC analysis of the system. Based on published power transformer measurement data as described below, an effective GIC of 75 A per phase is a conservative screening criterion. To provide an added measure of conservatism, the 75 A per phase threshold, although derived from measurements in single-phase units, is applicable to transformers with all core types (e.g., three-limb, three-phase).

Justification

Applicable entities are required to carry out a thermal assessment with GIC(t) calculated using the benchmark GMD event geomagnetic field time series or waveshape for effective GIC values above a screening threshold. The calculated GIC(t) for every transformer will be different because the length and orientation of transmission circuits connected to each transformer will be different even if the geoelectric field is assumed to be uniform. However, for a given thermal model and maximum effective GIC there are upper and lower bounds for the peak hot spot temperatures. These are shown in **Figure 1** using three available thermal models based on direct temperature measurements.

The results shown in **Figure 1** summarize the peak metallic hot spot temperatures when GIC(t) is calculated using (1), and systematically varying GIC_E and GIC_N to account for all possible orientation of circuits connected to a transformer. The transformer GIC (in A/phase) for any value of E_E (t) and E_N(t) can be calculated using equation (1) from reference [1].

$$GIC(t) = \left|E(t)\right| \cdot \left\{GIC_E \sin(\varphi(t)) + GIC_N \cos(\varphi(t))\right\} \quad (1)$$

where

$$|E(t)| = \sqrt{E_N^2(t) + E_E^2(t)} \tag{2}$$

$$\varphi(t) = \tan^{-1}\left(\frac{E_E(t)}{E_N(t)}\right) \tag{3}$$

$$GIC(t) = E_E(t) \cdot GIC_E + E_N(t) \cdot GIC_N \tag{4}$$

GIC_N is the effective GIC due to a northward geoelectric field of 1 V/km, and GIC_E is the effective GIC due to an eastward geoelectric field of 1 V/km. The units for GIC_N and GIC_E are A/phase/V/km.

It should be emphasized that with the thermal models used and the benchmark GMD event geomagnetic field waveshape, peak hot spot temperatures must lie below the envelope shown in **Figure 1**. The x-axis in Figure 1 corresponds to the absolute value of peak GIC(t). Effective maximum GIC for a transformer corresponds to a worst-case geoelectric field orientation, which is network-specific. Figure 1 represents a possible range, not the specific thermal response for a given effective GIC and orientation.

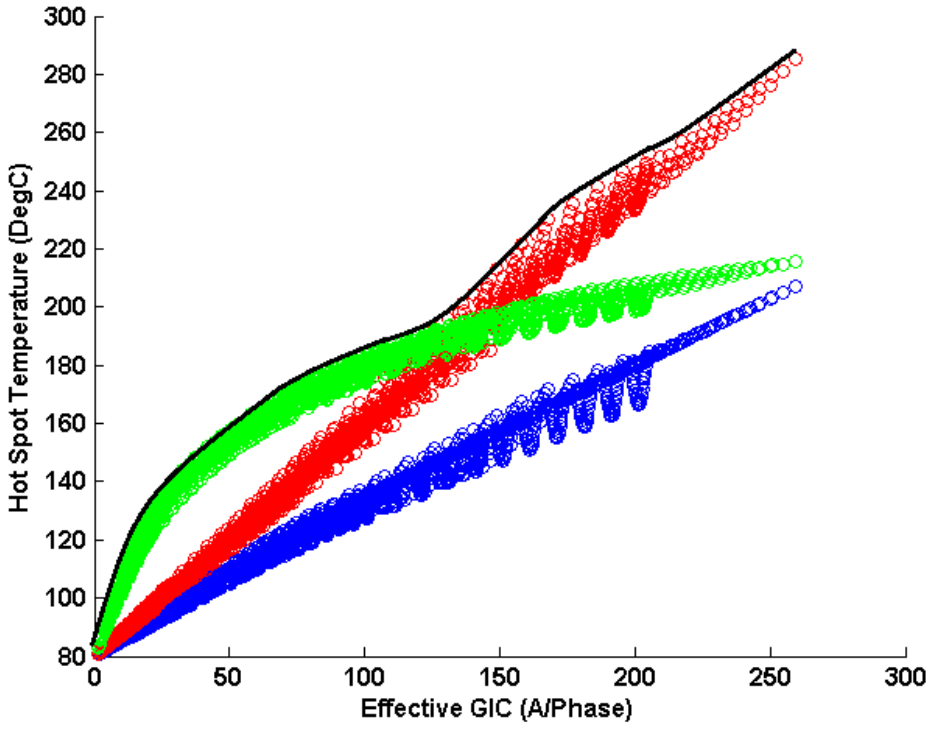

Figure 1: Metallic hot spot temperatures calculated using the benchmark GMD event. Red: SVC coupling transformer model [2]. Blue: Fingrid model [3]. Green: Autotransformer model [4].

Consequently, with the most conservative thermal models known at this point in time, the peak metallic hot spot temperature obtained with the benchmark GMD event waveshape assuming an effective GIC magnitude of 75 A per phase will result in a peak temperature between 160°C and 172°C when the bulk oil temperature is 80°C (full load bulk oil temperature). The upper boundary of 172°C remains well below the metallic hot spot 200°C threshold for short-time emergency loading suggested in IEEE Std C57.91-2011 [5] (see Table 1).

TABLE 1:
Excerpt from Maximum Temperature Limits Suggested in IEEE C57.91-2011

	Normal life expectancy loading	Planned loading beyond nameplate rating	Long-time emergency loading	Short-time emergency loading
Insulated conductor hottest-spot temperature °C	120	130	140	180
Other metallic hot-spot temperature (in contact and not in contact with insulation), °C	140	150	160	200
Top-oil temperature °C	105	110	110	110

The selection of the 75 A per phase screening threshold is based on the following considerations:

- A thermal assessment using the most conservative thermal models known to date will not result in peak hot spot temperatures above 172°C. Transformer thermal assessments should not be required by Reliability Standards when results will fall well below IEEE Std C57.91-2011 limits.
- Applicable entities may choose to carry out a thermal assessment when the effective GIC is below 75 A per phase to take into account the age or condition of specific transformers where IEEE Std C57.91- 2011 limits could be assumed to be lower than 200°C.
- The models used to determine the 75 A per phase screening threshold are known to be conservative at higher values of effective GIC, especially the SVC coupling transformer model in [2].
- Thermal models in peer-reviewed technical literature, especially those calculated models without experimental validation, are less conservative than the models used to determine the screening threshold. Therefore, a technically-justified thermal assessment for effective GIC below 75 A per phase using the benchmark GMD event geomagnetic field waveshape will always result in a "pass" on the basis of the state of the knowledge at this point in time.
- Based on simulations, the 75 A per phase screening threshold will result in a maximum instantaneous peak hot spot temperature of 172°C. However, IEEE Std C57.91- 2011 limits assume short term emergency operation (typically 30 minutes). As illustrated in **Figure 2**, simulations of the 75 A per phase screening threshold result in 30-minute duration hot spot temperatures of about

155°C. The threshold provides an added measure of conservatism in not taking into account the duration of hot spot temperatures.

- The models used in the determination of the threshold are conservative but technically justified.
- Winding hot spots are not the limiting factor in terms of hot spots due to half-cycle saturation, therefore the screening criterion is focused on metallic part hot spots only.

The 75 A per phase screening threshold was determined using single-phase transformers, but is applicable to all types of transformer construction. While it is known that some transformer types such as three-limb, three-phase transformers are intrinsically less susceptible to GIC, it is not known by how much, on the basis of experimentally-supported models.

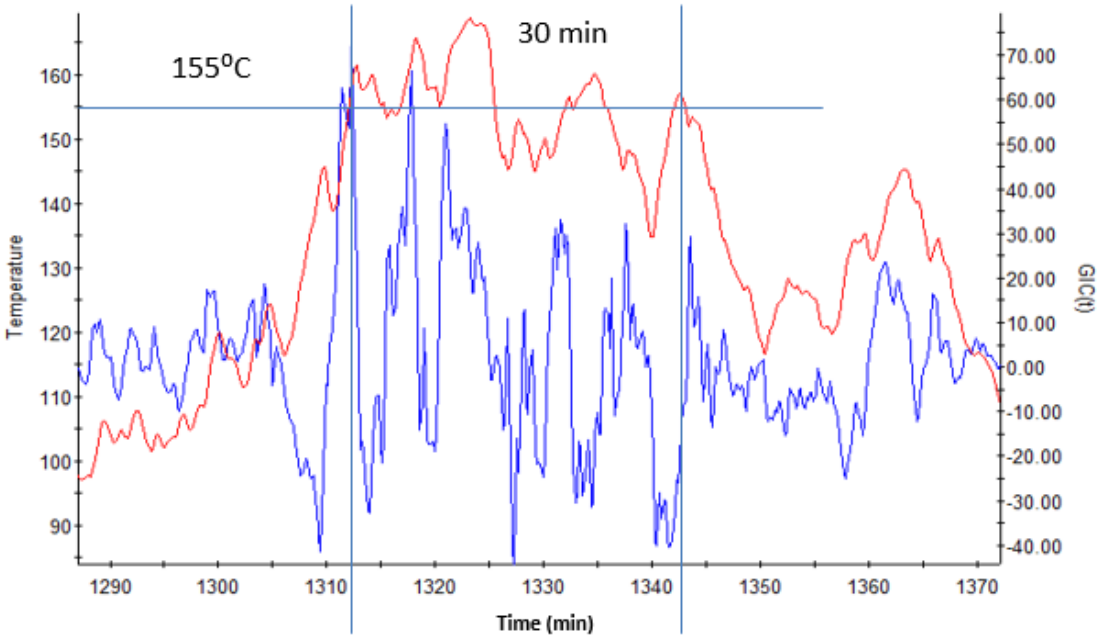

Figure 2: Metallic hot spot temperatures calculated using the benchmark GMD event. Red: metallic hot spot temperature. Blue: GIC(t) that produces the maximum hot spot temperature with peak GIC(t) scaled to 75 A/phase.

Appendix

The envelope used for thermal screening (Figure 1) is derived from two thermal models. The first is based on laboratory measurements carried out on 500/16.5 kV 400 MVA single-phase Static Var Compensator (SVC) coupling transformer [2]. Temperature measurements were carried out at relatively small values of GIC (see **Figure 3**). The asymptotic thermal response for this model is the linear extrapolation of the known measurement values. Although the near-linear behavior of the asymptotic thermal response is consistent with the measurements made on a Fingrid 400 kV 400 MVA five-leg core-type fully-wound transformer [3] (see **Figures 4 and 5**), the extrapolation from low values of GIC is very conservative, but reasonable for screening purposes.

The second transformer model is based on a combination of measurements and modeling for a 400 kV 400 MVA single-phase core-type autotransformer [4] (see **Figures 6 and 7**). The asymptotic thermal behavior of this transformer shows a "down-turn" at high values of GIC as the tie plate increasingly saturates but relatively high temperatures for lower values of GIC. The hot spot temperatures are higher than for the two other models for GIC less than 125 A per phase.

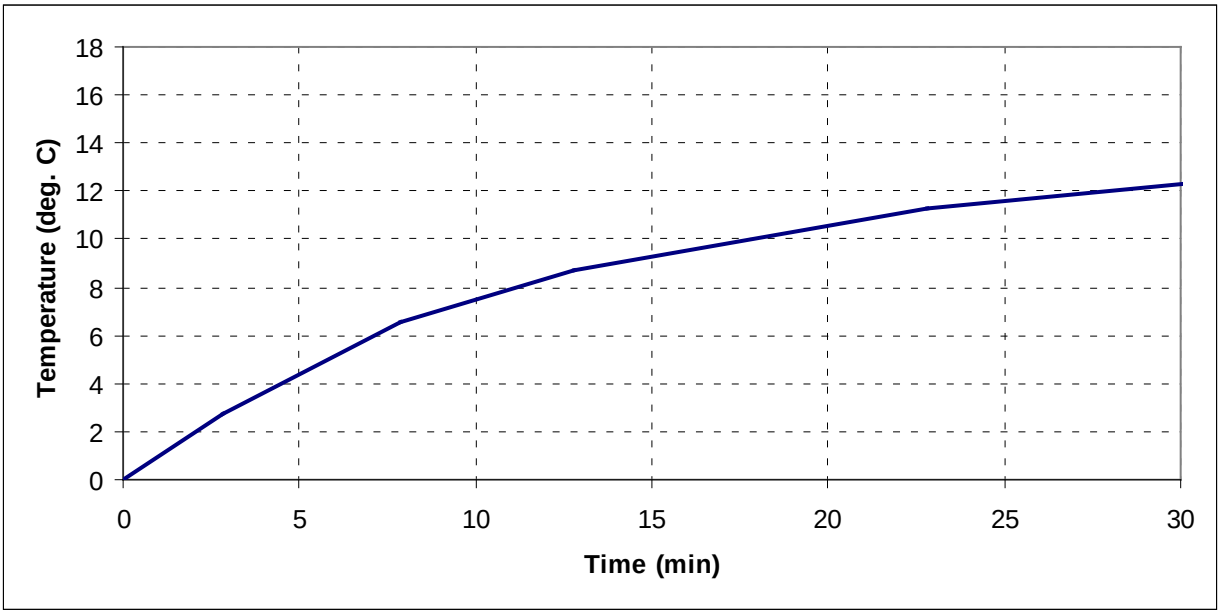

Figure 3: Thermal step response of the tie plate of a 500 kV 400 MVA single-phase SVC coupling transformer to a 5 A per phase dc step.

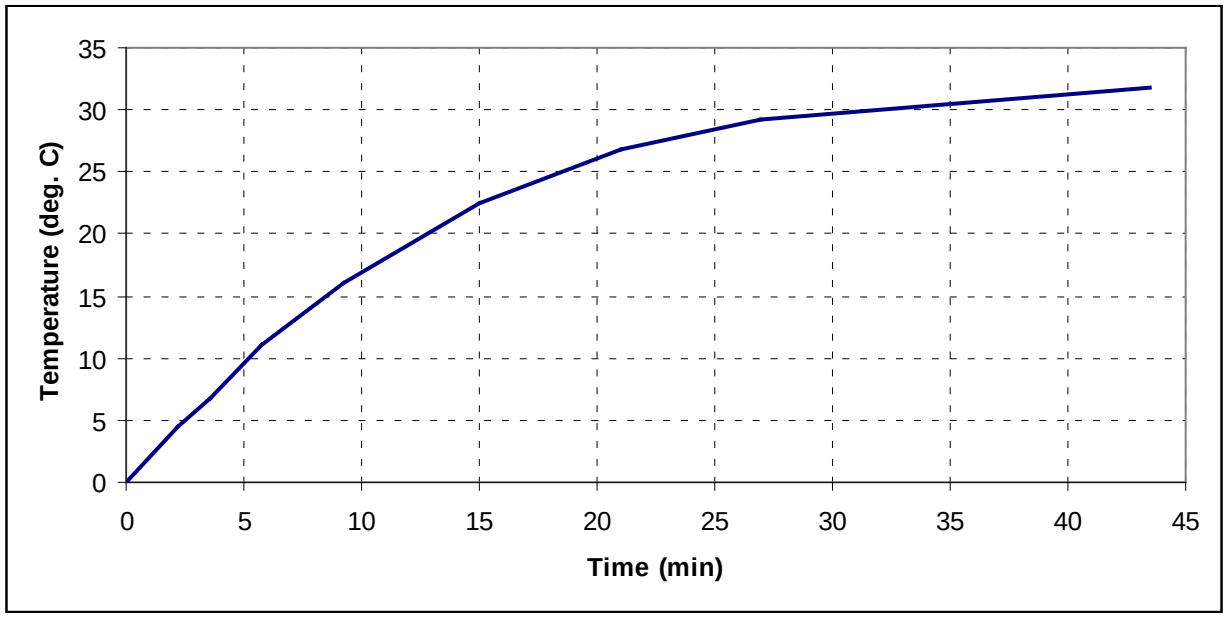

Figure 4: Step thermal response of the top yoke clamp of a 400 kV 400 MVA five-leg core-type fully-wound transformer to a 16.67 A per phase dc step.

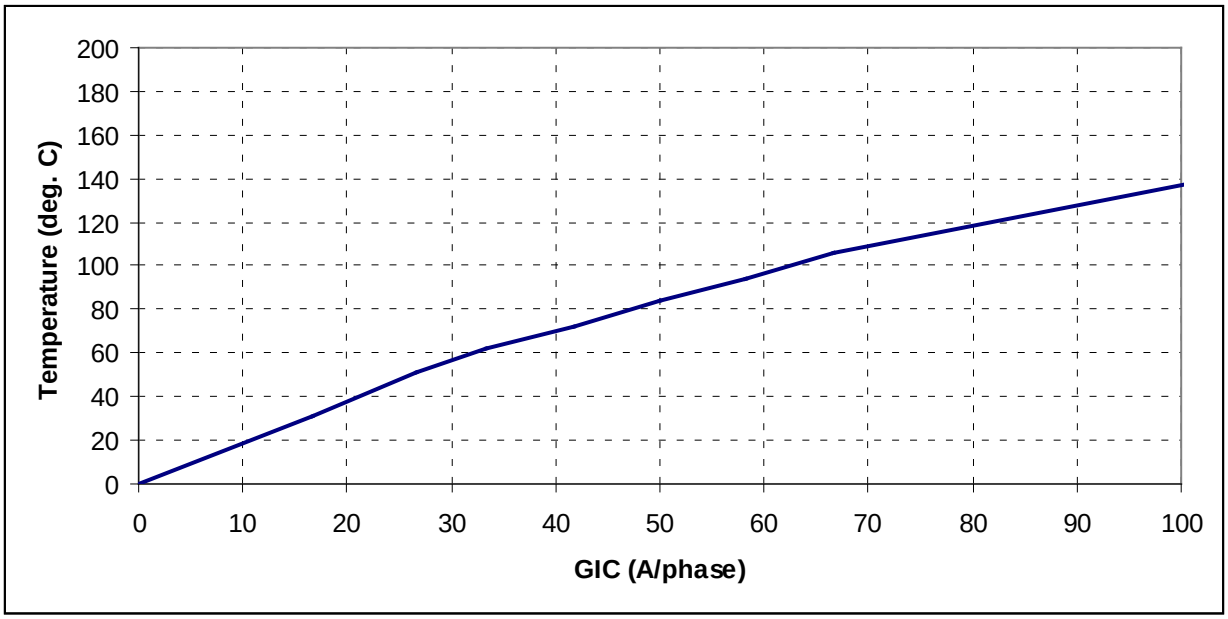

Figure 5: Asymptotic thermal response of the top yoke clamp of a 400 kV 400 MVA five-leg core-type fully-wound transformer.

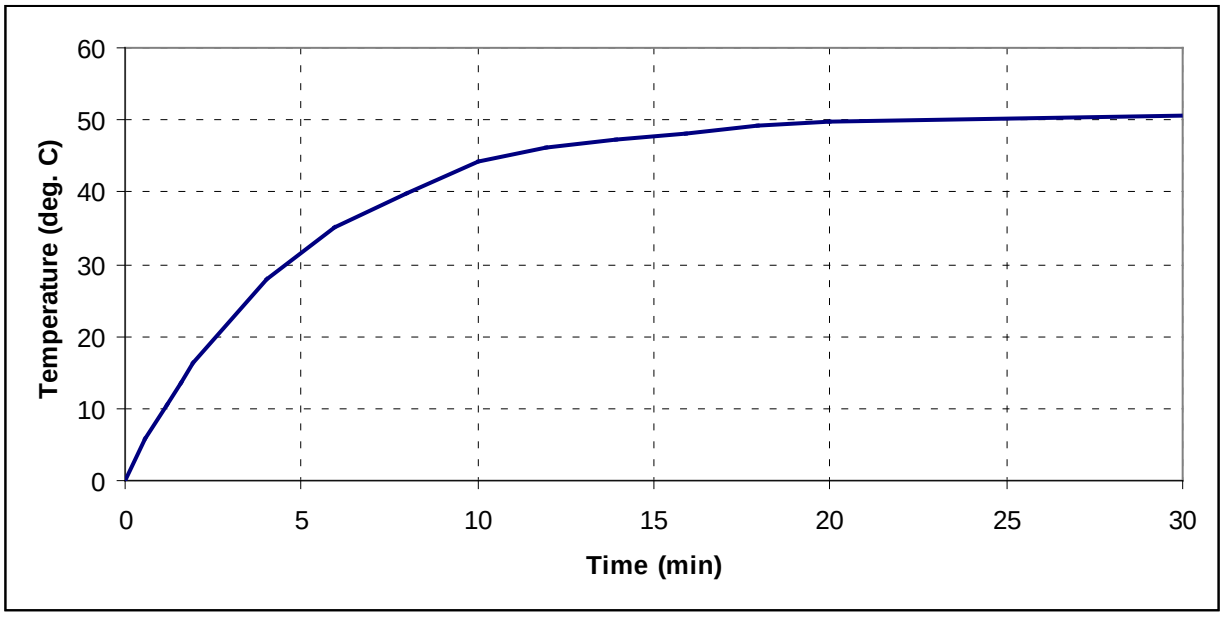

Figure 6: Step thermal response of the tie plate of a 400 kV 400 MVA single-phase core-type autotransformer to a 10 A per phase dc step.

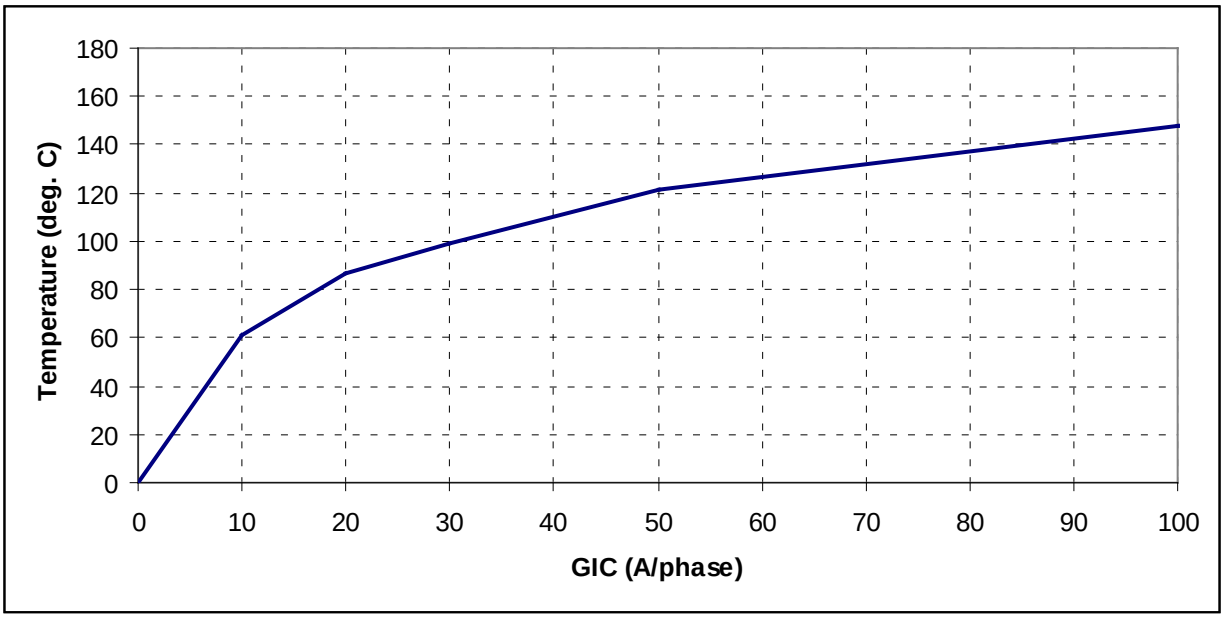

Figure 7: Asymptotic thermal response of the tie plate of a 400 kV 400 MVA single-phase core-type autotransformer.

The envelope in **Figure 1** can be used as a conservative thermal assessment for effective GIC values of 75 A per phase and greater (see Table 2).

Table 2: Upper Bound of Peak Metallic Hot Spot Temperatures Calculated Using the Benchmark GMD Event

Effective GIC (A/phase)	Metallic hot spot Temperature (°C)	Effective GIC(A/phase)	Metallic hot spot Temperature (°C)
0	80	100	182
10	107	110	186
20	128	120	190
30	139	130	193
40	148	140	204
50	157	150	213
60	169	160	221
70	170	170	230
75	172	180	234
80	175	190	241
90	179	200	247

For instance, if effective GIC is 130 A per phase and oil temperature is assumed to be 80°C, peak hot spot temperature is 193°C. This value is below the 200°C IEEE Std C57.91-2011 threshold for short time emergency loading and this transformer will have passed the thermal assessment. If the full heat run oil temperature is 67°C at maximum ambient temperature, then 150 A per phase of effective GIC translates into a peak hot spot temperature of 200°C and the transformer will have passed. If the limit is lowered to 180°C to account for the condition of the transformer, then this would be an indication to "sharpen the pencil" and perform a detailed assessment. Some methods are described in Reference [1].

The temperature envelope in Figure 1 corresponds to the values of effective GIC that result in the highest temperature for the benchmark GMD event. Different values of effective GIC could result in lower temperatures using the same model. For instance, the difference in upper and lower bounds of peak temperatures for the SVC coupling transformer model for 150 A per phase is approximately 30°C. In this case, GIC(t) should be generated to calculate the peak temperatures for the actual configuration of the transformer within the system as described in Reference [1]. Alternatively, a more precise thermal assessment could be carried out with a thermal model that more closely represents the thermal behavior of the transformer under consideration.

References

[1] Transformer Thermal Impact Assessment white paper. Developed by the Project 2013-03 (Geomagnetic Disturbance) standard drafting team. Available at:

http://www.nerc.com/pa/Stand/Pages/Project-2013-03-Geomagnetic-Disturbance-Mitigation.aspx

[2] Marti, L., Rezaei-Zare, A., Narang, A., "Simulation of Transformer Hotspot Heating due to Geomagnetically Induced Currents," *IEEE Transactions on Power Delivery,* vol.28, no.1, pp.320-327, Jan. 2013.

[3] Lahtinen, Matti. Jarmo Elovaara. "GIC occurrences and GIC test for 400 kV system transformer". IEEE Transactions on Power Delivery, Vol. 17, No. 2. April 2002.

[4] J. Raith, S. Ausserhofer: "GIC Strength verification of Power Transformers in a High Voltage Laboratory", GIC Workshop, Cape Town, April 2014

[5] "IEEE Guide for loading mineral-oil-immersed transformers and step-voltage regulators." IEEE Std C57.91-2011 (Revision of IEEE Std C57.91-1995).

NERC
NORTH AMERICAN ELECTRIC RELIABILITY CORPORATION

Screening Criterion for Transformer Thermal Impact Assessment

Project 2013-03 (Geomagnetic Disturbance Mitigation)

TPL-007-1 Transmission System Planned Performance for Geomagnetic Disturbance Events

Summary

Proposed standard TPL-007-1 – Transmission System Planned Performance for Geomagnetic Disturbance Events requires applicable entities to conduct assessments of the potential impact of benchmark GMD events on their systems. The standard requires transformer thermal impact assessments to be performed on power transformers with high side, wye-grounded windings with terminal voltage greater than 200 kV. Transformers are exempt from the thermal impact assessment requirement if the maximum effective geomagnetically-induced current (GIC) in the transformer is less than 75 A per phase as determined by GIC analysis of the system. Based on published power transformer measurement data as described below, an effective GIC of 75 A per phase is a conservative screening criterion. To provide an added measure of conservatism, the 75 A per phase threshold, although derived from measurements in single-phase units, is applicable to transformers with all core types (e.g., three-limb, three-phase).

Justification

Applicable entities are required to carry out a thermal assessment with GIC(t) calculated using the benchmark GMD event geomagnetic field time series or waveshape for effective GIC values above a screening threshold. The calculated GIC(t) for every transformer will be different because the length and orientation of transmission circuits connected to each transformer will be different even if the geoelectric field is assumed to be uniform. However, for a given thermal model and maximum effective GIC there are upper and lower bounds for the peak hot spot temperatures. These are shown in **Figure 1** using three available thermal models based on direct temperature measurements.

The results shown in **Figure 1** summarize the peak metallic hot spot temperatures when GIC(t) is calculated using (1), and systematically varying GIC_E and GIC_N to account for all possible orientation of circuits connected to a transformer. The transformer GIC (in A/phase) for any value of E_E (t) and E_N(t) can be calculated using equation (1) from reference [1].

$$GIC(t) = \left|E(t)\right| \cdot \left\{GIC_E \sin(\varphi(t)) + GIC_N \cos(\varphi(t))\right\} \quad (1)$$

where

$$|E(t)| = \sqrt{E_N^2(t) + E_E^2(t)} \quad (2)$$

$$\varphi(t) = \tan^{-1}\left(\frac{E_E(t)}{E_N(t)}\right) \quad (3)$$

$$GIC(t) = E_E(t) \cdot GIC_E + E_N(t) \cdot GIC_N \quad (4)$$

GIC_N is the effective GIC due to a northward geoelectric field of 1 V/km, and GIC_E is the effective GIC due to an eastward geoelectric field of 1 V/km. The units for GIC_N and GIC_E are A/phase/V/km.

It should be emphasized that with the thermal models used and the benchmark GMD event geomagnetic field waveshape, peak hot spot temperatures must lie below the envelope shown in **Figure 1**. The x-axis in Figure 1 corresponds to the absolute value of peak GIC(t). Effective maximum GIC for a transformer corresponds to a worst-case geoelectric field orientation, which is network-specific. Figure 1 represents a possible range, not the specific thermal response for a given effective GIC and orientation.

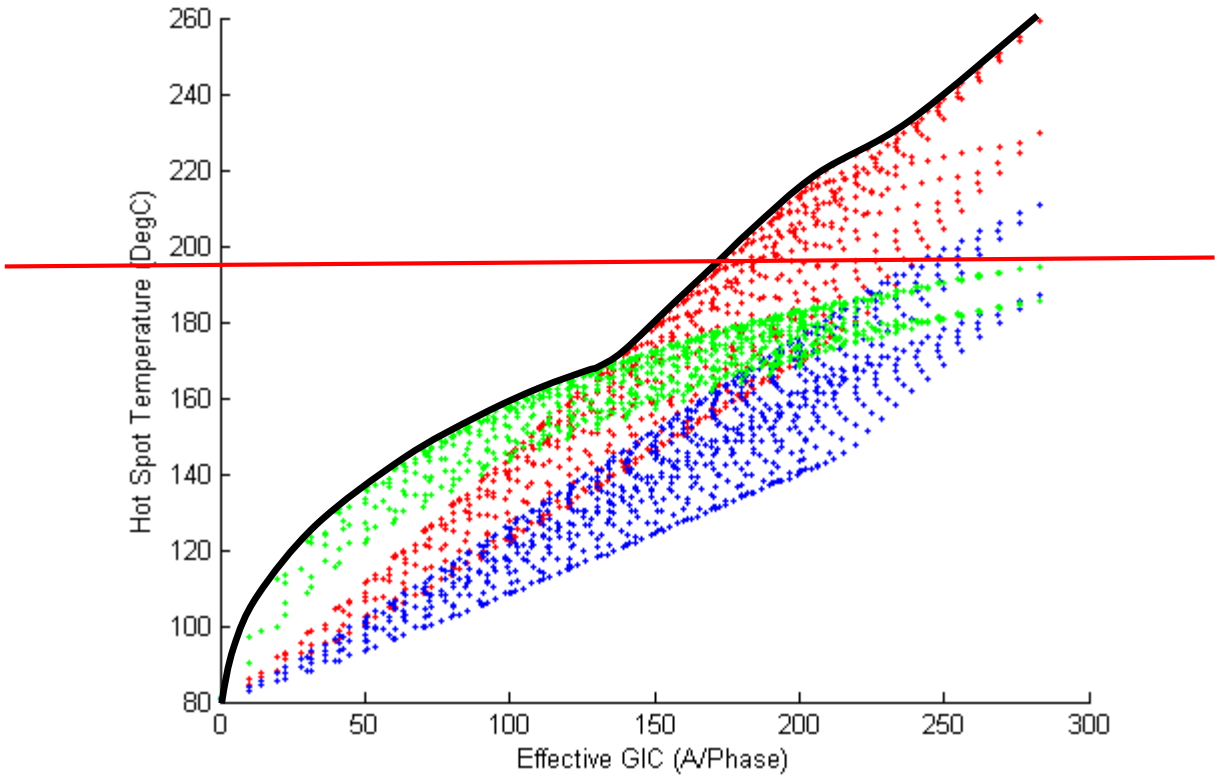
Hot Spot Temperature (DegC)
260
240
220
200
180
160
140
120
100
80
0
50
100
150
200
250
300
Effective GIC (A/Phase)

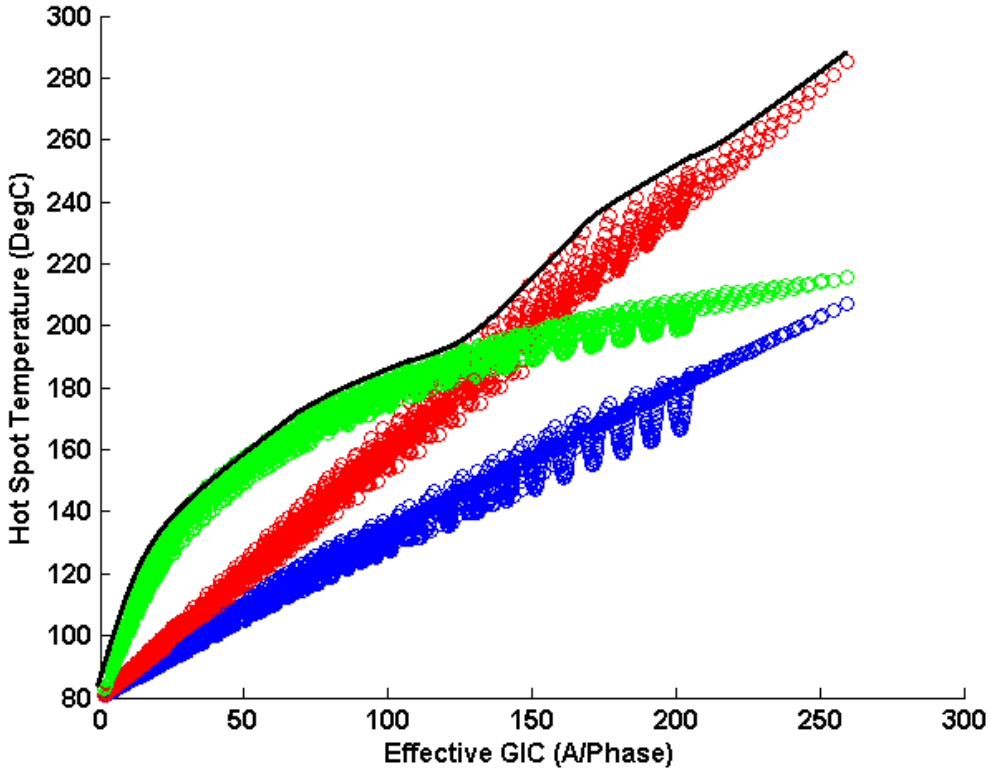

Figure 1: Metallic hot spot temperatures calculated using the benchmark GMD event. Red: ~~Screening~~SVC coupling transformer model [2]. Blue: Fingrid model [3]. Green: ~~SoCo~~Autotransformer model [4].

Consequently, with the most conservative thermal models known at this point in time, the peak metallic hot spot temperature obtained with the benchmark GMD event waveshape assuming an effective GIC magnitude of 75 A per phase will result in a peak temperature between ~~104~~160°C and ~~150~~172°C when the bulk oil temperature is 80°C (full load bulk oil temperature). The upper boundary of ~~150~~172°C ~~falls~~remains well below the metallic hot spot 200°C threshold for short-time emergency loading suggested in IEEE Std C57.91-2011 [5] (see Table 1).

TABLE 1:
Excerpt from Maximum Temperature Limits Suggested in IEEE C57.91-2011

	Normal life expectancy loading	Planned loading beyond	Long-time emergency loading	Short-time emergency loading

		nameplate rating		
Insulated conductor hottest-spot temperature °C	120	130	140	180
Other metallic hot-spot temperature (in contact and not in contact with insulation), °C	140	150	160	200
Top-oil temperature °C	105	110	110	110

The selection of the 75 A per phase screening threshold is based on the following considerations:

- A thermal assessment using the most conservative thermal models known to date will not result in peak hot spot temperatures above ~~150~~172°C. Transformer thermal assessments should not be required by Reliability Standards when results will fall well below IEEE Std C57.91-2011 limits.
- Applicable entities may choose to carry out a thermal assessment when the effective GIC is below 75 A per phase to take into account the age or condition of specific transformers where IEEE Std C57.91- 2011 limits could be assumed to be lower than 200°C.
- The models used to determine the 75 A per phase screening threshold are known to be conservative at higher values of effective GIC, especially the ~~screening~~SVC coupling transformer model in [2].
- Thermal models in peer-reviewed technical literature, especially those calculated models without experimental validation, are less conservative than the models used to determine the screening threshold. Therefore, a technically-justified thermal assessment for effective GIC below 75 A per phase using the benchmark GMD event geomagnetic field waveshape will always result in a "pass" on the basis of the state of the knowledge at this point in time.
- ~~The~~ Based on simulations, the 75 A per phase screening threshold ~~was determined on the basis of~~ will result in a maximum instantaneous peak hot spot temperature of 172°C. However, IEEE Std C57.91- 2011 limits assume short term emergency operation (typically 30 minutes). As illustrated in **Figure 2**, simulations of the 75 A per phase screening threshold result in 30-minute duration hot spot temperatures of about 155°C. The threshold provides an added measure of conservatism in not taking into account the duration of hot spot temperatures.
- The models used in the determination of the threshold are conservative but technically justified.
- Winding hot spots are not the limiting factor in terms of hot spots due to half-cycle saturation, therefore the screening criterion is focused on metallic part hot spots only.

The 75 A per phase screening threshold was determined using single-phase transformers, but is applicable to all types of transformer construction. While it is known that some transformer types such as three-limb, three-phase transformers are intrinsically less susceptible to GIC, it is not known by how much, on the basis of experimentally-supported models.

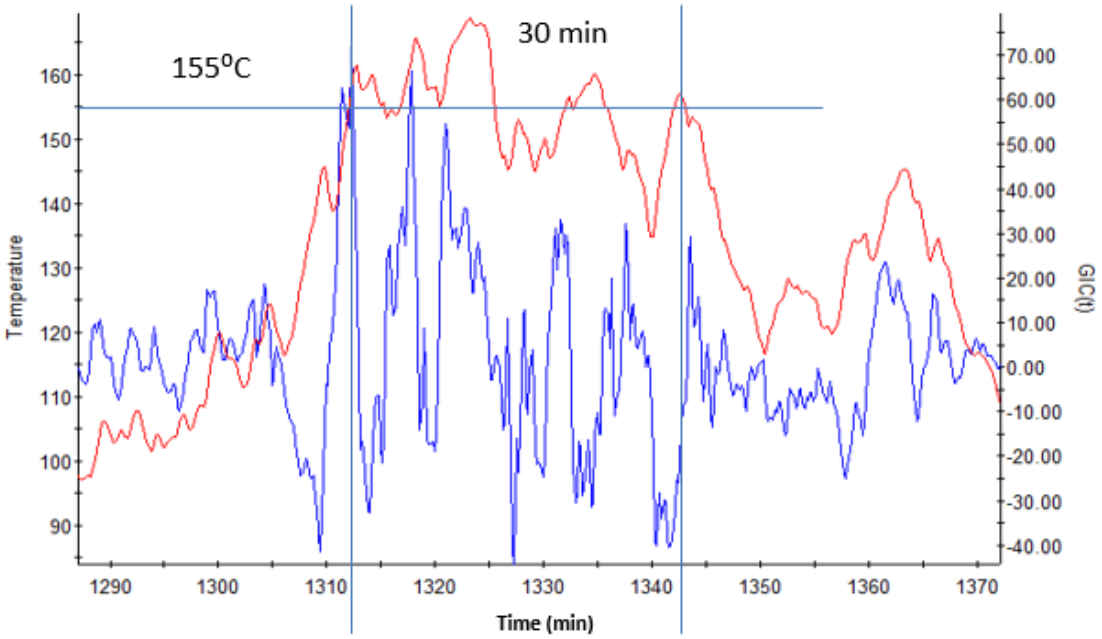

Figure 2: Metallic hot spot temperatures calculated using the benchmark GMD event. Red: metallic hot spot temperature. Blue: GIC(t) that produces the maximum hot spot temperature with peak GIC(t) scaled to 75 A/phase.

Appendix

The envelope used for thermal screening (Figure 1) is derived from two thermal ~~model~~models. The first is based on laboratory measurements carried out on 500/16.5 kV 400 MVA single-phase Static Var Compensator (SVC) coupling transformer [2]. Temperature measurements were carried out at relatively small values of GIC (see **Figure ~~2).~~ 3**). The asymptotic thermal response for this model is the linear extrapolation of the known measurement values. Although the near-linear behavior of the asymptotic thermal response is consistent with the measurements made on a Fingrid 400 kV 400 MVA five-leg core-type fully-wound transformer [3] (see **Figures ~~3~~4 and ~~4~~5**), the extrapolation from low values of GIC is very conservative, but reasonable for screening purposes.

The ~~third~~second transformer model is based on a combination of measurements and modeling for a 400 kV 400 MVA single-phase core-type autotransformer [4] (see **Figures ~~5~~6 and ~~6~~7**). The asymptotic thermal behavior of this transformer shows a "down-turn" at high values of GIC as the tie plate increasingly saturates but relatively high temperatures for lower values of GIC. The hot spot temperatures are higher than for the two other models for GIC less than 125 A per phase.

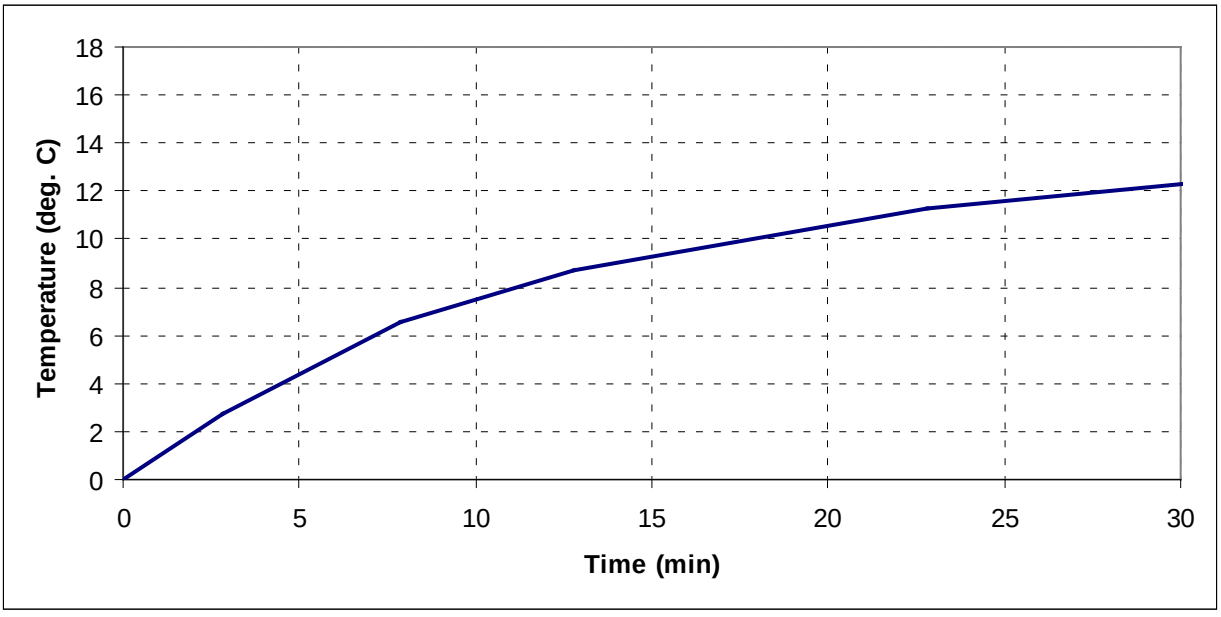

Figure ~~2~~3: Thermal step response of the tie plate of a 500 kV 400 MVA single-phase SVC coupling transformer to a 5 A per phase dc step.

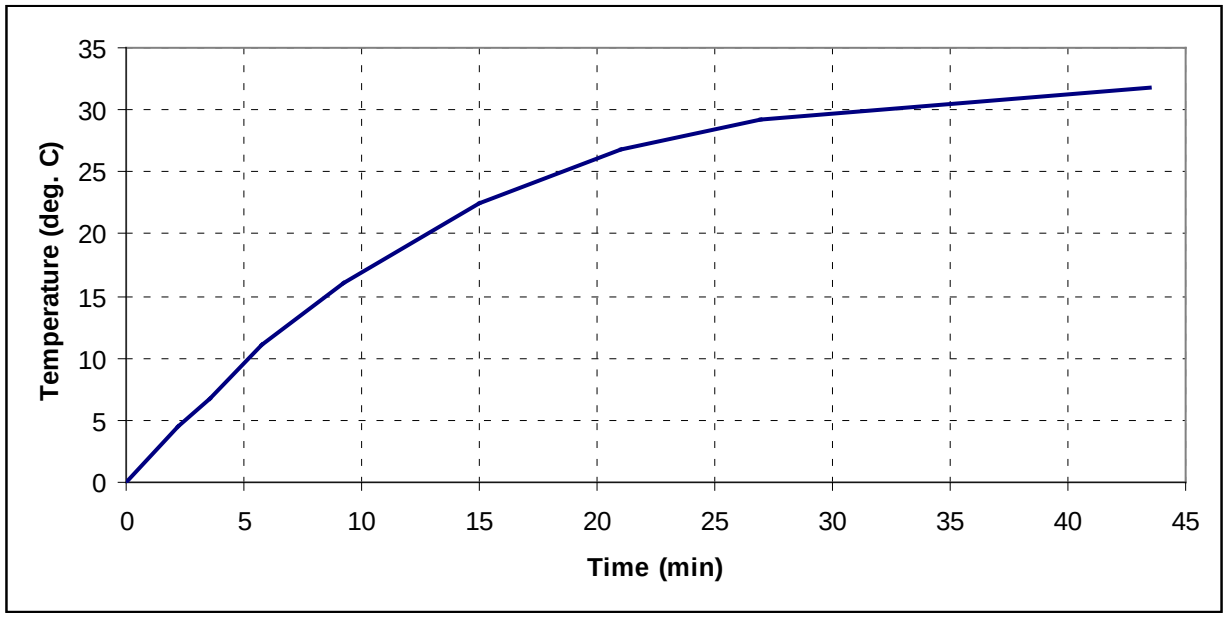

Figure ~~3~~4: Step thermal response of the ~~Flitch plate~~top yoke clamp of a 400 kV 400 MVA five-leg core-type fully-wound transformer to a ~~10~~16.67 A per phase dc step.

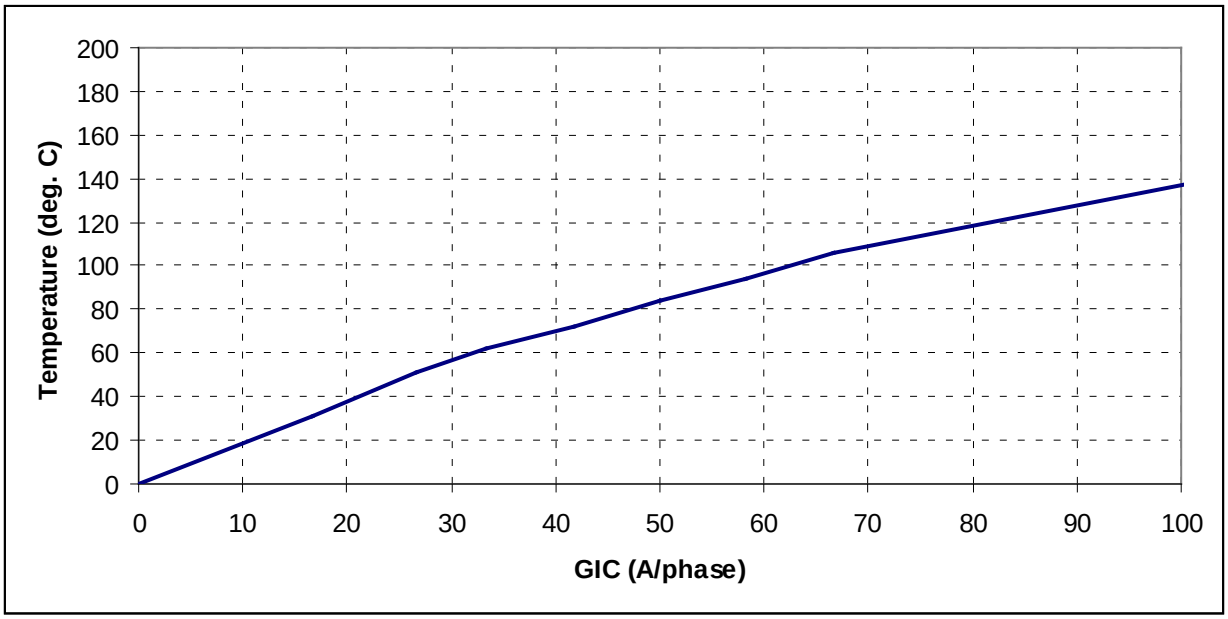

Figure ~~4~~5: Asymptotic thermal response of the ~~Flitch plate~~top yoke clamp of a 400 kV 400 MVA five-leg core-type fully-wound transformer.

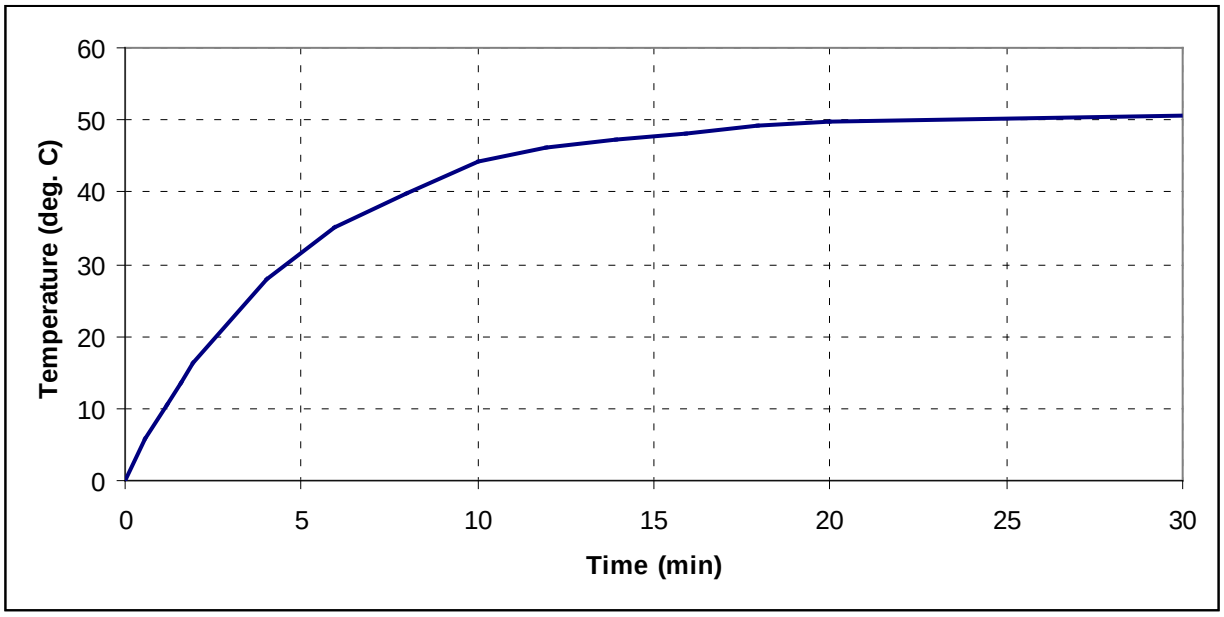

Figure ~~5~~6: Step thermal response of the tie plate of a 400 kV 400 MVA single-phase core-type autotransformer to a 10 A per phase dc step.

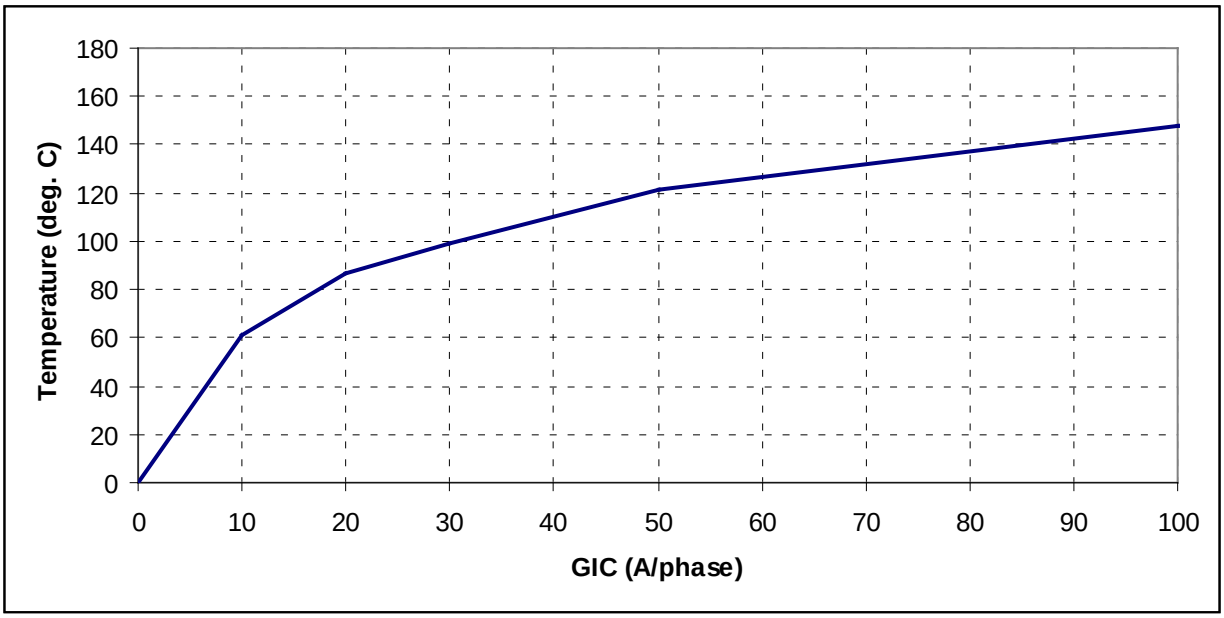

Figure ~~6~~7: Asymptotic thermal response of the ~~Flitch~~tie plate of a 400 kV 400 MVA single-phase core-type autotransformer.

The ~~composite~~ envelope in **Figure 1** can be used as a conservative thermal assessment for effective GIC values of 75 A per phase and greater (see Table 2).

Table 2: Upper Bound of Peak Metallic Hot Spot Temperatures Calculated Using the Benchmark GMD Event

Effective GIC (A/phase)	Metallic hot spot Temperature (°C)	Effective GIC(A/phase)	Metallic hot spot Temperature (°C)
0	80	~~140~~100	~~172~~182
10	~~106~~107	~~150~~110	~~180~~186
20	~~116~~128	~~160~~120	~~187~~190
30	~~125~~139	~~170~~130	~~194~~193
40	~~132~~148	~~180~~140	~~200~~204
50	~~138~~157	~~190~~150	~~208~~213
60	~~143~~169	~~200~~160	~~214~~221
70	~~147~~170	~~210~~170	~~221~~230
75	~~150~~172	~~220~~180	~~224~~234
80	~~152~~175	~~230~~190	~~228~~241
90	~~156~~179	~~240~~200	~~233~~247
~~100~~	~~159~~	~~250~~	~~239~~
~~110~~	~~163~~	~~260~~	~~245~~
~~120~~	~~165~~	~~270~~	~~251~~
~~130~~	~~168~~	~~280~~	~~257~~

For instance, if effective GIC is ~~150~~130 A per phase and oil temperature is assumed to be 80°C, peak hot spot temperature is ~~180~~193°C. This value is below the 200°C IEEE Std C57.91-2011 threshold for short time emergency loading and this transformer will have passed the thermal assessment. If the full heat run oil temperature is ~~59~~67°C at maximum ambient temperature, then ~~210~~150 A per phase of effective GIC translates ~~in~~into a peak hot spot temperature of 200°C and the transformer will have passed. If the limit is lowered to 180°C to account for the condition of the transformer, then this would be an indication to "sharpen the pencil" and perform a detailed assessment. Some methods are described in Reference [1].

The temperature envelope in Figure 1 corresponds to the values of ~~GIC_E and GIC_N~~effective GIC that result in the highest temperature for the benchmark GMD event. Different values of effective GIC could result in lower temperatures using the same ~~screening~~ model. For instance, the difference in upper and lower ~~bound~~bounds of peak temperatures for the ~~screening~~SVC coupling transformer model for ~~210~~150 A per phase is ~~165~~approximately 30°C. In this case, GIC(t) should be generated to calculate the peak temperatures for the actual configuration of the transformer within the system as described in Reference [1]. Alternatively, a more precise thermal assessment could be carried out with a thermal model that more closely represents the thermal behavior of the transformer under consideration.

References

[1] Transformer Thermal Impact Assessment white paper. Developed by the Project 2013-03 (Geomagnetic Disturbance) standard drafting team. Available at:

http://www.nerc.com/pa/Stand/Pages/Project-2013-03-Geomagnetic-Disturbance-Mitigation.aspx

[2] Marti, L., Rezaei-Zare, A., Narang, A., "Simulation of Transformer Hotspot Heating due to Geomagnetically Induced Currents," *IEEE Transactions on Power Delivery,* vol.28, no.1, pp.320-327, Jan. 2013.

[3] Lahtinen, Matti. Jarmo Elovaara. "GIC occurrences and GIC test for 400 kV system transformer". IEEE Transactions on Power Delivery, Vol. 17, No. 2. April 2002.

[4] J. Raith, S. Ausserhofer: "GIC Strength verification of Power Transformers in a High Voltage Laboratory", GIC Workshop, Cape Town, April 2014

[5] "IEEE Guide for loading mineral-oil-immersed transformers and step-voltage regulators." IEEE Std C57.91-2011 (Revision of IEEE Std C57.91-1995).

NERC
NORTH AMERICAN ELECTRIC RELIABILITY CORPORATION

Unofficial Comment Form

Project 2013-03 Geomagnetic Disturbance Mitigation

Do not use this form for submitting comments. Use the electronic form to submit comments on Project 2013-03 Geomagnetic Disturbance Mitigation TPL-007-1 White Papers. The electronic form must be submitted by **8 p.m. Eastern, June 13, 2016.**

Documents and information about this project are available on the Project 2013-03 Geomagnetic Disturbance Mitigation project page. If you have questions, contact Mark Olson, Senior Standards Developer (via email), or at 404.446-9760.

Background Information

On May 16, 2013 FERC issued Order No. 779, directing NERC to develop Standards that address risks to reliability caused by geomagnetic disturbances in two stages. Project 2013-03 responds to the FERC directives as follows:

- Stage 1. EOP-010-1 – Geomagnetic Disturbance Operations was approved by FERC in June, 2014.
- Stage 2. Proposed standard TPL-007-1 – Transmission System Planned Performance for Geomagnetic Disturbance Events requires applicable entities to conduct assessments of the potential impact of benchmark GMD events on their systems. If the assessments identify potential impacts, the proposed standard will require the applicable entity to develop corrective actions to mitigate the risk of voltage collapse, uncontrolled separation, or Cascading. The Stage 2 standard was filed for regulatory approval in January 2015. In May 2015, FERC issued a Notice of Proposed Rulemaking proposing to approve TPL-007-1 and direct NERC to develop some modifications through the standards development process. A FERC staff-led technical conference on the proposed standard was held March 1, 2016.

The standards drafting team (SDT) identified an error in Figure 1 of the *Screening Criterion for Transformer Thermal Impact Assessment* white paper (Screening Criterion white paper). The error resulted in incorrect plotting of simulated power transformer peak hot-spot heating from the Benchmark GMD Event. The SDT has corrected Figure 1 and revised related sections in the Screening Criterion white paper. The SDT has also made related revisions to other Project 2013-03 white papers. The revisions do not affect requirements in proposed TPL-007-1 but are being incorporated into the project white papers to maintain accuracy.

Questions

1. The SDT has corrected Figure 1 and revised related sections in the Screening Criterion white paper. The SDT has also made related revisions to other Project 2013-03 white papers. Do you agree with the revisions? If not, please provide specific recommendation(s) and technical justification.

   ☐ Yes
   ☐ No

   Comments:

NERC
NORTH AMERICAN ELECTRIC RELIABILITY CORPORATION

Standards Announcement

Project 2013-03 Geomagnetic Disturbance Mitigation Revised White Papers

Comment Period Open through June 13, 2016

Now Available

A comment period is open for **Project 2013-03 Geomagnetic Disturbance Mitigation** revised white papers. Stakeholders may provide comments using the link below through **8 p.m. Eastern, Monday, June 13, 2016.**

The standards drafting team (SDT) identified an error in Figure 1 of the *Screening Criterion for Transformer Thermal Impact Assessment* white paper (Screening Criterion white paper). The error resulted in incorrect plotting of simulated power transformer peak hot-spot heating from the Benchmark GMD Event. The SDT has corrected Figure 1 and revised related sections in the Screening Criterion white paper. The SDT has also made related revisions to other Project 2013-03 white papers. The revisions do not affect requirements in proposed TPL-007-1 but are being incorporated into the project white papers to maintain accuracy.

Commenting

Use the electronic form to submit comments. If you experience any difficulties in using the electronic form, contact Nasheema Santos. An unofficial Word version of the comment form is posted on the project page.

If you are having difficulty accessing the SBS due to a forgotten password, incorrect credential error messages, or system lock-out, contact NERC IT support directly at https://support.nerc.net/ (Monday – Friday, 8 a.m. - 8 p.m. Eastern).

For information on the Standards Development Process, refer to the Standard Processes Manual.

For more information or assistance, contact Senior Standards Developer, Mark Olson (via email) or by phone at (404) 446-9760.

North American Electric Reliability Corporation
3353 Peachtree Rd, NE
Suite 600, North Tower
Atlanta, GA 30326
404-446-2560 | www.nerc.com

Comment Report

Project Name:	2013-03 Geomagnetic Disturbance Mitigation White Papers
Comment Period Start Date:	5/12/2016
Comment Period End Date:	6/13/2016
Associated Ballots:	

There were 14 sets of responses, including comments from approximately 14 different people from approximately 14 companies representing 8 of the Industry Segments as shown in the table on the following pages.

Questions

1. The SDT has corrected Figure 1 and revised related sections in the Screening Criterion white paper. The SDT has also made related revisions to other Project 2013-03 white papers. Do you agree with the revisions? If not, please provide specific recommendation(s) and technical justification.

Organization Name	Name	Segment(s)	Region	Group Name	Group Member Name	Group Member Organization	Group Member Segment(s)	Group Member Region
ACES Power Marketing	Brian Van Gheem	6	NA - Not Applicable	ACES Standards Collaborators	Bob Solomon	Hoosier Energy Rural Electric Cooperative, Inc.	1	RF
					Ginger Mercier	Prairie Power, Inc.	1,3	SERC
					Michael Brytowski	Great River Energy	1,3,5,6	MRO
					Shari Heino	Brazos Electric Power Cooperative, Inc.	1,5	Texas RE
					Bill Hutchison	Southern Illinois Power Cooperative	1	SERC
					Mark Ringhausen	Old Dominion Electric Cooperative	3,4	SERC
					Chip Koloini	Golden Spread Electric Cooperative, Inc.	5	SPP RE
					Ellen Watkins	Sunflower Electric Power Corporation	1	SPP RE
					Ryan Strom	Buckeye Power, Inc.	4	RF
					Scott Brame	North Carolina Electric Membership Corporation	3,4,5	SERC
					Kevin Lyons	Central Iowa Power Cooperative	1	MRO
Duke Energy	Colby Bellville	1,3,5,6	FRCC,RF,SERC	Duke Energy	Doug Hils	Duke Energy	1	RF
					Lee Schuster	Duke Energy	3	FRCC
					Dale Goodwine	Duke Energy	5	SERC
					Greg Cecil	Duke Energy	6	RF

Southern Company - Southern Company Services, Inc.	Katherine Prewitt	1		Southern Company	Scott Moore	Alabama Power Company	3	SERC
					Bill Shultz	Southern Company Generation	5	SERC
					Jennifer Sykes	Southern Company Generation and Energy Marketing	6	SERC
Northeast Power Coordinating Council	Ruida Shu	1,2,3,4,5,6,7	NPCC	RSC	Paul Malozewski	Hydro One.	1	NPCC
					Guy Zito	Northeast Power Coordinating Council	NA - Not Applicable	NPCC
					Rob Vance	New Brunswick Power	1	NPCC
					Mark J. Kenny	Eversource Energy	1	NPCC
					Gregory A. Campoli	NY-ISO	2	NPCC
					Randy MacDonald	New Brunswick Power	2	NPCC
					Wayne Sipperly	New York Power Authority	4	NPCC
					David Ramkalawan	Ontario Power Generation	4	NPCC
					Glen Smith	Entergy Services	4	NPCC
					Brian Robinson	Utility Services	5	NPCC
					Bruce Metruck	New York Power Authority	6	NPCC
					Alan Adamson	New York State Reliability Council	7	NPCC
					Edward Bedder	Orange & Rockland Utilities	1	NPCC
					David Burke	UI	3	NPCC

					Michele Tondalo	UI	1	NPCC
					Kathleen Goodman	ISO-NE	2	NPCC
					Sylvain Clermont	Hydro Quebec	1	NPCC
					Si Truc Phan	Hydro Quebec	2	NPCC
					Helen Lainis	IESO	2	NPCC
					Brian Shanahan	National Grid	1	NPCC
					Michael Jones	National Grid	3	NPCC
					Michael Forte	Con-Edison	1	NPCC
					Kelly Silver	Con-Edison	3	NPCC
					Peter Yost	Con-Edison	4	NPCC
					Sean Bodkin	Dominion	4	NPCC
					Silvia Parada Mitchell	NextEra Energy	4	NPCC
					Brian O'Boyle	Con-Edison	5	NPCC
Southwest Power Pool, Inc. (RTO)	Shannon Mickens	2	SPP RE	SPP Standards Review Group	Shannon Mickens	Southwest Power Pool Inc.	2	SPP RE
					Jason Smith	Southwest Power Pool Inc	2	SPP RE
					Kim VanBrimer	Southwest Power Pool Inc	2	SPP RE
					kevin Giles	Westar Energy	1,3,5,6	SPP RE
					Jonathan Hayes	Southwest Power Pool Inc	2	SPP RE
					J.Scott Williams	City Utilities of Springfield	1,4	SPP RE

1. The SDT has corrected Figure 1 and revised related sections in the Screening Criterion white paper. The SDT has also made related revisions to other Project 2013-03 white papers. Do you agree with the revisions? If not, please provide specific recommendation(s) and technical justification.

Brian Van Gheem - 6 - NA - Not Applicable, Group Name ACES Standards Collaborators

Answer	No
Document Name	

Comment

We commend the SDT for revising the Screening Criterion and associated Project 2013-03 white papers. These revisions provide additional clarification on why 75 A per phase was chosen as the maximum effective geomagnetically-induced currents (GIC) value for the thermal impact assessment of applicable BES power transformers.

However, based on these clarifications, we believe this after-the-fact exercise to maintain accuracy misses the opportunity to revise the proposed TPL-007-1 reliability standard. The SDT should have justified its actions to revise these documents through the issuance of a SAR, as part of the standards development process. From these clarifications, it's further obvious that the 75 A per phase, while a step in the right direction away from the 15 A per phase value identified in the last draft revision of the standard, still misses the intent of why an overly conservative GIC value was chosen. Based on the information identified within the Screening Criterion and following the revised Table 2, it seems 130 A per phase is a better and more accurate selection for the GIC value.

We recommend the SDT develop a SAR, as part of the standards development process, with the intent to revise Requirement R6 of the standard and remove the maximum effective GIC value reference entirely. We suggest rephrasing the requirement to "each TO and GO shall conduct a thermal impact assessment for its solely and jointly owned applicable BES power transformers based on information provided in Requirement R5. The thermal impact assessment shall consist of [sub-requirements]." These documents could then be updated as part of the standards development process.

Likes 0	
Dislikes 0	

Response

Andrew Pusztai - 1

Answer	Yes
Document Name	

Comment

ATC is fine with the changes to the GMD white papers and have no comments.

Likes 0	
Dislikes 0	

Response

Thomas Foltz - 3,5	
Answer	Yes
Document Name	
Comment	
Though AEP has no objections to the revisions themselves, we do have a question regarding Figure 5 (formally Figure 4) in the document entitled "Screening Criterion for Transformer Thermal Impact Assessment". In short, what data source was used for this particular chart? Was it perhaps from the research conducted in Finland by ABB? If so, the plot does not appear to correlate correctly with this study's data. If this chart is *not* associated with the ABB study, please provide the data source used. In general, we would suggest that data sources be explicitly cited for all charts in the documents.	
Likes 0	
Dislikes 0	
Response	
Larisa Loyferman - 1 - Texas RE	
Answer	Yes
Document Name	
Comment	
CenterPoint Energy agrees with the revisions. CenterPoint Energy does not see any major impact with the SDT's proposed changes to the Screening Criterion White Paper, Thermal Impact Assessment, and Benchmark GMD Event White Paper. The changes were made based on the actual data received from the 2003 GMD Halloween storm, which clarified data shown by Figure 1. The SDT consisted of widely-recognized, knowledgeable experts. The Company believes that the members of the SDT are the most qualified to make justified adjustments to the white papers. The Company commends them for their open, thorough, and deliberative process, as well as careful consideration of the full range of technical issues and on the consistency of aligning all the documents at the same time. CenterPoint Energy greatly appreciates the SDT's effort in developing this Standard.	
Likes 0	
Dislikes 0	
Response	
Chris Scanlon - 1,3,5,6	
Answer	Yes
Document Name	

Comment
Responding on behalf of the Exelon Utilities and Generation companies. Exelon agrees with the revisions made to the Project 2013-03 white papers; we believe, however, that the drafting team missed the opportunity to include in these revisions any reference to the recently approved IEEE Std C57.163, *Guide for Establishing Power Transformer Capability while under Geomagnetic Disturbances*. At a minimum this IEEE Guide should be referenced on page 4 of the *Transformer Thermal Impact Assessment White Paper* as the source of IEEE guidance on conducting a detailed thermal impact assessment. The IEEE Guide also gives detailed information on thermal response of transformers to GIC, evaluation of transformer susceptibility to the effects of GIC, and recommendations regarding transformer specifications and monitoring. The IEEE Guide was developed in an open and collaborative process by more than 150 transformer experts composed of manufacturers, users and consultants from around the globe. Exelon recommends future revisions of the Project 2013-03 white papers should make a point to reference IEEE Std C57.163.

Likes 0	
Dislikes 0	

Response

Ruida Shu - 1,2,3,4,5,6,7 - NPCC, Group Name RSC	
Answer	Yes
Document Name	

Comment
The figure on page 3 of the Screening Criterion for Transformer Thermal Impact Assessment does not have a description. Should it be part of Figure 1? Is just the figure shown on page 4 Figure 1?

Likes 0	
Dislikes 0	

Response

Shannon Mickens - 2 - SPP RE, Group Name SPP Standards Review Group	
Answer	Yes
Document Name	

Comment
Our review group didn't see any major impacts with the drafting teams proposed changes to the three (3) White Papers. We commend them on the consistency of correcting all the documents at the same time. Thank you for all your efforts.

Likes 0	
Dislikes 0	

Response

Katherine Prewitt - 1, Group Name Southern Company	
Answer	Yes
Document Name	
Comment	
Likes 0	
Dislikes 0	
Response	
Nick Vtyurin - 1,3,5,6 - MRO	
Answer	Yes
Document Name	
Comment	
Likes 0	
Dislikes 0	
Response	
RoLynda Shumpert - 1,3,5,6 - SERC	
Answer	Yes
Document Name	
Comment	
Likes 0	
Dislikes 0	
Response	
Colby Bellville - 1,3,5,6 - FRCC,SERC,RF, Group Name Duke Energy	
Answer	Yes
Document Name	
Comment	

Likes 0	
Dislikes 0	
Response	
sean erickson - 1,6	
Answer	Yes
Document Name	
Comment	
Likes 0	
Dislikes 0	
Response	
Rachel Coyne - 10	
Answer	Yes
Document Name	
Comment	
Likes 0	
Dislikes 0	
Response	
Chris Gowder - 3,4,5,6 - FRCC	
Answer	Yes
Document Name	
Comment	
Likes 0	
Dislikes 0	
Response	

NERC
NORTH AMERICAN ELECTRIC RELIABILITY CORPORATION

Consideration of Comments

Project Name:	2013-03 Geomagnetic Disturbance Mitigation White Papers
Comment Period Start Date:	5/12/16
Comment Period End Date:	6/13/16

There were 14 responses, including comments from 7 people as shown in the table on the following pages.

All comments submitted can be reviewed in their original format on the project page.

If you feel that your comment has been overlooked, please let us know immediately. Our goal is to give every comment serious consideration in this process. If you feel there has been an error or omission, you can contact the Director of Standards, Howard Gugel (via email) or at (404) 446-9693.

Questions

1. The SDT has corrected Figure 1 and revised related sections in the *Screening Criterion for Transformer Thermal Impact Assessment* white paper (*Screening Criterion* white paper). The SDT has also made related revisions to other Project 2013-03 white papers. Do you agree with the revisions? If not, please provide specific recommendation(s) and technical justification.

The Industry Segments are:

1 — Transmission Owners
2 — RTOs, ISOs
3 — Load-serving Entities
4 — Transmission-dependent Utilities
5 — Electric Generators
6 — Electricity Brokers, Aggregators, and Marketers
7 — Large Electricity End Users
8 — Small Electricity End Users
9 — Federal, State, Provincial Regulatory or other Government Entities
10 — Regional Reliability Organizations, Regional Entities

Organization Name	Name	Segment(s)	Region	Group Name	Group Member Name	Group Member Organization	Group Member Segment(s)	Group Member Region
ACES Power Marketing	Brian Van Gheem	6	NA - Not Applicable	ACES Standards Collaborators	Bob Solomon	Hoosier Energy Rural Electric Cooperative, Inc.	1	RF
					Ginger Mercier	Prairie Power, Inc.	1,3	SERC
					Michael Brytowski	Great River Energy	1,3,5,6	MRO
					Shari Heino	Brazos Electric Power Cooperative, Inc.	1,5	Texas RE
					Bill Hutchison	Southern Illinois Power Cooperative	1	SERC
					Mark Ringhausen	Old Dominion Electric Cooperative	3,4	SERC
					Chip Koloini	Golden Spread Electric Cooperative, Inc.	5	SPP RE

					Ellen Watkins	Sunflower Electric Power Corporation	1	SPP RE
					Ryan Strom	Buckeye Power, Inc.	4	RF
					Scott Brame	North Carolina Electric Membership Corporation	3,4,5	SERC
					Kevin Lyons	Central Iowa Power Cooperative	1	MRO
Duke Energy	Colby Bellville	1,3,5,6	FRCC,RF,SERC	Duke Energy	Doug Hils	Duke Energy	1	RF
					Lee Schuster	Duke Energy	3	FRCC
					Dale Goodwine	Duke Energy	5	SERC
					Greg Cecil	Duke Energy	6	RF
Southern Company - Southern Company Services, Inc.	Katherine Prewitt	1		Southern Company	Scott Moore	Alabama Power Company	3	SERC
					Bill Shultz	Southern Company Generation	5	SERC
					Jennifer Sykes	Southern Company Generation and Energy Marketing	6	SERC

Northeast Power Coordinating Council	Ruida Shu	1,2,3,4,5,6,7	NPCC	RSC	Paul Malozewski	Hydro One.	1	NPCC
					Guy Zito	Northeast Power Coordinating Council	NA - Not Applicable	NPCC
					Rob Vance	New Brunswick Power	1	NPCC
					Mark J. Kenny	Eversource Energy	1	NPCC
					Gregory A. Campoli	NY-ISO	2	NPCC
					Randy MacDonald	New Brunswick Power	2	NPCC
					Wayne Sipperly	New York Power Authority	4	NPCC
					David Ramkalawan	Ontario Power Generation	4	NPCC
					Glen Smith	Entergy Services	4	NPCC
					Brian Robinson	Utility Services	5	NPCC
					Bruce Metruck	New York Power Authority	6	NPCC

Alan Adamson	New York State Reliability Council	7	NPCC
Edward Bedder	Orange & Rockland Utilities	1	NPCC
David Burke	UI	3	NPCC
Michele Tondalo	UI	1	NPCC
Kathleen Goodman	ISO-NE	2	NPCC
Sylvain Clermont	Hydro Quebec	1	NPCC
Si Truc Phan	Hydro Quebec	2	NPCC
Helen Lainis	IESO	2	NPCC
Brian Shanahan	National Grid	1	NPCC
Michael Jones	National Grid	3	NPCC
Michael Forte	Con-Edison	1	NPCC
Kelly Silver	Con-Edison	3	NPCC
Peter Yost	Con-Edison	4	NPCC
Sean Bodkin	Dominion	4	NPCC
Silvia Parada Mitchell	NextEra Energy	4	NPCC

					Brian O'Boyle	Con-Edison	5	NPCC
Southwest Power Pool, Inc. (RTO)	Shannon Mickens	2	SPP RE	SPP Standards Review Group	Shannon Mickens	Southwest Power Pool Inc.	2	SPP RE
					Jason Smith	Southwest Power Pool Inc	2	SPP RE
					Kim VanBrimer	Southwest Power Pool Inc	2	SPP RE
					kevin Giles	Westar Energy	1,3,5,6	SPP RE
					Jonathan Hayes	Southwest Power Pool Inc	2	SPP RE
					J.Scott Williams	City Utilities of Springfield	1,4	SPP RE

1. The SDT has corrected Figure 1 and revised related sections in the Screening Criterion white paper. The SDT has also made related revisions to other Project 2013-03 white papers. Do you agree with the revisions? If not, please provide specific recommendation(s) and technical justification.

Brian Van Gheem - 6 - NA - Not Applicable, Group Name ACES Standards Collaborators	
Answer	No
Comment	

We commend the SDT for revising the Screening Criterion and associated Project 2013-03 white papers. These revisions provide additional clarification on why 75 A per phase was chosen as the maximum effective geomagnetically-induced currents (GIC) value for the thermal impact assessment of applicable BES power transformers.

However, based on these clarifications, we believe this after-the-fact exercise to maintain accuracy misses the opportunity to revise the proposed TPL-007-1 reliability standard. The SDT should have justified its actions to revise these documents through the issuance of a SAR, as part of the standards development process. From these clarifications, it's further obvious that the 75 A per phase, while a step in the right direction away from the 15 A per phase value identified in the last draft revision of the standard, still misses the intent of why an overly conservative GIC value was chosen. Based on the information identified within the Screening Criterion and following the revised Table 2, it seems 130 A per phase is a better and more accurate selection for the GIC value.

We recommend the SDT develop a SAR, as part of the standards development process, with the intent to revise Requirement R6 of the standard and remove the maximum effective GIC value reference entirely. We suggest rephrasing the requirement to "each TO and GO shall conduct a thermal impact assessment for its solely and jointly owned applicable BES power transformers based on information provided in Requirement R5. The thermal impact assessment shall consist of [sub-requirements]." These documents could then be updated as part of the standards development process.

Response. Thank you for your comment. The SDT analyzed the corrected figure 1 in the *Screening Criterion* white paper and determined that the 75 A per phase threshold for thermal impact assessment remains a valid criterion. Consequently, a SAR to revise the proposed standard is not necessary. The SDT recognizes that 75 A per phase is a conservative screening criterion with a degree of margin, as

discussed on pages 2 and 3 of the *Screening Criterion* white paper. The criterion is used to identify transformers that must undergo a thermal impact assessment as specified in proposed TPL-007-1 Requirement R6 (i.e. 75 A per phase is a screening threshold and not a thermal impact assessment 'pass/fail' indication). The SDT believes it is appropriate to perform thermal impact assessments on transformers that meet or exceed the 75 A per phase threshold for the benchmark GMD event because the potential hot-spot heating in the transformer could exceed thermal limits. Factors such as transformer age and condition could lower the hot-spot heating limit from the 200◦ C value found in IEEE Std C57-91, so it is appropriate for the screening criterion to provide margin. The SDT does not believe revisions in the white paper support changes to Requirement R6 or removal of the thermal screening criterion as suggested by the commenter.
Andrew Pusztai – On Behalf of: American Transmission Company, LLC - 1

Answer	Yes
Comment	
ATC is fine with the changes to the GMD white papers and have no comments.	
Response. Thank you for your comment.	
Thomas Foltz – On Behalf of: AEP - 3,5	
Answer	Yes
Comment	
Though AEP has no objections to the revisions themselves, we do have a question regarding Figure 5 (formally Figure 4) in the document entitled “Screening Criterion for Transformer Thermal Impact Assessment”. In short, what data source was used for this particular chart? Was it perhaps from the research conducted in Finland by ABB? If so, the plot does not appear to correlate correctly with this study’s data. If this chart is *not* associated with the ABB study, please provide the data source used. In general, we would suggest that data sources be explicitly cited for all charts in the documents.	

Response. Thank you for your comment. Figure 5 in the *Screening Criterion* white paper is based on tests of a 400 kV 400 MVA five-leg core-type fully-wound transformer in Finland. The test results are published in the April 2002 IEEE Transactions paper noted as reference [3] in the *Screening Criterion* white paper. Figure 5 is derived from the temperature measurements plotted in reference [3], figure 8 (see Ch 14 plot), for the neutral dc step current profile in reference [3], figure 5.

Larisa Loyferman – On Behalf of: CenterPoint Energy Houston Electric, LLC, Texas RE -1	
Answer	Yes
Comment	
CenterPoint Energy agrees with the revisions. CenterPoint Energy does not see any major impact with the SDT's proposed changes to the Screening Criterion White Paper, Thermal Impact Assessment, and Benchmark GMD Event White Paper. The changes were made based on the actual data received from the 2003 GMD Halloween storm, which clarified data shown by Figure 1. The SDT consisted of widely-recognized, knowledgeable experts. The Company believes that the members of the SDT are the most qualified to make justified adjustments to the white papers. The Company commends them for their open, thorough, and deliberative process, as well as careful consideration of the full range of technical issues and on the consistency of aligning all the documents at the same time. CenterPoint Energy greatly appreciates the SDT's effort in developing this Standard.	

Response. Thank you for your comment.

Chris Scanlon – On Behalf of: Exelon - 1,3,5,6	
Answer	Yes
Comment	
Responding on behalf of the Exelon Utilities and Generation companies. Exelon agrees with the revisions made to the Project 2013-03 white papers; we believe, however, that the drafting team missed the opportunity to include in these revisions any reference to the recently approved IEEE Std C57.163, *Guide for Establishing Power*	

Transformer Capability while under Geomagnetic Disturbances. At a minimum this IEEE Guide should be referenced on page 4 of the *Transformer Thermal Impact Assessment White Paper* as the source of IEEE guidance on conducting a detailed thermal impact assessment. The IEEE Guide also gives detailed information on thermal response of transformers to GIC, evaluation of transformer susceptibility to the effects of GIC, and recommendations regarding transformer specifications and monitoring. The IEEE Guide was developed in an open and collaborative process by more than 150 transformer experts composed of manufacturers, users and consultants from around the globe. Exelon recommends future revisions of the Project 2013-03 white papers should make a point to reference IEEE Std C57.163.
Response. Thank you for your comment. The SDT added a footnote to page 4 of the *Thermal Impact Assessment* white paper referencing IEEE Std C57.163-2015 *Guide for Establishing Power Transformer Capability while under Geomagnetic Disturbances*.

Ruida Shu – Northeast Power Coordinating Council - 1,2,3,4,5,6,7 - NPCC, Group Name RSC	
Answer	Yes
Comment	
The figure on page 3 of the Screening Criterion for Transformer Thermal Impact Assessment does not have a description. Should it be part of Figure 1? Is just the figure shown on page 4 Figure 1?	
Response. Thank you for your comment. The figure on page 3 of the *Screening Criterion* white paper (redline version) is the deleted plot of figure 1 which is being replaced by the plot on page 4. The description for figure 1 is "Metallic hot spot temperatures calculated using the benchmark GMD event."	

Shannon Mickens - 2 - SPP RE, Group Name SPP Standards Review Group	
Answer	Yes
Comment	
Our review group didn't see any major impacts with the drafting teams proposed changes to the three (3) White Papers. We commend them on the consistency of correcting all the documents at the same time. Thank you for all your efforts.	

Response. Thank you for your comment.	
Katherine Prewitt - 1, Group Name Southern Company	
Answer	Yes
Nick Vtyurin – On Behalf of: Manitoba Hydro - 1,3,5,6 - MRO	
Answer	Yes
RoLynda Shumpert – On Behalf of: SCANA – South Carolina Electric and Gas Co. -1,3,5,6 - SERC	
Answer	Yes
Colby Bellville – Duke Energy - 1,3,5,6 - FRCC,SERC,RF, Group Name Duke Energy	
Answer	Yes
Sean Erickson – On Behalf of: Western Area Power Administration -1,6	
Answer	Yes
Rachel Coyne – On Behalf of: Texas Reliability Entity, Inc. -10	
Answer	Yes
Chris Gowder – On Behalf of: Florida Municipal Power Agency - 3,4,5,6 - FRCC	
Answer	Yes

NERC
NORTH AMERICAN ELECTRIC RELIABILITY CORPORATION

Benchmark Geomagnetic Disturbance Event Description

Project 2013-03 GMD Mitigation
Standard Drafting Team
May 12, 2016

RELIABILITY | ACCOUNTABILITY




Table of Contents

Preface

The North American Electric Reliability Corporation (NERC) is a not-for-profit international regulatory authority whose mission is to ensure the reliability of the Bulk-Power System (BPS) in North America. NERC develops and enforces Reliability Standards; annually assesses seasonal and long-term reliability; monitors the BPS through system awareness; and educates, trains, and certifies industry personnel. NERC's area of responsibility spans the continental United States, Canada, and the northern portion of Baja California, Mexico. NERC is the electric reliability organization (ERO) for North America, subject to oversight by the Federal Energy Regulatory Commission (FERC) and governmental authorities in Canada. NERC's jurisdiction includes users, owners, and operators of the BPS, which serves more than 334 million people.

The North American BPS is divided into several assessment areas within the eight Regional Entity (RE) boundaries, as shown in the map and corresponding table below.

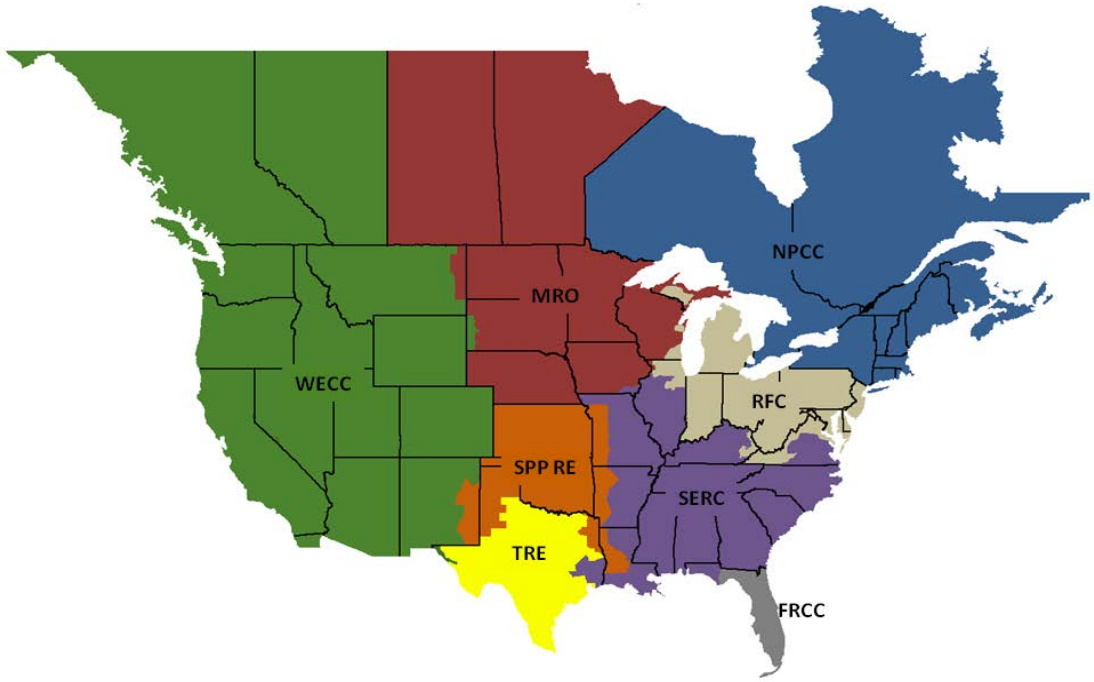

FRCC	Florida Reliability Coordinating Council
MRO	Midwest Reliability Organization
NPCC	Northeast Power Coordinating Council
RFC	Reliability*First* Corporation
SERC	SERC Reliability Corporation
SPP-RE	Southwest Power Pool Regional Entity
TRE	Texas Reliability Entity
WECC	Western Electric Coordinating Council

Introduction

Background

The purpose of the benchmark geomagnetic disturbance (GMD) event description is to provide a defined event for assessing system performance during a low probability, high magnitude GMD event as required by proposed standard TPL-007-1 – Transmission System Planned Performance for Geomagnetic Disturbance Events. The benchmark GMD event defines the geoelectric field values used to compute geomagnetically-induced current (GIC) flows for a GMD Vulnerability Assessment.

On May 16, 2013, FERC issued Order No. 779, directing NERC to develop Standards that address risks to reliability caused by geomagnetic disturbances in two stages:

- Stage 1 Standard(s) that require applicable entities to develop and implement Operating Procedures. EOP-010-1 – Geomagnetic Disturbance Operations was approved by FERC in June 2014.
- Stage 2 Standard(s) that require applicable entities to conduct assessments of the potential impact of benchmark GMD events on their systems. If the assessments identify potential impacts, the Standard(s) will require the applicable entity to develop and implement a plan to mitigate the risk.

TPL-007-1 is a new Reliability Standard developed to specifically address the Stage 2 directives in Order No. 779. The benchmark GMD event will define the scope of the Stage 2 Reliability Standard.

General Characteristics

The benchmark GMD event described herein takes into consideration the known characteristics of a severe GMD event and its impact on an interconnected transmission system. These characteristics include:

- Geomagnetic Latitude – The amplitude of the induced geoelectric field for a given GMD event is reduced as the observation point moves away from the earth's magnetic poles.
- Earth Conductivity – The amplitude and phase of the geoelectric field depends on the local or regional earth ground resistivity structure. Higher geoelectric field amplitudes are induced in areas of high resistivity.
- Transformer Electrical Response – Transformers can experience half-cycle saturation when subjected to GIC. Transformers under half-cycle saturation absorb increased amounts of reactive power (var) and inject harmonics into the system. However, half-cycle saturation does not occur instantaneously and depends on the electrical characteristics of the transformer and GIC amplitude [1]. Thus, the effects of transformer reactive power absorption and harmonic generation do not occur instantaneously, but instead may take up to several seconds. It is conservative, therefore, to assume that the effects of GIC on transformer var absorption and harmonic generation are instantaneous.
- Transformer Thermal Effects (e.g. hot spot transformer heating) – Heating of the winding and other structural parts can occur in power transformers during a GMD event. However, the thermal impacts are not instantaneous and are dependent on the thermal time constants of the transformer. Thermal time constants for hot spot heating in power transformers are in the 5-20 minute range.
- Geoelectric Field Waveshape – The geoelectric field waveshape has a strong influence on the hot spot heating of transformer windings and structural parts since thermal time constants of the transformer and time to peak of storm maxima are both on the order of minutes. The frequency content of the magnetic field (dB/dt) is a function of the waveshape, which in turn has a direct effect on the geoelectric field since the earth response to external dB/dt is frequency-dependent.
- Wide Area Geomagnetic Phenomena – The influence of GMD events is typically over a very broad area (e.g. continental scale); however, there can be pockets or very localized regions of enhanced geomagnetic activity. Since geomagnetic disturbance impacts within areas of influence of approximately 100-200 km do not have a widespread impact on the interconnected transmission system (see Appendix I), statistical methods used to assess the frequency of occurrence of a severe GMD event need to consider broad geographical regions to avoid bias caused by spatially localized geomagnetic phenomena.

Benchmark GMD Event Description

Severe geomagnetic disturbance events are high-impact, low-frequency (HILF) events [2]; thus, any benchmark event should consider the probability that the event will occur, as well as the impact or consequences of such an event. The benchmark event is composed of the following elements: 1) a reference peak geoelectric field amplitude (V/km) derived from statistical analysis of historical magnetometer data; 2) scaling factors to account for local geomagnetic latitude; 3) scaling factors to account for local earth conductivity; and 4) a reference geomagnetic field time series or waveshape to facilitate time-domain analysis of GMD impact on equipment.

Reference Geoelectric Field Amplitude

The reference geoelectric field amplitude was determined through statistical analysis using the plane wave method [3]-[10] geomagnetic field measurements from geomagnetic observatories in northern Europe [11] and the reference (Quebec) earth model shown in **Table 1** [12]. For details of the statistical considerations, see Appendix I. The Quebec earth model is generally resistive and the geological structure is relatively well understood.

Table 1: Reference earth model (Quebec)

Thickness (km)	Resistivity (Ω-m)
15	20,000
10	200
125	1,000
200	100
∞	3

The statistical analysis (see Appendix II) resulted in a conservative peak geoelectric field amplitude of approximately 8 V/km. For steady-state GIC and load flow analysis, the direction of the geoelectric field is assumed to be variable meaning that it can be in any direction (Eastward, Northward, or a vectorial combination thereof).

The frequency of occurrence of this benchmark GMD event is estimated to be approximately 1 in 100 years (see Appendix I). The selected frequency of occurrence is consistent with utility practices where a design basis frequency of 1 in 50 years is currently used as the storm return period for determining wind and ice loading of transmission infrastructure [13], for example.

The regional geoelectric field peak amplitude, E_{peak}, to be used in calculating GIC in the GIC system model can be obtained from the reference value of 8 V/km using the following relationship

$$E_{peak} = 8 \times \alpha \times \beta \text{ (V/km)} \quad (1)$$

where α is the scaling factor to account for local geomagnetic latitude, and β is a scaling factor to account for the local earth conductivity structure (see Appendix II).

Reference Geomagnetic Field Waveshape

The reference geomagnetic field waveshape was selected after analyzing a number of recorded GMD events, including the reference storm of the NERC interim report of 2012 [14], measurements at the Nurmijarvi (NUR) and Memanbetsu (MMB) geomagnetic observatories for the "Halloween event" of October 29-31, 2003, and the March 1989 GMD event that caused the Hydro Quebec blackout. The geomagnetic field measurement record of the March 13-14 1989 GMD event, measured at NRCan's Ottawa geomagnetic observatory, was selected as the

reference geomagnetic field waveform because it provides generally conservative results when performing thermal analysis of power transformers (see Appendix I). The reference geomagnetic field waveshape is used to calculate the GIC time series, GIC(t), required for transformer thermal impact assessment.

The geomagnetic latitude of the Ottawa geomagnetic observatory is 55°; therefore, the amplitude of the geomagnetic field measurement data were scaled up to the 60° reference geomagnetic latitude (see **Figure 1**) such that the resulting peak geoelectric field amplitude computed using the reference earth model was 8 V/km (see **Figures 2** and **3**). Sampling rate for the geomagnetic field waveshape is 10 seconds.

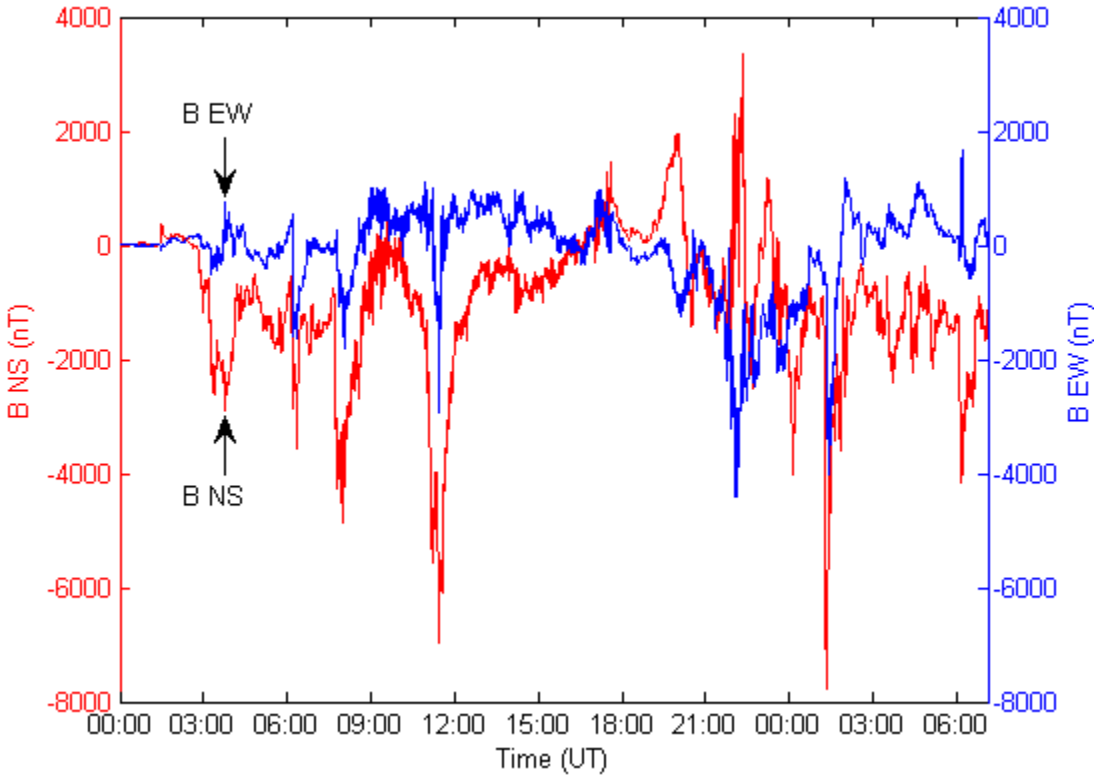

Figure 1: Benchmark Geomagnetic Field Waveshape
Red Bn (Northward), Blue Be (Eastward)
Referenced to pre-event quiet conditions

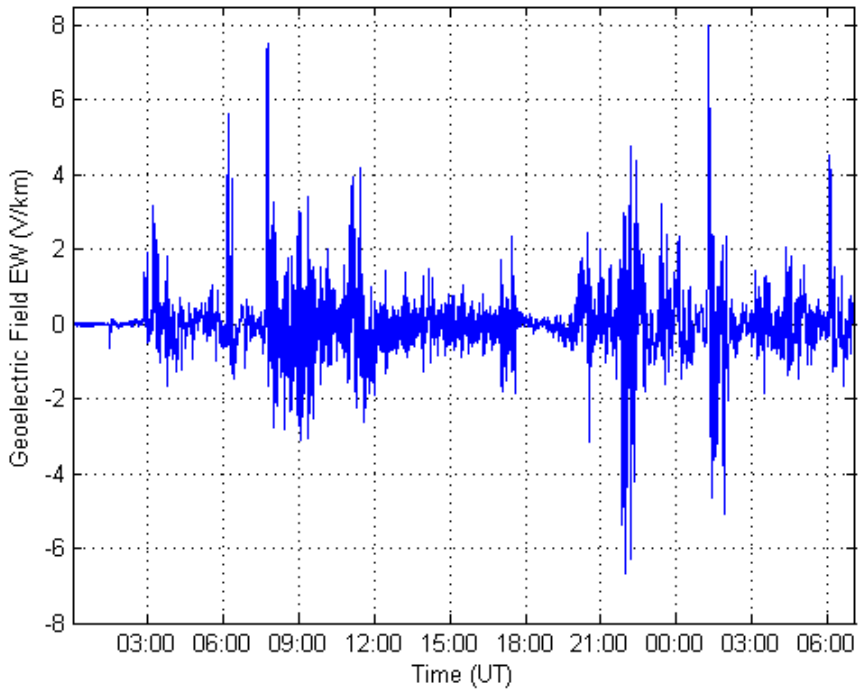

Figure 2: Benchmark Geoelectric Field Waveshape (E_E Eastward)

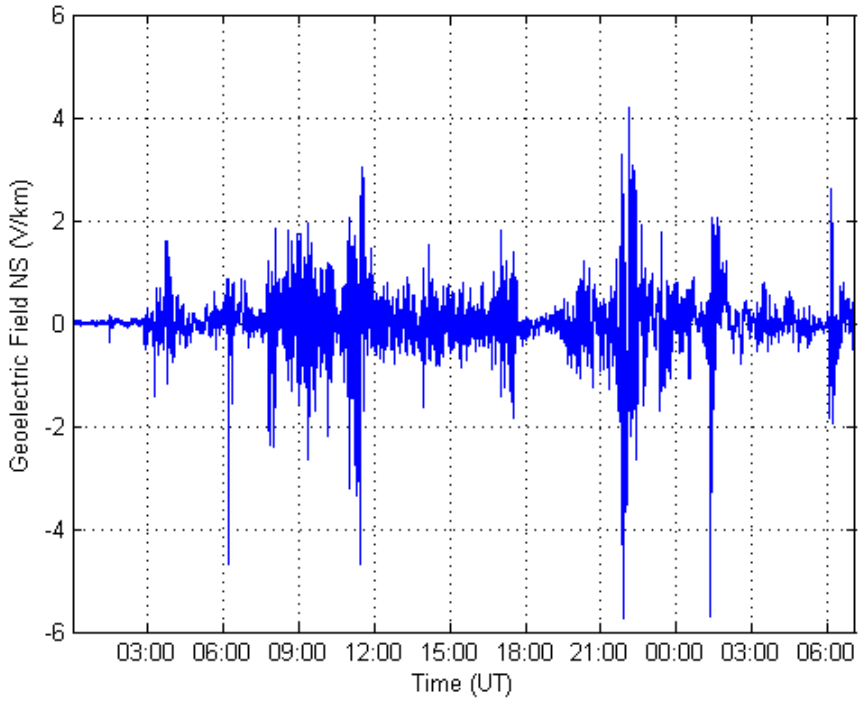

Figure 3: Benchmark Geoelectric Field Waveshape (E_N Northward)

Appendix I – Technical Considerations

The following sections describe the technical justification of the assumptions that were made in the development of the benchmark GMD event.

Statistical Considerations

Due to the lack of long-term accurate geomagnetic field observations, assigning probabilities to the occurrence of historical extreme geomagnetic storms is difficult because of the lack of high fidelity geomagnetic recordings of events prior to the 1980s. This is particularly true for the Carrington event for which data that allow the direct determination of the geoelectric fields experienced during the storm are not available [15].

The storm-time disturbance index Dst has often been used as a measure of storm strength even though it does not provide a direct correspondence with GIC[1]. One of the reasons for using Dst in statistical analysis is that Dst data are available for events occurring prior to 1980. Extreme value analysis of GMD events, including the Carrington, September 1859 and March 1989 events, has been carried out using Dst as an indicator of storm strength. In one such study [16], the (one sigma) range of 10-year occurrence probability for another March 1989 event was estimated to be between 9.4-27.8 percent. The range of 10-year occurrence probability for Carrington event in Love's analysis is 1.6-13.7 percent. These translate to occurrence rates of approximately 1 in 30-100 years for the March 1989 event and 1 in 70-600 years for the Carrington event. The error bars in such analysis are significant, however, it is reasonable to conclude that statistically the March 1989 event is likely more frequent than 1-in-100 years and the Carrington event is likely less frequent than 1-in-100 years.

The benchmark GMD event is based on a 1 in 100 year frequency of occurrence which is a conservative design basis for power systems. Also, the benchmark GMD event is not biased towards local geomagnetic field enhancements, since it must address wide-area effects in the interconnected power system. Therefore, the use of Dst-based statistical considerations is not adequate in this context and only relatively modern data have been used.

The benchmark GMD event is derived from modern geomagnetic field data records and corresponding calculated geoelectric field amplitudes. Using such data allows rigorous statistical analysis of the occurrence rates of the physical parameter (i.e. rate of change in geomagnetic field, dB/dt) directly related to the geoelectric field. Geomagnetic field measurements from the IMAGE magnetometer chain for 1993-2013 have been used to study the occurrence rates of the geoelectric field amplitudes.

With the use of modern data it is possible to avoid bias caused by localized geomagnetic field enhancements. The spatial structure of high-latitude geoelectric fields can be very complex during strong geomagnetic storm events [17]-[18]. One reflection of this spatial complexity is localized geomagnetic field enhancements that result in high amplitude geoelectric fields in regions of a few hundred kilometers or less. **Figure I-1**[2] illustrates this spatial complexity of the storm-time geoelectric fields. In areas indicated by the bright red location, the geoelectric field can be a factor of 2-3 larger than at neighboring locations. Localized geomagnetic phenomena should not be confused with local earth structure/conductivity features that result in consistently high geoelectric fields (e.g., coastal effects). Localized field enhancements can occur at any region exposed to auroral ionospheric electric current fluctuations.

[1] Dst index quantifies the amplitude of the main phase disturbance of a magnetic storm. The index is derived from magnetic field variations recorded at four low-latitude observatories. The data is combined to provide a measure of the average main-phase magnetic storm amplitude around the world.

[2] **Figure I-1** is for illustration purposes only, and is not meant to suggest that a particular area is more likely to experience a localized enhanced geoelectric field.

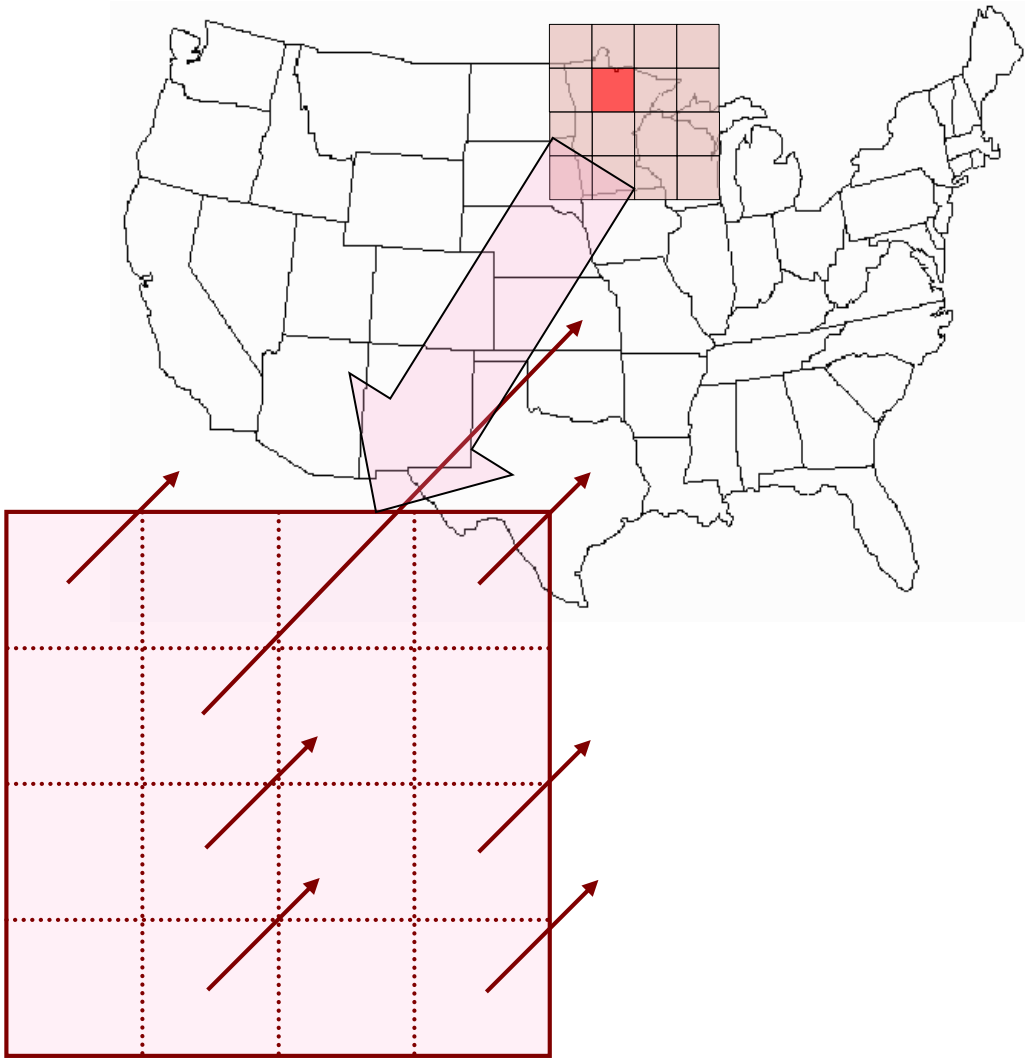

Figure I-1: Illustration of the Spatial Scale between Localized Enhancements and Larger Spatial Scale Amplitudes of Geoelectric Field Observed during a Strong Geomagnetic Storm.
In this illustration, the red square illustrates a spatially localized field enhancement.

The benchmark event is designed to address wide-area effects caused by a severe GMD event, such as increased var absorption and voltage depressions. Without characterizing GMD on regional scales, statistical estimates could be weighted by local effects and suggest unduly pessimistic conditions when considering cascading failure and voltage collapse. It is important to note that most earlier geoelectric field amplitude statistics and extreme amplitude analyses have been built for individual stations thus reflecting only localized spatial scales [10], [19]-[22]. A modified analysis is required to account for geoelectric field amplitudes at larger spatial scales. Consequently, analysis of spatially averaged geoelectric field amplitudes is presented below.

Figure I-2 shows statistical occurrence of spatially averaged high latitude geoelectric field amplitudes for the period of January 1, 1993 – December 31, 2013. The geoelectric field amplitudes were calculated using 10-s IMAGE magnetometer array observations and the Quebec ground conductivity model, which is used as a reference in the benchmark GMD event. Spatial averaging was carried out over four different station groups spanning a square area of approximately 500 km in width. For the schematic situation in **Figure I-1** the averaging process involves taking the average of the geoelectric field amplitudes over all 16 points or squares.

As can be seen from **Figure I-2**, the computed spatially averaged geoelectric field amplitude statistics indicate the 1-in-100 year amplitude is approximately between 3-8 V/km. Using extreme value analysis as described in the next section, it can be shown that the upper limit of the 95% confidence interval for a 100-year return level is more precisely 5.77 V/km.

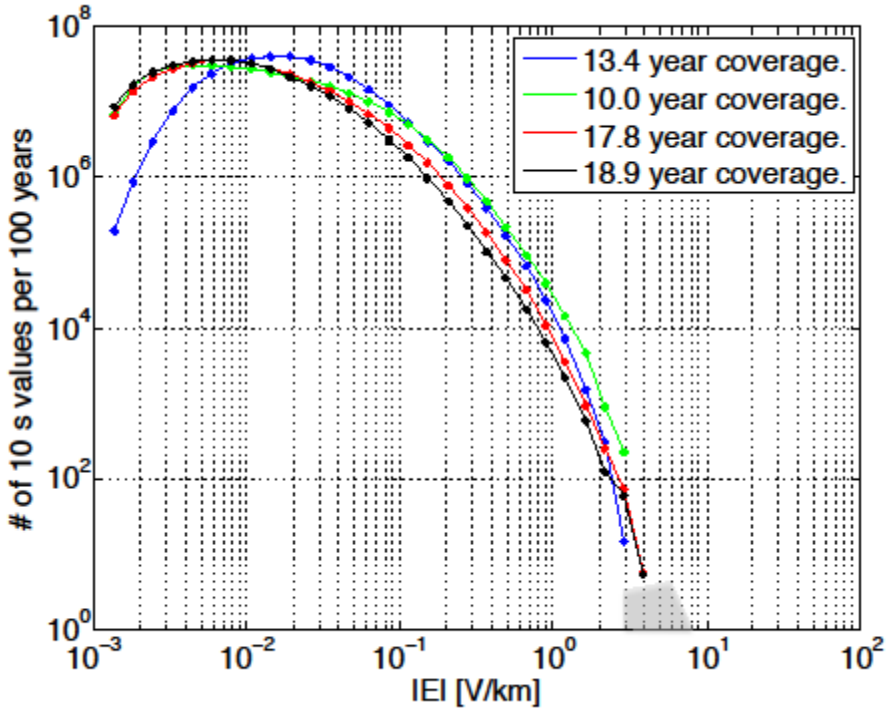

Figure I-2: Statistical Occurrence of Spatially Averaged Geoelectric Field Amplitudes.
Four curves with dots correspond to different station groups and the gray area shows a visual extrapolation to 1-in-100 year amplitudes. The legend shows the data coverage for each station group used in computing the averaged geoelectric field amplitudes.

Extreme Value Analysis

The objective of extreme value analysis is to describe the behavior of a stochastic process at extreme deviations from the median. In general, the intent is to quantify the probability of an event more extreme than any previously observed. In particular, we are concerned with estimating the 95 percent confidence interval of the maximum geoelectric field amplitude to be expected within a 100-year return period.[3] In the context of this document, extreme value analysis has been used to rigorously support the extrapolation estimates used in the statistical considerations of the previous section.

The data set consists of 21 years of daily maximum geoelectric field amplitudes derived from the IMAGE magnetometer chain, using the Quebec earth model as reference. **Figure I-3** shows a scatter plot of the 10-largest geoelectric field amplitudes per year across the IMAGE stations. The plot indicates that both the amplitude and standard deviation of extreme geoelectric fields are not independent of the solar cycle. The data clearly exhibits heteroskedasticity[4] and an 11-year seasonality in the mean.

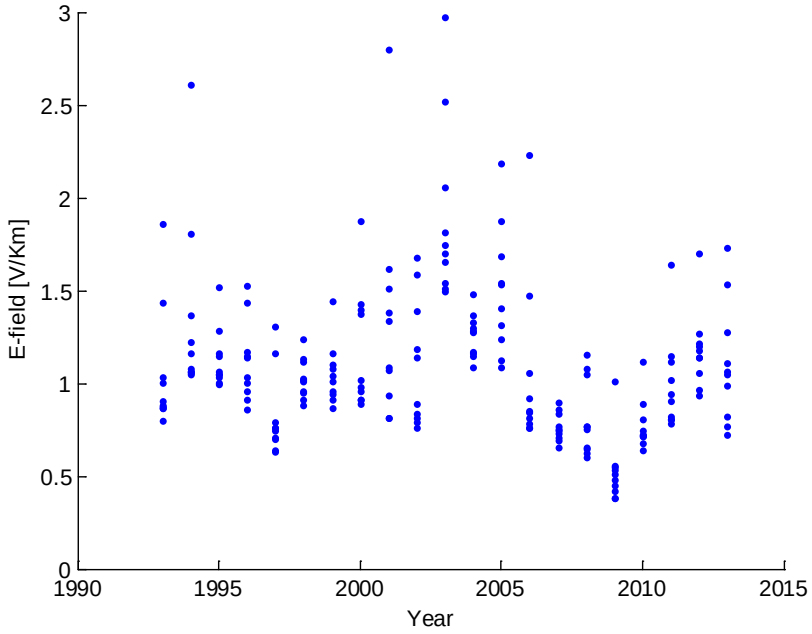

Figure I-3: Scatter Plot of Ten Largest Geoelectric Fields per Year

Data source: IMAGE magnetometer chain from 1993-2013

Several statistical methods can be used to conduct extreme value analysis. The most commonly applied include: Generalized Extreme Value (GEV), Point Over Threshold (POT), R-Largest, and Point Process (PP). In general, all methods assume independent and identically distributed (iid) data [23].

Two of these methods, GEV and POT, have been applied to the geoelectric field data, and their suitability for this application has been examined. **Table I-1** shows a summary of the estimated parameters and return levels obtained from GEV and POT methods. The parameters were estimated using the Maximum Likelihood Estimator (MLE). Since the distribution parameters do not have an intuitive interpretation, the expected geoelectric field amplitude for a 100-year return period is also included in **Table I-1.** The 95 percent confidence interval of the 100-year return level was calculated using the delta method and the profile likelihood. The delta method relies on the

[3] A 95 percent confidence interval means that, if repeated samples were obtained, the return level would lie within the confidence interval for 95 percent of the samples.

[4] Heteroskedasticity means that the skedastic function depends on the values of the conditioning variable; i.e., *var(Y|X=x) = f(x)*.

Gaussian approximation to the distribution of the MLE; this approximation can be poor for long return periods. In general, the profile likelihood provides a better description of the return level.

Table I-1: Extreme Value Analysis

Statistical Method	Estimated Parameters	Hypothesis Testing	100 Year Return Level Mean [V/km]	95% CI [V/km]	95% CI P-Likelihood [V/km]
(1) GEV	μ=1.4499 (0.1090) σ=0.4297 (0.0817) ξ=0.0305 (0.2011)	H0: ξ=0 p = 0.877	3.57	[1.77 , 5.36]	[2.71, 10.26]
(2) GEV $\mu = \beta_0 + \beta_1 \cdot \sin\left(\frac{t}{T} + \phi\right)$	β_0=1.5047 (0.0753) β_1=0.3722 (0.0740) σ=0.2894 (0.0600) ξ=0.1891 (0.2262)	H0: β_1=0 p= 0.0003 H0: ξ=0 p = 0.38	4	[2.64, 4.81]	[2.92, 12.33]
(3) POT, threshold=1V/km	σ=0.3163 (0.0382) ξ=0.0430 (0.0893)		3.4	[2.28, 4.52]	[2.72,5.64]
(4) POT, threshold=1V/km $\sigma = \alpha_0 + \alpha_1 \cdot \sin\left(\frac{t}{T} + \phi\right)$	α_0=0.2920 (0.0339) α_1=0.1660 (0.0368) ξ=-0.0308 (0.0826)	H0: α_1=0 p= 3.7e-5	3.724	[2.64, 4.81]	[3.02, 5.77]

Statistical model (1) in **Table I-1** is the traditional GEV estimation using blocks of 1 year maxima; i.e., only 21 data points are used in the estimation. The mean expected amplitude of the geolectric field for a 100-year return level is 3.57 V/km. Since GEV works with blocks of maxima, it is typically regarded as a wasteful approach. This is reflected in the comparatively large confidence intervals: [1.77, 5.36] V/km for the delta method and [2.71, 10.26] V/km for the profile likelihood.

As discussed previously, GEV assumes that the data is iid. Based on the scatter plot shown in **Figure 1-3**, the iid statistical assumption is not warranted by the data. Statistical model (2) in **Table I-1** is a re-parameterization of the GEV distribution contemplating the 11-year seasonality in the mean,

$$\mu = \beta_0 + \beta_1 \cdot \sin\left(\frac{t}{T} + \phi\right)$$

where β_0 represents the offset in the mean, β_1 describes the 11-year seasonality, T is the period (11 years), and ϕ is a constant phase shift.

A likelihood ratio test is used to test the hypothesis that β_1 is zero. The null hypothesis, H0: β_1=0, is rejected with a p-value of 0.0003; as expected, the 11-year seasonality has explanatory power. The blocks of maxima during the solar minimum are better represented in the re-parameterized GEV. The benefit is an increase in the mean return

level to 4 V/km and a wider confidence interval: [2.63, 4.81] V/km for the delta method and [2.92, 12.33] V/km for the profile likelihood (calculated at solar maximum).

Statistical model (3) in **Table I-1** is the traditional POT estimation using a threshold *u* of 1 V/km; the data was de-clustered using a 1-day run. The data set consists of normalized excesses over a threshold, and therefore, the sample size for POT is increased if more than one extreme observation per year is available (in the GEV approach, only the maximum observation over the year was taken; in the POT method, a single year can have multiple observations over the threshold). The selection of the threshold *u* is a compromise between bias and variance. The asymptotic basis of the model relies on a high threshold; a threshold that is too low will likely lead to bias. On the other hand, a threshold that is too high will reduce the sample size and result in high variance. The stability of parameter estimates can guide the selection of an appropriate threshold. **Figure I-4** shows the estimated parameters (modified scale $\sigma^*=\sigma_u-\xi\cdot u$, and shape ξ) for a range of thresholds. The objective is to select the lowest threshold for which the estimates remain near constant; 1V/km appears to be a good choice.

The mean return level for statistical model (3), 3.4 V/km, is similar to the GEV estimates. However, due to the larger sample size, the POT method is more efficient, and consequently, the confidence intervals are significantly reduced: [2.28, 4.52] V/km for the delta method, and [2.72, 5.64] V/km for the profile likelihood method.

In order to cope with the heteroskedasticity exhibited by the data, a re-parameterization of POT is used in statistical model (4) in **Table I-1**,

$$\sigma = \alpha_0 + \alpha_1 \cdot \sin\left(\frac{t}{T} + \phi\right)$$

where α_0 represents the offset in the standard deviation, α_1 describes the 11-year seasonality, *T* is the period ($365.25 \cdot 11$), and ϕ is a constant phase shift.

The parameter α_1 is statistically significant; the null hypothesis, H0: $\alpha_1=0$, is rejected with a p-value of 3.7e-5. The mean return level has slightly increased to 3.72 V/km. The upper limit of the confidence interval, calculated at solar maximum, also increases: [2.63, 4.81] V/km for the delta method and [3.02, 5.77] V/km for the profile likelihood method. As a final remark, it is emphasized that the confidence interval obtained using the profile likelihood is preferred over the delta method. **Figure I-5** shows the profile likelihood of the 100-year return level of statistical model (4). Note that the profile likelihood is highly asymmetric with a positive skew, rendering a larger upper limit for the confidence interval. Recall that the delta method assumes a normal distribution for the MLEs, and therefore, the confidence interval is symmetric around the mean.

To conclude, traditional GEV (1) and POT (3) models are misspecified; the statistical assumptions (iid) are not warranted by the data. The models were re-parameterized to cope with heteroskedasticity and the 11-year seasonality in the mean. Statistical model (4) better utilizes the available extreme measurements and it is therefore preferred over statistical model (2). The upper limit of the 95 percent confidence interval for a 100-year return level is 5.77 V/km. This analysis is consistent with the selection of a geoelectric field amplitude of 8 V/km for the 100-year GMD benchmark. .

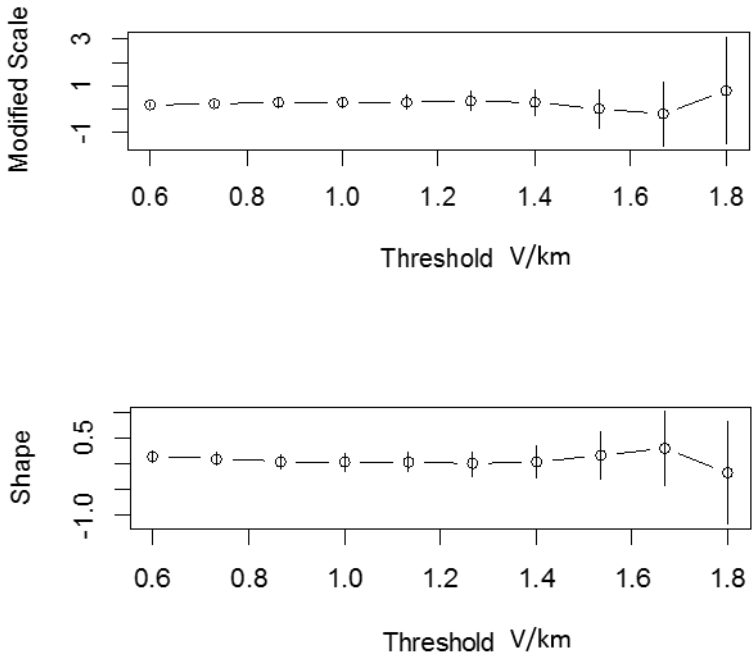

Figure I-4: Parameter Estimates Against Threshold for Statistical Model (3)

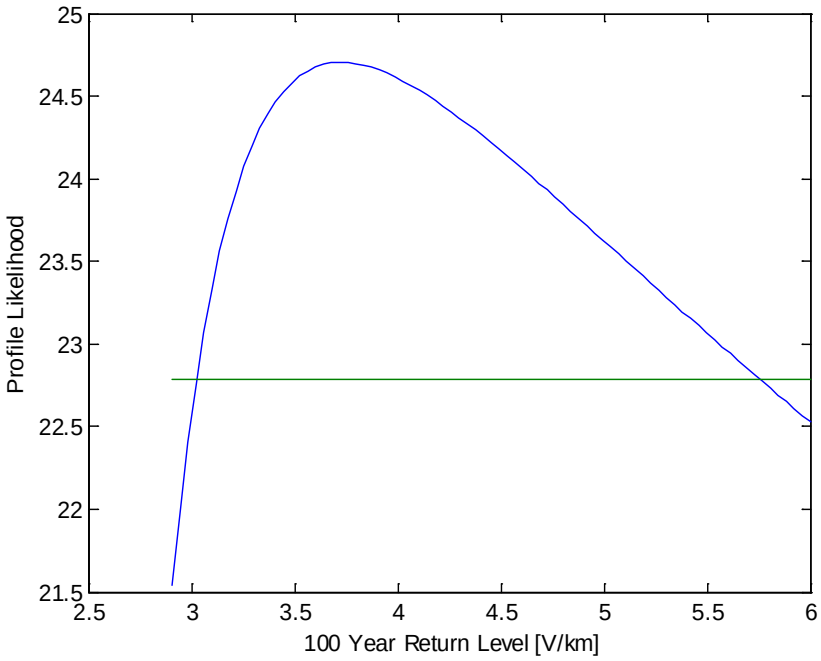

Figure I-5: Profile Likelihood for 100-year Return Level for Statistical Model (4)

Impact of Local Geomagnetic Disturbances on GIC

The impact of local disturbances on a power network is illustrated with the following example. A 500 km by 500 km section of a North American transmission network is subdivided into 100 km by 100 km sections. The geoelectric field is assumed to be uniform within each section. The analysis is performed by scaling the geoelectric field in each section individually by an intensification factor of 2.5 and computing the corresponding GIC flows in the network, resulting in a total of 25 GIC distribution simulations.[5] In these simulations the peak geomagnetic field amplitude has been scaled according to geomagnetic latitude of the network under study.

Figure I-6 shows the number of transformers that experience a GIC increase greater than 10 Amps (in red), those that experienced a reduction in GIC of more than 10 Amps (in blue), and those that remain essentially the same (in green). It can be observed that there is a small set of transformers that are affected by the local amplification of the geo-electric field but that the impact on the GIC distribution of the entire network due to a local intensification of the geoelectric field in a "local peak" is minor. Therefore, it can be concluded that the effect of local disturbances on the larger transmission system is relatively minor and does not warrant further consideration in network analysis.

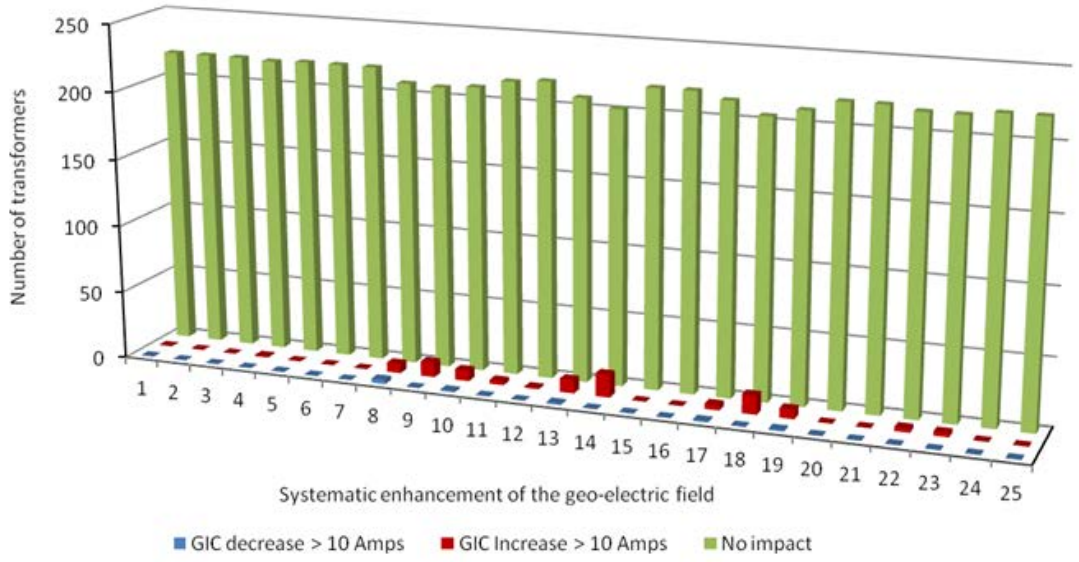

Figure I-6: Number of Transformers that see a 10 A/phase Change in GIC due to Local Geoelectric Field Intensification

Impact of Waveshape on Transformer Hot-spot Heating

Thermal effects (e.g. hot spot transformer heating) in power transformers are not instantaneous. Thermal time constants associated with hot spot heating in power transformers are in the 5-20 minute range; therefore, the waveshape of the geomagnetic and geoelectric field has a strong impact on transformer hot spot heating of windings and metallic parts since thermal time constants are of the same order of magnitude as the time-to-peak of storm maxima. The waveshape of the March 13-14 1989 GMD event measured at the Ottawa geomagnetic observatory was found to be a conservative choice when compared with other events of the last 20 years, such

[5] An intensification factor of 2.5 would make a general 8 V/km peak geoelectric field in the entire network show a 20 V/km intensified geoelectric field in one of the twenty five 100 km by 100 km sections.

as the measurements at the Nurmijarvi (NUR) and Memanbetsu (MMB) geomagnetic observatories for the "Halloween event" of October 29-31, 2003 described in the NERC GMD interim report of 2012 [14].

To illustrate, the results of a thermal analysis performed on a relatively large test network with a diverse mix of circuit lengths and orientations is provided in **Figures I-7** and **I-8**. **Figure I-9** shows a more systematic way to compare the relative effects of storm waveshape on the thermal response of a transformer. It shows the results of 33,000 thermal assessments for all combinations of effective GIC due to circuit orientation (similar **to Figures I-7** and **I-8** but systematically taking into account all possible circuit orientations). These results illustrate the relative effect of different waveshapes in a broad system setting and should not be interpreted as a vulnerability assessment of any particular network.

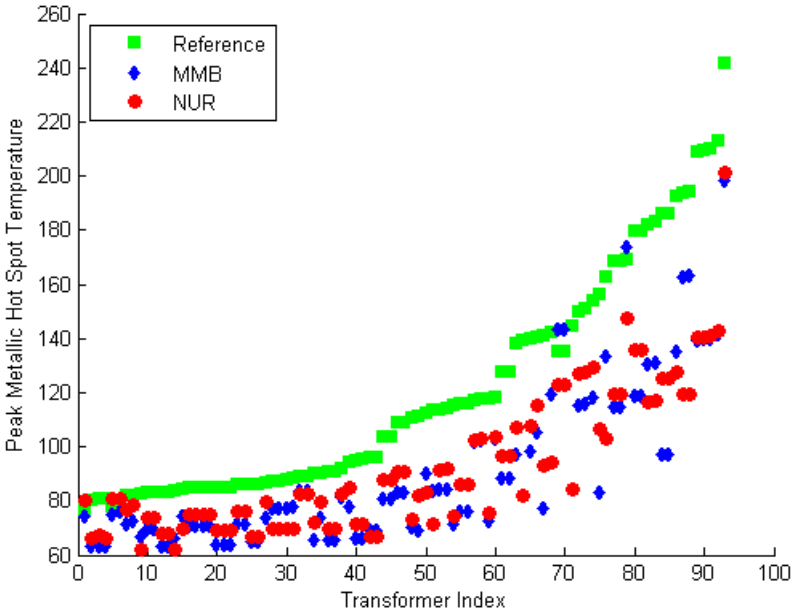

Figure I-7: Calculated Peak Metallic Hot Spot Temperature for All Transformers in a Test System with a Temperature Increase of More Than 20°C for Different GMD Events Scaled to the Same Peak Geoelectric Field

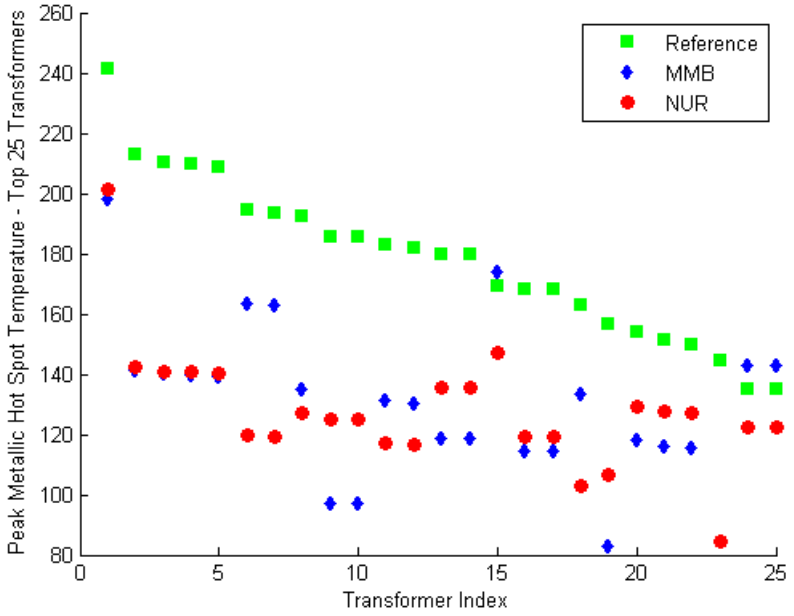

Figure I-8: Calculated Peak Metallic Hot Spot Temperature for the Top 25 Transformers in a Test System for Different GMD Events Scaled to the Same Peak Geoelectric Field

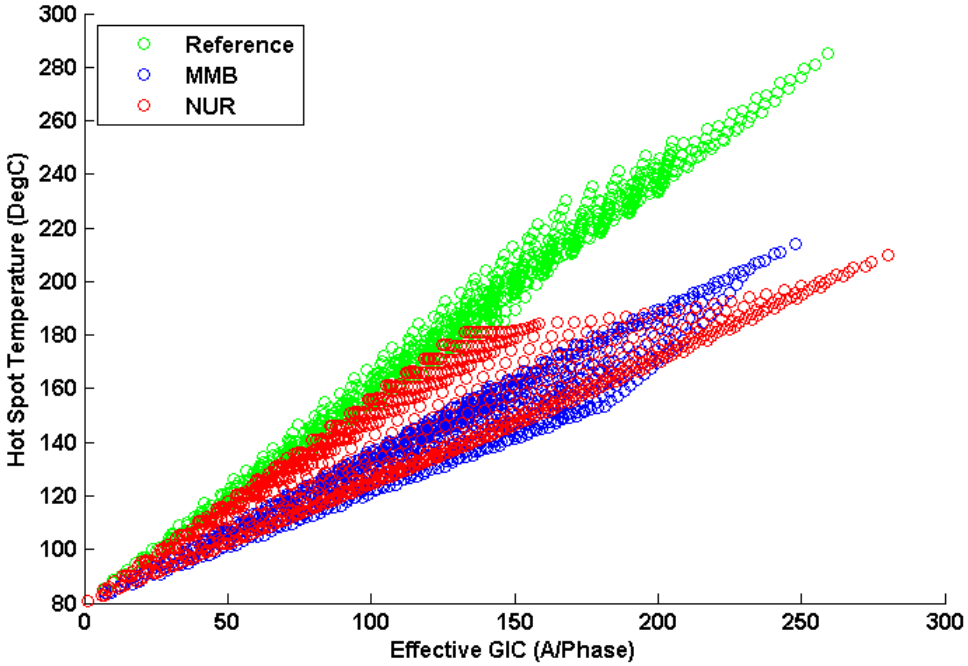

Figure I-9: Calculated Peak Metallic Hot Spot Temperature for all possible circuit orientations and effective GIC.

Appendix II – Scaling the Benchmark GMD Event

The intensity of a GMD event depends on geographical considerations such as geomagnetic latitude[6] and local earth conductivity[7] [3]**.** Scaling factors for geomagnetic latitude take into consideration that the intensity of a GMD event varies according to latitude-based geographical location. Scaling factors for earth conductivity take into account that the induced geoelectric field depends on earth conductivity, and that different parts of the continent have different earth conductivity and deep earth structure.

Scaling the Geomagnetic Field

The benchmark GMD event is defined for geomagnetic latitude of 60° and it must be scaled to account for regional differences based on geomagnetic latitude. To allow usage of the reference geomagnetic field waveshape in other locations, **Table II-1** summarizes the scaling factor α correlating peak geoelectric field to geomagnetic latitude as described in **Figure II-1** [3]. This scaling factor α has been obtained from a large number of global geomagnetic field observations of all major geomagnetic storms since the late 1980s [15], [24]-[25], and can be approximated with the empirical expression in (II.1)

$$\alpha = 0.001 \cdot e^{(0.115 \cdot L)} \qquad \text{(II.1)}$$

where L is the geomagnetic latitude in degrees and $0.1 \leq \alpha \leq 1.0$.

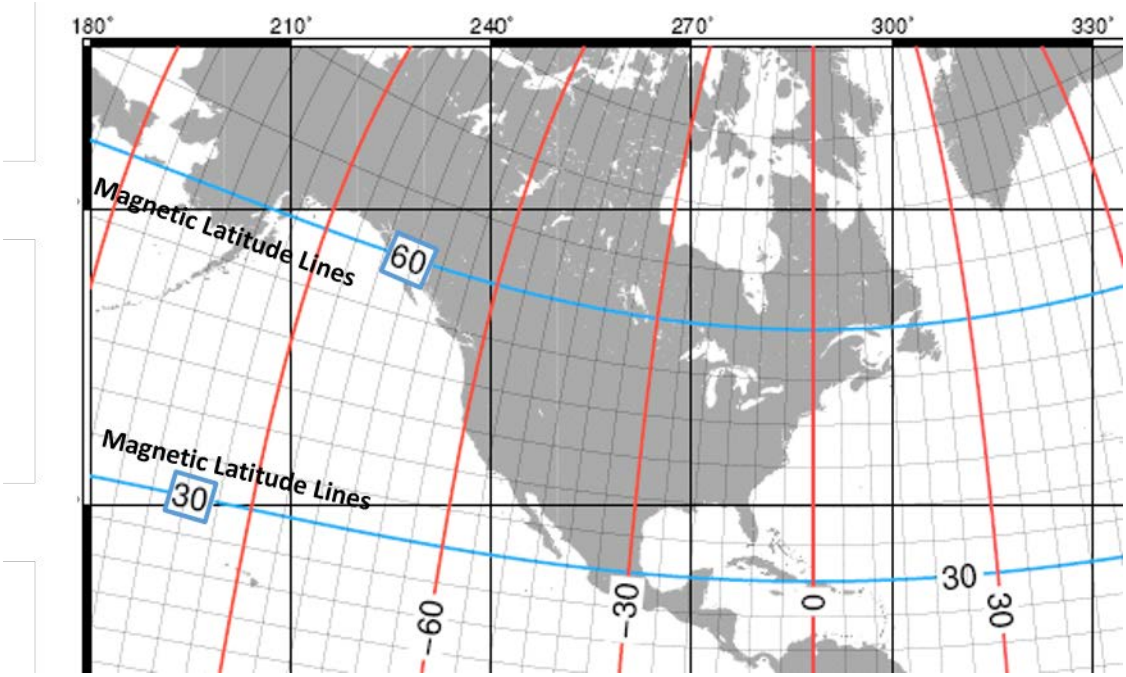

Figure II-1: Geomagnetic Latitude Lines in North America

[6] Geomagnetic latitude is analogous to geographic latitude, except that bearing is in relation to the magnetic poles, as opposed to the geographic poles. Geomagnetic phenomena are often best organized as a function of geomagnetic coordinates.

[7] Local earth conductivity refers to the electrical characteristics to depths of hundreds of km down to the earth's mantle. In general terms, lower ground conductivity results in higher geoelectric field amplitudes.

Table II-1: Geomagnetic Field Scaling Factors	
Geomagnetic Latitude (Degrees)	Scaling Factor1 (α)
≤ 40	0.10
45	0.2
50	0.3
54	0.5
56	0.6
57	0.7
58	0.8
59	0.9
≥ 60	1.0

Scaling the Geoelectric Field

The benchmark GMD event is defined for the reference Quebec earth model provided in **Table 1**. This earth model has been used in many peer-reviewed technical articles [12, 15]. The peak geoelectric field depends on the geomagnetic field waveshape and the local earth conductivity. Ideally, the peak geoelectric field, E_{peak}, is obtained by calculating the geoelectric field from the scaled geomagnetic waveshape using the plane wave method and taking the maximum value of the resulting waveforms

$$E_N = (z(t)/\mu_o) * B_E(t)$$
$$E_E = -(z(t)/\mu_o) * B_N(t) \qquad \text{(II.2)}$$
$$E_{peak} = \max\left\{\left|E_E(t), E_N(t)\right|\right\}$$

where,

* denotes convolution in the time domain,

z(t) is the impulse response for the earth surface impedance calculated from the laterally uniform or 1D earth model,

$B_E(t)$, $B_N(t)$ are the scaled Eastward and Northward geomagnetic field waveshapes,

$E_E(t)$, $E_N(t)|$ are the magnitudes of the calculated Eastward and Northward geoelectric field $E_E(t)$ and $E_N(t)$.

As noted previously, the response of the earth to B(t) (and dB/dt) is frequency dependent. **Figure II-2** shows the magnitude of Z(ω) for the reference earth model.

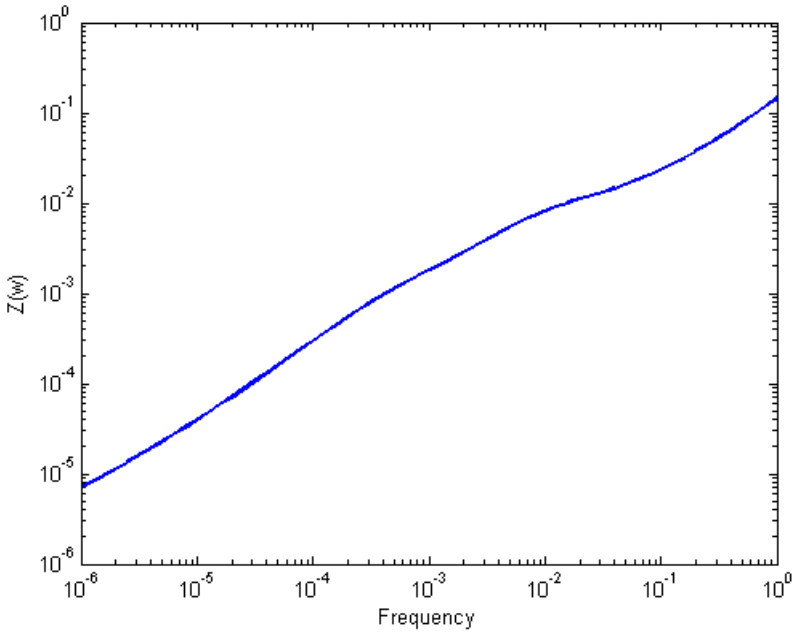

Figure II-2: Magnitude of the Earth Surface Impedance for the Reference Earth Model

If a utility does not have the capability of calculating the waveshape or time series for the geoelectric field, an earth conductivity scaling factor β can be obtained from **Table II-2**. Using α and β, the peak geoelectric field E_{peak} for a specific service territory shown in **Figure II-3** can be obtained using (II.3)

$$E_{peak} = 8 \times \alpha \times \beta \text{ (V/km)} \quad \text{(II.3)}$$

It should be noted that (II.3) is an approximation based on the following assumptions:

- The earth models used to calculate Table II-2 for the United States are from published information available on the USGS website.
- The models used to calculate Table II-2 for Canada were obtained from NRCan and reflect the average structure for large regions. When models are developed for sub-regions, there will be variance (to a greater or lesser degree) from the average model. For instance, detailed models for Ontario have been developed by NRCan and consist of seven major sub-regions.
- The conductivity scaling factor β is calculated as the quotient of the local geoelectric field peak amplitude in a physiographic region with respect to the reference peak amplitude value of 8 V/km. Both geoelectric field peaks amplitudes are calculated using the reference geomagnetic field time series. If a different geomagnetic field time series were used, the calculated scaling factors β would be different than the values in Table II-2 because the frequency content of storm maxima is, in principle, different for every storm. However, the reference time series produces generally more conservative values of β when compared to the time series of reference storm of the NERC interim report of 2012 [14], measurements at the Nurmijarvi (NUR) and Memanbetsu (MMB) geomagnetic observatories for the "Halloween event" of October 29-31, 2003, and other recordings of the March 1989 event at high latitudes (Meanook observatory, Canada). The average variation between minimum and maximum β is approximately 12 percent. **Figure II-4** illustrates the values of β calculated using the 10-second recordings for these geomagnetic field time series.
- If a utility has technically-sound earth models for its service territory and sub-regions thereof, then the use of such earth models is preferable to estimate E_{peak}.

- When a ground conductivity model is not available the planning entity should use the largest β factor of adjacent physiographic regions or a technically-justified value.

Physiographic Regions of the Continental United States

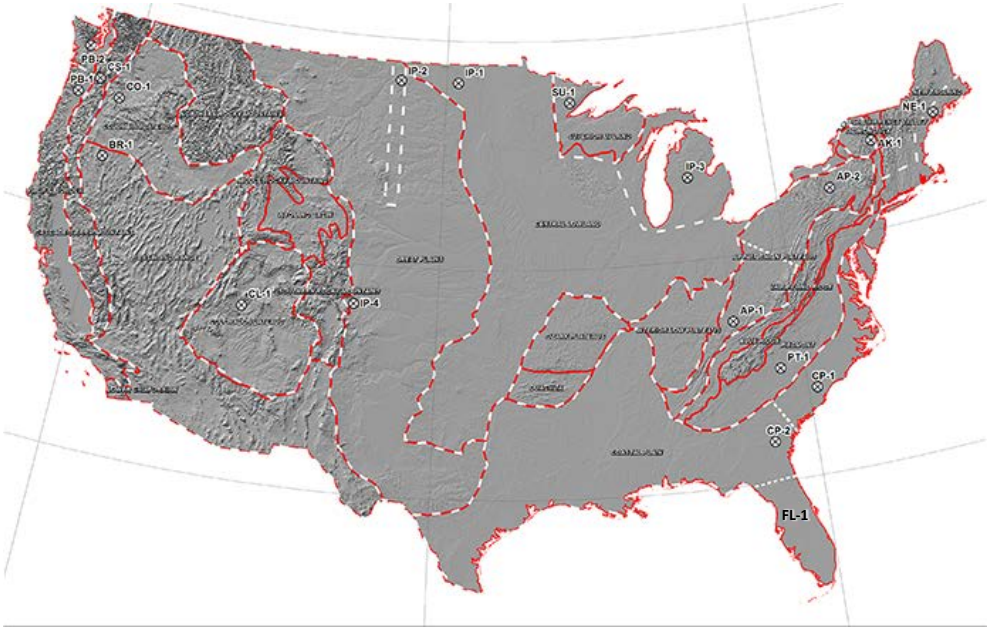

Physiographic Regions of Canada

Figure II-3: Physiographic Regions of North America

Table II-2 Geoelectric Field Scaling Factors	
USGS Earth model	Scaling Factor (β)
AK1A	0.56
AK1B	0.56
AP1	0.33
AP2	0.82
BR1	0.22
CL1	0.76
CO1	0.27
CP1	0.81
CP2	0.95
FL1	0.74
CS1	0.41
IP1	0.94
IP2	0.28
IP3	0.93
IP4	0.41
NE1	0.81
PB1	0.62
PB2	0.46
PT1	1.17
SL1	0.53
SU1	0.93
BOU	0.28
FBK	0.56
PRU	0.21
BC	0.67
PRAIRIES	0.96
SHIELD	1.0
ATLANTIC	0.79

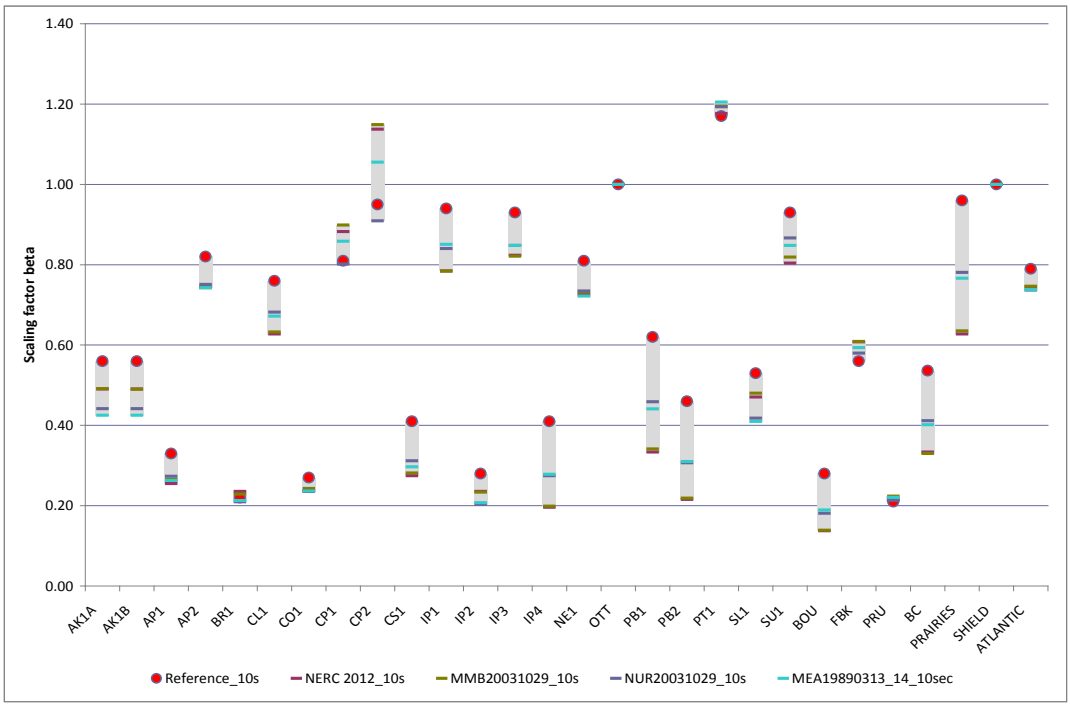

Figure II-4: Beta factors Calculated for Different GMD Events
Red circles correspond to the values in Table II-2

Example Calculations

Example 1

Consider a transmission service territory that lies in a geographical latitude of 45.5°, which translates to a geomagnetic latitude of 55°. The scaling factor α calculated using II.1 is 0.56; therefore, the benchmark waveshape and the peak geoelectric field will be scaled accordingly. If the service territory has the same earth conductivity as the benchmark then β=1, and the peak geoelectric field will be

$$\alpha = 0.56$$
$$\beta = 1.0$$
$$E_{peak} = 8 \times 0.56 \times 1 = 4.5 V/km$$

If the service territory spans more than one physiographic region (i.e. several locations within the service territory have a different earth model) then the largest α can be used across the entire service territory for conservative results. Alternatively, the network can be split into multiple subnetworks, and the corresponding geoelectric field amplitude can be applied to each subnetwork.

Example 2

Consider a service territory that lies in a geographical latitude of 45.5° which translates to a geomagnetic latitude of 55°. The scaling factor α calculated using II.1 is 0.56; therefore, the benchmark waveshape and the peak geoelectric field will be scaled accordingly.

The service territory has lower conductivity than the reference benchmark conductivity, therefore, according to the conductivity factor β from Table II-2., the calculation follows:

Conductivity factor β=1.17

$$\alpha = 0.56$$

$$E_{peak} = 8 \times 0.56 \times 1.17 = 5.2V / km$$

References

[1] L. Bolduc, A. Gaudreau, A. Dutil, "Saturation Time of Transformers Under dc Excitation", Electric Power Systems Research, 56 (2000), pp. 95-102

[2] *High-Impact, Low-Frequency Event Risk to the North American Bulk Power System*, A Jointly-Commissioned Summary Report of the North American Reliability Corporation and the U.S. Department of Energy's November 2009 Workshop.

[3] Application Guide: Computing Geomagnetically-Induced Current in the Bulk-Power System, NERC. NERC. http://www.nerc.com/comm/PC/Geomagnetic%20Disturbance%20Task%20Force%20GMDTF%202013/GIC%20Application%20Guide%202013_approved.pdf

[4] Kuan Zheng, Risto Pirjola, David Boteler, Lian-guang Liu, "Geoelectric Fields Due to Small-Scale and Large-Scale Source Currents", *IEEE Transactions on Power Delivery*, Vol. 28, No. 1, January 2013, pp. 442-449.

[5] Boteler, D. H. "Geomagnetically Induced Currents: Present Knowledge and Future Research", *IEEE Transactions on Power Delivery*, Vol. 9, No. 1, January 1994, pp. 50-58.

[6] Boteler, D. H. "Modeling Geomagnetically Induced Currents Produced by Realistic and Uniform Electric Fields", *IEEE Transactions on Power Delivery*, Vol. 13, No. 4, January 1998, pp. 1303-1308.

[7] J. L. Gilbert, W. A. Radasky, E. B. Savage, "A Technique for Calculating the Currents Induced by Geomagnetic Storms on Large High Voltage Power Grids", Electromagnetic Compatibility (EMC), 2012 IEEE International Symposium on.

[8] *How to Calculate Electric Fields to Determine Geomagnetically-Induced Currents.* EPRI, Palo Alto, CA: 2013. 3002002149.

[9] Pulkkinen, A., R. Pirjola, and A. Viljanen, Statistics of extreme geomagnetically induced current events, Space Weather, 6, S07001, doi:10.1029/2008SW000388, 2008.

[10] Boteler, D. H., Assessment of geomagnetic hazard to power systems in Canada, Nat. Hazards, 23, 101–120, 2001.

[11] Finnish Meteorological Institute's IMAGE magnetometer chain data available at: http://image.gsfc.nasa.gov/

[12] Boteler, D. H., and R. J. Pirjola, The complex-image method for calculating the magnetic and electric fields produced at the surface of the Earth by the auroral electrojet, Geophys. J. Int., 132(1), 31—40, 1998

[13] ANSI Standard C2, *National Electric Safety Code*, 2012, ISBN 978-0-7381-6588-2

[14] 2012 Special Reliability Assessment Interim Report: Effects of Geomagnetic Disturbances on the Bulk Power System. NERC. February 2012. http://www.nerc.com/pa/RAPA/ra/Reliability%20Assessments%20DL/2012GMD.pdf

[15] Pulkkinen, A., E. Bernabeu, J. Eichner, C. Beggan and A. Thomson, Generation of 100-year geomagnetically induced current scenarios, *Space Weather*, Vol. 10, S04003, doi:10.1029/2011SW000750, 2012.

[16] Love, J., Credible occurrence probabilities for extreme geophysical events: Earthquakes, volcanic eruptions, magnetic storms, Geophysical Research Letters, Vol. 39, L10301, doi:10.1029/2012GL051431, 2012.

[17] Pulkkinen, A., A. Thomson, E. Clarke, and A. Mckay, April 2000 geomagnetic storm: ionospheric drivers of large geomagnetically induced currents, Annales Geophysicae, 21, 709-717, 2003.

[18] Pulkkinen, A., S. Lindahl, A. Viljanen, and R. Pirjola, Geomagnetic storm of 29–31 October 2003: Geomagnetically induced currents and their relation to problems in the Swedish high-voltage power transmission system, Space Weather, 3, S08C03, doi:10.1029/2004SW000123, 2005.

[19] Pulkkinen, A., R. Pirjola, and A. Viljanen, Statistics of extreme geomagnetically induced current events, Space Weather, 6, S07001, doi:10.1029/2008SW000388, 2008.

[20] Langlois, P., L. Bolduc, and M. C. Chouteau, Probability of occurrence of geomagnetic storms based on a study of the distribution of the electric field amplitudes measured in Abitibi, Québec, in 1993–1994, J. Geomagn. Geoelectr., 48, 1033–1041, 1996.

[21] Pulkkinen, A., R. Pirjola, and A. Viljanen, Statistics of extreme geomagnetically induced current events, Space Weather, 6, S07001, doi:10.1029/2008SW000388, 2008.

[22] Campbell, W. C., Observation of electric currents in the Alaska oil pipeline resulting from auroral electrojet current sources, Geophys. J. R. Astron. Soc., 61, 437–449, 1980.

[23] Coles, Stuart (2001). An Introduction to Statistical Modelling of Extreme Values. Springer.

[24] Ngwira, C., A. Pulkkinen, F. Wilder, and G. Crowley, Extended study of extreme geoelectric field event scenarios for geomagnetically induced current applications, Space Weather, Vol. 11, 121–131, doi:10.1002/swe.20021, 2013.

[25] Thomson, A., S. Reay, and E. Dawson. Quantifying extreme behavior in geomagnetic activity, Space Weather, 9, S10001, doi:10.1029/2011SW000696, 2011.

NERC
NORTH AMERICAN ELECTRIC RELIABILITY CORPORATION

Screening Criterion for Transformer Thermal Impact Assessment

Project 2013-03 (Geomagnetic Disturbance Mitigation)

TPL-007-1 Transmission System Planned Performance for Geomagnetic Disturbance Events

Summary

Proposed standard TPL-007-1 – Transmission System Planned Performance for Geomagnetic Disturbance Events requires applicable entities to conduct assessments of the potential impact of benchmark GMD events on their systems. The standard requires transformer thermal impact assessments to be performed on power transformers with high side, wye-grounded windings with terminal voltage greater than 200 kV. Transformers are exempt from the thermal impact assessment requirement if the maximum effective geomagnetically-induced current (GIC) in the transformer is less than 75 A per phase as determined by GIC analysis of the system. Based on published power transformer measurement data as described below, an effective GIC of 75 A per phase is a conservative screening criterion. To provide an added measure of conservatism, the 75 A per phase threshold, although derived from measurements in single-phase units, is applicable to transformers with all core types (e.g., three-limb, three-phase).

Justification

Applicable entities are required to carry out a thermal assessment with GIC(t) calculated using the benchmark GMD event geomagnetic field time series or waveshape for effective GIC values above a screening threshold. The calculated GIC(t) for every transformer will be different because the length and orientation of transmission circuits connected to each transformer will be different even if the geoelectric field is assumed to be uniform. However, for a given thermal model and maximum effective GIC there are upper and lower bounds for the peak hot spot temperatures. These are shown in **Figure 1** using three available thermal models based on direct temperature measurements.

The results shown in **Figure 1** summarize the peak metallic hot spot temperatures when GIC(t) is calculated using (1), and systematically varying GIC_E and GIC_N to account for all possible orientation of circuits connected to a transformer. The transformer GIC (in A/phase) for any value of E_E (t) and E_N(t) can be calculated using equation (1) from reference [1].

$$GIC(t) = \left|E(t)\right| \cdot \left\{GIC_E \sin(\varphi(t)) + GIC_N \cos(\varphi(t))\right\} \quad (1)$$

where

$$|E(t)| = \sqrt{E_N^2(t) + E_E^2(t)} \tag{2}$$

$$\varphi(t) = \tan^{-1}\left(\frac{E_E(t)}{E_N(t)}\right) \tag{3}$$

$$GIC(t) = E_E(t) \cdot GIC_E + E_N(t) \cdot GIC_N \tag{4}$$

GIC_N is the effective GIC due to a northward geoelectric field of 1 V/km, and GIC_E is the effective GIC due to an eastward geoelectric field of 1 V/km. The units for GIC_N and GIC_E are A/phase/V/km.

It should be emphasized that with the thermal models used and the benchmark GMD event geomagnetic field waveshape, peak hot spot temperatures must lie below the envelope shown in **Figure 1**. The x-axis in Figure 1 corresponds to the absolute value of peak GIC(t). Effective maximum GIC for a transformer corresponds to a worst-case geoelectric field orientation, which is network-specific. Figure 1 represents a possible range, not the specific thermal response for a given effective GIC and orientation.

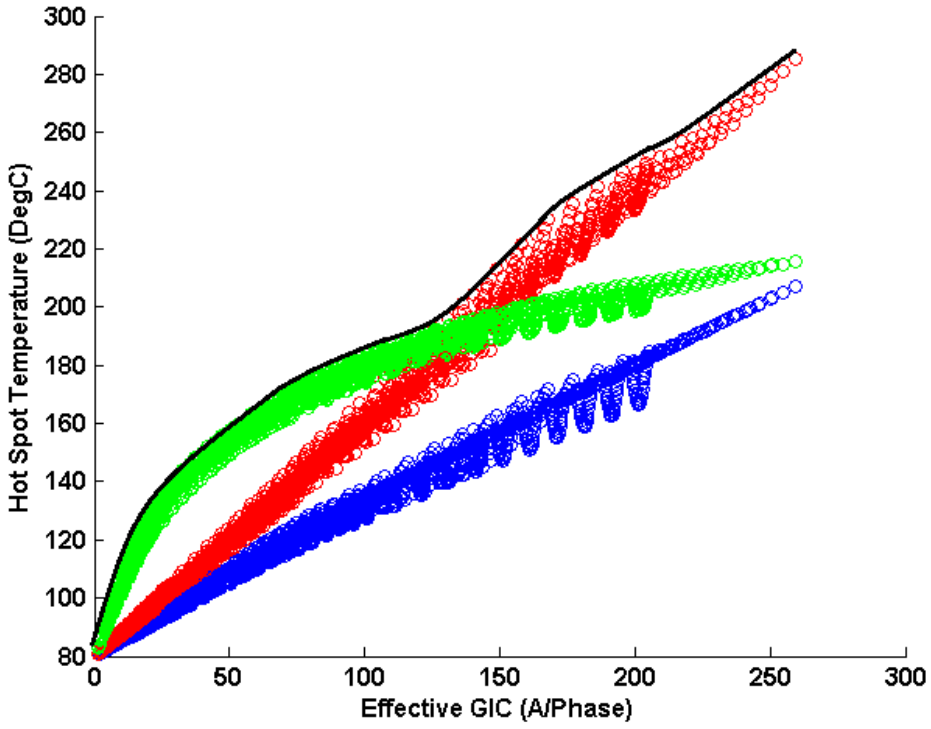

Figure 1: Metallic hot spot temperatures calculated using the benchmark GMD event. Red: SVC coupling transformer model [2]. Blue: Fingrid model [3]. Green: Autotransformer model [4].

Consequently, with the most conservative thermal models known at this point in time, the peak metallic hot spot temperature obtained with the benchmark GMD event waveshape assuming an effective GIC magnitude of 75 A per phase will result in a peak temperature between 160°C and 172°C when the bulk oil temperature is 80°C (full load bulk oil temperature). The upper boundary of 172°C remains well below the metallic hot spot 200°C threshold for short-time emergency loading suggested in IEEE Std C57.91-2011 [5] (see Table 1).

TABLE 1:
Excerpt from Maximum Temperature Limits Suggested in IEEE C57.91-2011

	Normal life expectancy loading	Planned loading beyond nameplate rating	Long-time emergency loading	Short-time emergency loading
Insulated conductor hottest-spot temperature °C	120	130	140	180
Other metallic hot-spot temperature (in contact and not in contact with insulation), °C	140	150	160	200
Top-oil temperature °C	105	110	110	110

The selection of the 75 A per phase screening threshold is based on the following considerations:

- A thermal assessment using the most conservative thermal models known to date will not result in peak hot spot temperatures above 172°C. Transformer thermal assessments should not be required by Reliability Standards when results will fall well below IEEE Std C57.91-2011 limits.
- Applicable entities may choose to carry out a thermal assessment when the effective GIC is below 75 A per phase to take into account the age or condition of specific transformers where IEEE Std C57.91- 2011 limits could be assumed to be lower than 200°C.
- The models used to determine the 75 A per phase screening threshold are known to be conservative at higher values of effective GIC, especially the SVC coupling transformer model in [2].
- Thermal models in peer-reviewed technical literature, especially those calculated models without experimental validation, are less conservative than the models used to determine the screening threshold. Therefore, a technically-justified thermal assessment for effective GIC below 75 A per phase using the benchmark GMD event geomagnetic field waveshape will always result in a "pass" on the basis of the state of the knowledge at this point in time.
- Based on simulations, the 75 A per phase screening threshold will result in a maximum instantaneous peak hot spot temperature of 172°C. However, IEEE Std C57.91- 2011 limits assume short term emergency operation (typically 30 minutes). As illustrated in **Figure 2**, simulations of the 75 A per phase screening threshold result in 30-minute duration hot spot temperatures of about

155°C. The threshold provides an added measure of conservatism in not taking into account the duration of hot spot temperatures.

- The models used in the determination of the threshold are conservative but technically justified.
- Winding hot spots are not the limiting factor in terms of hot spots due to half-cycle saturation, therefore the screening criterion is focused on metallic part hot spots only.

The 75 A per phase screening threshold was determined using single-phase transformers, but is applicable to all types of transformer construction. While it is known that some transformer types such as three-limb, three-phase transformers are intrinsically less susceptible to GIC, it is not known by how much, on the basis of experimentally-supported models.

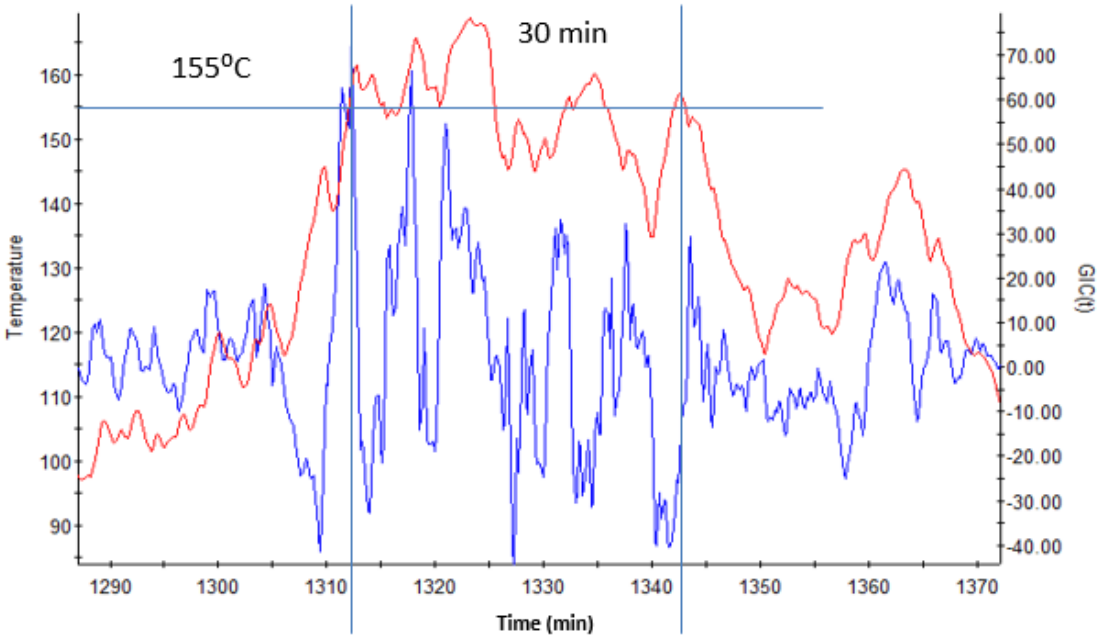

Figure 2: Metallic hot spot temperatures calculated using the benchmark GMD event. Red: metallic hot spot temperature. Blue: GIC(t) that produces the maximum hot spot temperature with peak GIC(t) scaled to 75 A/phase.

Appendix

The envelope used for thermal screening (Figure 1) is derived from two thermal models. The first is based on laboratory measurements carried out on 500/16.5 kV 400 MVA single-phase Static Var Compensator (SVC) coupling transformer [2]. Temperature measurements were carried out at relatively small values of GIC (see **Figure 3**). The asymptotic thermal response for this model is the linear extrapolation of the known measurement values. Although the near-linear behavior of the asymptotic thermal response is consistent with the measurements made on a Fingrid 400 kV 400 MVA five-leg core-type fully-wound transformer [3] (see **Figures 4 and 5**), the extrapolation from low values of GIC is very conservative, but reasonable for screening purposes.

The second transformer model is based on a combination of measurements and modeling for a 400 kV 400 MVA single-phase core-type autotransformer [4] (see **Figures 6 and 7**). The asymptotic thermal behavior of this transformer shows a "down-turn" at high values of GIC as the tie plate increasingly saturates but relatively high temperatures for lower values of GIC. The hot spot temperatures are higher than for the two other models for GIC less than 125 A per phase.

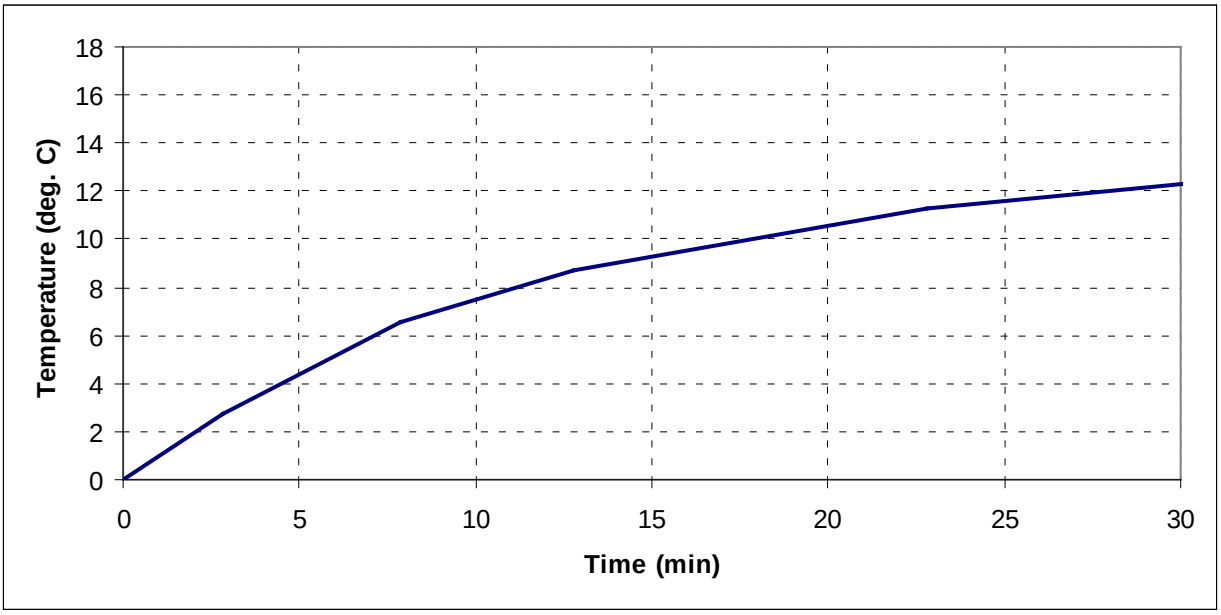

Figure 3: Thermal step response of the tie plate of a 500 kV 400 MVA single-phase SVC coupling transformer to a 5 A per phase dc step.

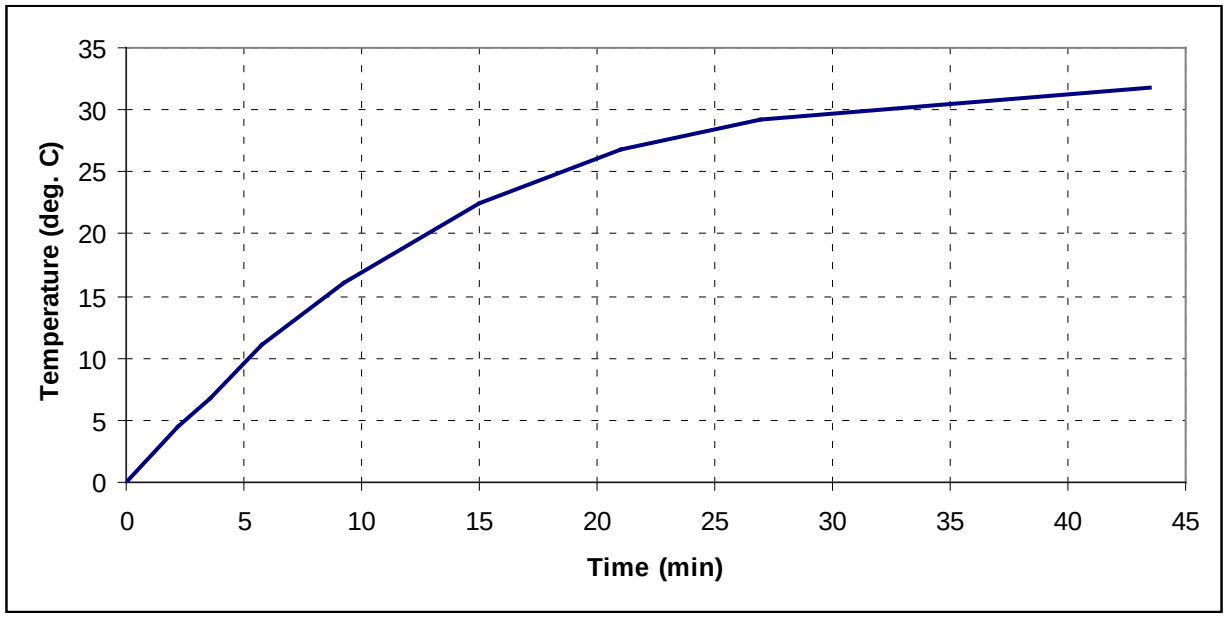

Figure 4: Step thermal response of the top yoke clamp of a 400 kV 400 MVA five-leg core-type fully-wound transformer to a 16.67 A per phase dc step.

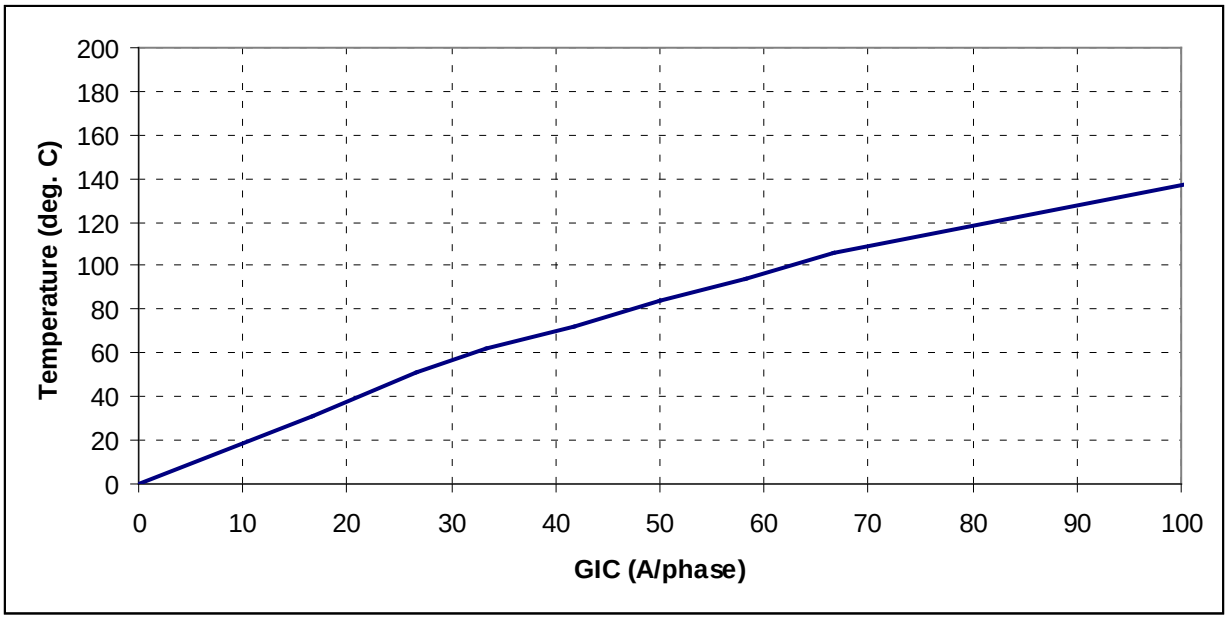

Figure 5: Asymptotic thermal response of the top yoke clamp of a 400 kV 400 MVA five-leg core-type fully-wound transformer.

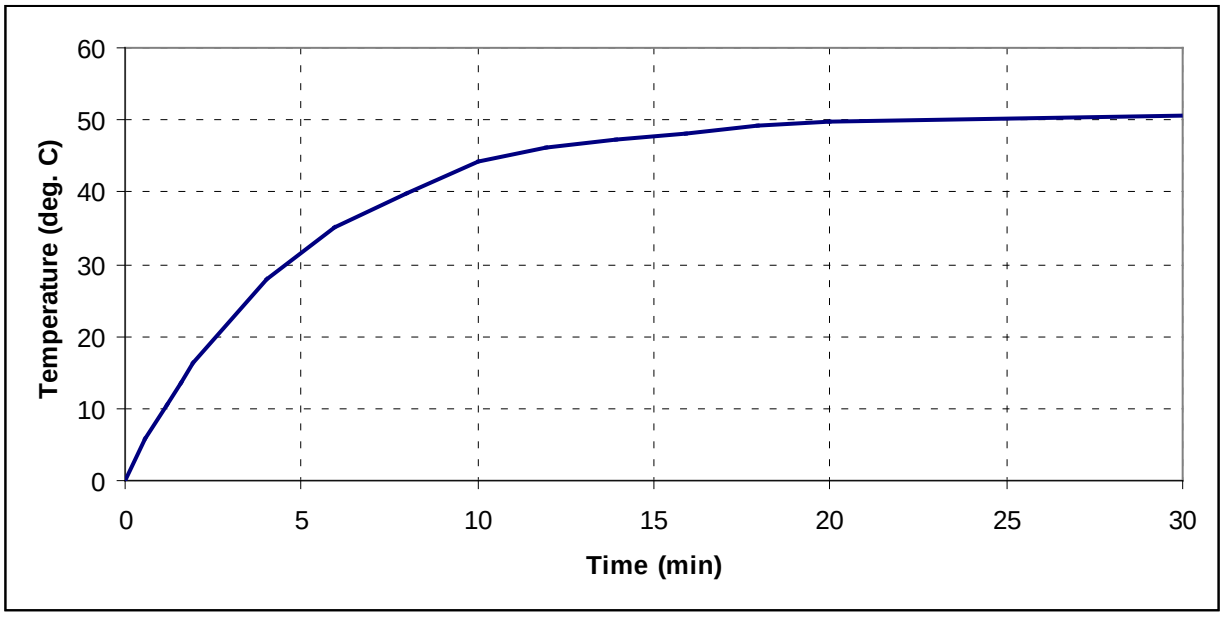

Figure 6: Step thermal response of the tie plate of a 400 kV 400 MVA single-phase core-type autotransformer to a 10 A per phase dc step.

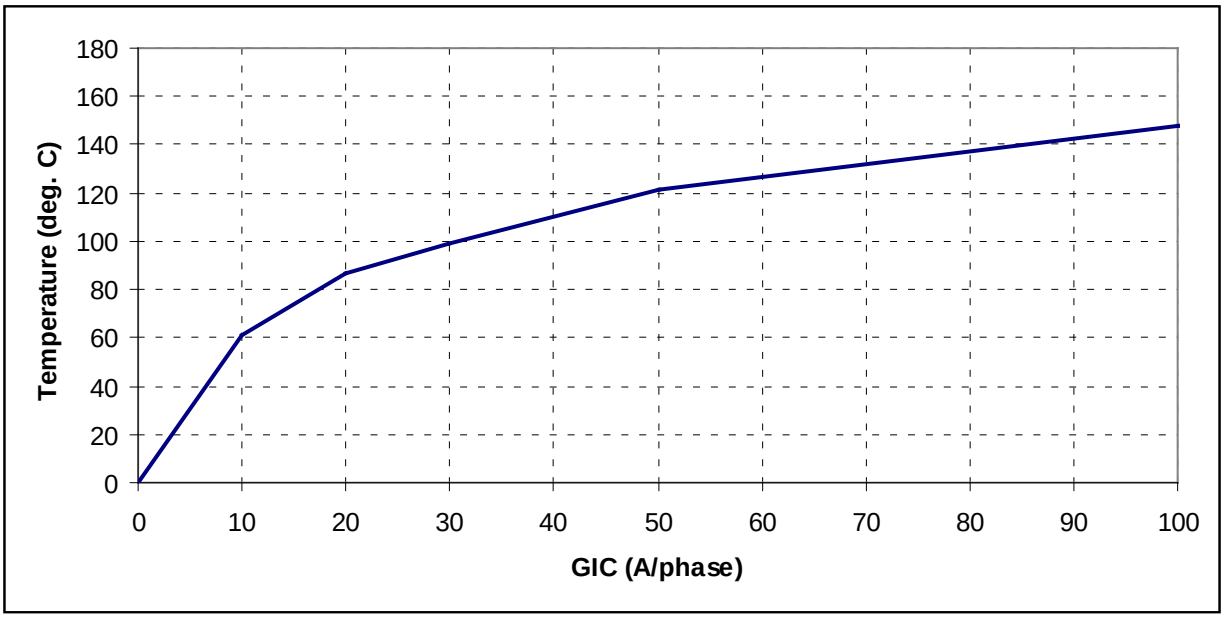

Figure 7: Asymptotic thermal response of the tie plate of a 400 kV 400 MVA single-phase core-type autotransformer.

The envelope in **Figure 1** can be used as a conservative thermal assessment for effective GIC values of 75 A per phase and greater (see Table 2).

Table 2: Upper Bound of Peak Metallic Hot Spot Temperatures Calculated Using the Benchmark GMD Event

Effective GIC (A/phase)	Metallic hot spot Temperature (°C)	Effective GIC(A/phase)	Metallic hot spot Temperature (°C)
0	80	100	182
10	107	110	186
20	128	120	190
30	139	130	193
40	148	140	204
50	157	150	213
60	169	160	221
70	170	170	230
75	172	180	234
80	175	190	241
90	179	200	247

For instance, if effective GIC is 130 A per phase and oil temperature is assumed to be 80°C, peak hot spot temperature is 193°C. This value is below the 200°C IEEE Std C57.91-2011 threshold for short time emergency loading and this transformer will have passed the thermal assessment. If the full heat run oil temperature is 67°C at maximum ambient temperature, then 150 A per phase of effective GIC translates into a peak hot spot temperature of 200°C and the transformer will have passed. If the limit is lowered to 180°C to account for the condition of the transformer, then this would be an indication to "sharpen the pencil" and perform a detailed assessment. Some methods are described in Reference [1].

The temperature envelope in Figure 1 corresponds to the values of effective GIC that result in the highest temperature for the benchmark GMD event. Different values of effective GIC could result in lower temperatures using the same model. For instance, the difference in upper and lower bounds of peak temperatures for the SVC coupling transformer model for 150 A per phase is approximately 30°C. In this case, GIC(t) should be generated to calculate the peak temperatures for the actual configuration of the transformer within the system as described in Reference [1]. Alternatively, a more precise thermal assessment could be carried out with a thermal model that more closely represents the thermal behavior of the transformer under consideration.

References

[1] Transformer Thermal Impact Assessment white paper. Developed by the Project 2013-03 (Geomagnetic Disturbance) standard drafting team. Available at:

http://www.nerc.com/pa/Stand/Pages/Project-2013-03-Geomagnetic-Disturbance-Mitigation.aspx

[2] Marti, L., Rezaei-Zare, A., Narang, A., "Simulation of Transformer Hotspot Heating due to Geomagnetically Induced Currents," *IEEE Transactions on Power Delivery,* vol.28, no.1, pp.320-327, Jan. 2013.

[3] Lahtinen, Matti. Jarmo Elovaara. "GIC occurrences and GIC test for 400 kV system transformer". IEEE Transactions on Power Delivery, Vol. 17, No. 2. April 2002.

[4] J. Raith, S. Ausserhofer: "GIC Strength verification of Power Transformers in a High Voltage Laboratory", GIC Workshop, Cape Town, April 2014

[5] "IEEE Guide for loading mineral-oil-immersed transformers and step-voltage regulators." IEEE Std C57.91-2011 (Revision of IEEE Std C57.91-1995).

NERC
NORTH AMERICAN ELECTRIC RELIABILITY CORPORATION

Transformer Thermal Impact Assessment White Paper

Project 2013-03 (Geomagnetic Disturbance Mitigation)

TPL-007-1 Transmission System Planned Performance for Geomagnetic Disturbance Events

Background

On May 16, 2013, FERC issued Order No. 779, directing NERC to develop Standards that address risks to reliability caused by geomagnetic disturbances (GMDs) in two stages:

- Stage 1 Standard(s) that require applicable entities to develop and implement Operating Procedures. EOP-010-1 – Geomagnetic Disturbance Operations was approved by FERC in June 2014.
- Stage 2 Standard(s) that require applicable entities to conduct assessments of the potential impact of benchmark GMD events on their systems. If the assessments identify potential impacts, the Standard(s) will require the applicable entity to develop and implement a plan to mitigate the risk.

TPL-007-1 is a new Reliability Standard to specifically address the Stage 2 directives in Order No. 779.

Large power transformers connected to the EHV transmission system can experience both winding and structural hot spot heating as a result of GMD events. TPL-007-1 will require owners of such transformers to conduct thermal analyses of their transformers to determine if the transformers will be able to withstand the thermal transient effects associated with the Benchmark GMD event. This paper discusses methods that can be employed to conduct such analyses, including example calculations.

The primary impact of GMDs on large power transformers is a result of the quasi-dc current that flows through wye-grounded transformer windings. This geomagnetically-induced current (GIC) results in an offset of the ac sinusoidal flux resulting in asymmetric or half-cycle saturation (see **Figure 1**).

Half-cycle saturation results in a number of known effects:

- Hot spot heating of transformer windings due to harmonics and stray flux;
- Hot spot heating of non-current carrying transformer metallic members due to stray flux;
- Harmonics;
- Increase in reactive power absorption; and
- Increase in vibration and noise level.

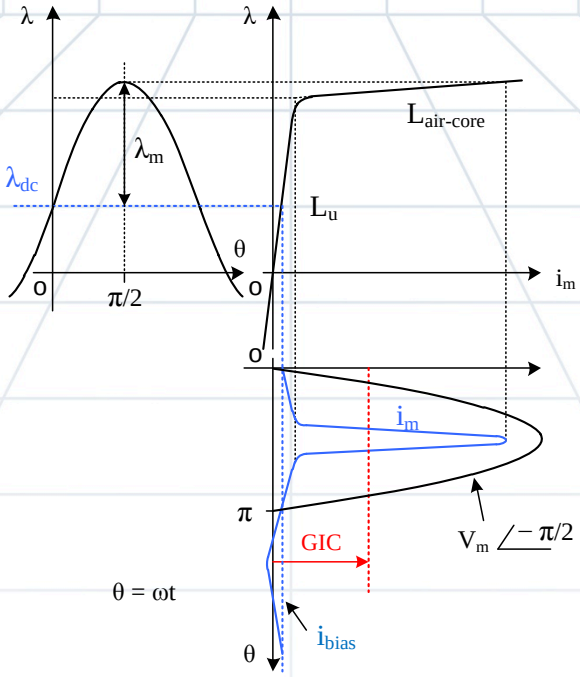

Figure 1: Mapping Magnetization Current to Flux through Core Excitation Characteristics

This paper focuses on hot spot heating of transformer windings and non current-carrying metallic parts. Effects such as the generation of harmonics, increase in reactive power absorption, vibration, and noise are not within the scope of this document.

Technical Considerations

The effects of half-cycle saturation on HV and EHV transformers, namely localized "hot spot" heating, are relatively well understood, but are difficult to quantify. A transformer GMD impact assessment must consider GIC amplitude, duration, and transformer physical characteristics such as design and condition (e.g., age, gas content, and moisture in the oil). A single threshold value of GIC cannot be justified as a "pass or fail" screening criterion where "fail" means that the transformer will suffer damage. A single threshold value of GIC only makes sense in the context where "fail" means that a more detailed study is required and that "pass" means that GIC in a particular transformer is so low that a detailed study is unnecessary. Such a threshold would have to be technically justifiable and sufficiently low to be considered a conservative value within the scope of the benchmark.

The following considerations should be taken into account when assessing the thermal susceptibility of a transformer to half-cycle saturation:

- In the absence of manufacturer specific information, use the temperature limits for safe transformer operation such as those suggested in the IEEE Std C57.91-2011 standard [1] for hot spot heating during short-term emergency operation. This standard does not suggest that exceeding these limits will result in transformer failure, but rather that it will result in additional aging of cellulose in the paper-oil insulation and the potential for the generation of gas bubbles in the bulk oil. Thus, from the point of view of evaluating

possible transformer damage due to increased hot spot heating, these thresholds can be considered conservative for a transformer in good operational condition.

- The worst case temperature rise for winding and metallic part (e.g., tie plate) heating should be estimated taking into consideration the construction characteristics of the transformer as they pertain to dc flux offset in the core (e.g., single-phase, shell, 5 and 3-leg three-phase construction).
- Bulk oil temperature due to ambient temperature and transformer loading must be added to the incremental temperature rise caused by hot spot heating. For planning purposes, maximum ambient and loading temperature should be used unless there is a technically justified reason to do otherwise.
- The time series or "waveshape" of the reference GMD event in terms of peak amplitude, duration, and frequency of the geoelectric field has an important effect on hot spot heating. Winding and metallic part hot spot heating have different thermal time constants, and their temperature rise will be different if the GIC currents are sustained for 2, 10, or 30 minutes for a given GIC peak amplitude.
- The "effective" GIC in autotransformers (reflecting the different GIC ampere-turns in the common and the series windings) must be used in the assessment. The effective current $I_{dc,eq}$ in an autotransformer is defined by [2].

$$I_{dc,eq} = I_H + (I_N/3 - I_H)V_X/V_H \quad (1)$$

where

I_H is the dc current in the high voltage winding;
I_N is the neutral dc current;
V_H is the rms rated voltage at HV terminals;
V_X is the rms rated voltage at the LV terminals.

Transformer Thermal Impact Assessment Process

A simplified thermal assessment may be based on Table 2 from the "Screening Criterion for Transformer Thermal Impact Assessment" white paper [7]. This table, shown as Table 1 below, provides the peak metallic hot spot temperatures that can be reached using conservative thermal models. To use Table 1, one must select the bulk oil temperature and the threshold for metallic hot spot heating, for instance, from reference [1] after allowing for possible de-rating due to transformer condition. If the effective GIC results in higher than threshold temperatures, then the use of a detailed thermal assessment as described below should be carried out.

Table 1: Upper Bound of Peak Metallic Hot Spot Temperatures Calculated Using the Benchmark GMD Event

Effective GIC (A/phase)	Metallic hot spot Temperature (°C)	Effective GIC(A/phase)	Metallic hot spot Temperature (°C)
0	80	100	182
10	107	110	186
20	128	120	190
30	139	130	193
40	148	140	204
50	157	150	213
60	169	160	221
70	170	170	230
75	172	180	234
80	175	190	241
90	179	200	247

Two different ways to carry out a detailed thermal impact assessment are discussed below. In addition, other approaches and models approved by international standard-setting organizations such as the Institute of Electrical and Electronic Engineers (IEEE)[1] or International Council on Large Electric Systems (CIGRE) may also provide technically justified methods for performing thermal assessments. All thermal assessment methods should be demonstrably equivalent to assessments that use the benchmark GMD event.

1. Transformer manufacturer GIC capability curves. These curves relate permissible peak GIC (obtained by the user from a steady-state GIC calculation) and loading, for a specific transformer. An example of manufacturer capability curves is provided in **Figure 2**. Presentation details vary between manufacturers, and limited information is available regarding the assumptions used to generate these curves, in particular, the assumed waveshape or duration of the effective GIC. Some manufacturers assume that the waveshape of the GIC in the transformer windings is a square pulse of 2, 10, or 30 minutes in duration. In the case of the transformer capability curve shown in **Figure 2** [3], a square pulse of 900 A/phase with a duration of 2 minutes would cause the Flitch plate hot spot to reach a temperature of 180 °C at full load. While GIC capability curves are relatively simple to use, an amount of engineering judgment is necessary to ascertain which portion of a GIC waveshape is equivalent to, for example, a 2 minute pulse. Also, manufacturers generally maintain that in

[1] For instance, IEEE Std C57.163-2015 Guide for Establishing Power Transformer Capability while under Geomagnetic Disturbances

the absence of transformer standards defining thermal duty due to GIC, such capability curves must be developed for every transformer design and vintage.

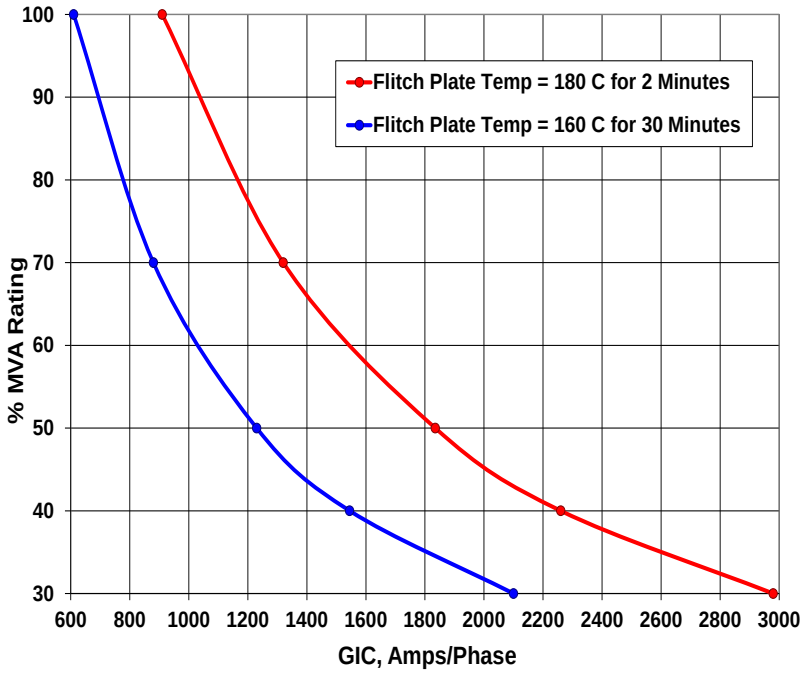

Figure 2: Sample GIC Manufacturer Capability Curve of a Large Single-Phase Transformer Design using the Flitch Plate Temperature Criteria [3]

2. Thermal response simulation[2]. The input to this type of simulation is the time series or waveshape of effective GIC flowing through a transformer (taking into account the actual configuration of the system), and the result of the simulation is the hot spot temperature (winding or metallic part) time sequence for a given transformer. An example of GIC input and hotspot temperature time series values from [4] are shown in **Figure 3**. The hot spot thermal transfer functions can be obtained from measurements or calculations provided by transformer manufacturers. Conservative default values can be used (e.g. those provided in [4]) when specific data are not available. Hot spot temperature thresholds shown in **Figure 3** are consistent with IEEE Std C57.91 emergency loading hot spot limits. Emergency loading time limit is usually 30 minutes.

[2] Technical details of this methodology can be found in [4].

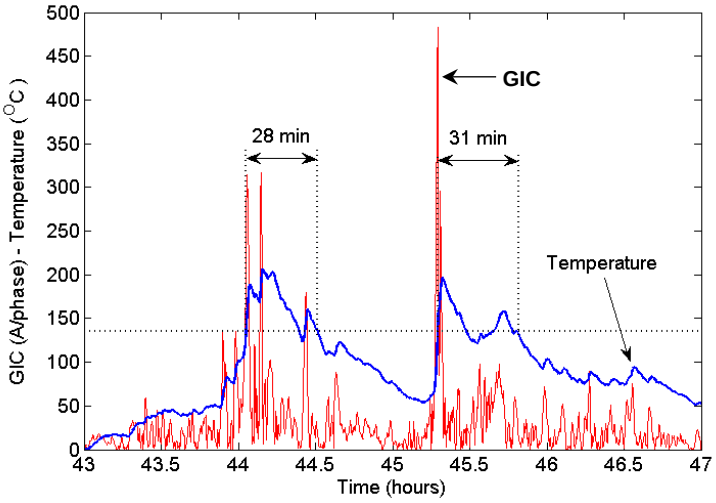

Figure 3: Sample Tie Plate Temperature Calculation
Blue trace is incremental temperature and red trace is the magnitude of the GIC/phase [4]

It is important to reiterate that the characteristics of the time sequence or "waveshape" are very important in the assessment of the thermal impact of GIC on transformers. Transformer hot spot heating is not instantaneous. The thermal time constants of transformer windings and metallic parts are typically on the order of minutes to tens of minutes; therefore, hot spot temperatures are heavily dependent on GIC history and rise time, amplitude and duration of GIC in the transformer windings, bulk oil temperature due to loading, ambient temperature and cooling mode.

Calculation of the GIC Waveshape for a Transformer

The following procedure can be used to generate time series GIC data, i.e. GIC(t), using a software program capable of computing GIC in the steady-state. The steps are as follows:

1. Calculate contribution of GIC due to eastward and northward geoelectric fields for the transformer under consideration;
2. Scale the GIC contribution according to the reference geoelectric field time series to produce the GIC time series for the transformer under consideration.

Most available GIC–capable software packages can calculate GIC in steady-state in a transformer assuming a uniform eastward geoelectric field of 1 V/km (GIC_E) while the northward geoelectric field is zero. Similarly, GIC_N can be obtained for a uniform northward geoelectric field of 1 V/km while the eastward geoelectric field is zero. GIC_E and GIC_N are the normalized GIC contributions for the transformer under consideration.

If the earth conductivity is assumed to be uniform (or laterally uniform) in the transmission system of interest, then the transformer GIC (in A/phase) for any value of $E_E(t)$ and $E_N(t)$ can be calculated using (2) [2].

$$GIC(t) = \left|E(t)\right| \cdot \left\{GIC_E \sin(\varphi(t)) + GIC_N \cos(\varphi(t))\right\} \quad (2)$$

where

$$|E(t)| = \sqrt{E_N^2(t) + E_E^2(t)} \quad (3)$$

$$\varphi(t) = \tan^{-1}\left(\frac{E_E(t)}{E_N(t)}\right) \quad (4)$$

$$GIC(t) = E_E(t) \cdot GIC_E + E_N(t) \cdot GIC_N \quad (5)$$

GIC_N is the effective GIC due to a northward geoelectric field of 1 V/km, and GIC_E is the effective GIC due to an eastward geoelectric field of 1 V/km. The units for GIC_N and GIC_E are A/phase/V/km)

The geoelectric field time series $E_N(t)$ and $E_E(t)$ is obtained, for instance, from the reference geomagnetic field time series [5] after the appropriate geomagnetic latitude scaling factor α is applied[3]. The reference geoelectric field time series is calculated using the reference earth model. When using this geoelectric field time series where a different earth model is applicable, it should be scaled with the conductivity scaling factor β[4]. Alternatively, the geoelectric field can be calculated from the reference geomagnetic field time series after the appropriate geomagnetic latitude scaling factor α is applied and the appropriate earth model is used. In such case, the conductivity scaling factor β is not applied because it is already accounted for by the use of the appropriate earth model.

Applying (5) to each point in $E_N(t)$ and $E_E(t)$ results in GIC(t).

GIC(t) Calculation Example

Let us assume that from the steady-state solution, the effective GIC in this transformer is GIC_E = -20 A/phase if E_N=0, E_E=1 V/km and GIC_N = 26 A/phase if E_N=1 V/km, E_E=0. Let us also assume the geomagnetic field time series corresponds to a geomagnetic latitude where α = 1 and that the earth conductivity corresponds to the reference earth model in [5]. The resulting geoelectric field time series is shown in **Figure 4**. Therefore:

$$GIC(t) = E_E(t) \cdot GIC_E + E_N(t) \cdot GIC_N \text{ (A/phase)} \quad (6)$$

$$GIC(t) = -E_E(t) \cdot 20 + \cdot E_N(t) \cdot 26 \text{ (A/phase)} \quad (7)$$

The resulting GIC waveshape GIC(t) is shown in **Figures 5 and 6** and can subsequently be used for thermal analysis.

[3] The geomagnetic factor α is described in [2] and is used to scale the geomagnetic field according to geomagnetic latitude. The lower the geomagnetic latitude (closer to the equator), the lower the amplitude of the geomagnetic field.

[4] The conductivity scaling factor β is described in [2], and is used to scale the geoelectric field according to the conductivity of different physiographic regions. Lower conductivity results in higher β scaling factors.

It should be emphasized that even for the same reference event, the GIC(t) waveshape in every transformer will be different, depending on the location within the system and the number and orientation of the circuits connecting to the transformer station. Assuming a single generic GIC(t) waveshape to test all transformers is incorrect.

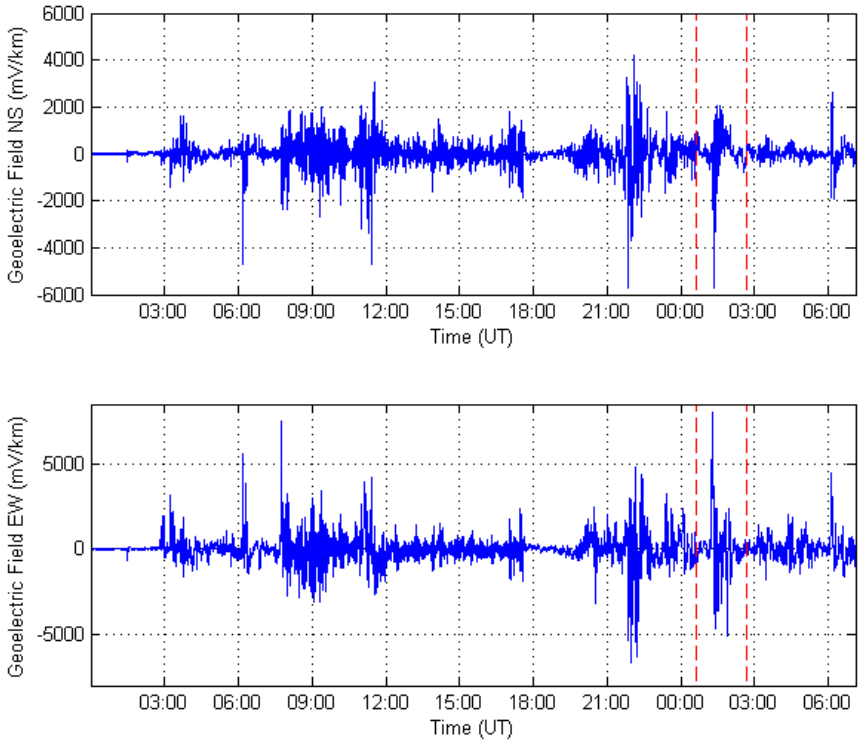

Figure 4: Calculated Geoelectric Field $E_N(t)$ and $E_E(t)$ Assuming $\alpha=1$ and $\beta=1$ (Reference Earth Model). Zoom area for subsequent graphs is highlighted. Dashed lines approximately show the close-up area for subsequent Figures.

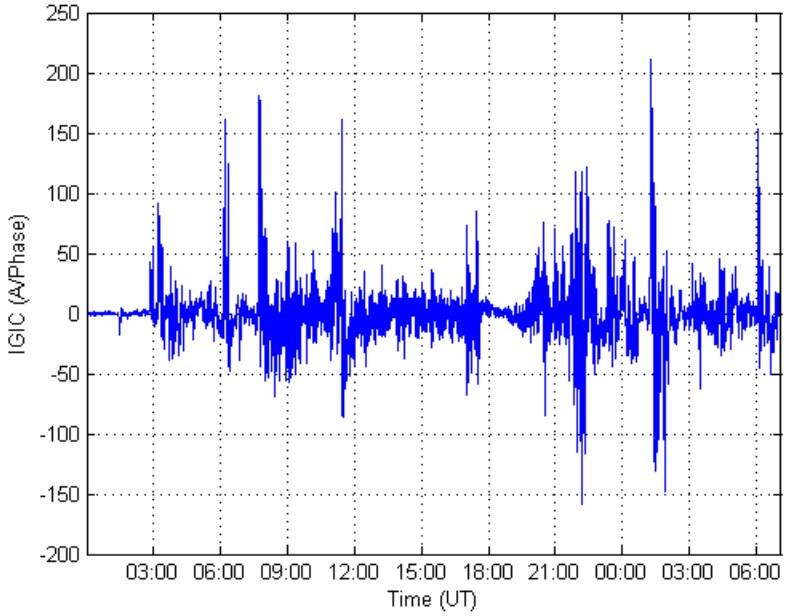

Figure 5: Calculated GIC(t) Assuming α=1 and β=1 (Reference Earth Model)

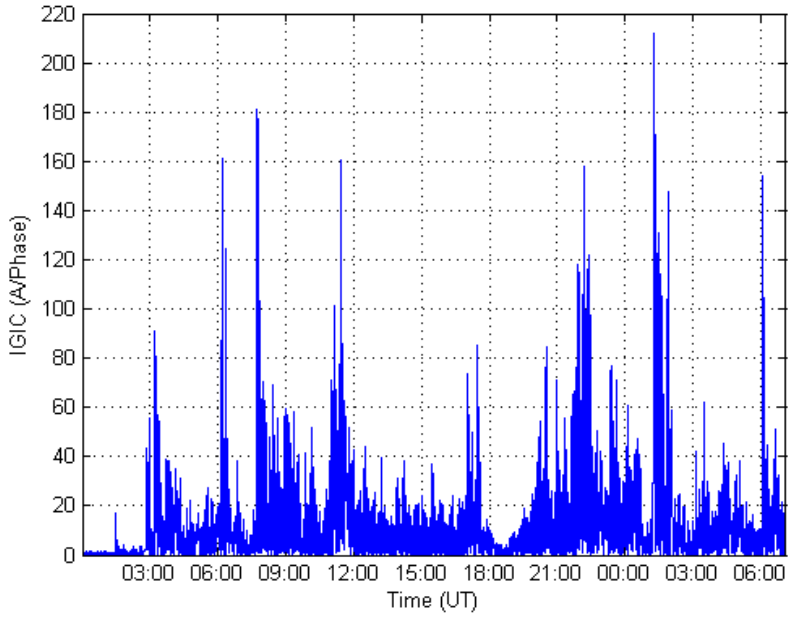

Figure 6: Calculated Magnitude of GIC(t) Assuming α=1 and β=1 (Reference Earth Model)

Transformer Thermal Assessment Examples

There are two basic ways to carry out a transformer thermal analysis once the GIC time series GIC(t) is known for a given transformer: 1) calculating the thermal response as a function of time; and 2) using manufacturer's capability curves.

Example 1: Calculating thermal response as a function of time using a thermal response tool

The thermal step response of the transformer can be obtained for both winding and metallic part hot spots from: 1) measurements; 2) manufacturer's calculations; or 3) generic published values. **Figure 7** shows the measured metallic hot spot thermal response to a dc step of 16.67 A/phase of the top yoke clamp from [6] that will be used in this example. **Figure 8** shows the measured incremental temperature rise (asymptotic response) of the same hot spot to long duration GIC steps.[5]

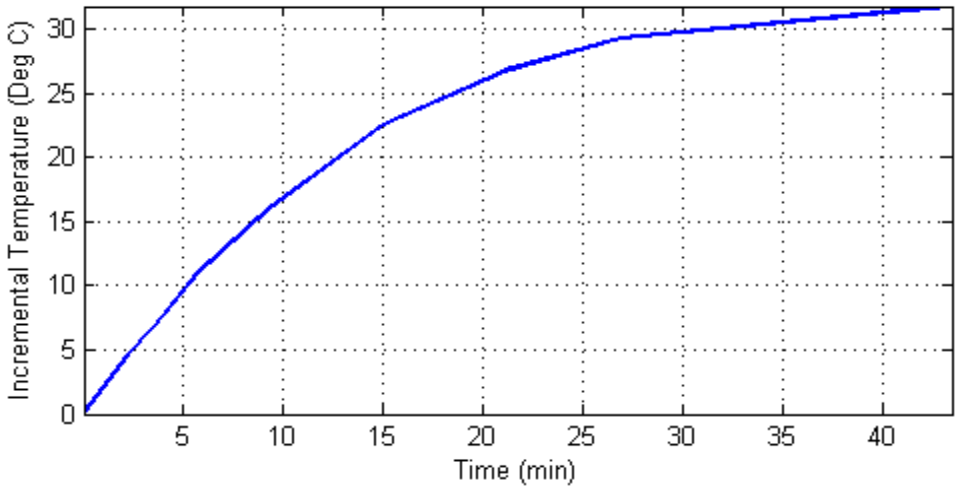

Figure 7: Thermal Step Response to a 16.67 Amperes per Phase dc Step
Metallic hot spot heating.

[5] Heating of bulk oil due to the hot spot temperature increase is not included in the asymptotic response because the time constant of bulk oil heating is at least an order of magnitude larger than the time constants of hot spot heating.

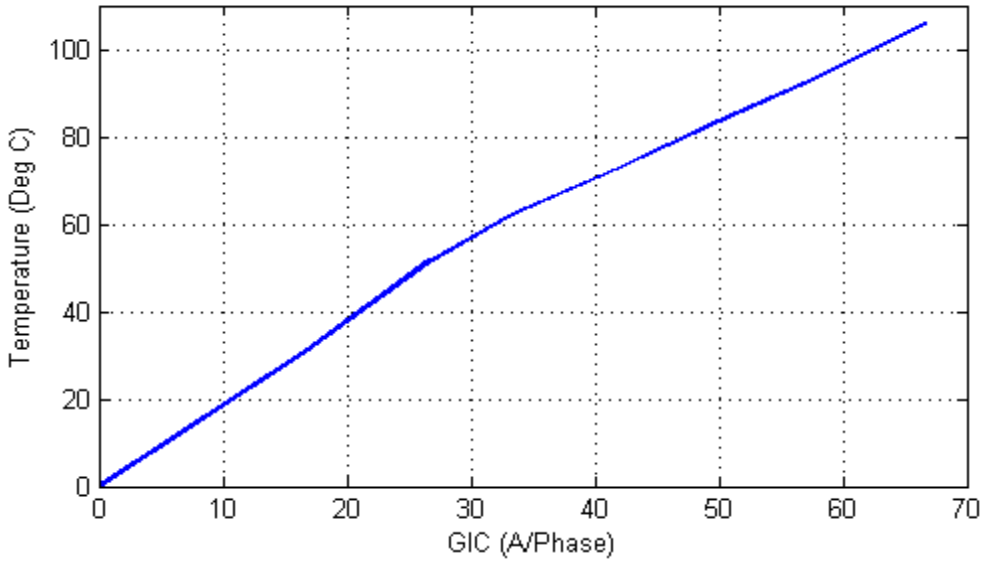

Figure 8: Asymptotic Thermal Step Response
Metallic hot spot heating.

The step response in **Figure 7** was obtained from the first GIC step of the tests carried out in [6]. The asymptotic thermal response in **Figure 8** was obtained from the final or near-final temperature values after each subsequent GIC step. **Figure 9** shows a comparison between measured temperatures and the calculated temperatures using the thermal response model used in the rest of this discussion.

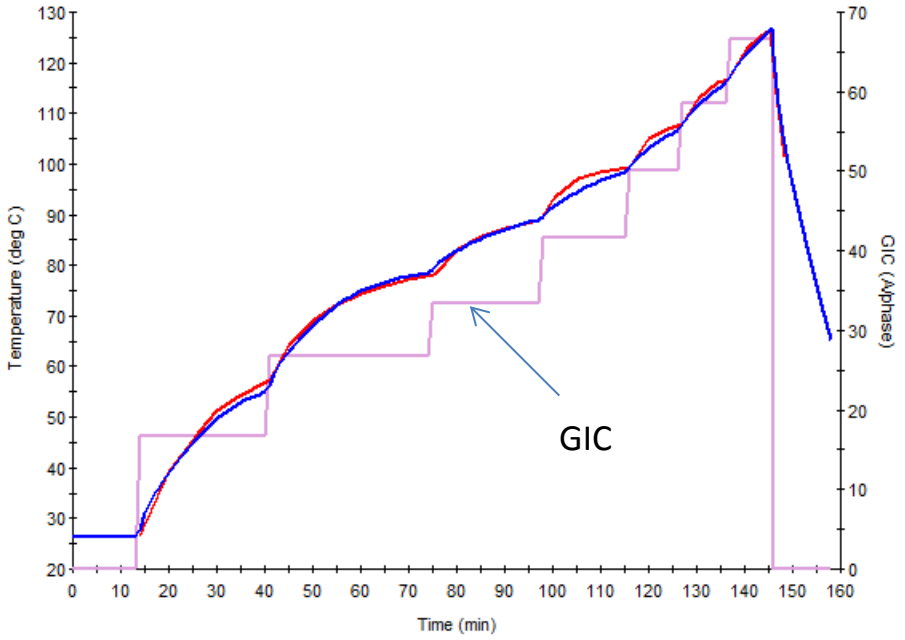

Figure 9: Comparison of measured temperatures (red trace) and simulation results (blue trace). Injected current is represented by the magenta trace.

To obtain the thermal response of the transformer to a GIC waveshape such as the one in **Figure 6**, a thermal response model is required. To create a thermal response model, the measured or manufacturer-calculated transformer thermal step responses (winding and metallic part) for various GIC levels are required. The GIC(t) time series or waveshape is then applied to the thermal model to obtain the incremental temperature rise as a function of time $\theta(t)$ for the GIC(t) waveshape. The total temperature is calculated by adding the oil temperature, for example, at full load.

Figure 10 illustrates the calculated GIC(t) and the corresponding hot spot temperature time series $\theta(t)$. **Figure 11** illustrates a close-up view of the peak transformer temperatures calculated in this example.

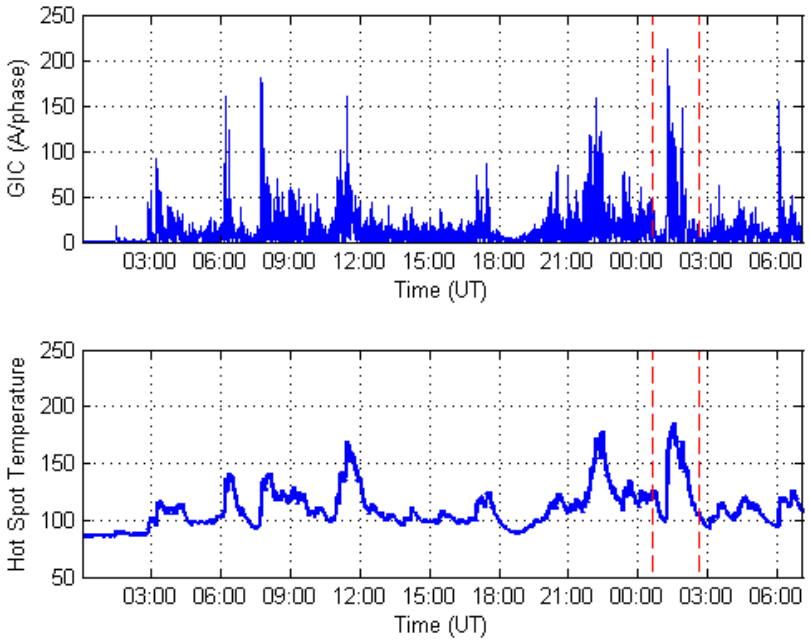

Figure 10: Magnitude of GIC(t) and Metallic Hot Spot Temperature $\theta(t)$ Assuming Full Load Oil Temperature of 85.3°C (40°C ambient). Dashed lines approximately show the close-up area for subsequent Figures.

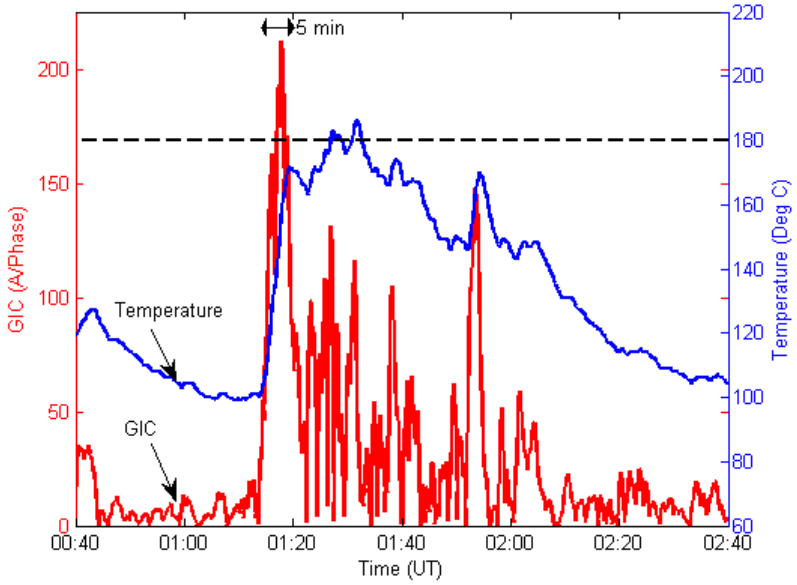

Figure 11: Close-up of Metallic Hot Spot Temperature Assuming a Full Load
(Blue trace is θ(t). Red trace is GIC(t))

In this example, the IEEE Std C57.91 emergency loading hot spot threshold of 200°C for metallic hot spot heating is not exceeded. Peak temperature is 186°C. The IEEE standard is silent as to whether the temperature can be higher than 200°C for less than 30 minutes. Manufacturers can provide guidance on individual transformer capability.

It is not unusual to use a lower temperature threshold of 180°C to account for calculation and data margins, as well as transformer age and condition. **Figure 11** shows that 180°C will be exceeded for 5 minutes.

At 75% loading, the initial temperature is 64.6 °C rather than 85.3 °C, and the hot spot temperature peak is 165°C, well below the 180°C threshold (see **Figure 12**).

If a conservative threshold of 160°C were used to account for the age and condition of the transformer, then the full load limits would be exceeded for approximately 22 minutes.

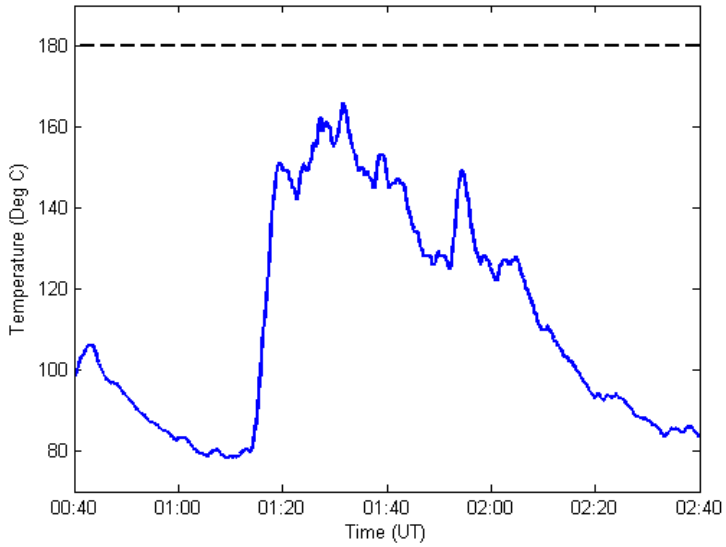

Figure 12: Close-up of Metallic Hot Spot Temperature Assuming a 75% Load
(Oil temperature of 64.5°C)

Example 2: Using a Manufacturer's Capability Curves

The capability curves used in this example are shown in **Figure 13**. To maintain consistency with the previous example, these particular capability curves have been reconstructed from the thermal step response shown in **Figures 7** and **8**, and the simplified loading curve shown in **Figure 14** (calculated using formulas from IEEE Std C57.91).

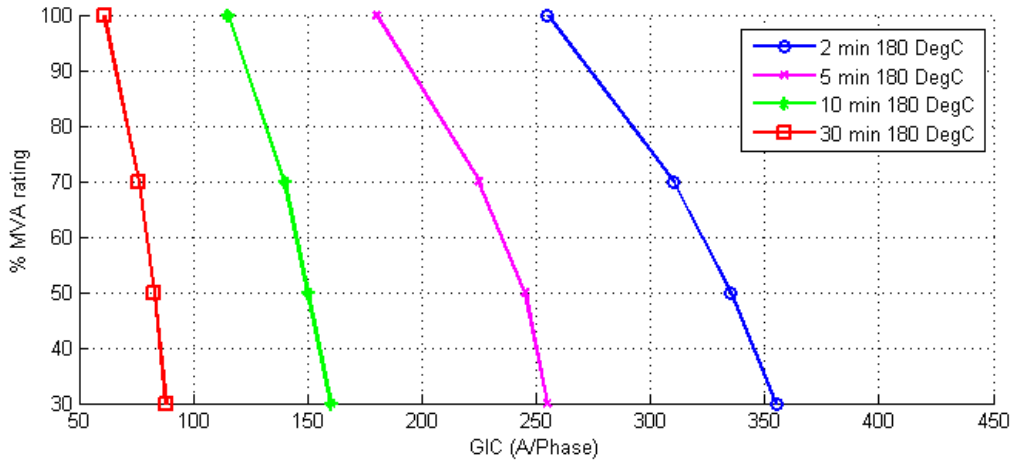

Figure 13: Capability Curve of a Transformer Based on the Thermal Response Shown in Figures 8 and 9.

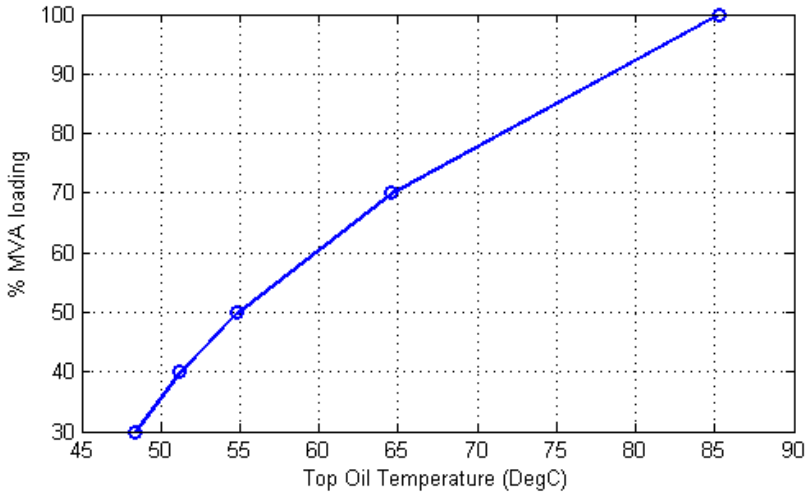

Figure 14: Simplified Loading Curve Assuming 40°C Ambient Temperature.

The basic notion behind the use of capability curves is to compare the calculated GIC in a transformer with the limits at different GIC pulse widths. A narrow GIC pulse has a higher limit than a longer duration or wider one. If the calculated GIC and assumed pulse width falls below the appropriate pulse width curve, then the transformer is within its capability.

To use these curves, it is necessary to estimate an equivalent square pulse that matches the waveshape of GIC(t), generally at a GIC(t) peak. **Figure 15** shows a close-up of the GIC near its highest peak superimposed to a 255 Amperes per phase, 2 minute pulse at 100% loading from **Figure 13**. Since a narrow 2-minute pulse is not representative of GIC(t) in this case, a 5 minute pulse with an amplitude of 180 A/phase at 100% loading has been superimposed on **Figure 16**. It should be noted that a 255 A/phase, 2 minute pulse is equivalent to a 180 A/phase 5 minute pulse from the point of view of transformer capability. Deciding what GIC pulse is equivalent to the portion of GIC(t) under consideration is a matter of engineering judgment.

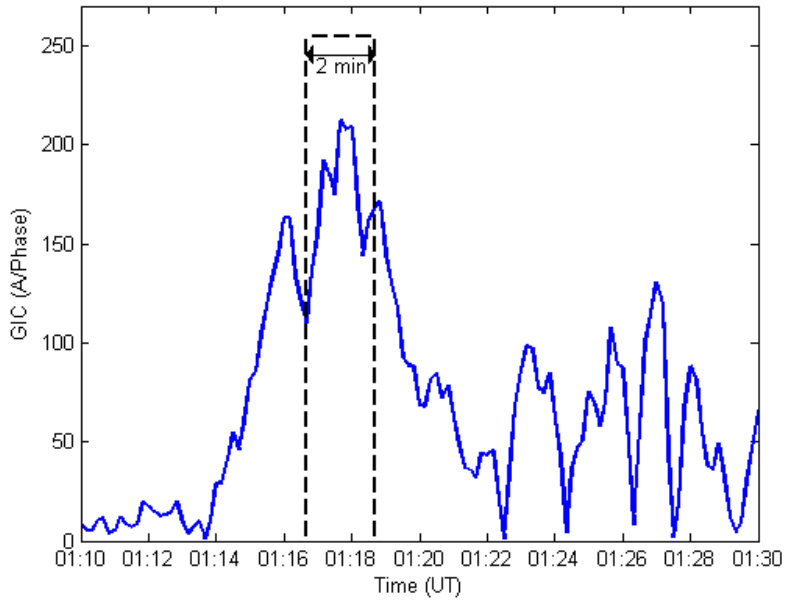

Figure 15: Close-up of GIC(t) and a 2 minute 255 A/phase GIC pulse at full load

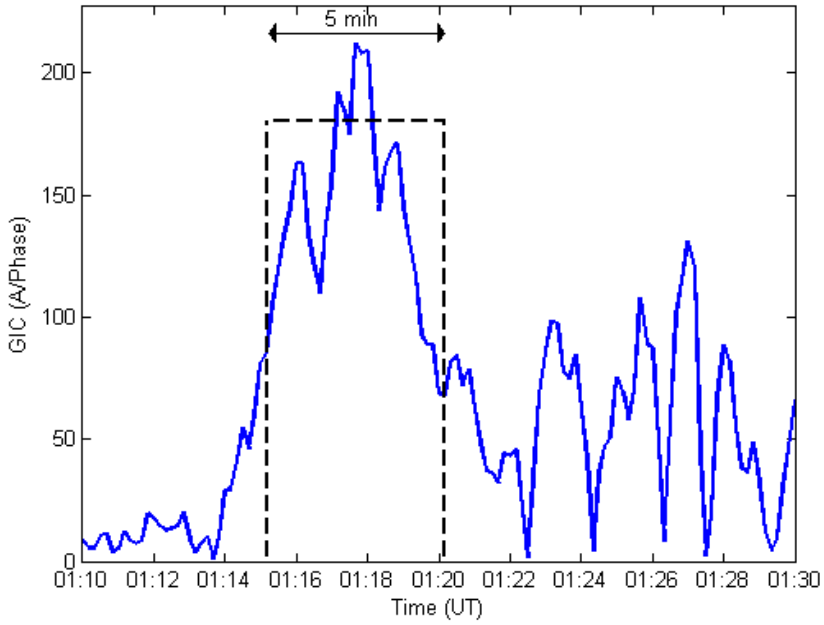

Figure 16: Close-up of GIC(t) and a Five Minute 180 A/phase GIC Pulse at Full Load

When using a capability curve, it should be understood that the curve is derived assuming that there is no hot spot heating due to prior GIC at the time the GIC pulse occurs (only an initial temperature due to loading). Therefore, in addition to estimating the equivalent pulse that matches GIC(t), prior hot spot heating must be accounted for. From

these considerations, it is unclear whether the capability curves would be exceeded at full load with a 180 °C threshold in this example.

At 70% loading, the two and five minute pulses from **Figure 13** would have amplitudes of 310 and 225 A/phase, respectively. The 5 minute pulse is illustrated in **Figure 17**. In this case, judgment is also required to assess if the GIC(t) is within the capability curve for 70% loading. In general, capability curves are easier to use when GIC(t) is substantially above, or clearly below the GIC thresholds for a given pulse duration.

If a conservative threshold of 160°C were used to account for the age and condition of the transformer, then a new set of capability curves would be required.

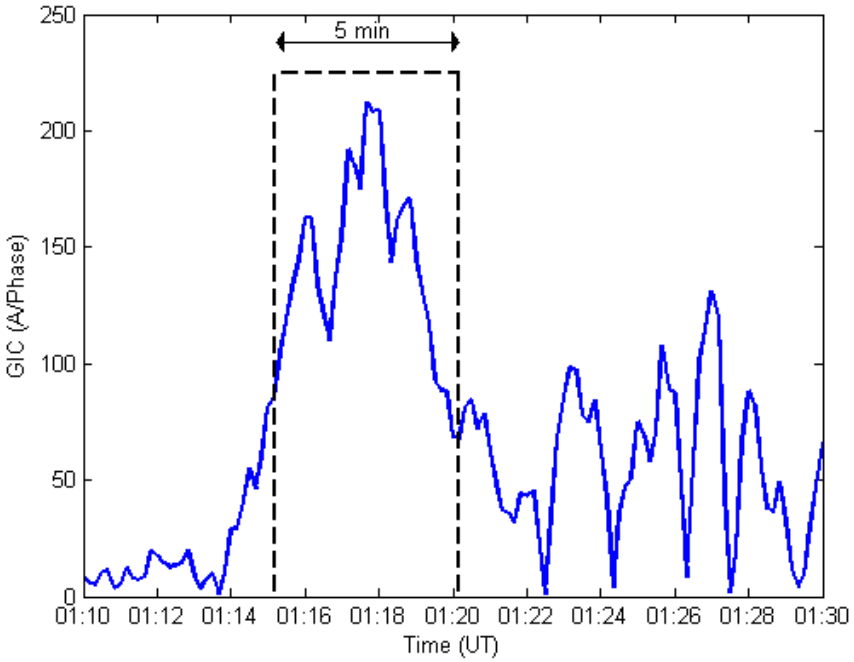

Figure 17: Close-up of GIC(t) and a 5 Minute 225 A/phase GIC Pulse Assuming 75% Load

References

[1] "IEEE Guide for loading mineral-oil-immersed transformers and step-voltage regulators." IEEE Std C57.91-2011 (Revision of IEEE Std C57.91-1995).

[2] Application Guide: Computing Geomagnetically-Induced Current in the Bulk-Power System, NERC. Available at: http://www.nerc.com/comm/PC/Geomagnetic%20Disturbance%20Task%20Force%20GMDTF%202013/GIC%20Application%20Guide%202013_approved.pdf

[3] Girgis, R.; Vedante, K. "Methodology for evaluating the impact of GIC and GIC capability of power transformer designs." IEEE PES 2013 General Meeting Proceedings. Vancouver, Canada.

[4] Marti, L., Rezaei-Zare, A., Narang, A. "Simulation of Transformer Hotspot Heating due to Geomagnetically Induced Currents." IEEE Transactions on Power Delivery, vol.28, no.1. pp 320-327. January 2013.

[5] Benchmark Geomagnetic Disturbance Event Description white paper. Developed by the Project 2013-03 (Geomagnetic Disturbance) standard drafting team. Available at:

http://www.nerc.com/pa/Stand/Pages/Project-2013-03-Geomagnetic-Disturbance-Mitigation.aspx

[6] Lahtinen, Matti. Jarmo Elovaara. "GIC occurrences and GIC test for 400 kV system transformer". IEEE Transactions on Power Delivery, Vol. 17, No. 2. April 2002.

[7] "Screening Criterion for Transformer Thermal Impact Assessment". Developed by the Project 2013-03 (Geomagnetic Disturbance) standard drafting team. Available at:

http://www.nerc.com/pa/Stand/Pages/Project-2013-03-Geomagnetic-Disturbance-Mitigation.aspx

NERC
NORTH AMERICAN ELECTRIC RELIABILITY CORPORATION

Transformer Thermal Impact Assessment White Paper

Project 2013-03 (Geomagnetic Disturbance Mitigation)

TPL-007-1 Transmission System Planned Performance for Geomagnetic Disturbance Events

Background

On May 16, 2013, FERC issued Order No. 779, directing NERC to develop Standards that address risks to reliability caused by geomagnetic disturbances (GMDs) in two stages:

- Stage 1 Standard(s) that require applicable entities to develop and implement Operating Procedures. EOP-010-1 – Geomagnetic Disturbance Operations was approved by FERC in June 2014.
- Stage 2 Standard(s) that require applicable entities to conduct assessments of the potential impact of benchmark GMD events on their systems. If the assessments identify potential impacts, the Standard(s) will require the applicable entity to develop and implement a plan to mitigate the risk.

TPL-007-1 is a new Reliability Standard to specifically address the Stage 2 directives in Order No. 779.

Large power transformers connected to the EHV transmission system can experience both winding and structural hot spot heating as a result of GMD events. TPL-007-1 will require owners of such transformers to conduct thermal analyses of their transformers to determine if the transformers will be able to withstand the thermal transient effects associated with the Benchmark GMD event. This paper discusses methods that can be employed to conduct such analyses, including example calculations.

The primary impact of GMDs on large power transformers is a result of the quasi-dc current that flows through wye-grounded transformer windings. This geomagnetically-induced current (GIC) results in an offset of the ac sinusoidal flux resulting in asymmetric or half-cycle saturation (see **Figure 1**).

Half-cycle saturation results in a number of known effects:

- Hot spot heating of transformer windings due to harmonics and stray flux;
- Hot spot heating of non-current carrying transformer metallic members due to stray flux;
- Harmonics;
- Increase in reactive power absorption; and
- Increase in vibration and noise level.

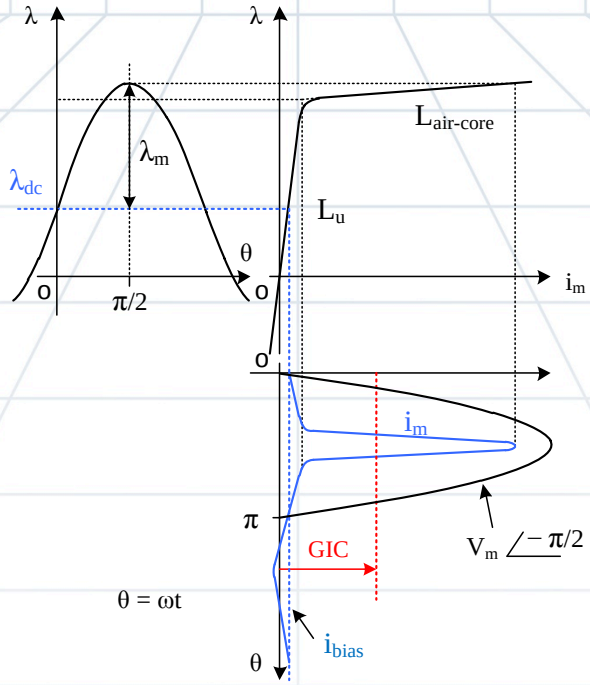

Figure 1: Mapping Magnetization Current to Flux through Core Excitation Characteristics

This paper focuses on hot spot heating of transformer windings and non current-carrying metallic parts. Effects such as the generation of harmonics, increase in reactive power absorption, vibration, and noise are not within the scope of this document.

Technical Considerations

The effects of half-cycle saturation on HV and EHV transformers, namely localized "hot spot" heating, are relatively well understood, but are difficult to quantify. A transformer GMD impact assessment must consider GIC amplitude, duration, and transformer physical characteristics such as design and condition (e.g., age, gas content, and moisture in the oil). A single threshold value of GIC cannot be justified as a "pass or fail" screening criterion where "fail" means that the transformer will suffer damage. A single threshold value of GIC only makes sense in the context where "fail" means that a more detailed study is required and that "pass" means that GIC in a particular transformer is so low that a detailed study is unnecessary. Such a threshold would have to be technically justifiable and sufficiently low to be considered a conservative value within the scope of the benchmark.

The following considerations should be taken into account when assessing the thermal susceptibility of a transformer to half-cycle saturation:

- In the absence of manufacturer specific information, use the temperature limits for safe transformer operation such as those suggested in the IEEE Std C57.91-2011 standard [1] for hot spot heating during short-term emergency operation. This standard does not suggest that exceeding these limits will result in transformer failure, but rather that it will result in additional aging of cellulose in the paper-oil insulation and the potential for the generation of gas bubbles in the bulk oil. Thus, from the point of view of evaluating

possible transformer damage due to increased hot spot heating, these thresholds can be considered conservative for a transformer in good operational condition.

- The worst case temperature rise for winding and metallic part (e.g., tie plate) heating should be estimated taking into consideration the construction characteristics of the transformer as they pertain to dc flux offset in the core (e.g., single-phase, shell, 5 and 3-leg three-phase construction).
- Bulk oil temperature due to ambient temperature and transformer loading must be added to the incremental temperature rise caused by hot spot heating. For planning purposes, maximum ambient and loading temperature should be used unless there is a technically justified reason to do otherwise.
- The time series or "waveshape" of the reference GMD event in terms of peak amplitude, duration, and frequency of the geoelectric field has an important effect on hot spot heating. Winding and metallic part hot spot heating have different thermal time constants, and their temperature rise will be different if the GIC currents are sustained for 2, 10, or 30 minutes for a given GIC peak amplitude.
- The "effective" GIC in autotransformers (reflecting the different GIC ampere-turns in the common and the series windings) must be used in the assessment. The effective current $I_{dc,eq}$ in an autotransformer is defined by [2].

$$I_{dc,eq} = I_H + (I_N/3 - I_H)V_X/V_H \quad (1)$$

where

I_H is the dc current in the high voltage winding;
I_N is the neutral dc current;
V_H is the rms rated voltage at HV terminals;
V_X is the rms rated voltage at the LV terminals.

Transformer Thermal Impact Assessment Process

A simplified thermal assessment may be based on Table 2 from the "Screening Criterion for Transformer Thermal Impact Assessment" white paper [7]. This table, shown as Table 1 below, provides the peak metallic hot spot temperatures that can be reached using conservative thermal models. To use Table 1, one must select the bulk oil temperature and the threshold for metallic hot spot heating, for instance, from reference [1] after allowing for possible de-rating due to transformer condition. If the effective GIC results in higher than threshold temperatures, then the use of a detailed thermal assessment as described below should be carried out.

Table 1: Upper Bound of Peak Metallic Hot Spot Temperatures Calculated Using the Benchmark GMD Event

Effective GIC (A/phase)	Metallic hot spot Temperature (°C)	Effective GIC(A/phase)	Metallic hot spot Temperature (°C)
0	80	100	182
10	107	110	186
20	128	120	190
30	139	130	193
40	148	140	204
50	157	150	213
60	169	160	221
70	170	170	230
75	172	180	234
80	175	190	241
90	179	200	247

Two different ways to carry out a detailed thermal impact assessment are discussed below. In addition, other approaches and models approved by international standard-setting organizations such as the Institute of Electrical and Electronic Engineers (IEEE)[1] or International Council on Large Electric Systems (CIGRE) may also provide technically justified methods for performing thermal assessments. All thermal assessment methods should be demonstrably equivalent to assessments that use the benchmark GMD event.

1. Transformer manufacturer GIC capability curves. These curves relate permissible peak GIC (obtained by the user from a steady-state GIC calculation) and loading, for a specific transformer. An example of manufacturer capability curves is provided in **Figure 2**. Presentation details vary between manufacturers, and limited information is available regarding the assumptions used to generate these curves, in particular, the assumed waveshape or duration of the effective GIC. Some manufacturers assume that the waveshape of the GIC in the transformer windings is a square pulse of 2, 10, or 30 minutes in duration. In the case of the transformer capability curve shown in **Figure 2** [3], a square pulse of 900 A/phase with a duration of 2 minutes would cause the Flitch plate hot spot to reach a temperature of 180 °C at full load. While GIC capability curves are relatively simple to use, an amount of engineering judgment is necessary to ascertain which portion of a GIC waveshape is equivalent to, for example, a 2 minute pulse. Also, manufacturers generally maintain that in

[1] For instance, IEEE Std C57.163-2015 Guide for Establishing Power Transformer Capability while under Geomagnetic Disturbances

the absence of transformer standards defining thermal duty due to GIC, such capability curves must be developed for every transformer design and vintage.

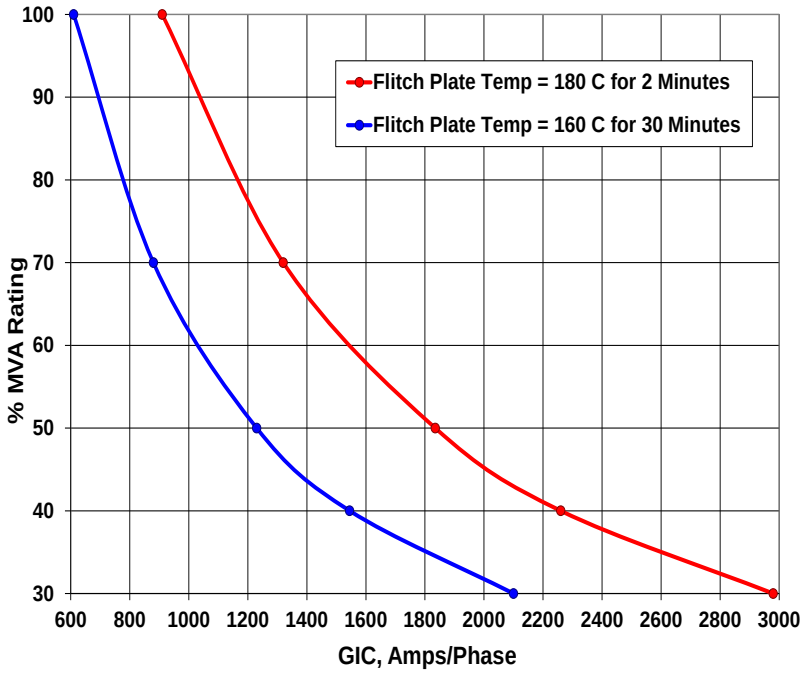

Figure 2: Sample GIC Manufacturer Capability Curve of a Large Single-Phase Transformer Design using the Flitch Plate Temperature Criteria [3]

2. Thermal response simulation[2]. The input to this type of simulation is the time series or waveshape of effective GIC flowing through a transformer (taking into account the actual configuration of the system), and the result of the simulation is the hot spot temperature (winding or metallic part) time sequence for a given transformer. An example of GIC input and hotspot temperature time series values from [4] are shown in **Figure 3**. The hot spot thermal transfer functions can be obtained from measurements or calculations provided by transformer manufacturers. Conservative default values can be used (e.g. those provided in [4]) when specific data are not available. Hot spot temperature thresholds shown in **Figure 3** are consistent with IEEE Std C57.91 emergency loading hot spot limits. Emergency loading time limit is usually 30 minutes.

[2] Technical details of this methodology can be found in [4].

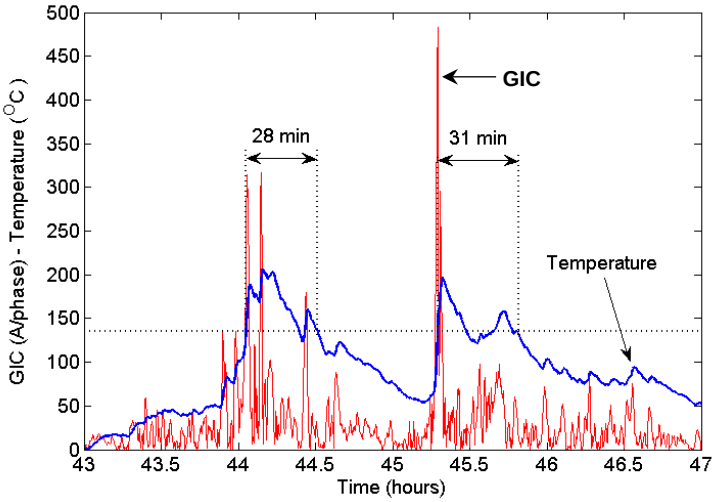

Figure 3: Sample Tie Plate Temperature Calculation
Blue trace is incremental temperature and red trace is the magnitude of the GIC/phase [4]

It is important to reiterate that the characteristics of the time sequence or "waveshape" are very important in the assessment of the thermal impact of GIC on transformers. Transformer hot spot heating is not instantaneous. The thermal time constants of transformer windings and metallic parts are typically on the order of minutes to tens of minutes; therefore, hot spot temperatures are heavily dependent on GIC history and rise time, amplitude and duration of GIC in the transformer windings, bulk oil temperature due to loading, ambient temperature and cooling mode.

Calculation of the GIC Waveshape for a Transformer

The following procedure can be used to generate time series GIC data, i.e. GIC(t), using a software program capable of computing GIC in the steady-state. The steps are as follows:

1. Calculate contribution of GIC due to eastward and northward geoelectric fields for the transformer under consideration;
2. Scale the GIC contribution according to the reference geoelectric field time series to produce the GIC time series for the transformer under consideration.

Most available GIC–capable software packages can calculate GIC in steady-state in a transformer assuming a uniform eastward geoelectric field of 1 V/km (GIC_E) while the northward geoelectric field is zero. Similarly, GIC_N can be obtained for a uniform northward geoelectric field of 1 V/km while the eastward geoelectric field is zero. GIC_E and GIC_N are the normalized GIC contributions for the transformer under consideration.

If the earth conductivity is assumed to be uniform (or laterally uniform) in the transmission system of interest, then the transformer GIC (in A/phase) for any value of $E_E(t)$ and $E_N(t)$ can be calculated using (2) [2].

$$GIC(t) = |E(t)| \cdot \{GIC_E \sin(\varphi(t)) + GIC_N \cos(\varphi(t))\} \quad (2)$$

where

$$|E(t)| = \sqrt{E_N^2(t) + E_E^2(t)} \quad (3)$$

$$\varphi(t) = \tan^{-1}\left(\frac{E_E(t)}{E_N(t)}\right) \quad (4)$$

$$GIC(t) = E_E(t) \cdot GIC_E + E_N(t) \cdot GIC_N \quad (5)$$

GIC_N is the effective GIC due to a northward geoelectric field of 1 V/km, and GIC_E is the effective GIC due to an eastward geoelectric field of 1 V/km. The units for GIC_N and GIC_E are A/phase/V/km)

The geoelectric field time series $E_N(t)$ and $E_E(t)$ is obtained, for instance, from the reference geomagnetic field time series [5] after the appropriate geomagnetic latitude scaling factor α is applied[3]. The reference geoelectric field time series is calculated using the reference earth model. When using this geoelectric field time series where a different earth model is applicable, it should be scaled with the conductivity scaling factor β[4]. Alternatively, the geoelectric field can be calculated from the reference geomagnetic field time series after the appropriate geomagnetic latitude scaling factor α is applied and the appropriate earth model is used. In such case, the conductivity scaling factor β is not applied because it is already accounted for by the use of the appropriate earth model.

Applying (5) to each point in $E_N(t)$ and $E_E(t)$ results in GIC(t).

GIC(t) Calculation Example

Let us assume that from the steady-state solution, the effective GIC in this transformer is GIC_E = -20 A/phase if E_N=0, E_E=1 V/km and GIC_N = 26 A/phase if E_N=1 V/km, E_E=0. Let us also assume the geomagnetic field time series corresponds to a geomagnetic latitude where α = 1 and that the earth conductivity corresponds to the reference earth model in [5]. The resulting geoelectric field time series is shown in **Figure 4**. Therefore:

$$GIC(t) = E_E(t) \cdot GIC_E + E_N(t) \cdot GIC_N \text{ (A/phase)} \quad (6)$$

$$GIC(t) = -E_E(t) \cdot 20 + \cdot E_N(t) \cdot 26 \text{ (A/phase)} \quad (7)$$

The resulting GIC waveshape GIC(t) is shown in **Figures 5 and 6** and can subsequently be used for thermal analysis.

[3] The geomagnetic factor α is described in [2] and is used to scale the geomagnetic field according to geomagnetic latitude. The lower the geomagnetic latitude (closer to the equator), the lower the amplitude of the geomagnetic field.

[4] The conductivity scaling factor β is described in [2], and is used to scale the geoelectric field according to the conductivity of different physiographic regions. Lower conductivity results in higher β scaling factors.

It should be emphasized that even for the same reference event, the GIC(t) waveshape in every transformer will be different, depending on the location within the system and the number and orientation of the circuits connecting to the transformer station. Assuming a single generic GIC(t) waveshape to test all transformers is incorrect.

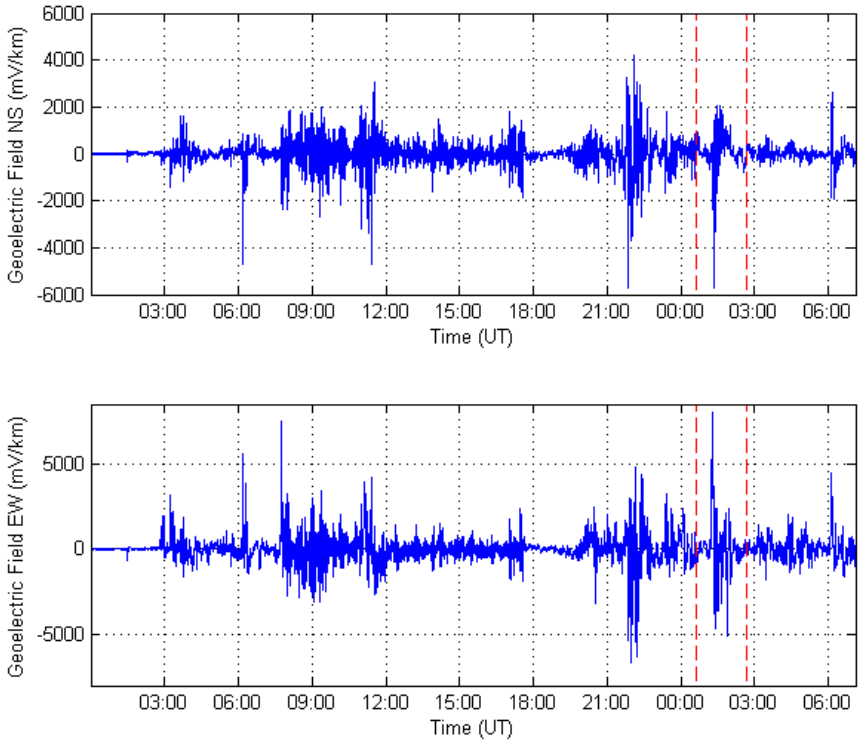

Figure 4: Calculated Geoelectric Field $E_N(t)$ and $E_E(t)$ Assuming $\alpha=1$ and $\beta=1$ (Reference Earth Model). Zoom area for subsequent graphs is highlighted. Dashed lines approximately show the close-up area for subsequent Figures.

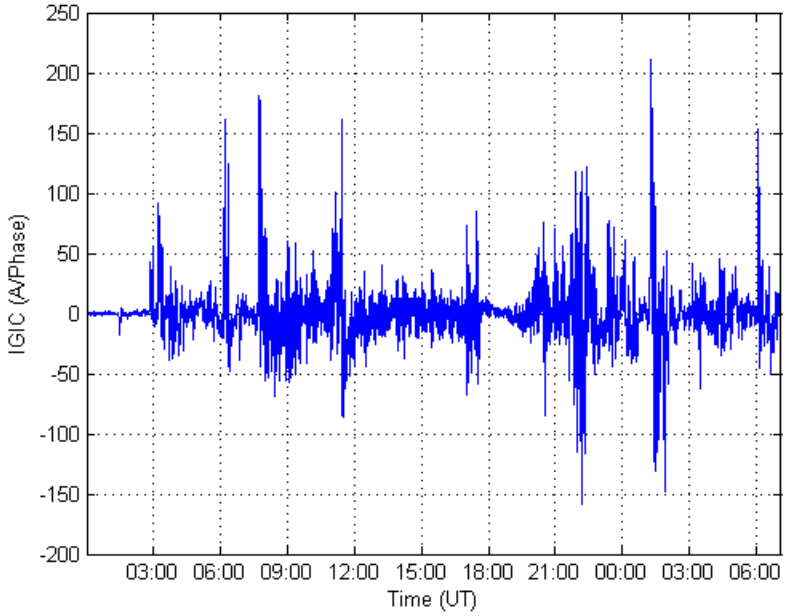

Figure 5: Calculated GIC(t) Assuming α=1 and β=1 (Reference Earth Model)

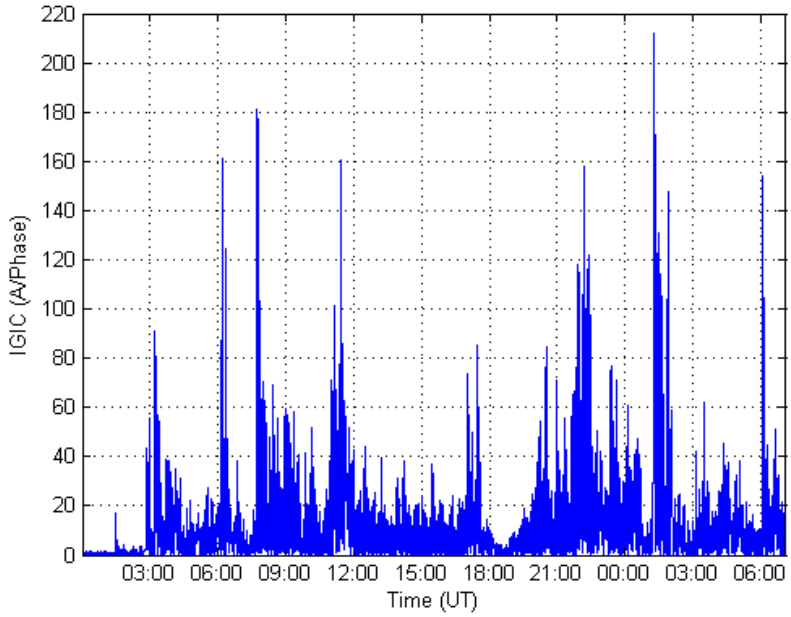

Figure 6: Calculated Magnitude of GIC(t) Assuming α=1 and β=1 (Reference Earth Model)

Transformer Thermal Assessment Examples

There are two basic ways to carry out a transformer thermal analysis once the GIC time series GIC(t) is known for a given transformer: 1) calculating the thermal response as a function of time; and 2) using manufacturer's capability curves.

Example 1: Calculating thermal response as a function of time using a thermal response tool

The thermal step response of the transformer can be obtained for both winding and metallic part hot spots from: 1) measurements; 2) manufacturer's calculations; or 3) generic published values. **Figure 7** shows the measured metallic hot spot thermal response to a dc step of 16.67 A/phase of the top yoke clamp from [6] that will be used in this example. **Figure 8** shows the measured incremental temperature rise (asymptotic response) of the same hot spot to long duration GIC steps.[5]

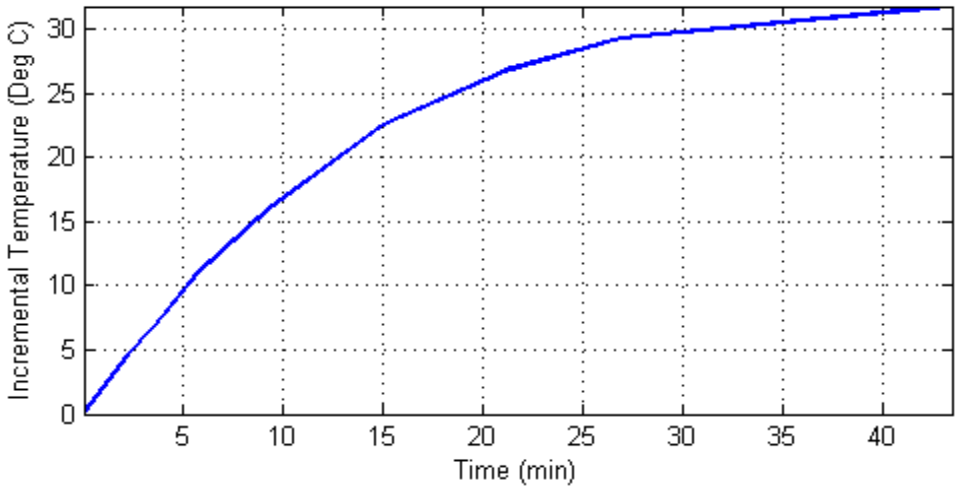

Figure 7: Thermal Step Response to a 16.67 Amperes per Phase dc Step
Metallic hot spot heating.

[5] Heating of bulk oil due to the hot spot temperature increase is not included in the asymptotic response because the time constant of bulk oil heating is at least an order of magnitude larger than the time constants of hot spot heating.

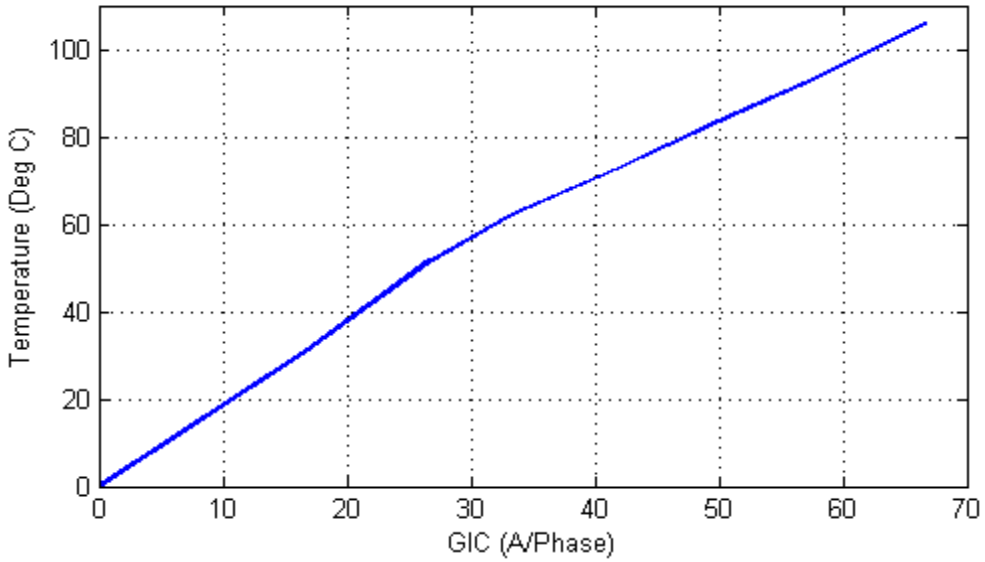

Figure 8: Asymptotic Thermal Step Response
Metallic hot spot heating.

The step response in **Figure 7** was obtained from the first GIC step of the tests carried out in [6]. The asymptotic thermal response in **Figure 8** was obtained from the final or near-final temperature values after each subsequent GIC step. **Figure 9** shows a comparison between measured temperatures and the calculated temperatures using the thermal response model used in the rest of this discussion.

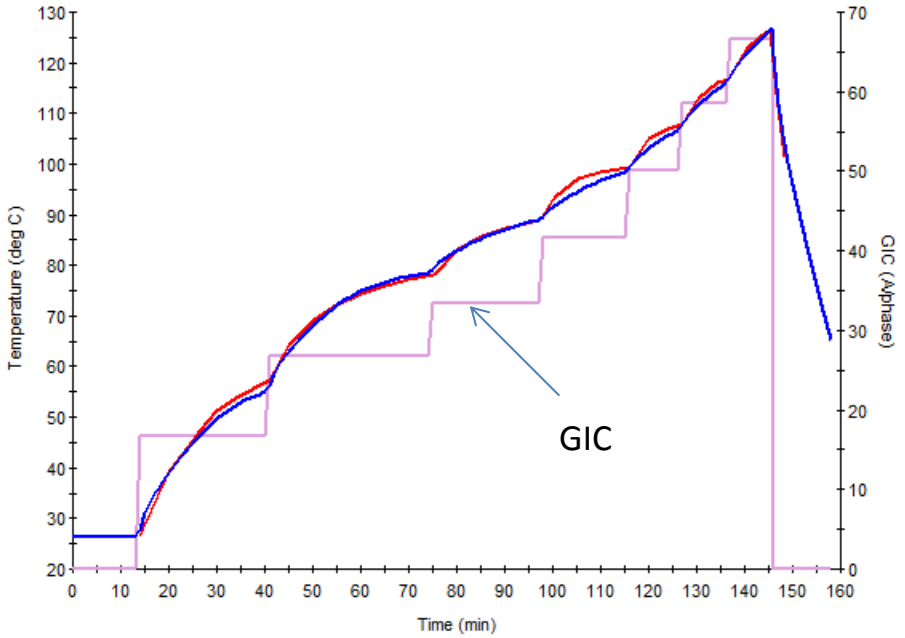

Figure 9: Comparison of measured temperatures (red trace) and simulation results (blue trace). Injected current is represented by the magenta trace.

To obtain the thermal response of the transformer to a GIC waveshape such as the one in **Figure 6**, a thermal response model is required. To create a thermal response model, the measured or manufacturer-calculated transformer thermal step responses (winding and metallic part) for various GIC levels are required. The GIC(t) time series or waveshape is then applied to the thermal model to obtain the incremental temperature rise as a function of time $\theta(t)$ for the GIC(t) waveshape. The total temperature is calculated by adding the oil temperature, for example, at full load.

Figure 10 illustrates the calculated GIC(t) and the corresponding hot spot temperature time series $\theta(t)$. **Figure 11** illustrates a close-up view of the peak transformer temperatures calculated in this example.

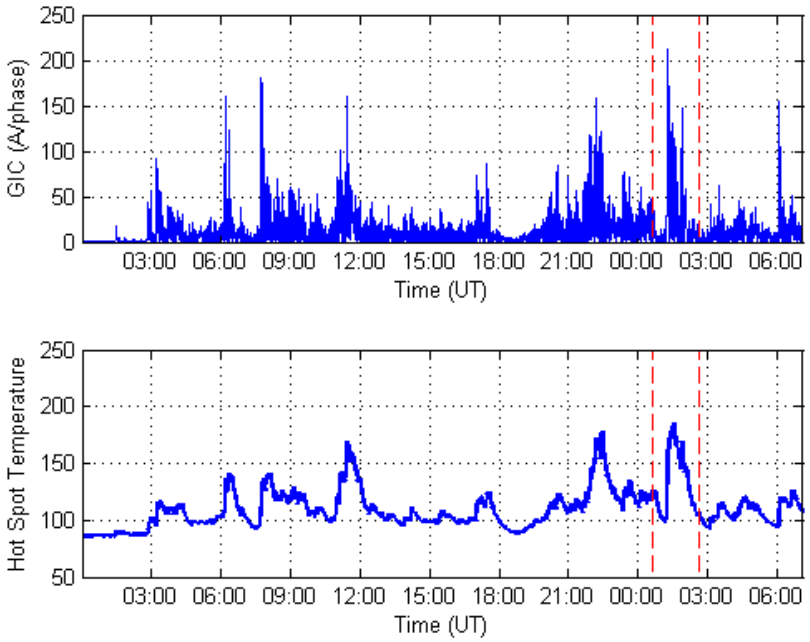

Figure 10: Magnitude of GIC(t) and Metallic Hot Spot Temperature $\theta(t)$ Assuming Full Load Oil Temperature of 85.3°C (40°C ambient). Dashed lines approximately show the close-up area for subsequent Figures.

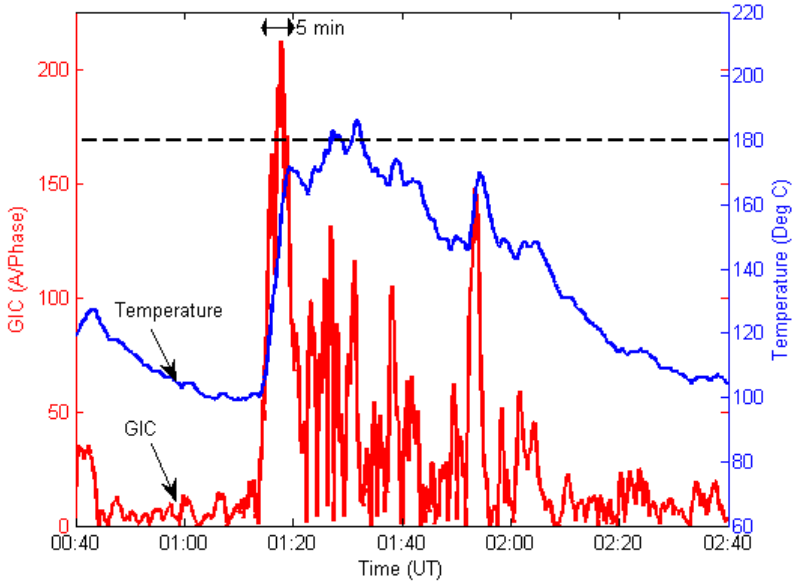

Figure 11: Close-up of Metallic Hot Spot Temperature Assuming a Full Load
(Blue trace is θ(t). Red trace is GIC(t))

In this example, the IEEE Std C57.91 emergency loading hot spot threshold of 200°C for metallic hot spot heating is not exceeded. Peak temperature is 186°C. The IEEE standard is silent as to whether the temperature can be higher than 200°C for less than 30 minutes. Manufacturers can provide guidance on individual transformer capability.

It is not unusual to use a lower temperature threshold of 180°C to account for calculation and data margins, as well as transformer age and condition. **Figure 11** shows that 180°C will be exceeded for 5 minutes.

At 75% loading, the initial temperature is 64.6 °C rather than 85.3 °C, and the hot spot temperature peak is 165°C, well below the 180°C threshold (see **Figure 12**).

If a conservative threshold of 160°C were used to account for the age and condition of the transformer, then the full load limits would be exceeded for approximately 22 minutes.

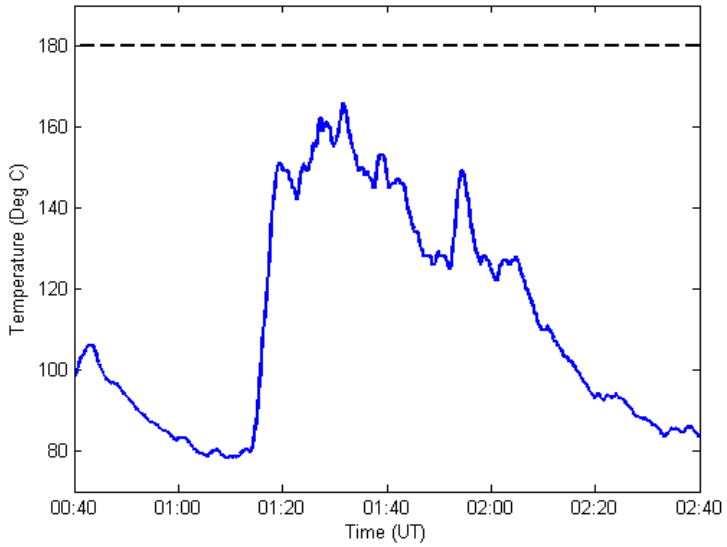

Figure 12: Close-up of Metallic Hot Spot Temperature Assuming a 75% Load
(Oil temperature of 64.5°C)

Example 2: Using a Manufacturer's Capability Curves

The capability curves used in this example are shown in **Figure 13**. To maintain consistency with the previous example, these particular capability curves have been reconstructed from the thermal step response shown in **Figures 7** and **8**, and the simplified loading curve shown in **Figure 14** (calculated using formulas from IEEE Std C57.91).

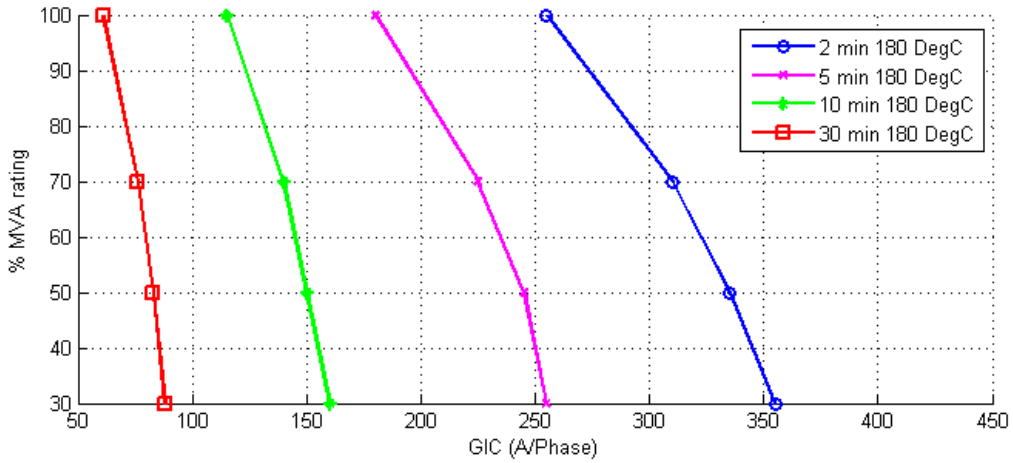

Figure 13: Capability Curve of a Transformer Based on the Thermal Response Shown in Figures 8 and 9.

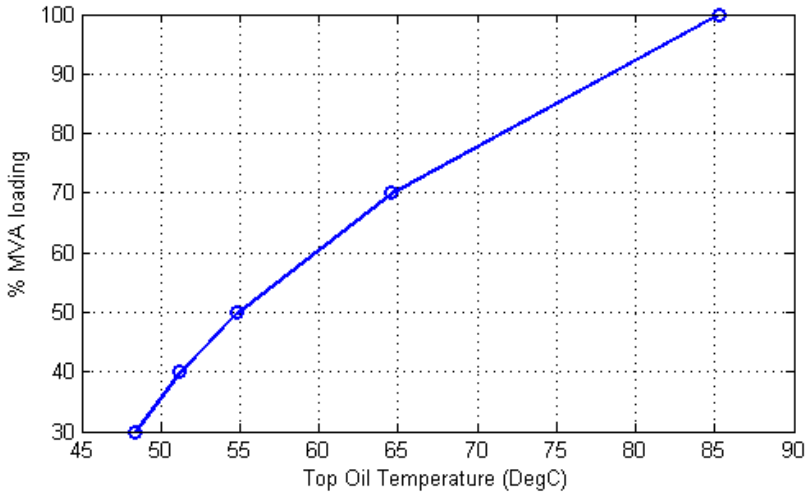

Figure 14: Simplified Loading Curve Assuming 40°C Ambient Temperature.

The basic notion behind the use of capability curves is to compare the calculated GIC in a transformer with the limits at different GIC pulse widths. A narrow GIC pulse has a higher limit than a longer duration or wider one. If the calculated GIC and assumed pulse width falls below the appropriate pulse width curve, then the transformer is within its capability.

To use these curves, it is necessary to estimate an equivalent square pulse that matches the waveshape of GIC(t), generally at a GIC(t) peak. **Figure 15** shows a close-up of the GIC near its highest peak superimposed to a 255 Amperes per phase, 2 minute pulse at 100% loading from **Figure 13**. Since a narrow 2-minute pulse is not representative of GIC(t) in this case, a 5 minute pulse with an amplitude of 180 A/phase at 100% loading has been superimposed on **Figure 16**. It should be noted that a 255 A/phase, 2 minute pulse is equivalent to a 180 A/phase 5 minute pulse from the point of view of transformer capability. Deciding what GIC pulse is equivalent to the portion of GIC(t) under consideration is a matter of engineering judgment.

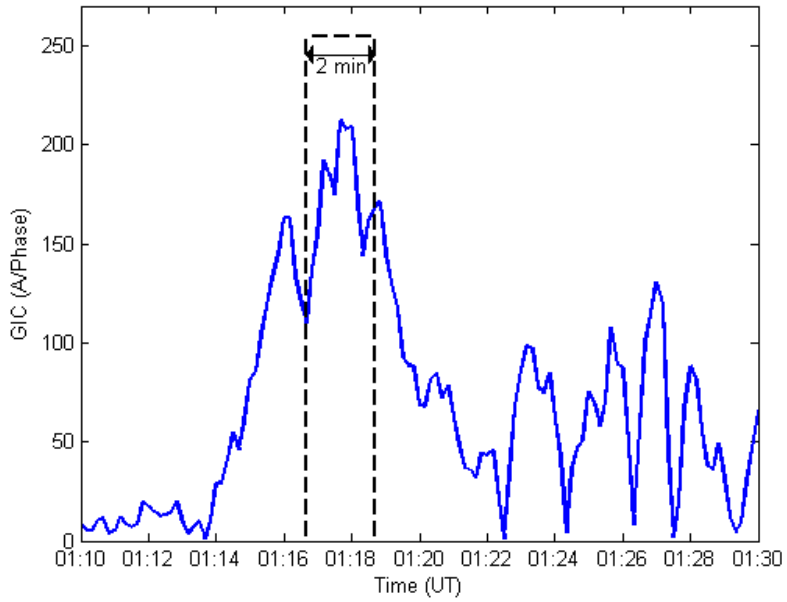

Figure 15: Close-up of GIC(t) and a 2 minute 255 A/phase GIC pulse at full load

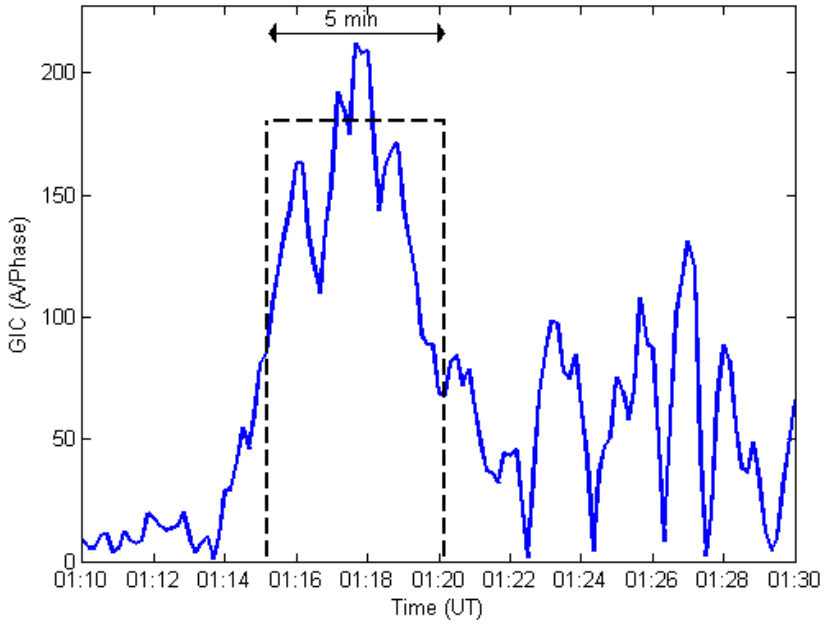

Figure 16: Close-up of GIC(t) and a Five Minute 180 A/phase GIC Pulse at Full Load

When using a capability curve, it should be understood that the curve is derived assuming that there is no hot spot heating due to prior GIC at the time the GIC pulse occurs (only an initial temperature due to loading). Therefore, in addition to estimating the equivalent pulse that matches GIC(t), prior hot spot heating must be accounted for. From

these considerations, it is unclear whether the capability curves would be exceeded at full load with a 180 °C threshold in this example.

At 70% loading, the two and five minute pulses from **Figure 13** would have amplitudes of 310 and 225 A/phase, respectively. The 5 minute pulse is illustrated in **Figure 17**. In this case, judgment is also required to assess if the GIC(t) is within the capability curve for 70% loading. In general, capability curves are easier to use when GIC(t) is substantially above, or clearly below the GIC thresholds for a given pulse duration.

If a conservative threshold of 160°C were used to account for the age and condition of the transformer, then a new set of capability curves would be required.

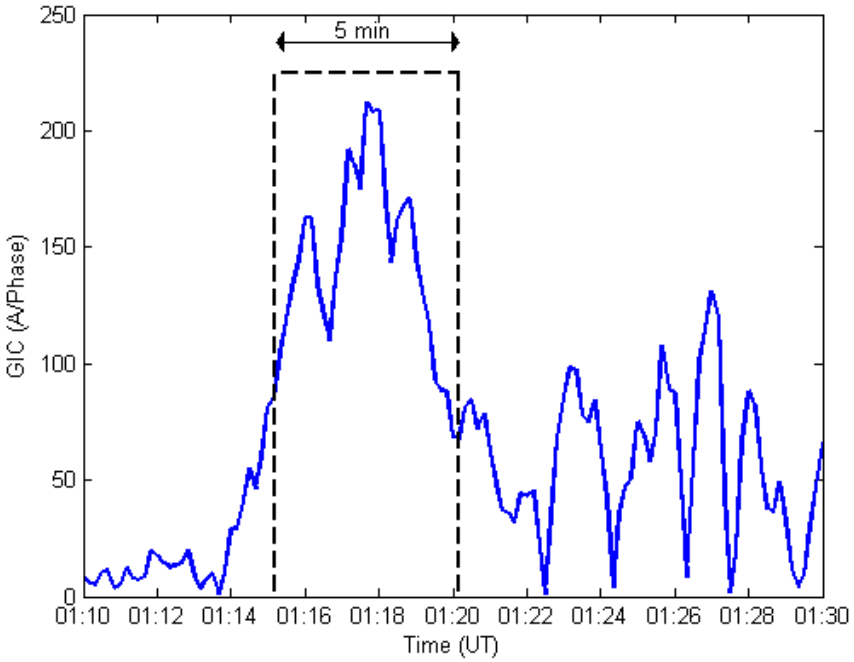

Figure 17: Close-up of GIC(t) and a 5 Minute 225 A/phase GIC Pulse Assuming 75% Load

References

[1] "IEEE Guide for loading mineral-oil-immersed transformers and step-voltage regulators." IEEE Std C57.91-2011 (Revision of IEEE Std C57.91-1995).

[2] Application Guide: Computing Geomagnetically-Induced Current in the Bulk-Power System, NERC. Available at: http://www.nerc.com/comm/PC/Geomagnetic%20Disturbance%20Task%20Force%20GMDTF%202013/GIC%20Application%20Guide%202013_approved.pdf

[3] Girgis, R.; Vedante, K. "Methodology for evaluating the impact of GIC and GIC capability of power transformer designs." IEEE PES 2013 General Meeting Proceedings. Vancouver, Canada.

[4] Marti, L., Rezaei-Zare, A., Narang, A. "Simulation of Transformer Hotspot Heating due to Geomagnetically Induced Currents." IEEE Transactions on Power Delivery, vol.28, no.1. pp 320-327. January 2013.

[5] Benchmark Geomagnetic Disturbance Event Description white paper. Developed by the Project 2013-03 (Geomagnetic Disturbance) standard drafting team. Available at:

http://www.nerc.com/pa/Stand/Pages/Project-2013-03-Geomagnetic-Disturbance-Mitigation.aspx

[6] Lahtinen, Matti. Jarmo Elovaara. "GIC occurrences and GIC test for 400 kV system transformer". IEEE Transactions on Power Delivery, Vol. 17, No. 2. April 2002.

[7] "Screening Criterion for Transformer Thermal Impact Assessment". Developed by the Project 2013-03 (Geomagnetic Disturbance) standard drafting team. Available at:

http://www.nerc.com/pa/Stand/Pages/Project-2013-03-Geomagnetic-Disturbance-Mitigation.aspx

NERC
NORTH AMERICAN ELECTRIC RELIABILITY CORPORATION

Meeting Announcement

Project 2013-03 Geomagnetic Disturbance Mitigation Standard Drafting Team

May 11, 2016 | 8:00 – 10:00 a.m. Eastern

Conference Call with Web Access

ReadyTalk Webinar | Enter Access Code: 6251541

Dial-in: 1-866-740-1260 | Access Code: 6251541 | Security Code: 201303

The purpose of this web meeting is to review and discuss a correction to the *Screening Criterion for Transformer Thermal Impact Assessment* white paper related to the proposed TPL-007-1 reliability standard. The proposed standard and related white papers are available on the project page.

For more information or assistance, contact Senior Standards, Mark Olson (via email) or by phone at (404) 446-9760.

3353 Peachtree Road NE
Suite 600, North Tower
Atlanta, GA 30326
404-446-2560 | www.nerc.com

NERC
NORTH AMERICAN ELECTRIC RELIABILITY CORPORATION

Standards Announcement

Project 2013-03 Geomagnetic Disturbance Mitigation | Revised White Papers

Comment Period Open through June 13, 2016

Now Available

A comment period is open for **Project 2013-03 Geomagnetic Disturbance Mitigation** revised white papers. Stakeholders may provide comments using the link below through **8 p.m. Eastern, Monday, June 13, 2016.**

The standards drafting team (SDT) identified an error in Figure 1 of the *Screening Criterion for Transformer Thermal Impact Assessment* white paper (Screening Criterion white paper). The error resulted in incorrect plotting of simulated power transformer peak hot-spot heating from the Benchmark GMD Event. The SDT has corrected Figure 1 and revised related sections in the Screening Criterion white paper. The SDT has also made related revisions to other Project 2013-03 white papers. The revisions do not affect requirements in proposed TPL-007-1 but are being incorporated into the project white papers to maintain accuracy.

Commenting

Use the electronic form to submit comments. If you experience any difficulties in using the electronic form, contact Nasheema Santos. An unofficial Word version of the comment form is posted on the project page.

If you are having difficulty accessing the SBS due to a forgotten password, incorrect credential error messages, or system lock-out, contact NERC IT support directly at https://support.nerc.net/ (Monday – Friday, 8 a.m. - 8 p.m. Eastern).

For information on the Standards Development Process, refer to the Standard Processes Manual.

For more information or assistance, contact Senior Standards Developer, Mark Olson (via email) or by phone at (404) 446-9760.

3353 Peachtree Road NE
Suite 600, North Tower
Atlanta, GA 30326
404-446-2560 | www.nerc.com

NERC
NORTH AMERICAN ELECTRIC RELIABILITY CORPORATION

Meeting Announcement

Project 2013-03 Geomagnetic Disturbance Mitigation Standard Drafting Team

June 24, 2016 | 8:30 – 10:30 a.m. Eastern

Conference Call with Web Access

ReadyTalk Webinar | Enter Access Code: 6251541

Dial-in: 1-866-740-1260 | Access Code: 6251541 | Security Code: 201303

The Standard Drafting Team (SDT) will review and discuss stakeholder comments and recommendations on the white papers associated with proposed reliability standard TPL-007-1. In May, the SDT corrected Figure 1 of the *Screening Criterion for Transformer Thermal Impact Assessment* white paper, and made corresponding revisions to text in the project white papers. The revisions were posted on May 13, 2016, for a 30-day comment period. Proposed standard TPL-007-1 and related white papers are available on the project page.

For more information or assistance, contact Senior Standards Developer, Mark Olson (via email) or by phone at (404) 446-9760.

3353 Peachtree Road NE
Suite 600, North Tower
Atlanta, GA 30326
404-446-2560 | www.nerc.com